

CHARACTERIZATION OF ENDOGENOUS NUCLEOBINDIN-2/NESFATIN-1 IN RODENTS

A Thesis Submitted to the College of

Graduate Studies and Research

In Partial Fulfillment of the Requirements

For the Degree of Doctor of Philosophy

In the Department of Veterinary Biomedical Sciences

University of Saskatchewan

Saskatoon

By

HANEESHA MOHAN

PERMISSION TO USE

In presenting this thesis/dissertation in partial fulfillment of the requirements for a Postgraduate degree from the University of Saskatchewan, I agree that the Libraries of this University may make it freely available for inspection. I further agree that permission for copying of this thesis/dissertation in any manner, in whole or in part, for scholarly purposes may be granted by the professor or professors who supervised my thesis/dissertation work or, in their absence, by the Head of the Department or the Dean of the College in which my thesis work was done. It is understood that any copying or publication or use of this thesis/dissertation or parts thereof for financial gain shall not be allowed without my written permission. It is also understood that due recognition shall be given to me and to the University of Saskatchewan in any scholarly use which may be made of any material in my thesis/dissertation.

Requests for permission to copy or to make other uses of materials in this thesis/dissertation in whole or part should be addressed to:

Head of the Department of Veterinary Biomedical Science
Western College of Veterinary Medicine
University of Saskatchewan
Saskatoon, Saskatchewan S7N 5B4
Canada

OR

Dean
College of Graduate Studies and Research
University of Saskatchewan
107 Administration Place
Saskatoon, Saskatchewan S7N 5A2
Canada

ABSTRACT

The regulation of whole body energy balance is regulated by the endocrine system. Nesfatin-1 is a newly identified multifunctional metabolic peptide with insulinotropic, endocrine, glucoregulatory, fat reducing and cardiovascular functions. There is no evidence on NUCB2/nesfatin-1 during development. While nesfatin-1 is meal responsive, it is unknown whether macronutrients regulate its secretion. Is endogenous nesfatin-1 critical for energy balance? The central hypothesis of this thesis research is that the tissue specific expression of NUCB2/nesfatin-1 is regulated developmentally, and by nutrients, and that the endogenous NUCB2/nesfatin-1 is critical for the maintenance of energy homeostasis. The specific objectives of this research were to determine the developmental, and nutrient regulated expression of NUCB2/nesfatin-1, and to characterize the metabolic phenotype of mice lacking NUCB2/nesfatin-1. There were three key findings made in this research. First, it was found that NUCB2/nesfatin-1 presents an ontogenic pattern of expression in the gastroenteropancreatic tissues and serum of rats. An age-dependent co-expression of related peptides, ghrelin and its processing enzyme, ghrelin-O-acyl transferase (GOAT), and nesfatin-1 processing prohormone convertases were also found in the endocrine pancreas. Second, it was determined that the NUCB2 mRNA expression and NUCB2/nesfatin-1 secretion in mice are influenced by nutrients in a tissue specific manner *in vitro* and *in vivo*, and it depends on the duration of exposure to specific diets tested. This research identified macronutrients as major regulators of endogenous NUCB2/nesfatin-1. Third, a sexually dimorphic effect of NUCB2/nesfatin-1 disruption in mice was found, with alterations in body weight, food intake, insulin secretion, glucose homeostasis and energy homeostasis. These data support a metabolic role for endogenous nesfatin-1. Together, this research provides important new information on developmental and cell specific

regulation of nesfatin-1 expression, nutrient regulation of its expression and secretion, and an essential role for endogenous nesfatin-1 in maintaining energy homeostasis. For example, endocrine pancreas is an abundant source of nesfatin-1. Absence of endogenous nesfatin-1 causes defects in insulin secretion from islet beta cells, and alters glucose homeostasis. Exogenous nesfatin-1 causes a reduction in body weight. NUCB2 gene disruption resulted in abnormal body weight, further confirming that nesfatin-1 indeed influences body mass.

ACKNOWLEDGEMENTS

The generous financial support for this research came from two Open Operating Grants from the Canadian Institute of Health Research (CIHR), a Leader's Opportunities Fund (LOF) from the Canada Foundation for Innovation (CFI) and an Establishment Grant from the Saskatchewan Health Research Foundation (SHRF) to Suraj Unniappan. The facilities and research infrastructure provided by the Department of Veterinary Biomedical Sciences and University of Saskatchewan are also deeply appreciated.

I would like to sincerely thank my supervisor, Dr. Suraj Unniappan and my committee members, Drs. Karen Machin, George Forsyth, Linda Hiebert, and Kaushik Desai for their constant support, constructive criticism and exceptional advice during my graduate studies. I would also like to thank my external examiner, Dr. Prasanth Chelikani for reviewing my thesis and for serving as a member of the thesis examining committee.

DEDICATION

I dedicate this thesis to everyone who has guided and supported me throughout my graduate studies. Firstly, I would like to dedicate this thesis to Suraj for his continued guidance, assistance, encouragement and compassion throughout the duration of my graduate studies. I am privileged to be your student! Thank you for being a great advisor, allowing me to learn and improve from my mistakes. Your constant drive, confidence and enthusiasm for research have helped me succeed strengthening my passion in the field of endocrinology. I deeply appreciate your constant advice as a friend over the past years during my graduate studies at York University and University of Saskatchewan. Your traits of independency, determination, ambitiousness and professionalism are qualities I hope to take with me in my future endeavors. I am grateful for the several operating grants that you have achieved over the years which has helped me to accomplish my projects in a timely manner. I would also like to thank members of the Unniappan lab who I have worked with for teaching me multiple lab techniques and always being available to answer my questions. I will surely miss the lab when I am not here! I hold many memories dear to my heart and shall cherish them forever! I wish you all the best in future and profound success in research in many years to come. Next, I would like to dedicate this thesis to my family for their constant support during my past years. You'll are the backbone to my success! Most of all, this thesis is dedicated to my mother, father, and brother, Yerram Sowdhamini, Mohan Srinivasan and Harsha Mohan who I believe I would not have reached this stage to become a successful individual in life without their constant care and wisdom. You were always there to listen to my complains, wipe my tears and bring a smile to my face, when I needed it the most! I am blessed to be your daughter and sister, and hope to keep you'll proud for many years to follow! Thank you for loving me and always being there for me!

TABLE OF CONTENTS

PERMISSION TO USE.....	i
ABSTRACT.....	ii
ACKNOWLEDGEMENTS.....	iv
DEDICATION.....	v
TABLE OF CONTENTS.....	vi
LIST OF TABLES.....	xiv
LIST OF FIGURES.....	xv
LIST OF ABBREVIATIONS.....	xix
CHAPTER 1 INTRODUCTION.....	1
1.1 The Nervous and Hormonal Systems: Integrators of Homeostasis.....	1
1.1.1 Hormone Synthesis.....	2
1.1.2 Mechanism of Hormonal Action.....	3
1.1.3 Hormones Involved in the Regulation of Energy Balance.....	3
1.1.4 Neuroendocrine Control of Feeding.....	4
1.2 Nucleobindins.....	7
1.2.1 Discovery of Nucleobindin-2 and Nesfatin-1.....	7
1.2.2 Tissue-Specific Expression of NUCB2/Nesfatin-1: Comparative Aspects.....	15
1.2.2.1 Region-Specific Expression of NUCB2/Nesfatin-1 in Mammals and Non-Mammals.....	15
1.2.2.1.1 Mammals.....	15
1.2.2.1.2 Non-Mammals.....	18
1.2.2.2 G-Protein Coupled Receptors (GPCRs) – potential receptor of nesfatin-1?.....	19
1.2.3 Biological Actions of Nesfatin-1 in Mammals and Fish.....	20

1.2.3.1	Nesfatin-1 Regulation of Feeding and Metabolism.....	20
1.2.3.1.1	Nesfatin-1 Mediated Inhibition of Feeding.....	20
1.2.3.1.2	Mechanism of Nesfatin-1 <i>In Vivo</i> Action on Food Intake.....	22
1.2.3.2	Nesfatin-1 Regulation of Insulin Secretion and Glucose Metabolism.....	24
1.2.3.3	Nesfatin-1 Metabolic Control of Reproduction.....	25
1.2.4	Summary.....	28
	Regulation of Energy Balance during Growth.....	30
1.3	Ghrelin.....	32
1.3.1	Ghrelin mRNA and Protein Expression in Tissues.....	35
1.3.2	Biological Actions of Ghrelin.....	37
	Ghrelin Function is Dependent on GOAT.....	39
1.4	GOAT.....	40
1.4.1	GOAT mRNA and Protein Expression in Tissues.....	41
1.4.2	Biological Actions of GOAT.....	43
1.5	NUCB2/Nesfatin-1 – Ghrelin Relationship.....	46
1.6	Rationale.....	48
1.7	Hypothesis and Specific Objectives.....	49
	Transition.....	50
	CHAPTER 2 ONTOGENIC PATTERN OF NUCLEOBINDIN-2/NESFATIN-1 EXPRESSION IN THE GASTROENTEROPANCREATIC TISSUES AND SERUM OF SPRAGUE DAWLEY RATS.....	51
2.1	Introduction.....	51
2.2	Materials and Methods.....	55
2.2.1	Animals.....	55

2.2.2	Immunohistochemistry.....	55
2.2.3	Real time quantitative PCR.....	57
2.2.4	Serum NUCB2/Nesfatin-1 levels.....	61
2.3	Results.....	62
2.3.1	NUCB2/nesfatin-1 IR in the rat stomach.....	62
2.3.2	NUCB2/nesfatin-1 IR in the rat duodenum.....	64
2.3.3	Co-localization of NUCB2/nesfatin-1 and Chromogranin A (CgA) IR in the rat duodenum.....	66
2.3.4	NUCB2/nesfatin-1 IR in the rat pancreas.....	68
2.3.5	Co-localization of NUCB2/nesfatin-1 and insulin IR in the rat pancreas.....	70
2.3.6	Developmental expression of NUCB2 mRNA in the rat gastroenteropancreatic tissues.....	75
2.3.7	Serum NUCB2/nesfatin-1 levels during development.....	77
2.4	Discussion.....	79
2.5	Conclusions.....	83
	Transition.....	84
CHAPTER 3 GHRELIN, GHRELIN-O-ACYL TRANSFERASE, NUCLEOBINDIN- 2/NESFATIN-1 AND PROHORMONE CONVERTASES IN THE PANCREATIC ISLETS OF SPRAGUE DAWLEY RATS DURING DEVELOPMENT.....		85
3.1	Introduction.....	85
3.2	Material and Methods.....	89
3.2.1	Animals.....	89
3.2.2	Immunohistochemistry.....	89
3.2.3	Real Time Quantitative PCR.....	90

3.3	Results.....	92
3.3.1	Ghrelin and GOAT Immunoreactivity in the Rat Pancreas.....	92
3.3.2	NUCB2/nesfatin-1, PC1/3 and PC2 Immunoreactivity in the Rat Pancreas.....	94
3.3.3	Developmental Expression of GOAT mRNA in the Rat Pancreas.....	97
3.4	Discussion.....	99
3.5	Conclusions.....	102
	Transition.....	103
CHAPTER 4 NUTRIENTS DIFFERENTIALLY REGULATE NUCLEOBINDIN-2/NESFATIN-1 <i>IN VIVO</i> IN CULTURED STOMACH GHRELINOMA (MGN3-1) AND <i>IN VIVO</i> IN MALE MICE.....		105
4.1	Introduction.....	105
4.2	Material and Methods.....	108
4.2.1	Ethics Statement.....	108
4.2.2	<i>In Vitro</i> Studies.....	108
4.2.3	<i>In Vivo</i> Studies.....	109
4.2.4	Total RNA Extraction and cDNA Synthesis.....	110
4.2.5	RT-PCR and Quantitative Real Time-PCR.....	110
4.2.6	Immunocytochemistry and Microscopy.....	113
4.2.7	Western Blot Analysis, Immunohistochemistry and Fluorescence Microscopy.....	115
4.2.8	Nesfatin-1/NUCB2 Levels in Serum and Media.....	117
4.2.9	NUCB2/Nesfatin-1 Levels in Serum and Media and Total Ghrelin levels in media.....	117
4.2.10	Statistical Analysis.....	118
4.3	Results.....	119

4.3.1	NUCB2, PC 1/3 and PC 2 mRNAs are expressed in MGN3-1 cells and NUCB2 mRNA is expressed in the stomach, liver, small intestine and large intestine of male mice.....	119
4.3.2	MGN3-1 cells are immunopositive for ghrelin, NUCB2/nesfatin-1, PC1/3 and PC2.....	122
4.3.3	NUCB2 protein expression in large intestine, small intestine and liver from male mice.....	125
4.3.4	Effects of glucose and L-Tryptophan on NUCB2 mRNA expression in, and NUCB2/nesfatin-1 secretion from MGN3-1 cells.....	128
4.3.5	Effect of linolenic acid, octanoic acid and oleic acid on NUCB2 mRNA expression in, and NUCB2/nesfatin-1 secretion from MGN3-1 cells.....	131
4.3.6	Effect of L-tryptophan, linolenic acid, octanoic acid and oleic acid independently on ghrelin mRNA expression in, and total ghrelin secretion from MGN3-1 cells.....	134
4.3.7	Chronic effects of nutrients on NUCB2 mRNA expression and serum NUCB2/nesfatin-1 in mice.....	138
4.3.8	Acute effects of nutrients on NUCB2 mRNA expression, blood glucose and serum NUCB2/nesfatin-1 in mice.....	145
4.4	Discussion.....	150
4.5	Conclusion.....	156
	Transition.....	157
	CHAPTER 5 PRELIMINARY CHARACTERIZATION OF NUCLEOBINDIN-2 KNOCKOUT MICE: SEXUALLY DIMORPHIC DEFECTS IN WHOLE BODY ENERGY HOMEOSTASIS, GLUCOSE TOLERANCE AND INSULIN SECRETION.....	158
5.1	Introduction.....	158

5.2	Materials and Methods.....	160
5.2.1	Generation of the NKO mice.....	160
5.2.2	Genotyping.....	163
5.2.3	Western Blot Analysis.....	163
5.2.4	Immunohistochemistry.....	166
5.2.5	Weekly Body Weight and Food Intake Measurement.....	167
5.2.6	In Vitro Effects on Glucose Stimulated Insulin Secretion (GSIS) from Isolated Islets.....	168
5.2.7	Assessment of Whole-Body Energy Homeostasis Using Comprehensive Laboratory Animals Monitoring System (CLAMS).....	170
5.2.8	Intraperitoneal Glucose Tolerance Test (IPGTT).....	171
5.2.9	Insulin Tolerance Test (ITT).....	172
5.2.10	Absolute Terminal Organ/Tissue Weight.....	173
5.2.11	Serum Insulin, Glucagon, Ghrelin and Leptin Levels.....	173
5.2.12	Statistical Software.....	174
5.3	Results.....	175
5.3.1	Confirmation of NUCB2 Gene Disruption in NKO Male and Female Mice.....	175
5.3.2	Loss of NUCB2/nesfatin-1 protein expression in the Liver, Stomach, Duodenum, Pancreas from NKO Male and Female Mice.....	178
5.3.3	Insulin producing β -cells are immunonegative for NUCB2/nesfatin-1 but Not for Insulin in NKO Male and Female Pancreatic Islets.....	184
5.3.4	Body weight of NKO Male and Female Mice.....	186
5.3.5	Food Intake of NKO Male and Female Mice.....	189

5.3.6	GSIS on Pancreatic Islets Isolated from Female Wildtype and NKO Mice.....	192
5.3.7	Organ/Tissue Weight of NKO Male and Female Mice.....	194
5.3.8	Whole-Body Energy Homeostasis in NKO Male Mice Using CLAMS.....	197
5.3.9	Blood Glucose and Insulin Levels in NKO Male and Female Mice during an IPGTT.....	199
5.3.10	ITT and Blood Glucose Levels in NKO Male and Female Mice.....	204
5.3.11	Serum Insulin, Glucagon, Ghrelin and Leptin in NKO Male and Female Mice.....	207
5.4	Discussion.....	210
5.6	Limitations of the Study and Reasons for the Lack of Complete Characterization..	217
5.7	Ongoing Studies on NKO Mice Characterization and Future Directions.....	219
	Transition.....	220
	CHAPTER 6 GENERAL DISCUSSION.....	221
6.1	Contribution 1: Tissue Specific Expression of NUCB2/Nesfatin-1-PCs, and Ghrelin- GOAT – Developmental Perspectives.....	221
6.2	Contribution 2: MGN3 Cells as a Tool to Study Regulation of NUCB2/Nesfatin-1.....	222
6.3	Contribution 3: NUCB2/Nesfatin-1 in the Small Intestine.....	223
6.4	Contribution 4: Nutrient Regulation of NUCB2/Nesfatin-1.....	223
6.5	Contribution 5: Is NUCB2/Nesfatin-1 Critical for Energy Homeostasis?.....	224
6.6	Nesfatin-1 and the Neuroendocrine Regulation of Energy Balance.....	227
6.7	Limitations of this Research.....	229
6.7.1	Antibody Specificity.....	229
6.7.2	Gender Specific Expression of NUCB2/Nesfatin-1.....	229

6.7.3	Lack of Protein Determination.....	230
6.7.4	NKO = NUCB2 knockout or Nesfatin-1 knockout?.....	230
6.8	Ongoing Research and Future Directions.....	231
6.9	Conclusions.....	233
APPENDIX.....		234
REFERENCES.....		237

LIST OF TABLES

Table 2.1. Primers used for quantitative real-time PCR of NUCB2 cDNA from embryonic and prenatal SD rat tissue.....	60
Table 4.1. Sequences of forward and reverse primers, and the conditions employed in PCR and qRT-PCR analyses of the expression of mRNAs of interest.....	112
Table 4.2. Antibodies used for immunofluorescence microscopy.....	114
Table 6.1. Preliminary Characterization of NKO Male and Female Mice.....	226

LIST OF FIGURES

Figure 1.1 Evolutionary Relationships of NUCB1 and NUCB2 Sequences in Vertebrates.....	12
Figure 1.2 Nesfatin-1 is an Emerging Multifunctional Protein.....	29
Figure 1.3 An Overview of Ghrelin Synthesis and Secretion.....	33
Figure 2.1 NUCB2/nesfatin-1 IR in the rat stomach.....	63
Figure 2.2 NUCB2/nesfatin-1 IR in the rat duodenum.....	65
Figure 2.3 Co-localization of NUCB2/nesfatin-1 and Chromogranin A (CgA) IR in the rat duodenum.....	67
Figure 2.4 NUCB2/nesfatin-1 IR in the rat pancreas.....	69
Figure 2.5 Co-localization of NUCB2/nesfatin-1 and insulin IR in the rat pancreas.....	71
Figure 2.6 Co-localization of NUCB2/nesfatin-1 and insulin IR in the rat pancreas.....	73
Figure 2.7 Developmental expression of NUCB2 mRNA in the rat gastroenteropancreatic tissues.....	76
Figure 2.8 Serum NUCB2/nesfatin-1 levels during development.....	78
Figure 3.1 Co-localization of Ghrelin and GOAT in the Pancreatic Islets.....	93
Figure 3.2 Co-localization of NUCB2/nesfatin-1 and PC 1/3 in the Pancreatic Islets.....	95
Figure 3.3 Localization of NUCB2/nesfatin-1 and PC 2 in the Pancreatic Islets.....	96
Figure 3.4 GOAT mRNA levels at different development stages.....	98
Figure 4.1 NUCB2, PC 1/3 and PC 2 mRNAs are expressed in MGN3-1 cells and NUCB2 mRNA is expressed in the stomach, liver, small intestine and large intestine of male mice.....	120
Figure 4.2 MGN3-1 cells are immunopositive for ghrelin, NUCB2/nesfatin-1, PC1/3 and PC2.....	123
Figure 4.3 MGN3-1 cells are immunopositive for ghrelin, NUCB2/nesfatin-1, PC1/3 and PC2.....	124

Figure 4.4 NUCB2 protein expression in large intestine, small intestine and liver from male mice.....	126
Figure 4.5 Effects of glucose and L-Tryptophan on NUCB2 mRNA expression in, and NUCB2/nesfatin-1 secretion from MGN3-1 cells.....	129
Figure 4.6 Effect of linolenic acid, octanoic acid and oleic acid on NUCB2 mRNA expression in, and NUCB2/nesfatin-1 secretion from MGN3-1 cells.....	132
Figure 4.7 Effect of L-tryptophan, linolenic acid, octanoic acid and oleic acid independently on ghrelin mRNA expression in, and total ghrelin secretion from MGN3-1 cells.....	136
Figure 4.8 Chronic effects of nutrients on NUCB2 mRNA expression in mice.....	141
Figure 4.9 Chronic effects of nutrients on serum NUCB2/nesfatin-1 in mice.....	143
Figure 4.10 Acute effects of nutrients on NUCB2 mRNA expression NUCB2/nesfatin-1 in mice.....	146
Figure 4.11 Acute effects of nutrients on blood glucose and serum NUCB2/nesfatin-1 in mice.....	148
Supporting Figure S4.1 Ghrelin mRNA Expression (A) and Total Ghrelin Secretion (B) from MGN3-1 Cells Incubated for 1 Hour with Different Concentrations of Glucose (5.6 mM, 25 mM, 50 mM and 100 mM).....	135
Supporting Figure S4.2 Weekly Body Weight (A), Blood Glucose (B) and Food Intake to Body Weight Ratio (C) on Mice Fed Chronically on Various Nutrient Diets for 17 Weeks.....	139
Figure 5.1 Creation of the NUCB2 KO Model.....	162
Figure 5.2 Confirmation of NUCB2 Gene Presence in WT Male and Female Mice.....	176
Figure 5.3 Confirmation of NUCB2 Gene Disruption in NKO Male and Female Mice.....	177
Figure 5.4 Western Blot Display the Loss of NUCB2 Protein Expression in the Liver from NKO Male and Female Mice.....	179
Figure 5.5 Western Blot Display the Loss of NUCB2 Protein Expression in the Stomach from NKO Male and Female Mice.....	180
Figure 5.6 Western Blot Display the Loss of NUCB2 Protein Expression in the Duodenum from NKO Male and Female Mice.....	181

Figure 5.7 Western Blot Display the Loss of NUCB2 Protein Expression in the Pancreas from NKO Male and Female Mice.....	182
Figure 5.8 Insulin producing β -cells are immunonegative for NUCB2/nesfatin-1 but Not for Insulin in NKO Male and Female Pancreatic Islets.....	185
Figure 5.9 Body Weight of NKO and WT Mice fed <i>Ad Libitum</i> on Regular Chow.....	187
Figure 5.10 Body Weight of NKO and WT Mice fed <i>Ad Libitum</i> on 10% and 45% kcal Fat Diet.....	188
Figure 5.11 Food Intake of NKO Mice and WT Mice fed <i>Ad Libitum</i> on Regular Chow.....	190
Figure 5.12 Food Intake of NKO and WT Mice fed <i>Ad Libitum</i> on 10% and 45% kcal Fat Diet.....	191
Figure 5.13 GSIS on Pancreatic Islets Isolated from Wildtype (C57BL/6) and NKO Female Mice.....	193
Figure 5.14 Organ/tissue Weight of WT and NKO Male Mice.....	195
Figure 5.15 Organ/tissue Weight of WT and NKO Female Mice.....	196
Figure 5.16 Whole-Body Energy Homeostasis in NKO Male Mice Using CLAMS.....	198
Figure 5.17 IPGTT in NKO and WT Male Mice fed <i>Ad Libitum</i> on Regular Chow.....	200
Figure 5.18 IPGTT in NKO and WT Female Mice fed <i>Ad Libitum</i> on Regular Chow.....	201
Figure 5.19 IPGTT in NKO and WT Mice fed <i>Ad Libitum</i> on 10% and 45% kcal Fat Diet.....	202
Figure 5.20 ITT in NKO and WT Mice fed <i>Ad Libitum</i> on Regular Chow.....	205
Figure 5.21 ITT in NKO and WT Mice fed <i>Ad Libitum</i> on 10% and 45% kcal Fat Diet.....	206
Figure 5.22 Serum Protein Levels in NKO and WT (C57BL/6) Mice fed <i>Ad Libitum</i> on Regular Chow.....	208
Figure 5.23 Serum Protein Levels in NKO and WT (129Sv) Mice fed <i>Ad Libitum</i> on Regular Chow.....	209
Supporting Figure S5.1 Western Blot Display the Attenuation of Preproghrelin Protein Expression in the Stomach from NKO Male and Female Mice.....	183

Figure 6.1 Summary of Thesis Findings.....	228
Figure A GPR3, GPR6 and GPR12 mRNAs are expressed in the stomach, liver, pancreas of male mice.....	234
Figure B Co-localization of GPR12 and insulin IR in the mouse pancreas.....	235
Figure C Localization of GPR12 and glucagon IR in the mouse pancreas.....	236

LIST OF ABBREVIATIONS

ARC.....	arcuate nucleus
as-MON.....	antisense morpholino oligonucleotide
ATCC.....	American type culture collection
AUC.....	area under the curve
BAT.....	brown adipose tissue
CCK.....	cholecystokinin
CgA.....	chromogranin A
CLAMS.....	comprehensive laboratory animal monitoring system
CRH.....	corticotropin-releasing hormone
DAPI.....	4', 6-diamidino-2-phenylindole
DIO.....	diet induced obese
DMN.....	dorso-medial nucleus
DMNV.....	dorsal motor nucleus of vagus
DON.....	deoxynivalenol
dsDNA.....	double stranded DNA
DVC.....	dorsal vagal complex
ELISA.....	enzyme-linked immunosorbent assay
EW.....	edinger westphal
FMH.....	fluoromethyl histidine
FSH.....	follicle-stimulating hormone
G6PC.....	glucose-6-phosphatase
GH.....	growth hormone
GHS.....	growth hormone secretagogues
GHS-R.....	growth hormone secretagogue receptor
GI.....	gastrointestinal
GLP-1.....	glucagon-like peptide-1
GOAT.....	ghrelin-O-acyl transferase
GPCR.....	G-protein coupled receptor
GSIS.....	glucose stimulated insulin secretion
HBSS.....	Hank's balanced salt solution
Hcrt.....	hypocretin
HFD.....	high-fat diet
HPLC.....	high protein liquid chromatography
iBAT.....	interscapular brown adipose tissue
ICV.....	Intracerebroventricular
IL.....	interleukin
INS.....	insulinoma
IP.....	intraperitoneal
IPGTT.....	intraperitoneal glucose tolerance test
IR.....	immunoreactivity
ITT.....	insulin tolerance test
Kiss1r.....	kisspeptin receptor
KRB.....	Krebs-ringer bicarbonate buffer
LC.....	locus coeruleus
LH.....	lateral hypothalamus

LH.....	luteinizing hormone
LPN.....	lateral parabrachial nucleus
LTR.....	long terminal repeats
MBOAT.....	membrane-bound O-acyl transferase
MGN3-1.....	mouse ghrelinoma 3-1
MT.....	mutant primers
NEO.....	neomycin phosphotransferase
NKO.....	nucleobindin2/nesfatin-1 knockout
NLT.....	nucleus lateralis tuberis
NPY.....	neuropeptide Y
NPY/AgRP.....	neuropeptide Y and Agouti-related peptide
NTS.....	nucleus tractus solitarius
NUCB1.....	nucleobindin-1
NUCB2.....	nucleobindin-2
OD.....	optical density
OTKO.....	oxytocin KO
PBS.....	phosphate buffered saline
PC 1/3.....	prohormone convertases 1/3
PC 2.....	prohormone convertases 2
PCOS.....	polycystic ovary syndrome
PCR.....	polymerase chain reaction
PEPCK.....	phosphoenolpyruvate carboxykinase
PI.....	pars intermedia
POMC.....	pro-opiomelanocortin
POMC/CART.....	pro-opiomelanocortin and cocaine- and amphetamine-related transcript
PVN.....	paraventricular nucleus
RACE.....	rapid amplification of cDNA ends
RER.....	respiratory exchange ratio
RIA.....	radioimmunoassay
RPD.....	rostral pars distalis
RT-PCR.....	reverse transcription-PCR
SD.....	Sprague Dawley
SFO.....	subfornical organ
SON.....	supraoptic nucleus
STZ.....	streptozotocin
TRH.....	thyrotropin-releasing hormone
TSNO.....	Tsumura Suzuki non obese mice
TSOD.....	Tsumura Suzuki obese diabetes
V1aRKO.....	vasopression V1a receptor knockout
VLM.....	ventrolateral medulla
VMN.....	ventro-medial
WT.....	wildtype
ZI.....	zona incerta

Chapter 1

Introduction

1.1 The Nervous and Hormonal Systems: Integrators of Homeostasis

The emergence of multicellular organisms involves, in large part, the communication of multiple signalling systems (Stoka, 1999). These systems are organized in a structured network to carry out several signals from one cell to another, either between or within multiple environmental compartments. Communication on a cellular level is defined as chemical signalling, sensing, and response, which is central to evolutionary history (Stoka, 1999). Chemical signals are in the form of information molecules which include hormones, bioregulators, receptors, transducers, effectors and secondary messengers (Stoka, 1999). As we know, vertebrates being multicellular, are made up of several tissues and organs that constitute the circulatory, respiratory, digestive, musculoskeletal and nervous systems. To function properly, these organs systems must communicate with each other to ensure that the physiological homeostasis is maintained (Nussey and Saffron, 2001). Two systems ensure that communication is achieved between the organs systems: the nervous and the hormonal (neuroendocrine) system (Nussey and Saffron, 2001).

The nervous system allows rapid transmission of information to several regions of the body within fractions of seconds. Information is communicated from neurons to other neurons or peripheral tissues through electrical signals along axons. These signals stimulate the release of chemical neurotransmitters into the synaptic cleft between pre- and post-synaptic neurons (Hiller-Sturmhöfel and Bartke, 1999). Neurotransmitters bind to receptors on target cells to mediate their signal via intracellular signalling cascades (Hiller-Sturmhöfel and Bartke, 1999). In addition to neurotransmitters, neurons and cells also communicate via chemical messengers that

are derived from fatty acids, cholesterol and amino acids. The most diverse group of chemical messengers are comprised of linked amino-acids, known as peptides (Nussey and Saffron, 2001). To date, there are several different types of peptide hormones discovered. Peptide hormones can range in size from 3 to over 200 amino acids. The hormones are transported via the blood to their target cells. Some hormones have few target cells whereas other hormones have numerous target cells throughout the body (Nussey and Saffron, 2001). Conversely, the hormone system relies on the production and release of these peptide hormones from various organ systems to bind to their receptors inducing a chemical signal either by endocrine, paracrine, autocrine and/or intracrine mechanisms (Nussey and Saffron, 2001). The interaction between the hormone and their respective receptors triggers a cascade of biochemical reactions implementing the cell's regulatory action. Hence, both communication systems complement each other to respond to changes in the internal and external environments (Nussey and Saffron, 2001).

1.1.1 Hormone synthesis

Most hormones require the transcription of a single gene, although there are some hormones that consist of multiple subunits that are derived from several genes. The initial RNA undergoes modification to form the messenger RNA. Introns are excised and the 3' and 5' of the RNA are altered (Nussey and Saffron, 2001). The mature RNA is used as a template for the assembly of amino acids via the transfer RNA on the endoplasmic reticulum. Inside the endoplasmic reticulum, the protein translated from mRNA, moves into the golgi apparatus by fission. Secretory granules are formed from the budding of the golgi apparatus (Nussey and Saffron, 2001). These prohormones are stored and secreted from the secretory granules within the cell. Peptidases cleave the prohormones into biologically active hormones prior to their release into the cytoplasm (Nussey and Saffron, 2001).

1.1.2 Mechanism of Hormonal Action

Hormones are involved in a variety of functions, some of which include, reproduction, sexual differentiation, development and growth, regulation of metabolism and nutrient supply (Hiller-Sturmhöfel and Bartke, 1999). A single hormone may induce one or multiple functions and each function may be modulated by several hormones. Hormones exist in several classes: steroids, amino acid derivatives, polypeptides and proteins. Mostly the hormone's class define the basis of their putative action. The hormone classes differ in the molecular structure and chemical properties. As of result of structural differences, their mechanisms of action are diverse (Hiller-Sturmhöfel and Bartke, 1999). Steroids, mainly produced from the adrenal cortex and gonads, have a molecular structure similar to cholesterol. These molecules can enter into the cells and bind to their receptors present in the cytoplasm or in the nucleus. The hormone-receptor complex binds to the DNA regulating the activation of genes specific to the hormone bound (Hiller-Sturmhöfel and Bartke, 1999). Amino acid derivatives mediate their action similar to that of steroids, which are mainly secreted from the thyroid gland and the adrenal medulla. In contrast, proteins and polypeptides are chains of amino acids found primarily in the hypothalamus, pituitary gland and several peripheral organs (Hiller-Sturmhöfel and Bartke, 1999). They are usually derived as inactive prohormones which are then cleaved into one or more active proteins. Due to their complex structure, they are incapable of entering the cells and thereby interact with receptors on the cell surface to initiate their cell specific function (Hiller-Sturmhöfel and Bartke, 1999).

1.1.3 Hormones Involved in the Regulation of Energy Balance

To maintain the body's homeostasis and to respond to changes in the environment, it is vital that hormone production and secretion be tightly controlled (Murphy and Bloom, 2006).

Homeostasis is a process that is tightly regulated in order to maintain constant energy reserves over a long period of time. In order to maintain a constant energy balance, energy intake, determined by feeding behavior, thermogenesis and energy expenditure must be regulated. These components of energy balance are modulated by two interconnected, yet separate systems (Murphy and Bloom, 2006). The first system is identified as a short-term system that controls the beginning and termination of ingestion depending on the quality and quantity of nutrient availability. Neural and hormonal signals from the peripheral sources convey their information on the nutritional contents in the gastrointestinal tract. The second system is a long term system that works to maintain stable energy reserves and constant body weight (Murphy and Bloom, 2006). During feeding, excess energy consumed is stored for later use in the form of fats and carbohydrates. Both systems work together to balance the energy reserves in response to the changing environmental conditions (Murphy and Bloom, 2006). Gastrointestinal hormones are modulated as a result of short term regulation of hunger and satiety, which tend to have less influence on food intake and body weight which are controlled by long term regulation. Therefore, the body relies predominantly on the long-term system, which includes hormones such as leptin secreted by adipose tissue and insulin from the pancreas to maintain a constant energy balance (Murphy and Bloom, 2006).

1.1.4 Neuroendocrine Control of Feeding

The gastrointestinal tract secretes several hormones for different physiological actions (Schwartz et al., 2000, Boguszewski and Van der Lely, 2015). Appetite, satiety regulation, gastrointestinal tract functional, nutrient digestion, absorption, distribution and energy homeostasis are regulated by a complex system of central and peripheral effects that interact in order to modulate nutrient ingestion (Schwartz et al., 2000, Boguszewski and Van der Lely,

2015). Central control of gut hormones are mainly due to actions of two distinct neuronal populations present within the arcuate nucleus (ARC) of the hypothalamus (Schwartz et al., 2000, Boguszewski and Van der Lely, 2015). These neuron populations are identified as ‘first order neurons’ because of their contact with circulation and are key targets of appetite regulatory factors, serving as the central neuronal processors of orexigenic (appetite stimulatory) and anorexigenic (appetite inhibitory) signals. The first neuron population consists of anorexigenic neurons that express pro-opiomelanocortin and cocaine- and amphetamine-related transcripts (POMC/CART). In contrast, the second orexigenic neurons express neuropeptide Y and agouti-related peptide (NPY/AgRP). These neurons project on to ‘second-order neurons’ residing in other regions, which include the paraventricular nucleus (PVN), dorso-medial nucleus (DMN), ventro-medial nucleus (VMN) and the lateral hypothalamus (LH) (Schwartz et al., 2000, Boguszewski and Van der Lely, 2015). This peripheral information is then integrated with behavioral, hormonal and nutritional inputs coming from the periphery and higher cortical centers. The orexigenic and anorexigenic neuron groups are interconnected at several regions of the central nervous system (Schwartz et al., 2000). Activation of one neuronal group leads to the activation of other neurons via neural firing that modulates the transcription and translation of multiple genes involved in regulating energy balance. In addition, the blood brain barrier (BBB) is important for the gastrointestinal-brain axis, by modulating hormone transportation (Schwartz et al., 2000).

The gastrointestinal tract secretes many anorexigenic factors, which include cholecystokinin (CCK), peptide YY (PYY), oxyntomodulin (OXM), gastric inhibitory polypeptide (GIP) and glucagon-like peptide 1 (GLP-1). The stomach mucosa secretes ghrelin and nucleobindin-2/nesfatin-1 (NUCB2/nesfatin-1) that are mainly involved in regulating food

intake and increasing energy expenditure (Schwartz et al., 2000, Boguszewski and Van der Lely, 2015). Due to the scope of our research, this chapter will only focus on NUCB2/nesfatin-1 and ghrelin, that aid in playing major roles in feeding and energy homeostasis.

1.2 Nucleobindins

Nucleobindins are a class of multidomain Ca^{2+} binding proteins that interact with nucleic acids and different regulatory proteins, thereby playing an important role in various signaling pathways. Initially, nucleobindin was identified as a transcription factor as it demonstrated the ability to bind to DNA fragments *in vitro*, thus the name nucleobindin (Miura et al., 1992). To date, two nucleobindins, nucleobindin-1 (NUCB1) and nucleobindin-2 (NUCB2) (Lin et al., 1998, Miura et al., 1992) have been identified. Although two separate and unlinked genes encode for these proteins, human NUCB1 and NUCB2 exhibit 62% amino acid sequence identity (Valencia et al., 2008). The first focus of this chapter is to summarize the most recent findings on the functional significance of NUCB2 and its encoded protein, nesfatin-1.

1.2.1 Discovery of Nucleobindin-2 and Nesfatin-1

NUCB2 belongs to the EF-hand family of calcium-binding proteins (Moncrief et al., 1990, Lee et al., 1991, Nakayama et al., 1992). These proteins share a structural motif of calcium binding domain known as the EF-hand (Moncrief et al., 1990, Lee et al., 1991, Nakayama et al., 1992). The name EF-hand was coined by Kretsinger and Nockolds (Kretsinger et al., 1973) to visually describe the calcium-binding motif they observed in parvalbumin, a calcium-binding protein (Henrotte et al., 1952, Celio et al., 1981). Several proteins with the EF-hand motif have been extensively characterized and were shown to undergo several genetic processes including splicing, translocation, fusion and gene replication. Phylogenetic analyses were conducted to determine the primary ancestor of these proteins. This approach helps to understand the origin of the protein and how it changed during evolution. From recent discoveries, one protein that demonstrated rooted phylogeny from the EF-hand domain is nucleobindin-2/NEFA (Nucleic Acid/DNA binding/EF-hand/acidic amino acid rich region) (Nakayama et al., 1992).

Phylogenetic and sequence analysis has shown that through a series of genetic modifications, such as duplication and fusion, NEFA arised from the UR/CTER EF-hand domains (Nakayama et al., 1992). This common domain led to the formation of a four-domain precursor ancestor. With ultimate steps of domain deletion, duplication and fusion, two sequences were fused together leading to NEFA-N and NEFA-C (Nakayama et al., 1992). A signal peptide is present at the N-terminal region of NEFA-N, and two functional EF-hand calcium binding domains are present at the N-terminal region of NEFA-C (Nakayama et al., 1992). With subsequent divergence of this precursor protein sequence with other domains such as the heptad repeat domain, a putative hydrophilic DNA-binding region and a leucine zipper region resulted in the genetic evolution of NEFA. Gene duplication of NEFA led to the formation of nucleobindin-2 and NEFA-like proteins (Nakayama et al., 1992).

The initial discovery of nucleobindin came from research conducted in lupus-prone MRL/l mice. These mice are known to secrete large amounts of antibodies targeted against single stranded and double stranded DNA (Theofilopoulos et al., 1985). A cell line (KML1-7) that produced a soluble protein which induced the formation of antibodies against ss and ds DNA in-vivo and in-vitro was established from the MRL/l mice (Kanai et al., 1986, Kanai et al., 1990). From this cell line, a 55-kDa protein was purified (Kanai et al., 1992) and the gene encoding this protein was later cloned (Miura et al., 1992). Despite the fact that this protein is secreted and consists of a signal peptide, its capability to bind to DNA resulted in the name, nucleobindin. Since nucleobindin is found in the sera of MRL/l mice, it has a possible role in the development of autoimmune disorders of MRL/l mice (Kanai et al., 1993).

While studying the cDNA libraries of human acute lymphoblastic leukemia KM3 cell line for screening common acute lymphoblastic leukemia antigens, a protein sequence that was

identical to nucleobindin was identified, suggesting it to be an isoform of nucleobindin (Barnikol-Watanabe et al., 1994). This protein was produced in the plasma membrane and cytosol, and was secreted into the culture medium. It was found to have a molecular mass of 55 KDa protein band determined by SDS-PAGE (Barnikol-Watanabe et al., 1994). Structural characteristics depicted that it consisted of a nuclear localization signal with an amino acid region present between the two EF-hand motifs, demonstrating to have sequence similarity to NEFA at 61.56%. As a result of its sequence similarity to NEFA it was instead named as nucleobindin-2 (Karabinos et al., 1996). While investigating small proteins in the mineral phase of the bone tissue led to the discovery of nucleobindin in some other organisms. A 63-KDa protein from the mineralized matrix of the bovine bone was characterized (Wendel et al., 1995). This protein shared structural similarity with mouse and human nucleobindin, where the presence of N-terminal signal sequence, two EF-hand motifs, a heptad repeat-leucine zipper regions and a bipartite-nuclear localization signal was observed (Wendel et al., 1995).

The gene organization of nucleobindin is conserved across many species. Some of the organisms have untranslated regions at both their 3' and 5' ends with more than 11 exons in their gene (Guo et al., 2007). The size of the nucleobindin gene in every organism determines the number of the introns in these genes. With an increase in the gene size, an increase in the number of introns is observed (Aradhyam et al., 2010). Despite differences observed in the C-terminal region of the gene and incidence of exon shuffling, the primary structure of the nucleobindin gene is highly conserved across various species (Aradhyam et al., 2010). Differences in the gene structure despite the presence of conserved sites may raise the possibility of species- and tissue-specific functions as a consequence of the evolution of this gene. Analysis of the amino acid sequence suggests a clear difference of this gene and its processing in organisms (Kanuru et al.,

2009, Miura et al., 1994). More complex organisms tend to have multiple isoforms of nucleobindin whereas simple organisms express a single polypeptide chain. The degree of conservation is greater in the highly evolved organisms in comparison to the less complex organisms. Differences in the function and expression of these nucleobindin isoforms are yet to be determined (Kanuru et al., 2009, Miura et al., 1994).

In evolution, a single ancestral domain undergoes several genetic modifications in time, giving rise to multiple genes implicated in various functions. It is believed that NUCB2 and nucleobindin-1 (NUCB1) arose from a single EF-hand domain (Karabinos et al., 1996). Both NUCB1 and NUCB2 belong to a homologous gene family (Miura et al., 1992). The NUCB2 gene structure is highly conserved across various species. The NUCB2 gene in rats shares a high percentage similarity to NUCB2 of other species including: 87.4% homology to humans (*Homo sapiens*) and 95.7% to mice (*Mus musculus*) (Oh-I et al., 2006). In cyprinids, there is a high conservation of NUCB2 gene between goldfish (*Carassius auratus*) and zebrafish (*Danio rerio*) (Gonzalez et al., 2010). A broad phylogenetic analysis of NUCB2 gene sequence identified several isoforms of NUCB2 within one species, which include NUCB2A and NUCB2B. The differences in these isoforms are attributed mainly to the number of exons and introns present in the gene (Gonzalez et al., 2010). For instance, NUCB2A and NUCB2B gene sequences in zebrafish (*Danio rerio*), medaka (*Oryzias latipes*) and stickleback (*Gasterosteus aculeatus*) are composed of 13 exons by 12 introns (Gonzalez et al., 2010). In contrast, as a result of the deletion of exon 1 in both fugu (*Takifugu rubripes*) and green pufferfish (*Tetraodon nigroviridis*), the genes are composed of 12 exons and 11 introns (Gonzalez et al., 2010). The presence of these isoforms in teleost fishes could be a result of independent tetraploidization, named 3R, identified as the third stage of genome replication (Christoffels et al., 2004, Jaillon et

al., 2004). The nesfatin-1 region of NUCB2A sequences in goldfish shares a high percentage homology with the NUCB2A isoform of teleosts which includes: 94% to zebrafish (*Danio rerio*), 91% to medaka (*Oryzias latipes*), 86% to stickleback (*Gasterosteus aculeatus*), 84% to green pufferfish (*Tetraodon nigroviridis*), and 83% to fugu (*Takifugu rubripes*) (Gonzalez et al., 2010). The nesfatin-1 region of NUCB2A sequences in goldfish shares a higher percentage similarity to NUCB2 gene in other species which includes: 64% to Western clawed frog (*Xenopus tropicalis*), 66% to chicken (*Gallus gallus*), 57% to mouse (*Mus musculus*), and 63% to humans (*Homo sapiens*) (Gonzalez et al., 2010). **Figure 1.1** is a phylogram showing evolutionary relationships of NUCB1 and NUCB2 sequences in vertebrates. Further elucidation of gene structure and function in individual species will be an important aspect of future nesfatin-1 research.

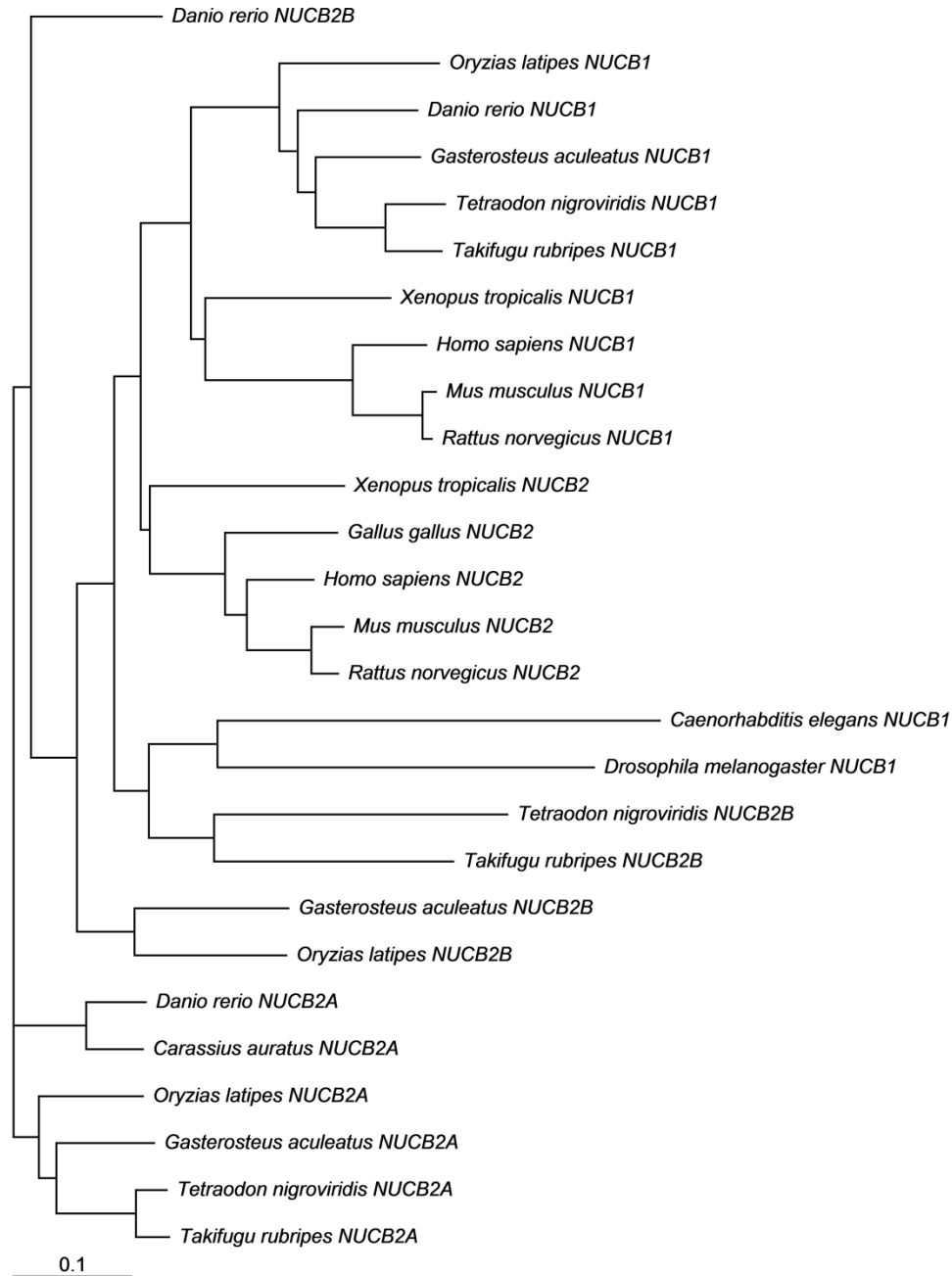


Figure 1.1 Evolutionary Relationships of NUCB1 and NUCB2 Sequences in Vertebrates

Figure 1.1. A phylogram showing relationships between NUCB1 and NUCB2 sequences among vertebrates. The details of sequences used to create this figure are listed in our previous publication Gonzalez et al., 2010. The phylogram is created using the program Treeview (<http://taxonomy.zoology.gla.ac.uk/rod/treeview.html>).

In 2006, Oh-I and colleagues identified a novel protein named nesfatin-1, which is encoded in NUCB2, and found in several hypothalamic and brainstem neurons of rats (Oh et al., 2006). Nesfatin-1 is the N-terminal fragment of NUCB2 and the name stands for the acronym NEFA/nucleobindin-2 Encoded Satiety- and Fat-Influencing protein-1 (Oh et al., 2006, Shimizu et al., 2009). Reports to date implicate a role for nesfatin-1 in inducing satiety [Oh et al., 2006, Shimizu et al., 2009, Maejima et al., 2009, Stengel et al., 2009a, Su et al., 2010, Atsuchi et al., 2010, Yosten et al., 2010, Goebel et al., 2010], development (Garcia-Galiano et al., 2010), regulation of blood glucose (Su et al., 2010), gonadotrope regulation (Su et al., 2010), gut motility (Stengel et al., 2009), stress mediation (Goebel et al., 2009), adipose differentiation (Ramanjaneya et al., 2010) and hypertension (Yosten et al., 2010). Prohormone convertases (PC 1/3 and PC 2) are the enzymes proposed to cleave NUCB2 precursor protein to nesfatin-1 (Oh et al., 2006, Lee et al., 1999). Upon cleavage of NUCB2 by PCs, 3 smaller proteins: nesfatin-1 (82 amino acids), nesfatin-2 (79 amino acids), and nesfatin-3 (231 amino acids) are expected to be produced (Oh et al., 2006). Recent study determined the protein expression of nesfatin-1 in PC 1/3 deficient patients (Catli et al., 2013). Congenital PC 1/3 deficiency is a very rare syndrome with abnormal prohormone processing, early-onset obesity, small intestinal dysfunction, impaired glucose homeostasis. These patients have low levels of nesfatin-1 protein in circulation suggesting that decreased levels of nesfatin-1 may be one of the contributing factor for the development of obesity (Catli et al., 2013).

The C-terminal fragments of NUCB2, nesfatin-2 and nesfatin-3 have no known biological effects in comparison to nesfatin-1 (Oh-I et al., 2006). The mid-segment of nesfatin-1 (M30) from amino acids 23 to 53 is identified as the bioactive core that induces the anorectic response. The M30 region of nesfatin-1 shows a great degree of sequence identity among the

nesfatin-1 encoded in both NUCB1 and NUCB2 (Gonzalez et al., 2010). It has been shown that intraperitoneal injections of M30 in *db/db*, *ob/ob* and diet-induced obese mice significantly decreases food intake (Shimizu et al., 2009). Also, recent studies on nesfatin-1 (30-59; M30) but not the N- and C- terminal fragment, showed that intracerebroventricular injection induced satiety in the dark phase with reduced meal number 4 hours post injection. These studies further support previous studies that nesfatin-1(30-59) is the active core of nesfatin-1 (1-82) that induces the satiety effect (Stengel et al., 2012a).

1.2.2 Tissue-Specific Expression of NUCB2/Nesfatin-1: Comparative Aspects

Nesfatin-1 is present in various regions of the brain and peripheral tissues that are involved in the regulation of feeding and appetite and it is been suggested that the neuronal effects of nesfatin-1 are mediated through a G-protein coupled receptor.

1.2.2.1 Region-Specific Expression of NUCB2/Nesfatin-1 in Mammals and Non-Mammals

1.2.2.1.1 Mammals

The broad distribution of NUCB2/nesfatin-1 in the hypothalamus and regions of the brainstem which are primarily involved in the regulation of food intake supports a crucial role for this protein in the maintenance of energy homeostasis. In mammals, NUCB2 is expressed in the rat brain, mainly in the hypothalamic paraventricular nucleus (PVN), arcuate nucleus (ARC), lateral hypothalamus (LHA), supraoptic nucleus (SON), and the zona incerta (ZI) of the thalamus (Oh et al., 2006). NUCB2/nesfatin-1 immunopositive cells are also localized in the brainstem of rats, in the nucleus tractus solitarius (NTS), Edinger Westphal (EW), dorsal motor nucleus of vagus (DMNV; Xia et al., 2012), and caudal raphe nuclei (Oh et al., 2006, Foo et al., 2008, Brailoiu et al., 2007, Geobel-Stengel et al., 2011). In addition, NUCB2/nesfatin-1 immunoreactivity was detected in cortical areas including piriform, insular, cingulate and somatomotor cortices, the limbic system including amygdaloid nuclei, hippocampus and septum, the basal ganglia, bed nucleus of the stria terminalis (Geobel-Stengel et al., 2011). Colocalization of NUCB2/nesfatin-1 with neuropeptide regulators of appetite, like proopiomelanocortin, cocaine- and amphetamine-regulated transcript, melanin concentrating hormone and neuropeptide Y (Brailoiu et al., 2007, Foo et al., 2008, Fort et al., 2008, Price et al., 2008) has been reported. In addition, co-immunostaining of NUCB2/nesfatin-1 was found with

vasopression, oxytocin, cocaine amphetamine regulated transcript and melanin concentrating hormone (Kohno et al., 2008). Histamine H1 receptor (H1-R) expression was co-immunoreactive with NUCB2/nesfatin-1 expression in the PVN of the hypothalamus (Gotch et al., 2013). Mature nesfatin-1 elution peak was obtained from the cerebrospinal fluid and rat hypothalamic extracts during high performance liquid chromatography (HPLC) (Oh et al., 2006). Studies have also shown that NUCB2 is found in the sympathetic and parasympathetic preganglion neurons in rats (Goebel et al., 2009). NUCB2/nesfatin-1 immunoreactivity was detected in the raphe nuclei, Edinger-Westphal nucleus, locus coeruleus (LC), lateral parabrachial nucleus, ventrolateral medulla (VLM) and dorsal vagal complex (Geobel-Stengel M et al., 2011). Nesfatin-1 is able to cross the blood-brain barrier without saturation, which suggests that peripherally administered or produced nesfatin-1 could reach the brain to elicit its central actions (Pan et al., 2007, Price et al., 2007). In addition to the brain, NUCB2/nesfatin-1-like immunoreactivity was found in the anterior pituitary gland of rats (Stengel et al., 2009a) and mouse (Chang et al., 2015). As many studies determine NUCB2 localization in the brain regions, researches have branched into determining their expression in domestic animals as well. The presence of NUCB2/nesfatin-1 neurons was also evident in the VLM, DVC, PVN, ARC and SON of pig brain, supporting previous studies. Study also reveals that these NUCB2 neurons are activated during deoxynivalenol (DON) intoxication in the pig (Gaige et al., 2013). DON is a major mycotoxin product from *Fusarium* species responsible for mycotoxicosis in many farm animals (Gaige et al., 2013).

NUCB2/nesfatin-1 is also found in several peripheral tissues. In the pancreas, NUCB2/nesfatin-1 is expressed in the insulin producing beta-cells of rats, mice and humans (Foo et al., 2010, Gonzalez et al., 2009, Stengal et al., 2009). However, NUCB2/nesfatin-1

immunoreactivity is not found in the glucagon producing alpha-cells (Foo et al., 2010, Gonzalez et al., 2009, Stengal et al., 2009), pancreatic polypeptide cells (Foo et al., 2010) and somatostatin producing D-cells (Foo et al., 2010). In the stomach, NUCB2/nesfatin-1 was found in the gastric X/A-like cells located in the lower and middle third region of the gastric mucosal glands (Zhang et al., 2010). In the periphery, decreased NUCB2 mRNA expression levels were also found in the gastric endocrine glands of rodents during fasting and increase in NUCB2 mRNA in the stomach (Stengel et al., 2009b). Similarly, NUCB2/nesfatin-1 positive enteroendocrine cells were also observed in the anterior part of the goldfish gastrointestinal tract (Gonzalez et al., 2010; Kerbel et al., 2012). NUCB2/nesfatin-1 expression is also observed in the adipose tissue of mouse and humans (Ramanjaneya et al., 2010). The expression of NUCB2 mRNA was highest in the subcutaneous adipocytes in both mice and humans (Ramanjaneya et al., 2010). During the differentiation of preadipocytes to adipocytes, NUCB2 mRNA and nesfatin-1 protein synthesis increases (Ramanjaneya et al., 2010). In rats NUCB2/nesfatin-1 expression was also observed in the liver, with moderate expression in the subcutaneous and visceral fat mass as well as the interscapular brown adipose tissue (iBAT) (Osaki et al., 2012). Weak expression of NUCB2/nesfatin-1 was found in the skeletal muscle (gastrocnemius) and fat tissue. In this study they found that a lesion in the ventromedial hypothalamus region of rats increased the expression of NUCB2/nesfatin-1 in the white adipose tissue (Osaki et al., 2012). NUCB2/nesfatin-1 was increased in the subcutaneous and visceral fat mass in comparison to the skeletal muscle mass (gastrocnemius) (Osaki et al., 2012).

1.2.2.1.2 Non-Mammals

In contrast to mammals, fish express two NUCB2 isoforms: NUCB2A and NUCB2B. Nesfatin-1 has been identified in zebrafish (Hatef et al., 2014, Gonzalez et al., 2012b, Kerbel et al., 2012, Lin et al., 2014), goldfish (Gonzalez et al., 2010, Kerbel et al., 2012) and Ya fish (Lin et al., 2014). NUCB2 in goldfish was found in the nucleus lateralis tuberis (NLT) (Gonzalez et al., 2010), the teleostean homologue of the mammalian arcuate nucleus (Cerdeira-Reverte et al., 2003, Peng et al., 1994, Kerbel et al., 2012). The NLT of goldfish is considered a key region of the brain that regulates food intake (Cerdeira-Reverte et al., 2003, Peng et al., 1994). Similarly, abundance of nesfatin-1 expression was also detected in the brain and olfactory bulbs of frogs, especially in the hypothalamic regions involved in the regulation of food intake (Senejani et al., 2014).

In zebrafish, both NUCB2A and NUCB2 mRNAs are most abundant in the liver, while less expression was found in other tissues including the brain and gut. NUCB2/nesfatin-1-like immunoreactivity was detected in the mucosal layer cells of zebrafish anterior gastrointestinal tract. NUCB2 mRNA expression is found in multiple tissues of goldfish as well, with highest expression in the liver, followed by pituitary, with lowest expression found in the muscle and gill (Gonzalez et al., 2010). Similarly, the Ya-fish NUCB2A mRNA expressed ubiquitously in various organs. Expression was found high in the hepatopancreas, hypothalamus, intestines, gonad, pituitary and kidney (Lin et al., 2014). NUCB2 mRNA was also detected in the olfactory bulbs, hypothalamus, telencephalon, midbrain and hindbrain, adipose tissue, ovary, eye, kidney, and midgut (Gonzalez et al., 2010). In agreement with this, most recent studies have identified NUCB2/nesfatin-1 immunoreactivity in the goldfish pituitary, and goldfish and zebrafish ovarian theca and/or follicular cells (Gonzalez et al., 2012b).

1.2.2.2 G-Protein Coupled Receptors (GPCRs) - potential receptors of nesfatin-1?

The identity of the nesfatin-1 receptor currently remains unknown. However, there are several lines of evidence that suggest that the neuronal effects of nesfatin-1 are mediated via a G-protein coupled receptor (GPCR) (Brailoiu et al., 2007, Iwasaki et al., 2009). Preliminary findings suggest that GPR3, GPR6 and/or GPR12 are potential receptors for nesfatin-1 (Mori et al., 2008, Osei-Hyiaman et al., 2011). Nesfatin-1 can cause an increase in the intracellular calcium concentrations in cultured hypothalamic neurons of rats, an effect that was attenuated by pertussis toxin, a calcium channel blocker (Brailoiu et al., 2007). It is suggested that nesfatin-1 interacts with the G-protein-coupled receptor causing an increase in the intracellular calcium concentration mediated via the N-type and L-type calcium channels (Brailoiu et al., 2007, Iwasaki et al., 2009). In the vagal afferent ganglion of mice, nesfatin-1 stimulates an influx of calcium ions through N-type channels present in these neurons (Iwasaki et al., 2009). Nesfatin-1 stimulates an influx of calcium ions mediated by the L-type calcium channels present in the insulin producing beta-cells (Nakata et al., 2011). Although the nesfatin-1 receptor remains unknown, it appears that the effects of nesfatin-1, at least on the neurons and the beta cells are elicited via a calcium mediated pathway.

1.2.3 Biological Actions of Nesfatin-1 in Mammals and Fish

Nesfatin-1 has multiple biological actions in rodents, which include stress modulation (Ueta et al., 2003), thermogenesis (Fan et al., 2005; Konczol et al., 2012), osteogenesis (Li et al., 2013), energy expenditure (Gonzalez et al., 2012a), development (Mohan et al., 2012), pregnancy (Garces et al., 2014), autonomic response (Maejima et al., 2013), visceral hypersensitivity (Jia et al., 2013), sleep regulation (Vas et al., 2013) and cardiac functions (Angelone et al., 2012, Brailoiu et al., 2013). The NUCB2 gene sequences in rodents and teleosts have been shown to be highly conserved (Gonzalez et al., 2010), which suggests that some functions of nesfatin-1 amongst these species are similar.

1.2.3.1 Nesfatin-1 Regulation of Feeding and Metabolism

1.2.3.1.1 Nesfatin-1 Mediated Inhibition of Feeding

Nesfatin-1-induced inhibition of feeding is a common function that has been characterized in both rodents and goldfish. NUCB2/nesfatin-1 is expressed in various hypothalamic regions and the brainstem of rodents that play a major role in the inhibition of feeding (Maejima et al., 2009). In mammals, nesfatin-1 is a meal-responsive hormone (Stengel et al., 2009a, Gonzalez et al., 2012a). The SON and PVN play a major role in appetite regulation (Balthasar et al., 2005, Horvath et al., 2006, Morton et al., 2006, Schwartz et al., 2000). In rodents, NUCB2 mRNA expression was decreased upon fasting in the hypothalamic neurons. Upon re-feeding, SON and PVN neurons were activated with an increase in NUCB2 mRNA expression (Garcio-Galiano et al., 2010, Kohno et al., 2008). In addition, the SON, PVN along with subfornical organ (SFO) are involved in body fluid regulation. A recent study has shown that the NUCB2 mRNA was increased 2 to 3 fold in the SFO, SON and PVN following a 48 hour water deprivation in a time dependent manner. This study suggested that NUCB2/nesfatin-1

is a critical peptide involved in dehydration-induced anorexia (Yoshimura et al., 2014). Also, a study on PVN expressing nesfatin-1 neurons, determined that insulin and glucose directly interact with and increase the cytosolic calcium concentrations in nesfatin-1 neurons in the PVN, thereby inducing satiety (Gantulga et al., 2012). There are many glucosensing neurons located in the hypothalamus that are involved in glucoprivic feeding and homeostatic control of blood glucose. Nesfatin-1 injection into the PVN, LHA, VMN of the hypothalamus of *ad libitum* fed rats during the dark phase excited most of the glucose-inhibited neurons and inhibited most of the glucose-excited neurons. This study suggested that nesfatin-1 inhibits feeding by modulating the excitability of glucosensing neurons in the PVN, LHA, VMN, regions involved in feeding behavior (Chen et al., 2012). Nesfatin-1 influenced the excitability of glucose-inhibited neurons in the dorsal vagal complex (DVC), inhibiting food ingestion (Dong et al., 2014). Nesfatin-1 injection studies in the fourth cerebral ventricle of chronically cannulated rats helped determine that 2 µg of nesfatin-1 is a sufficient dose to inhibit food intake during the dark phase for more than 3 hours as well inhibit vagally stimulated secretion of gastric acid (Xia et al., 2012).

Nesfatin-1 has also been studied in gastrointestinal function. Nesfatin -1 has shown to regulate the activity of gastric distention sensitive neurons and gastric motility mediated via the melanocortin pathway in the central nucleus of the amygdala (Wang et al., 2014). Nesfatin-1 injection has been shown to activate the DMNV in the medulla *in vivo* and also trigger calcium signaling in cultured DMNV neurons (Xia et al., 2012). It was found that the hyperphagic feeding mechanism in Tsumura Suzuki obese diabetes (TSOD) mice is different from that of *db/db* mice, which lack a leptin receptor. It was found that TSOD mice had decreased levels of NUCB2 mRNA in the hypothalamus of age-matched non-diabetic control Tsumura Suzuki non obese Mice (TSNO) but no change in *db/db* mice. This finding suggests that NUCB2-mediated

signaling could be disrupted in the hypothalamus of TSOD mice (Miyata et al., 2012). Corticotropin-releasing hormone (CRH), thyrotropin-releasing hormone (TRH), and hypothalamic neuronal histamine act as anorexigenics in the hypothalamus along with nesfatin-1 (Gotch et al., 2013). Histamine increased nesfatin-1 expression and nesfatin-1 increased brain CRH and TRH levels. Histidine decarboxylase inhibitor (α -fluoromethyl histidine; FMH), a CRH antagonist and anti-TRH antibody attenuated nesfatin-1-suppressed feeding in rats. This study suggests that CRH, TRH and hypothalamic neural histamine may mediate the satiety effects on nesfatin-1 on feeding behavior (Gotch et al., 2013). Also, neuro-circuits in the ARC and PVN secrete neuropeptides in the hypothalamus, which in turn can regulate NUCB2/nesfatin-1 neurons in a dual manner. NPY inhibits, while α -MSH activates NUCB2/nesfatin-1 neurons to elicit its effects on feeding (Sedbazar et al., 2014).

1.2.3.1.2 Mechanism of Nesfatin-1 *In Vivo* Action on Food Intake

Several other studies in rodents confirm that central and/or peripheral administration of nesfatin-1 causes a reduction in food intake (Oh et al., 2006, Shimizu et al., 2009, Maejima et al., 2009, Stengal et al., 2009, Su et al., 2010, Atsuchi et al., 2010, Yosten et al., 2010, Goebel et al., 2010, Gonazalez et al., 2012) and water intake (Yosten et al., 2010, Yosten et al., 2012). The method of administration unravels several mechanistic pathways that NUCB2/nesfatin-1 could elicit its action.

Intracerebroventricular (ICV) injection of nesfatin-1 into the third ventricle (3V) in leptin-resistant Zucker (*db/db*) rats caused a reduction in food intake (Oh et al., 2006). The effect on food intake was attenuated when a melanocortin receptor antagonist SHU9119 was co-administered with nesfatin-1. This suggests that NUCB2/nesfatin-1 acts via a leptin-independent melanocortin-dependant signaling pathway (Oh et al., 2006). Recent evidence further confirms

these findings that NUCB2/nesfatin-1 neurons in the PVN are directly influenced by leptin, mediating its anorexigenic effect (Darambazar et al., 2015). Nesfatin-1 ICV and intraperitoneal (IP) injections cause a reduction in food intake in goldfish (Gonzalez et al., 2010, Kerbel et al., 2012). It has been shown that ICV injection of nesfatin-1 inhibits gastric emptying in rats (Stengel et al., 2009a). This specific role of nesfatin-1 is not yet studied in teleosts. Further, cholecystokinin (CCK) has shown to activate NUCB2/nesfatin-1 neurons in the PVN and NTS mediated via a corticotropin-releasing hormone (CRH)₂-receptor-dependent pathway (Stengel et al., 2009). When astressin₂-B, a CRH receptor antagonist was coinjected with nesfatin-1, the effects of nesfatin-1 on food intake in rats were attenuated (Stengel et al., 2009). Under conditions of stress in rats, nesfatin-1 was shown to stimulate other hormones which include CRH, noradrenalin, and serotonin neurons of the rat hypothalamus (Yoshida et al., 2010). NUCB2/nesfatin-1 may also act via the central oxytocin system, where studies have shown that nesfatin-1 stimulates the release of oxytocin from the PVN neurons (Maejima et al., 2009). Oxytocin release sends a message to the NTS pro-opiomelanocortin (POMC) neurons in the brainstem, which results in the inhibition of food intake independent of the leptin mediated pathway (Maejima et al., 2009). In addition, oxytocin receptor antagonist, H4928, suppressed the effects of nesfatin-1 on food intake. These results suggest that nesfatin-1 may act via an oxytocin mediated pathway (Maejima et al., 2009) to elicit the satiety effect. Other studies suggest that nesfatin-1 may directly influence the POMC neurons in the ARC nucleus stimulating the release of alpha-melanocortin stimulating hormone, thus activating the oxytocin neurons in the PVN (Yosten et al., 2010). Furthermore, it was shown that nesfatin-1 hyperpolarizes neuropeptide Y (NPY) neurons in the ARC nucleus resulting in an inhibition of food intake (Price et al., 2008). The mammalian equivalent of the arcuate nucleus in goldfish is the NLT (Cerdeira-Reverte et al.,

2003, Peng et al., 1994), where other neuropeptides are present, suggesting that nesfatin-1 may interact with these appetite regulators in modulating food intake. Studies have shown that NUCB2/nesfatin-1 colocalized with pSEK1, which is a downstream target of mammalian target of rapamycin (mTOR). mTOR activity and gastric NUCB2/nesfatin-1 were downregulated by fasting and was found to be high in high fat diet induced obese mice. Inhibition of mTOR activity by rapamycin affects and attenuates the expression of NUCB2 mRNA in gastric tissues of both lean and obese mice as well as in MIN6 cells. This study suggests that modulation of mTOR signaling regulates gastric NUCB2/nesfatin-1 expression (Li et al., 2012).

1.2.3.2 Nesfatin-1 Regulation of Insulin Secretion and Glucose Metabolism

NUCB2/nesfatin-1 immunoreactivity in the insulin producing pancreatic beta cells provides the first evidence that NUCB2/nesfatin-1 might influence glucose metabolism (Foo et al., 2010, Gonzalez et al., 2009). In hyperglycemic *db/db* mice, nesfatin-1 administration resulted in an anti-hyperglycemic effect (Su et al., 2010). Upon the use of PPAR- γ antagonist, GW9662 or the AMPK inhibitor, compound C, the anti-hyperglycemic effect of nesfatin-1 was attenuated suggesting that nesfatin-1 is mediated via the insulin signaling pathway (Su et al., 2010). In addition, NUCB2/nesfatin-1 immunoreactivity was low in the isolated islets of Goto-Kakizaki (a T2DM model) rats in comparison to Wistar control rats (Foo et al., 2010). Isolated islets of Wistar rats, when incubated in high glucose, released NUCB2/nesfatin-1 *in vitro*. Furthermore, there was a significant decrease of nesfatin-1 levels 30 minutes post-glucose intraperitoneal injection and an increase at 120 and 240 minutes post-injection (Foo et al., 2010). NUCB2 mRNA expression and NUCB2/nesfatin-1 immunoreactivity was higher in the pancreatic islets of high fat diet induced obese, type 2 diabetic mice (Gonzalez et al., 2011). NUCB2 mRNA and NUCB2/nesfatin-1 immunoreactivity was attenuated, but still detectable in the pancreatic islets

of streptozotocin (STZ)-induced type 1 diabetic mice (Gonzalez et al., 2011). Nesfatin-1 stimulates glucose dependent insulin secretion in isolated mouse pancreatic beta-cells (Nakata et al., 2011, Gonzalez et al., 2011). Nesfatin-1 infusion caused a significant increase in physical activity, energy derived from fat and total number of feeding bouts. Simultaneously, it caused a significant reduction in duration of feeding bouts, respiratory exchange ratio and energy derived from carbohydrates (Gonzalez et al., 2012a). In an oral glucose tolerance test in *ab libitum* fed rats infused with nesfatin-1, significantly increased amounts of circulating insulin levels were detected (Gonzalez et al., 2012). However, no changes in glucose levels coincided with this insulin increase. Nesfatin-1 stimulates glucose uptake in the white adipose tissue and inhibits glucose uptake in L6 muscle cells (Gonzalez et al., 2012a). Also, it is found that mRNA expression of two regulators of gluconeogenesis, phosphoenolpyruvate carboxykinase (PEPCK) and glucose-6-phosphatase (G6PC) were upregulated following nesfatin-1 infusion (Gonzalez et al., 2012a). These findings suggest that nesfatin-1 has tissue specific effects on glucose uptake and it influences production of glucose. These tissue specific peripheral effects are likely causing the lack of changes in glucose, when insulin levels were elevated. In contrast to rodents, goldfish under fasted conditions have increased NUCB2 mRNA expression in the liver (Gonzalez et al., 2010). This upregulation of NUCB2 suggests that nesfatin-1 might be involved in the regulation of glucose metabolism in the liver of fasted goldfish.

1.2.3.3 Nesfatin-1 Metabolic Control of Reproduction

NUCB2/nesfatin-1 also plays a major role in the reproduction of rodents and teleost fishes (Garcio-Galiano et al., 2013; Gonzalez et al., 2012). NUCB2/nesfatin-1 immunoreactivity was evident in human, rat and mouse testes and rat ovaries (Garcio-Galiano et al., 2010). NUCB2/nesfatin-1 immunoreactivity was also found in Leydig cells suggesting its

possible role in testosterone production. During the pubertal period of female rats, NUCB2 mRNA and protein expression was significantly higher in the hypothalamus (Garcio-Galiano et al., 2010). There was a nine fold increase in circulating LH levels at 15 min post-ICV injection of nesfatin-1 after a 48-hour fast (Garcio-Galiano et al., 2010). During pubertal maturation, central injection of anti-NUCB2 morpholino oligonucleotides caused a decrease in ovarian weight, delayed vaginal opening and reduction in circulating levels of LH in pubertal female rats (Garcio-Galiano et al., 2010). In adult female rats, no changes to LH and FSH pre-ovulatory levels were found as a result of central injection of nesfatin-1 or anti-NUCB2 morpholino oligonucleotides (Garcio-Galiano et al., 2010). In addition, these researchers have also determined the presence of NUCB2/nesfatin-1 in the testis, where its expression was found to be regulated by developmental, metabolic, and hormonal cues and multiple Leydig cell-derived factors (Garcio-Galiano et al., 2012). NUCB2 mRNA was found in the rat, mouse, and human testes, where NUCB2/nesfatin-1 protein was identified in interstitial mature Leydig cells. NUCB2/nesfatin-1 content in rats was suppressed after fasting and was increasing along the puberty-to-adult transitional phase (Garcio-Galiano et al., 2012). NUCB2/nesfatin-1 became expressed in Sertoli cells upon Leydig cell elimination in rats. Human choriogonadotropin replacement enhanced NUCB2/nesfatin-1 mRNA and peptide levels. Testicular NUCB2/nesfatin-1 expression was found to be up-regulated by pituitary LH (Garcio-Galiano et al., 2012). Also, nesfatin-1 increased human choriogonadotropin-stimulated testosterone secretion using rat testicular explants *ex vivo*. The findings from these studies suggest that nesfatin-1 plays a vital role in energy homeostasis, puberty onset, and gonadal function in the testis (Garcio-Galiano et al., 2012). On the other hand, in domestic animals, i.c.v. injection of nesfatin-1 increases LH secretion and also affects the gonadotropic axis of prepubertal pigs

(Lents et al., 2013). Studies have also shown that NUCB2/nesfatin-1 was found highest in the pituitary regulating reproduction via the hypothalamic-pituitary ovarian axis (Chung et al., 2014). In humans, plasma nesfatin-1 was found to be high in circulation in patients with polycystic ovary syndrome (PCOS), suggesting that nesfatin-1 might play a role in the development of PCOS (Ademoglu et al., 2014).

NUCB2/nesfatin-1 immunoreactivity was evident within the cellular areas of the rostral pars distalis (RPD) and pars intermedia (PI) of goldfish anterior pituitary (Gonzalez et al., 2012b). NUCB2/nesfatin-1 immunoreactivity was also evident in the goldfish and zebrafish ovaries (Gonzalez et al., 2012b). Peripheral injection of nesfatin-1 in goldfish caused a significant reduction in circulating LH levels (Gonzalez et al., 2012b). Nesfatin-1 treatment has also been shown to decrease mRNA expression of hypothalamic hypophysiotropic hormones sGnRH and cGnRH (Gonzalez et al., 2012b). Nesfatin-1 also causes a suppression of oocyte maturation in zebrafish ovaries (Gonzalez et al., 2012b). In contrast, studies have been conducted to determine whether energy availability after spawning can affect plasma levels of nesfatin-1 in female rainbow trout fish (*Oncorhynchus mykiss*), (Caldwell et al., 2014). It was observed that plasma nesfatin-1 was not affected by long-term food restriction and does not aid in the prediction of rematuration in these fish (Caldwell et al., 2014). Overall, nesfatin-1 acts directly on all three tissues in the hypothalamo-pituitary-ovarian axis to regulate reproduction in teleosts.

1.2.4 Summary

NUCB2 gene organization and nesfatin-1 sequence are very highly conserved among species studied from the animal kingdom. Many studies have been conducted in recent years to unravel the functions of NUCB2/nesfatin-1. **Figure 1.2** summarizes the actions of nesfatin-1 in various groups of animals in which nesfatin-1 has been studied. In humans, rodents and teleost fishes, studies demonstrate tissue-specific expression of NUCB2/nesfatin-1. In rodents and humans, NUCB2/nesfatin-1 plays a major role in energy balance and glucose metabolism. In rodents and teleost fishes, nesfatin-1 plays a major role in the regulation of food intake, energy balance, and reproduction. In addition, several studies have been shown that in rodents, nesfatin-1 is also involved in the regulation of gastric emptying, development, stress modulation, thermogenesis, and cardiovascular functions. While all these studies unequivocally enhanced our understanding on nesfatin-1 biology, several aspects of nesfatin-1 still remain poorly understood. This necessitates future research on NUCB2 and nesfatin-1 using multiple model organisms.

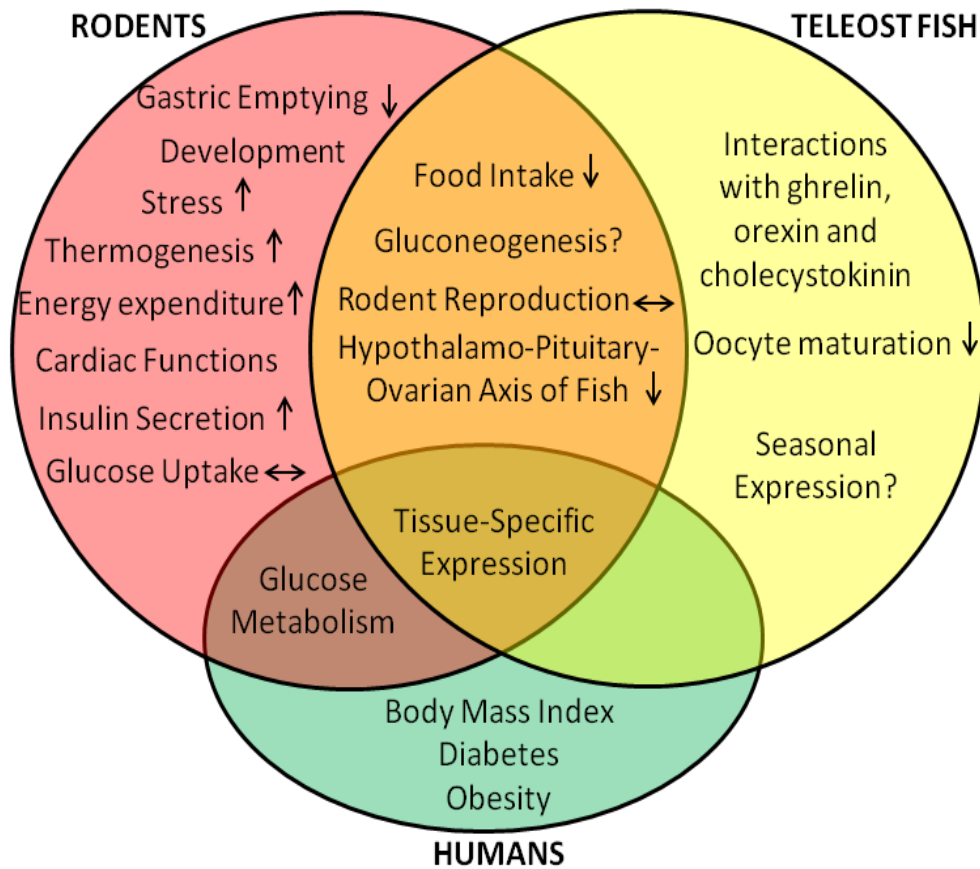


Figure 1.2 Nesfatin-1 is an Emerging Multifunctional Protein

Figure 1.2. A diagram listing the biological actions of nesfatin-1 in Teleosts (Yellow), Rodents (Orange), and Humans (Green) are listed separately. Overlapping regions of circles show functions or features that are common in one or more groups

Regulation of Energy Balance During Growth

Growing rat pups undergo major transitions in food intake. Fetal growth is mainly dependent on mother's nutrition. A decrease in the size of the neonatal pups is evident from mothers who are fed decreased amount of food compared to mothers fed *ad libitum* (Ferré et al., 1986, Ferré et al., 1977, Lorenz et al., 1982). Fetuses receive glucose, lactate and amino acids through the placenta, but at birth, the main source of energy intake comes from mother's milk (Ferré et al., 1986, Ferré et al., 1977, Lorenz et al., 1982). It has been observed that anatomical variation in peptide levels exists during pregnancy and in fetuses, and peptide levels can be modified due to changes in nutrition which could result in morphological and metabolic changes (Ferré et al., 1986, Ferré et al., 1977, Lorenz et al., 1982). Rat pups at post-natal day 1 regulate their milk intake depending on how much deprived they are of energy (Ferré et al., 1986, Ferré et al., 1977, Lorenz et al., 1982). In suckling rats, the regulation of milk intake is based on the distension by gastrointestinal fill. This response is controlled by the vagus nerve activity rather than by the hypothalamus at early stages of development (Lorenz et al., 1982). Energy regulation by milk intake at this early stage favours for optimizing growth and is restricted by full stomach to prevent over eating. Thus, in suckling pups, energy balance is regulated by short term regulation of milk intake rather than long term regulation (Ferré et al., 1986, Ferré et al., 1977, Lorenz et al., 1982). A few weeks later, when the pups begin to wean, they begin to make a steady conversion to high-carbohydrate, low-fat adult diet where their main energy source is mediated by feeding and drinking (Ferré et al., 1986, Ferré et al., 1977, Lorenz et al., 1982). Energy balance is modulated during development by changes in mRNA expression and protein levels of many orexigenic and anorexigenic peptides localized in both central and peripheral tissues (Stoka, 1999). An important orexigenic hormone, involved in appetite regulation during

development is ghrelin. Ghrelin and nesfatin-1 share several commonalities in their expression and processing, but have opposing physiological actions. The second focus of this chapter is to discuss the biological importance of ghrelin and its processing enzyme, GOAT, and to compare ghrelin and nesfatin-1, two predominant metabolic regulators in animals.

1.3 Ghrelin

Synthetic growth hormone secretagogues (GHS) with potent growth hormone (GH)-secreting properties were developed in 1970 (Bowers. 2001). These GHS bind to the GH secretagogue receptor (GHS-R) that was cloned in 1996 (Howard et al., 1996). This receptor is known to be expressed in both peripheral and central organs and is highly conserved from teleost fish to humans (Howard et al., 1996). In 1999, a 28 amino acid orexigenic peptide known as ghrelin was discovered in gastric extracts, which was the first natural ligand of the GHS-R (Kojima et al., 1999). The major active product of the ghrelin gene is ghrelin (amino acids 24 to 51) derived from posttranslational processing of preproghrelin (117 amino acids) by prohormone convertase (PC) 1/3. A 23 amino acid peptide named obestatin (amino acid 76 to 98) is also derived from preproghrelin, but in contrast to ghrelin, obestatin is proposed to have anorexigenic properties (Zhu et al., 2006). Ghrelin is secreted into the circulation as both acylated ('active') and des-acylated ghrelin. **Figure 1.3** provides an overview of cellular events leading to the synthesis and secretion of ghrelin.

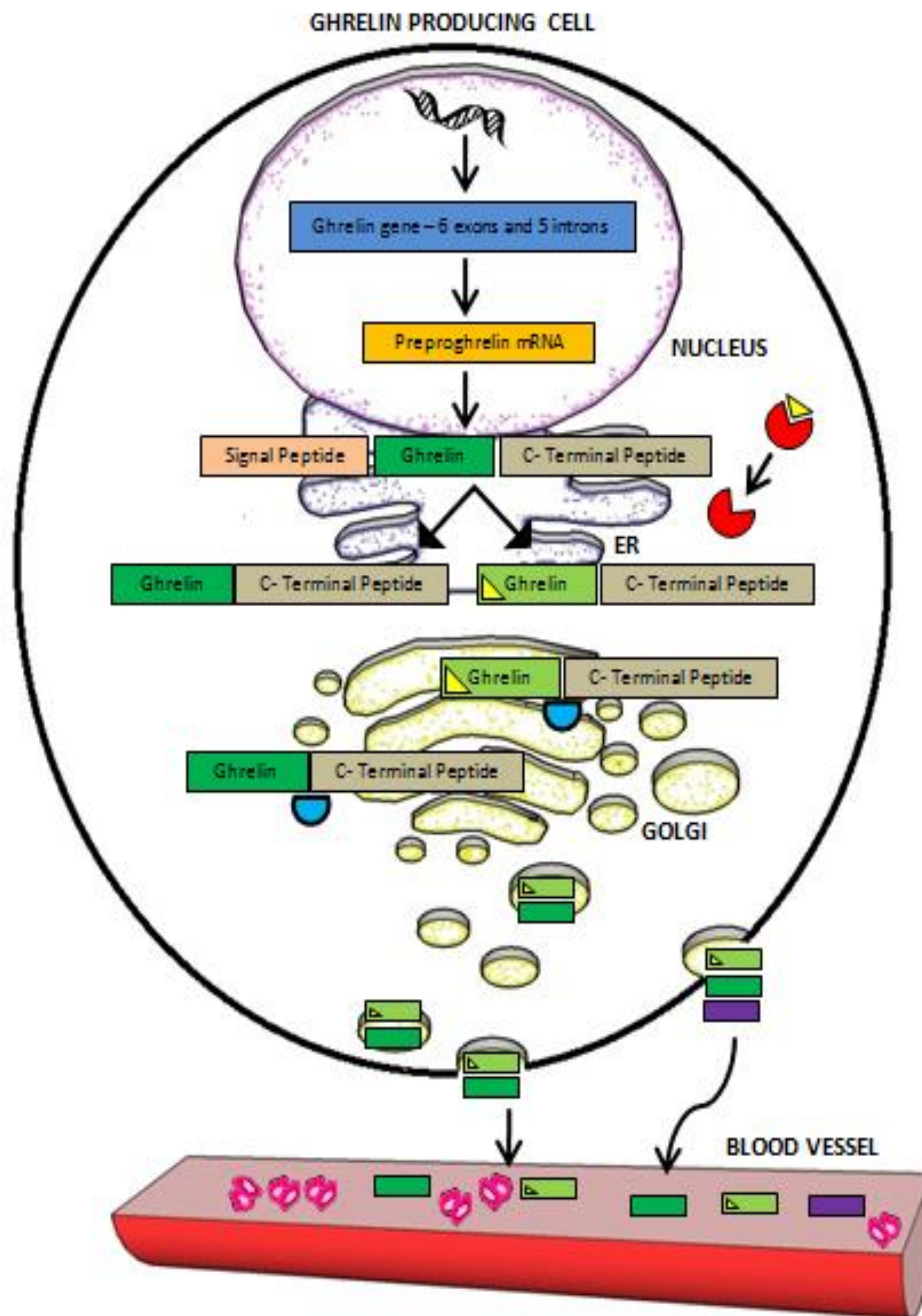

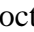

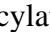
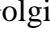



Figure 1.3 An Overview of Ghrelin Synthesis and Secretion

Figure 1.3. Schematic Illustration of the Post-Translational Processing of Ghrelin Gene. Preproghrelin mRNA is transcribed from the ghrelin gene in the nucleus. A precursor peptide is formed in the ER following the translation of preproghrelin mRNA which consists of a signal peptide, mature ghrelin and a C-terminal peptide. After the cleavage of the signal sequence by signal peptide peptidase, pro-ghrelin is produced either as acylated proghrelin or unacylated proghrelin. Acylated proghrelin is produced when ghrelin O-acyl transferase (GOAT; ) in the ER translocates octanoyl-CoA () to acylate pro-ghrelin before it reaches the Golgi where prohormone convertases 1/3 (PC 1/3; ) post-translationally cleave acylated or unacylated pro-ghrelin to form mature ghrelin forms. Acylated () , unacylated () , and other shorter forms of ghrelin () are packaged into vesicles from the Golgi and released into blood circulation.

Both forms of ghrelin, des-acyl ghrelin and acylated ghrelin exist in the stomach in significant amounts. In circulation, des-acyl ghrelin is present in greater amounts than acylated ghrelin (Kitamura et al., 1998). Thus far, there have been no studies that have shown that des-acyl ghrelin possess any endocrine function (Baldanzi et al., 2002). Ghrelin in the plasma binds to high-density lipoprotein (HDLs) that consists of amino acids that are either esterase, paraoxonase and clusterin (Beaumont et al., 2003). The acylation of a hydroxyl group of one of its serine residues (Ser 3) by n-octanoic acid is a unique characteristic to ghrelin, which is necessary for the binding of ghrelin to GHS-R (Kojima et al., 1999). The enzyme that facilitates this modification is ghrelin-O-acyl transferase (GOAT) (Yang et al., 2008, Gutierrez et al., 2008). A review on GOAT will be provided at the latter half of this chapter. The amino acid sequence of ghrelin in mammals is highly conserved, especially the 10 amino acids in the NH₂ termini are identical. In non-mammals, ghrelin has also been identified in amphibians, birds and fishes. The amino acid sequence of ghrelin in fish varies in their length and their acyl modification, thus existing in variant forms.

1.3.1 Ghrelin mRNA and Protein Expression in Tissues

In the brain, ghrelin is found in the hypothalamic arcuate nucleus, where other appetite regulatory peptides are found (Kojima et al., 1999, Lu et al., 2002). Ghrelin is expressed in very low amount in the brain (Hosoda et al., 2002, Kojima et al., 1999). Ghrelin is also found in the pituitary gland, where is it found to influence the release of growth hormone (Korbonit et al., 2001a, Korbonit et al., 2001b). At birth, ghrelin expression levels are high and gradually decline with puberty (Korbonit et al., 2001a, Korbonit et al., 2001b).

Ghrelin is found to be expressed predominantly in the stomach in all vertebrate species (Ariyasu et al., 2001). Immunohistochemical analysis and in-situ hybridization indicates that ghrelin containing cells are endocrine cells (Date et al., 2000, Rindi et al., 2002). Ghrelin is

primarily secreted in the X/A cells of the oxyntic glands (Solcia et al., 1975) expressed abundantly in the mucosal layer of the fundus of the stomach (Kojima et al., 1999). The X/A-like cells are identified to be round and compact, as electron dense granules filled with ghrelin (Date et al., 2000). They account for 20% of the endocrine cell population in the oxyntic glands. Also, sexual dimorphism is observed in the expression of ghrelin gene and ghrelin cell differentiation in the stomach (Sakata et al., 2002). The concentration of ghrelin is age and gender dependent. In the fetal stomach and at birth, ghrelin concentration is low and gradually increases until 5 weeks of age (Hayashida et al., 2002). Ghrelin-immunoreactive cells are also present in the duodenum, jejunum, ileum and colon (Sakata et al., 2002). The concentration of ghrelin decreases gradually from the duodenum to the colon (Date et al., 2000). In addition, ghrelin is also found in the pancreas. Ghrelin is identified in a new cell type identified as the epsilon (ϵ) cell (Wierup et al., 2004). Ghrelin-RIA and HPLC has determined that both ghrelin and des-acyl ghrelin exist in the rat pancreas (Date et al., 2002). Ghrelin expressing cells in the pancreas are numerous from mid-gestation to early postnatal periods, comprising 10% of all endocrine cells. It gradually decreases after birth. Total ghrelin concentration and ghrelin mRNA are 6 to 7 fold higher in the fetal pancreas than in the fetal stomach. Therefore the onset of pancreatic ghrelin precedes gastric ghrelin. On the other hand, gastric ghrelin is low at prenatal periods and increases after birth (Hayashida et al., 2002). Pancreatic ghrelin is moreover not affected by fasting (Kishimoto et al., 2003). Nkx2.2 is an important protein required for the differentiation of islet β and α cells, and a study has identified that the mice lacking Nkx2.2 have all their β -cells replaced by ghrelin producing cells (Prado et al., 2004). Ghrelin is also expressed in the kidney in the glomeruli (Gnanapavan et al., 2002, Mori et al., 2000). In addition, ghrelin-immunoreactive cells are detected in the cytotrophoblast cells in the first-trimester of human

placenta (Gualillo et al., 2001). Ghrelin-immunoreactive cells have also been identified in the interstitial Leydig cells and in Sertoli cells (Barreiro et al., 2002, Tena-Sempere et al., 2002).

Ghrelin is also expressed in cell lines, some of which that include, human thyroid medullary carcinoma cell line TT (Kanamoto et al., 2001), kidney-derived cell line NRK-49F (Mori et al., 2000), gastric carcinoid ECC10 cells (Kishimoto et al., 2003, and the cardiomyocyte cell line HL-1 (Iglesias et al., 2004). A recent discovery identified the mouse ghrelinoma 3-1 (MGN3-1) cells from a gastric ghrelin-producing cell tumor derived from ghrelin-promoter Simian virus 40-T-antigen transgenic mice. These cells produce ghrelin that is 5000 times higher than that observed in TT cells. These cells as well produce GOAT and PC 1/3 that are required for the acyl modification and maturation of ghrelin. The newly established MGN3-1 is currently a useful tool for *in vitro* study of ghrelin production and secretion (Iwakura et al., 2010).

1.3.2 Biological Actions of Ghrelin

Ghrelin plays a major role in hormone secretion. Ghrelin stimulates the secretion of GH both *in vitro* and *in vivo* in a dose-dependent manner (Arvat et al., 2000, Arvat et al., 2001, Date et al., 2002, Kojima et al., 1999, Peino et al., 2000, Takaya et al., 2000). Ghrelin in humans stimulates increases in ACTH, prolactin and cortisol (Arvat et al., 2000, Takaya et al., 2000). Ghrelin is a potent appetite stimulatory peptide. The levels of ghrelin in circulation increase prior to meal and decrease post meal, which suggest its potential role in meal initiation. Ghrelin stimulates appetite by binding to GHS-R, which activates neuropeptide Y/agouti-related protein (NPY), which are potent orexigenic agents in the arcuate nucleus of the hypothalamus (ARH) (Chen et al., 2004). Rats have increased food intake when ghrelin is injected into the cerebral ventricles (Kamegai et al., 2001, Nakazato et al., 2001, Shintani et al., 2001, Tschop et al., 2000, Wren et al., 2000a). Intracerebroventricular, intravenous and subcutaneous injections of ghrelin

have been shown to increase food intake (Nakazato et al., 2001, Tschop et al., 2000, Wren et al., 2000b).

In addition, ghrelin stimulates adipogenesis to promote a positive energy balance by mediating GHS-R-independent pathways (Tschop et al., 2000). This effect is independent of food intake (Tschop et al., 2000). Also, studies have found that ghrelin gene expression in the stomach is high when fasting and attenuated when leptin and interleukin (IL)-1 β is administered (Asakawa 2001, Kim et al., 2003, Toshinai et al., 2001). Study suggests that ghrelin produces a positive energy balance by decreasing energy expenditure and promoting food intake by blocking IL-1 β -induced anorexia. Studies have identified that ghrelin is further involved in gastric acid secretion (Tschop et al., 2000), gut motility (Trosello et al., 2003), insulin and gastrin secretion (Prado et al., 2004) and the cardiovascular system (Nagaya et al., 2001). Furthermore, a study conducted on neonates treated with ghrelin during the first 2 weeks after birth, have shown increased eye and vaginal opening than the saline treated group, which signifies its additional role in growth (Torsello et al., 2003). Ghrelin influences insulin secretion, but there is much controversy as some studies have shown that ghrelin inhibits insulin secretion while others show that it stimulates insulin secretion (Adeghate et al., 2002, Broglio et al., 2001, Date et al., 2002, Lee et al., 2002, Reimer et al., 2003). Ghrelin increases insulin secretion from islet cells in high glucose compared to low glucose medium (Date et al., 2002). In rat hepatoma cell line, H4-II-E cells, ghrelin inhibited the effect of insulin on PEPCK mRNA levels, suggesting that it may be involved in the regulation of gluconeogenesis *in vivo*.

Ghrelin Function is Dependent on GOAT

The unique structure of ghrelin, its expression in multiple tissues and its biological functions is groundbreaking in the field of endocrinology. Among all bioactive peptides in literature, ghrelin by far is the only peptide that is modified by a fatty acid that requires an n-octanoyl modification that is essential for it for function (Yang et al., 2008, Gutierrez et al., 2008). Addition of this acyl group is critical for the growth hormone releasing activity and several other actions of ghrelin described above. However, the process of acylation, as well as the possible enzyme(s) behind this process remained unsolved. Meanwhile, in the unrelated area of enzyme research, several new ideas were forming. Specifically, Hofmann (2000), using novel combinations of bioinformatics tools, identified a family of O-acyl transferases that catalyses the O-acylation reaction. These findings were rooted in genetic studies performed earlier on *Drosophila*, based on a gene called *porcupine* (Kadowaki et al., 1996). *Porcupine* has conserved regions that is also found in many membrane bound hydrophobic enzymes that are involved in translocating long chain fatty acids to membrane bound hydroxyl receptors. These enzymes were called membrane-bound O-acyl transferases (MBOATs) (Kadowaki et al., 1996). This advance in the MBOAT research eventually led to the discovery of what we know now as the **Ghrelin O-Acy Transferase (GOAT)**

1.4 GOAT

GOAT was identified independently by two research groups, and was reported to the scientific community in two elegant articles (Yang et al., 2008, Gutierrez et al., 2008) published months apart in 2008. In the article that came first in the public domain, Yang et al., (2008) determined that the mouse genome encodes for 16 membrane bound MBOAT protein sequences produced by 11 genes. Later studies on cultured endocrine cells lines co-transfected with preproghrelin sequence and MBOATs, revealed that one of these MBOATs catalyzed the octanoylation of ghrelin. This MBOAT facilitating ghrelin acylation was then named GOAT (Yang et al., 2008). There were 11 catalytic regions that are highly conserved in all 16 MBOAT sequences in the mouse genome. The conserved regions contain the putative asparagine and histidine residues that are thought to take part in the catalytic reactions (Yang et al., 2008). A series of transfection experiments demonstrated that octanylation of ghrelin was facilitated by GOAT in three different murine endocrine cell lines. When mouse pituitary AtT-20 cells, rat insulinoma INS-1 cells, and mouse insulinoma MIN-6 cells were co-transfected with preproghrelin and GOAT, acylated ghrelin was produced. Mutation of the serine at position 3 to alanine prevented the acyl modification of ghrelin by GOAT, indicating that the presence of a third serine is essential for GOAT-dependent octanylation of ghrelin (Yang et al., 2008). Overall, these results by Yang and colleagues (2008) provide the first reported experimental evidence for GOAT. Meanwhile, the second group led by Gutierrez et al. (2008) studied ghrelin octanoylation *in vitro* using human medullary thyroid carcinoma (TT) cells to identify which member of the MBOAT family is involved in ghrelin acylation. Less than 10% of ghrelin protein secreted by the TT cells were acylated, leading them to think that there is a low expression of the acylating machinery in TT cells (Gutierrez et al., 2008). Silencing the GOAT gene in the TT cells using

several GOAT specific siRNAs resulted in an inhibition of ghrelin acylation. Gene silencing of other MBOAT members present in the TT cells did not affect ghrelin octanoylation, implicating solely GOAT in the acylation of ghrelin. In addition, HEK-293 cells that express neither ghrelin nor GOAT, when co-transfected with preproghrelin and GOAT, started secreting octanoylated ghrelin (Gutierrez et al., 2008). Further experiments conclusively showed that ghrelin octanoylation was only achieved with GOAT, although these cells were co-expressed with other members of the MBOAT family, including MBOAT1, MBOAT2, MBOAT3, MBOAT5, human-BB1, porcupine, and FKSG89. The replacement of the conserved histidine residue in GOAT to alanine (H338A) inhibited its activity, demonstrating further that GOAT is a member of the MBOAT protein family (Gutierrez et al., 2008). Also, HEK-293 cell medium treated with a variety of substrate lipids, including tetradecanoic acid caused acylation of ghrelin. This suggests that GOAT could use a selection of fatty acids in addition to octanoic and decanoic acid to acylate ghrelin (Gutierrez et al., 2008).

1.4.1 GOAT mRNA and Protein Expression in Tissues

Yang et al. found that the highest levels of GOAT mRNA expression were limited to the stomach and intestine followed by the testis of mice (Gonzalez et al., 2008). In rats, GOAT mRNA expression is also identified in the hypothalamus, stomach, intestine, ovary, serum, placenta, muscle, heart, and adrenal glands (Gonzalez et al., 2008). Gutierrez et al., (2008) demonstrated that in humans GOAT transcript levels are most abundant in the stomach and pancreas. From these results, it is highly evident that the stomach is the main tissue for acyl ghrelin production and changes in the secretion of acylated ghrelin can modulate changes in metabolism of many species (Gutierrez et al., 2008). GOAT immunopositive ghrelin cells found in mice (95%) are higher in comparison to rats (56%) in the stomach (Stengel et al., 2010).

GOAT mRNA and protein are present in the whole pancreas, isolated islets and INS-1 cells. GOAT immunopositive cells are mainly localized in the periphery of rat islets (An et al., 2010). In diet-induced obese (DIO) and ob/ob mice, it was found that the GOAT mRNA levels were decreased in the pituitary in comparison to the hypothalamus. Although GOAT mRNA expression increased in the pituitary after a 24 hour fast, it increased in the hypothalamus at 48 hours of fasting. GOAT is also expressed in the hypothalamus and pituitary of mice (Gahete et al., 2010). Overall, GOAT appears to be predominantly expressed in the gut, brain and the pancreas, three tissues that play major roles in feeding and energy homeostasis.

GOAT expression is modulated by nutrition. For instance, mice in a state of negative energy balance, or fasted for 24 or 48 hours have shown increased GOAT expression. While, in a positive energy balance state, GOAT expression decreases (Gahete et al., 2010, Xu et al., 2009). However, in another study performed by Gonzalez et al., (2008) there was no change in GOAT mRNA expression after 48 hours of fasting in rats. Meanwhile, they found that chronic malnutrition achieved by 70% restriction in food intake for 21 days led to an increase in GOAT expression in the gastric mucosa (Gonzalez et al., 2008). This is contradictory to another study where 35% of dietary food restriction for 5 months significantly reduced the levels of GOAT expression in the stomach (Reimer et al., 2010). Furthermore, a study by Kirchner et al. (2009) found that when mice are fed *ad libitum*, expression of GOAT was evidently high but decreased after 12, 24, 36, and 48 hours of fasting. While variations exist between tissues, species and strains, it is important to learn that metabolic status influences the expression of GOAT. These data suggest that GOAT is possibly linked to metabolic regulation.

1.4.2 Biological Actions of GOAT

GOAT is the only known enzyme that acylates ghrelin. However, it is possible that GOAT might have other effects on homeostasis, especially by acting on other hormones or physiological processes. In line with this possibility, a very recent study by Kang and colleagues (Bando et al., 2012) showed that GOAT has a crucial role in the regulation of bile acid reabsorption. GOAT null mice exhibited an approximately 2.5 fold increase in secondary bile acids. GOAT null mice have an increase in the expression of ileal sodium dependant bile acid transporter mRNA and protein in both the biliary tract and the gastrointestinal (GI) tract. A similar ~10 fold increase in the solute carrier family 5 (Slc5a12), a sodium/glucose co-transporter was also detected in the small intestine and bile duct. This study provides the first glimpse of GOAT effects unrelated to ghrelin (Bando et al., 2012). More studies are essential to identify the physiology of GOAT and complete functional implications of GOAT absence.

As GOAT protein is highly similar across many vertebrates, the function of GOAT is conserved across species (Gutierrez et al., 2008). HEK-293 cells transfected with rat, mouse or zebrafish GOAT resulted in successful octanoylation of human ghrelin, demonstrating that the function of GOAT is highly conserved across vertebrates (Gutierrez et al., 2008). Further studies on GOAT gene knockout mice, confirmed that GOAT is the critical lipid acyl transferase for acylating ghrelin as there was no detectable levels of octanoylated ghrelin in the GOAT knockout mice compared to wild-type controls (Gutierrez et al., 2008). GOAT knockout mice produced large amounts of des-acyl ghrelin only, and were unable to produce acyl ghrelin. Collectively, these results from Gutierrez and colleagues (Gutierrez et al., 2008) confirmed Yang et al.'s (2008) findings and strengthened the notion that GOAT is the enzyme responsible for ghrelin acylation.

As GOAT is co-expressed with ghrelin in the pancreas, GOAT has been implicated in the regulation of insulin secretion and glucose metabolism. GOAT knockout mice fasted for 16 hours have increased insulin secretion and improved glucose tolerance (Zhao et al., 2010). In addition, GOAT knock-out mice provided with a 60% caloric restriction diet develop severe hypoglycaemia, with 2% reduction in body fat compared to wild type mice and were morbid after 7 days (Zhao et al., 2010). When these mice were infused with ghrelin or GH, their blood glucose reached normal levels and prevented death. These studies suggest that caloric deficiency can modulate the expression of ghrelin and GH levels in the absence of GOAT and thus implicate its role in glucose metabolism (Zhao et al., 2010). Recently, GOAT has been associated with anorexia nervosa as a result of genetic variations found in the GOAT gene.

Ghrelin has been actively pursued as a potential anti-obesity target. Discovery of GOAT led to a new line of translational research aimed to develop GOAT inhibitors. The idea behind this approach is to inhibit GOAT, thereby inhibiting synthesis of active ghrelin, which is involved in stimulating a positive energy balance and inhibiting insulin secretion. Thus far, two effective GOAT inhibitors have been validated. The first one developed by Yang and colleagues (Soriano-Guillen et al., 2004) is a potent inhibitor of GOAT activity *in vitro*. The first and rather extensive *in vivo* characterization of a different type of GOAT inhibitor named GO-CoA-Tat was reported by Barnett and colleagues (Yang et al., 2008). *In vivo* administration of GO-CoA-Tat resulted in a significant reduction in body weight, an increase in glucose stimulated insulin secretion (GSIS). This effect is mediated by inhibiting UCP2, which has negative effects on GSIS. It was also found that islet GOAT mRNA expression is inhibited by insulin, and that the insulin effects on GOAT are mediated via the PI3 kinase/AkT pathway and by inhibiting the GOAT promoter activity (Barnett et al., 2010). These results clearly indicate an important role

for GOAT on insulin synthesis and secretion from pancreatic islets. Collectively, the data obtained from GOAT null mice and studies using GOAT inhibitors clearly indicate a role for GOAT in the regulation of energy balance. These metabolic effects of GOAT appear to be mediated mainly via its modulatory roles on ghrelin. At least one study suggests that the inraislet ghrelin/GOAT is not responsible for modulating insulin secretion. Bando et al., (2012) developed a new mouse strain that has inraislet over expression of both ghrelin and GOAT under the rat insulin promoter. These mice have normal portal vein ghrelin levels, glucose homeostasis, insulin levels and islet morphology. A suggested possibility is that the islet beta cells are unable to make acylated ghrelin due to the absence of critical cellular components that are present in the gastric ghrelin cells. Further studies are required to determine the tissue specific presence and function of GOAT.

1.5 NUCB2/Nesfatin-1 - Ghrelin Relationship

NUCB2/nesfatin-1 and ghrelin have been found to be co-expressed in the X/A or ghrelin cells of the stomach (Stengal et al., 2009). However, nesfatin-1 and ghrelin are present in different vesicles of the same cell suggest differential roles in feeding regulation (Stengel et al., 2012b). NUCB2 is processed by PC 1/3 and PC 2. Previous studies have determined that the same enzymes also process proghrelin and GOAT. Being processed by the same enzymes and localized in the same cell but different vesicles raises the possibility of opposing actions for these peptides. Nesfatin-1, an anorexigen, decreases food intake and body weight gain, while ghrelin, an orexigen, increases food intake and body weight gain (Stengel et al., 2012a, Stengel et al., 2013). In non-mammals, NUCB2/nesfatin-1 and ghrelin immunoreactivity was observed in the enteroendocrine cells of the goldfish anterior intestine (Kerbel et al., 2012). Co-localization of both these peptides was observed in the posterior nucleus lateralis tuberis of the goldfish hypothalamus, a region involved in regulating food intake. I.c.v. administration of nesfatin-1 decreased food intake and mRNAs encoding preproghrelin, ghrelin receptor and NUCB2 in the forebrain of fed fish (Kerbel et al., 2012). In contrast, i.c.v. injection of ghrelin stimulated food intake and suppressed NUCB2 and preproghrelin mRNAs, Ghrelin had no effect on ghrelin receptor mRNA expression in the forebrain (Kerbel et al., 2012). The Unniappan lab performed an additional study in Fischer 344 Rats to determine whether such relationships between nesfatin-1 and ghrelin exist in mammals. It was found that nesfatin-1 indeed colocalizes with ghrelin, GOAT and GHS-R1a in gastric endocrine cells. Ghrelin infusion significantly increased dark phase cumulative food intake and duration of feeding bouts, but decreased light phase total activity. Ghrelin infusion tissue-specifically decreased NUCB2 mRNA in the liver, but did not affect NUCB2 and preproGOAT mRNA in the stomach and serum NUCB2 levels. Nesfatin-1

infusion in postprandial conditions significantly decreased preproGOAT and preproghrelin mRNA expression levels. Ghrelin and nesfatin-1 co-administration cancelled out all metabolic effects. These results (manuscript under preparation) indicate opposing metabolic effects for ghrelin and nesfatin-1.

1.6 Rationale

The neuroendocrine regulation of energy homeostasis in mammals is the core focus of this thesis research. Hormones play an integral role in energy homeostasis. Since its discovery in 2006, there are just over 250 articles on nesfatin-1 in PubMed. Ongoing research on NUCB2/nesfatin-1 has identified it as multifunctional protein, but many of the biological actions found are mainly based on the studies where exogenous nesfatin-1 was administered. The goal of the studies outlined in this thesis is to gain a deeper understanding of nesfatin-1. They were focused on addressing the void in our knowledge base on nesfatin-1.

NUCB2 is co-expressed with insulin and is an insulintropic peptide (Foo et al., 2010, Gonzalez et al., 2009, Gonzalez et al., 2011, Gonzalez et al., 2012a). PCs, the same enzymes that process proinsulin and proghrelin, cleave NUCB2 to produce nesfatin-1 (Stengel et al., 2009, Stengel et al., 2012a, Stengel et al., 2013). How are NUCB2/nesfatin-1, ghrelin and their processing enzymes expressed during pancreatic development? NUCB2/nesfatin-1 is widely distributed in several peripheral tissues (Zhang et al., 2010). Hormone secretion from endocrine cells of these tissues can be influenced by nutrient intake (Dauncey et al., 2001). Nesfatin-1 indeed is a meal responsive hormone (Stengel et al., 2009a, Gonzalez et al., 2009, Gonzalez et al., 2011), and circulating nesfatin-1 increases after the ingestion of a meal (Stengel et al., 2009a, Gonzalez et al., 2009, Gonzalez et al., 2011). Which nutrients regulate nesfatin-1 synthesis and secretion? If nutrients do regulate nesfatin-1, are such effects tissue-specific? While nesfatin-1 is a multifunctional peptide, whether NUCB2/nesfatin-1 is critical for energy homeostasis remain unclear. Disruption of the NUCB2 gene resulting in a lack of the bioactive protein will allow us to identify specific functions of this gene and its encoded proteins. This thesis aims to address

the above questions. Outcome of this thesis is expected to better our understanding of nesfatin-1, an important, naturally occurring bioactive orphan ligand.

1.7 Hypothesis and Specific Objectives

The **central hypothesis** of this thesis research is that the tissue specific expression of NUCB2/nesfatin-1 is regulated developmentally, and by nutrients, and that the endogenous NUCB2/nesfatin-1 is critical for the maintenance of energy homeostasis.

Specific Objective 1: To investigate the ontogenic expression of NUCB2 mRNA and NUCB2/nesfatin-1 immunoreactivity in the rat stomach, duodenum and pancreas; to compare the developmental co-localization of insulin and NUCB2/nesfatin-1 in the pancreas; and to determine the circulating levels of NUCB2/nesfatin-1 during various developmental stages of Sprague Dawley rats.

Specific Objective 2: To elucidate the developmental expression of GOAT mRNA and colocalization of ghrelin, GOAT, NUCB2/nesfatin-1, PC 1/3 and PC 2 immunoreactivity in the pancreas during fetal and postnatal periods in Sprague Dawley rats.

Specific Objective 3: To determine how different nutrients modulate NUCB2/nesfatin-1 and ghrelin secretion *in vitro* in cultured stomach ghrelinoma (MGN3-1) cells from mice and *in vivo* in male mice.

Specific Objective 4: To learn whether the genetic loss of nesfatin-1 alters whole body energy homeostasis, islet morphology, islet hormone release, and glucose homeostasis in NUCB2 knockout (NKO) mice.

Transition

The following chapter focuses on my first set of objectives: To investigate the ontogenic expression of NUCB2 mRNA and NUCB2/nesfatin-1 immunoreactivity in the stomach, duodenum and pancreas, to compare the developmental co-localization of insulin and NUCB2/nesfatin-1 in the pancreas, and to determine the circulating levels of NUCB2/nesfatin-1 during various developmental stages of Sprague Dawley rats. As stated earlier, NUCB2 is expressed in the gastrointestinal tissues and is co-expressed with insulin in islet β -cells with glucose-responsive insulintropic actions. Although it has been identified as a multifunctional hormone, there are no reports on the developmental expression of NUCB2/nesfatin-1. We found that all islet β -cells colocalize NUCB2/nesfatin-1 in an age-dependent manner. In the stomach and duodenum, NUCB2/nesfatin-1 expression shows a tissue specific developmental expression in rats. Serum NUCB2/nesfatin-1 gradually increased with growth and was highest in adults, suggesting an increase in its production and secretion from tissues including the gastrointestinal tract and pancreas. ***This is the first study that has focused on the tissue specific expression of NUCB2/nesfatin-1 in rats during development.*** These results collectively suggest that NUCB2/nesfatin-1 has important age- and tissue-specific roles in the developmental physiology of rats.

Publication: Mohan, H., Unniappan, S. 2012. Ontogenic pattern of nucleobindin-2/nesfatin-1 expression in the gastroenteropancreatic tissues and serum of Sprague Dawley rats. *Regulatory Peptides*, 175 (1-3), 61-9.

Contributions: Haneesha Mohan conducted all *in vivo* studies, collected and processed the tissue samples for RNA extraction, conducted immunohistochemistry, protein assays, analysed data and wrote the first draft of the manuscript. Suraj Unniappan helped with the experimental design, provided the research infrastructure, edited the manuscript and funded the project to completion.

Chapter 2

Ontogenic Pattern of Nucleobindin-2/Nesfatin-1 Expression in the Gastroenteropancreatic Tissues and Serum of Sprague Dawley Rats

2.1 Introduction

Nesfatin-1 is an eighty two amino acid anorexigenic peptide encoded in the N-terminal region of its precursor protein, nucleobindin 2 (NUCB2). NUCB2 is a 396 amino acid protein with approximately 85% amino acid sequence homology among humans, mice, and rats (Oh-I et al., 2006, Myres et al., 2006, Cowley et al., 2006). Prohormone convertases, PC-1/3 and PC-2, the same enzymes responsible for the proteolytic conversion of proinsulin to insulin (Steiner et al., 1992) are proposed to cleave NUCB2 to nesfatin-1 (1–82 amino acids), nesfatin-2 (85–163 amino acids), and nesfatin-3 (166–386 amino acids) respectively (Oh-I et al., 2006). To date, the processed nesfatin-1 has been detected only in the cerebrospinal fluid (Oh-I et al., 2006). In rats, NUCB2/nesfatin-1 is expressed in many brain regions including the arcuate nucleus (ARC), paraventricular nucleus (PVN) and the supraoptic nucleus (SON), which are involved in the regulation of energy balance (Oh-I et al., 2006, Yosten et al., 2010, Brailoiu et al., 2007, Foo et al., 2008, Kohno et al., 2007). NUCB2 mRNA expression analysis of purified endocrine cells of the gastric mucosa has shown that mRNA levels at this region are higher than in the brain (Stengel et al., 2009b). NUCB2/nesfatin-1 immunoreactivity has also been identified in the middle and lower segments of the gastric mucosal glands and in the submucosal layer of the duodenum in rats (Zhang et al., 2009). NUCB2/nesfatin-1 is also co-localized with insulin in the pancreatic islet β -cells, but not in other islet cell types in rats and mice (Gonzalez et al., 2009) and human pancreas (Foo et al., 2010). This extensive distribution of NUCB2/nesfatin-1 in

tissues that are involved in metabolic regulation suggests important physiological roles for this novel protein.

Several studies have found that nesfatin-1 induces anorectic responses after central and peripheral administration in rodents (Oh-I et al., 2005, Yosten et al., 2010, Shimizu et al., 2009, Stengel et al., 2009a, Goebel et al., 2011, Atsuchi et al., 2010, Maejima et al., 2009). Rats receiving chronic intracerebroventricular (i.c.v) injection of nesfatin-1 for 10 days resulted in a reduction in food intake and body weight. A decrease in the weights of subcutaneous, epididymal and mesenteric fat tissues was also detected (Oh-I et al., 2006). Similarly, continuous administration of nesfatin-1 into the third ventricle of the rat brain gradually decreased body weight with a reduction in white adipose tissue weight (Shimizu et al., 2009). Our own studies on the whole-body metabolic effects revealed that peripheral infusion of nesfatin-1 reduces food intake, lowers the duration of feeding bouts, and increases the total number of feeding bouts (Gonzalez et al., 2012a). A decrease in respiratory exchange ratio (RER) was also observed, that coincided with an increase in energy production being met by increased fat oxidation (Gonzalez et al., 2012a). Together, these studies provide considerable data supporting the metabolic effects of nesfatin-1.

Nesfatin-1 also regulates glucose metabolism and insulin secretion. In MIN6 cells, a 4-fold increase in nesfatin-1 levels was observed when the cells were incubated in high glucose (16.7 mM) compared to low glucose (2.0 mM) (Gonzalez et al., 2011). In addition, nesfatin-1 stimulates glucose stimulated insulin secretion from rat and mouse β -cells that were incubated in high glucose in a dose dependent manner (Gonzalez et al., 2011, Gonzalez et al., 2012a). In the pancreas of streptozotocin (STZ)-injected mice with type 1 diabetes, it was found that both NUCB2 and preproinsulin mRNA expression were significantly lower while there was a

significant increase in proglucagon mRNA expression. In contrast, nesfatin-1 and insulin colocalizes in β -cells in the pancreatic islets of high-fat diet (HFD)-induced obese (DIO) mice with Type 2 Diabetes. There was a significant increase in the density, size, and distribution of pancreatic islets in diet induced obese (DIO) mice (Gonzalez et al., 2012a). Intravenous injection of nesfatin-1 has shown to induce an antihyperglycemic effect lowering blood glucose in hyperglycaemic *db/db* mice for 6 h (Su et al., 2010). Furthermore, nesfatin-1 also stimulates insulin secretion *in vivo* in rats (Gonzalez et al., 2012a). Our studies have identified that nesfatin-1 treatment induced insulin-stimulated glucose uptake in adipocytes, but not muscle cells, implicating nesfatin-1 in regulating glucose homeostasis. In human studies, glucose treated subjects have shown higher basal nesfatin-1 levels compared to control subjects (Li et al., 2010). Overall, these results provide several results in support of nesfatin-1 as an insulinotropic protein with modulatory effects on glucose homeostasis.

While data available to date implicate nesfatin-1 on metabolic regulation, many aspects of this protein remain undetermined. One such question that still remains unanswered is whether and how NUCB2/nesfatin-1 is expressed in the peripheral tissues during development. From earlier studies on NUCB2/nesfatin-1 in the periphery, it appears that NUCB2/nesfatin-1 is mainly expressed in the gastrointestinal tract and pancreas. Studying the developmental expression of NUCB2/nesfatin-1 in the gastroenteropancreatic tissues will be beneficial for future functional studies. The objectives of this study were to determine the ontogenic expression of NUCB2 mRNA and NUCB2/nesfatin-1 immunoreactivity in the rat stomach, duodenum and pancreas, to compare the developmental co-localization of insulin and NUCB2/nesfatin-1 in the pancreas, and to determine the circulating levels of NUCB2/nesfatin-1 during various developmental stages. Our findings indicate that NUCB2/nesfatin-1 mRNA and protein

expression are tissue specific and in general increases from embryonic day 21 through postnatal day 27. These results suggest an age- and tissue-specific role for NUCB2/nesfatin-1 in the developmental physiology of rats.

2.2 Materials and Methods

2.2.1 Animals

Timed pregnant Sprague Dawley rats (Charles River Laboratories, St Constant, QU, Canada) were housed from day 13 of pregnancy in a 12 h light:12 h dark cycle (lights off at 7 PM and on at 7 AM), temperature and humidity controlled vivarium. Pregnant dams had *ad libitum* access to standard rat chow (60% carbohydrate, 27% protein, and 13% fat; with energy density = 3.43 kcal/g; LabDiets Inc., St. Louis, MO) and water. All experiments using rats complied with the Canadian Council of Animal Care guidelines, and the animal care protocol (# 2010-31-R3) was reviewed and approved by the York University Animal Care Committee.

2.2.2 Immunohistochemistry

For immunohistochemical studies, we used 2 pregnant rats that were housed in the vivarium. All dissections and tissue collection were conducted at the same time of the day (13:00–14:00 h) to provide consistency. One pregnant rat was euthanized under deep carbon dioxide inhalation followed by cardiac puncture on day 21 of pregnancy. Out of 13 embryos, tissues (corpus region of the stomach, the duodenal region immediately after the pyloric sphincter, and the head region of the pancreas) from 5 embryos on gestational day 21 (embryonic day 21) were dissected. The second pregnant dam was allowed to deliver (n = 11 pups) and nurse normally. Tissues were collected as described above from neonatal pups on postnatal days 1 (n = 3), 6 (n = 2), 13 (n = 2), 20 (n = 2) and 27 (n = 2) and fixed in 4% formaldehyde for 24 h at 4 °C. Fixative was replaced with ethanol (three 70% ethanol), each followed by a 10 minute incubation at 4 °C. Tissues were then stored in 70% ethanol at 4 °C and were processed and sectioned at the Pathology Core Facility of the Centre for Modeling Human Disease, Toronto Center for Phenogenomics. Paraffin sections of 4 µm thickness were prepared for

immunostaining. These sections were deparaffinized with xylene (incubated twice in 100% xylene; 5 min, 25 °C) and rehydrated in a graded ethanol series (incubated twice in 100% ethanol, and once in each 95% ethanol, 70% ethanol, 50% ethanol; 2 min each, 25 °C). The sections were then incubated with 3% hydrogen peroxide in distilled water to block endogenous peroxidase activity (30 min at room temperature). The sections were then blocked with serum-free protein block reagent (DAKO® Corporation, California) for 10 min before being incubated with primary antibodies. These sections, except for the stomach (Rabbit anti-nesfatin-1; catalog number H-003-22; 1:100 dilution; Phoenix Pharmaceuticals, California) were then incubated with rabbit anti-nesfatin-1 (Catalog number H-003-22; 1:500 dilution; Phoenix Pharmaceuticals, California) alone or co-incubated with rabbit anti-nesfatin-1, mouse monoclonal anti-chromogranin A (Catalog number ab 80787; 1:500 dilution; Abcam, Massachusetts) and guinea pig anti-insulin (Catalog number ab 7842; 1:100 dilution; Abcam, Massachusetts) for 24 h at room temperature. All primary and secondary antibodies were diluted in antibody diluent reagent (DakoCytomation®, Mississauga, Ontario).

All slides were subsequently washed three times with 1 × PBS and incubated with goat anti-rabbit Texas Red® IgG (Red-Nesfatin-1; Catalog number TI-1000; 1:100 dilution; Vector Laboratories, California), goat polyclonal anti-mouse FITC IgG (H & L) (Green-Chromogranin A (CgA); Catalog number ab 6785; 1:100 dilution; Abcam, Massachusetts) and either goat anti-guinea pig FITC IgG (Green-Insulin; Catalog number ab 6904; 1:200 dilution; Abcam, Massachusetts) secondary antibodies for 1 h at room temperature. The slides were washed three times with 1 × PBS and seven times with distilled water. Finally, the slides were mounted with Vectashield® medium that contain nuclear dye DAPI (Blue; Vector Laboratories, Burlingame, California) (Gonzalez et al., 2011). Sections were viewed under a Nikon Eclipse Ti-E inverted

fluorescence microscope (Nikon Canada, Mississauga, Canada). Images were captured using a Nikon DS-QI1MC cooled monochrome camera connected to a Dell HP Workstation computer and NIS elements basic research imaging software (Nikon Canada, Mississauga, Canada) (Gonzalez et al., 2011). Approximately 8 slides (from multiple rats) containing two sections each of the stomach, duodenum and pancreas from each developmental stage were stained using the above protocol and analyzed. Only representative images of tissues from each stage staining for NUCB2/nesfatin-1 alone, co-localization of NUCB2/nesfatin-1 and CgA, and colocalization of NUCB2/nesfatin-1 and insulin are shown in the Results section.

The NUCB2/nesfatin-1 antibody has been tested and validated in our lab before and preabsorption controls did not show any immunoreactivity (Gonzalez et al., 2011, Gonzalez et al., 2009, Kerbel et al., 2011). The primary antibody used in this study can detect the unprocessed precursor (NUCB2) in addition to the nesfatin-1 fragment. Therefore, the immunoreactivity detected is presented as NUCB2/nesfatin-1.

2.2.3 Real time quantitative PCR

For real time quantitative PCR analysis, 6 rats were housed in the vivarium from day 13 of pregnancy. Three pregnant dams were sacrificed on day 21 of pregnancy to gather tissues (stomach, duodenum and pancreas) from the embryos on embryonic day 21. Tissues (stomach, duodenum and pancreas) were collected from neonatal pups born from the remaining 3 pregnant dams on postnatal days 1, 6, 13, 20 and 27. Similar to immunohistochemical studies, tissue regions were harvested for RNA extraction. In addition, the whole pancreas including the head, corpus and tail was extracted for total RNA. The tissues collected above were harvested at the same time of the day and thus, this study was repeated thrice to ensure reproducibility in the data obtained. Tissues were also collected from 4 adult male SD rats (n = 4, average

weight = 200.35 g and approximate age: 43–46 days) to compare NUCB2 mRNA expression during each development stage versus adult hood.

Total RNA was extracted from the embryonic, postnatal and adult rat stomach, duodenum and pancreas using the TRIzol® RNA isolation reagent (Invitrogen, Canada). RNA purity was validated by optical density (OD) absorption ratio (OD 260 nm/OD 280 nm) using a Multiskan® Spectrum spectrophotometer (Thermo, Vantaa, Finland). Only samples with an absorption ratio greater than 1.7 were used for cDNA synthesis. Synthesis of cDNAs was conducted using iScript™ cDNA synthesis kit as directed by the manufacturer (BioRad, Canada). The cDNAs were used as templates for reverse transcription-PCR (RT-PCR) with forward and reverse primers and the primer sequences are listed in **Table 2.1**. The qRT-PCR protocol used for NUCB2 was 95 °C for 3 min heat activation, followed by 43 cycles of 95 °C for 30 s denaturation of double stranded DNA (dsDNA), 63 °C for 30 s annealing of primers, and 73 °C for 30 s elongation on the Chromo4™ Multicolor Real-Time PCR Detection System (BioRad, Canada). For the analysis, mRNA expression of NUCB2 was normalized using beta-actin as a housekeeping gene. Based on previous studies conducted (Oliver et al., 2002, Chanoine et al., 2004, Cunha et al., 2006), we used beta-actin as an internal control to normalize the signal of NUCB2 mRNA. When using stomach, duodenal and pancreatic total RNA where mRNA quantification was very precise, the critical threshold values for beta-actin showed no variability. All values were reported as means \pm SEM. Tukey's multiple comparison test was performed to compare the difference between each pair of means of different growth stages with appropriate adjustment for multiple testing. Data were analyzed with GraphPad Prism Version 5.0 (GraphPad Software Inc.). The absolute levels of NUCB2 mRNA for each of the tissues

collected from the adult rat and at different stages of development are depicted in the results section.

Table 2.1. Primers used for quantitative real-time PCR of NUCB2 cDNA from embryonic and prenatal SD rat tissue

Primer	Sequence (5' → 3')
β-actin forward	CTTCTACAATGAGCTGCGTGTG
β-actin reverse	GTCAGGATCTTCATGAGGTAGTCTGTC
NUCB2 forward	CAAGGATAGAACCGCCAGAC
NUCB2 reverse	TTCATCCAGTCTCGTCCTCA

2.2.4 Serum NUCB2/Nesfatin-1 levels

Enzyme-linked immunosorbent assay (ELISA) was used to measure the circulating levels of nesfatin-1. To investigate age-related variation in nesfatin-1 levels, serum samples were collected from the embryos of *ad libitum* rats (n = 8), neonatal pups on postnatal days 1 (n = 8), 6 (n = 5), 13(n = 4), 20 (n = 4), 27 (n = 4) and adult rats (n = 4). Blood samples were collected immediately pre-dissection. In order to preserve the integrity of blood serum proteins, serum was immediately separated from the blood samples were withdrawn (Hanash, 2002). Therefore, to avoid ongoing movement of analytes as well as limit cellular metabolic activities between serum and blood, serum was immediately separated (Boyanton and Blick, 2002) by centrifugation (7000 rpm for 9 min at 4 °C) and stored at – 20 °C. Similar methodology was performed by studies conducted previously (Gonzalez et al., 2011, Gonzalez et al., 2012a). We did not use any anticoagulant such as lithium heparin and ethylenediaminetetraacetic acid (EDTA) to collect plasma. The blood was allowed to clot and centrifuged as mentioned above to separate pure serum, devoid of additives. The collected serum has the same composition of plasma, but is devoid of clotting factors, including fibrinogen. Serum nesfatin-1 levels were measured using the Nesfatin-1 (1–82) (Rat) ELISA kit (Catalog number EK-003-22, Phoenix Pharmaceuticals Inc., California). The limit of assay sensitivity was 1.2 ng/ml for nesfatin-1, with detectable range from 0.1 to 1000 ng/ml. This assay was previously validated in our lab for use in rodents and fish. We used a new tip between repeat samples and ensured that the tip was secure and free of air bubbles. For better intra-assay variation, the serum sample was aspirated and expelled back into the container few times prior to loading. The amount of immunoreactive material was determined using a non-linear regression curve-fit, which was used to quantify and compare the concentration of nesfatin-1 in serum samples during different growth stages versus adulthood.

Although this ELISA kit is able to detect both nesfatin-1 and NUCB2, many studies have used it despite its cross-reactivity (Foo et al., 2010, Stengel et al., 2009a, Gonzalez et al., 2011). Therefore results obtained from using this kit are referred to as NUCB2/nesfatin-1.

2.3 Results

2.3.1 NUCB2/nesfatin-1 IR in the rat stomach

NUCB2/nesfatin-1 IR was detected in the gastric cells present in the oxyntic glands of the stomach at all stages of development. NUCB2/nesfatin-1 immunoreactive cells were rare at embryonic day 21 and relatively less NUCB2/nesfatin-1 immunoreactive cells were observed in the gastric mucosal glands at postnatal days 1 (data not shown), 6 and 13 (data not shown). The NUCB2/nesfatin-1 IR in the oxyntic mucosa progressively increased from postnatal days 20 (**Figures 2.1A–B**), 27 (**Figures 2.1B–C**) to adult (**Figures 2.1D–E**)

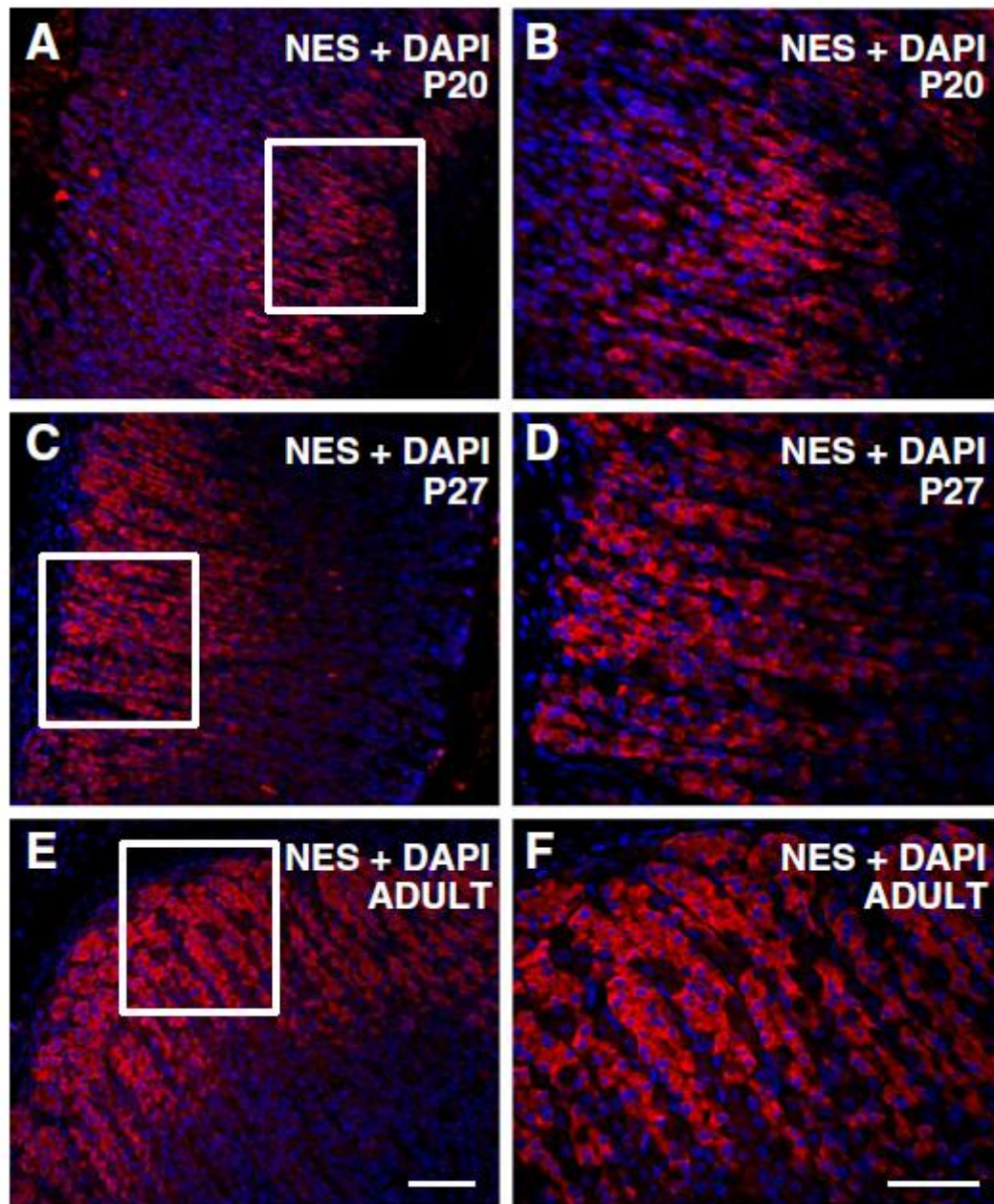


Figure 2.1 NUCB2/nesfatin-1 IR in the rat stomach

Figure 2.1. NUCB2/nesfatin-1 immunohistochemical staining of the rat stomach at postnatal days 20 (A and B), 27 (C and D) and adult (E and F). Figure 1 displays a merged image of cells immunoreactive for NUCB2/nesfatin-1 (red) and DAPI (nuclei; blue). There is a gradual increase in the number of NUCB2/nesfatin-1 immunopositive cells detected in the oxyntic glands of the stomach. Immunohistochemical images display a distributive pattern of endocrine gastric cells staining for NUCB2/nesfatin-1 at postnatal day 20, postnatal day 27, and adult (selected area) final magnification, 20 \times ; and higher power view of the selected area, final magnification, 40 \times . Representative images were taken of 8 slides (16 sections) from 2 neonatal stomach tissues at postnatal days 20, 27, and adult. Scale bar (A, C, and E) = 50 μ m and (B, D and F) = 100 μ m. (E, embryonic day; P, postnatal).

2.3.2 NUCB2/nesfatin-1 IR in the rat duodenum

NUCB2/nesfatin-1 IR was undetectable from embryonic day 21 to postnatal day 6 in the duodenum (data not shown). NUCB2/nesfatin-1 IR was first identified in the enteroendocrine cells of the duodenum beginning from postnatal days 13 to 27. NUCB2/nesfatin-1 IR was detected on postnatal day 13 (**Figures 2.2A–B**) and postnatal day 27 (**Figures 2.2C–D**) in the enteroendocrine cells present in the villi.

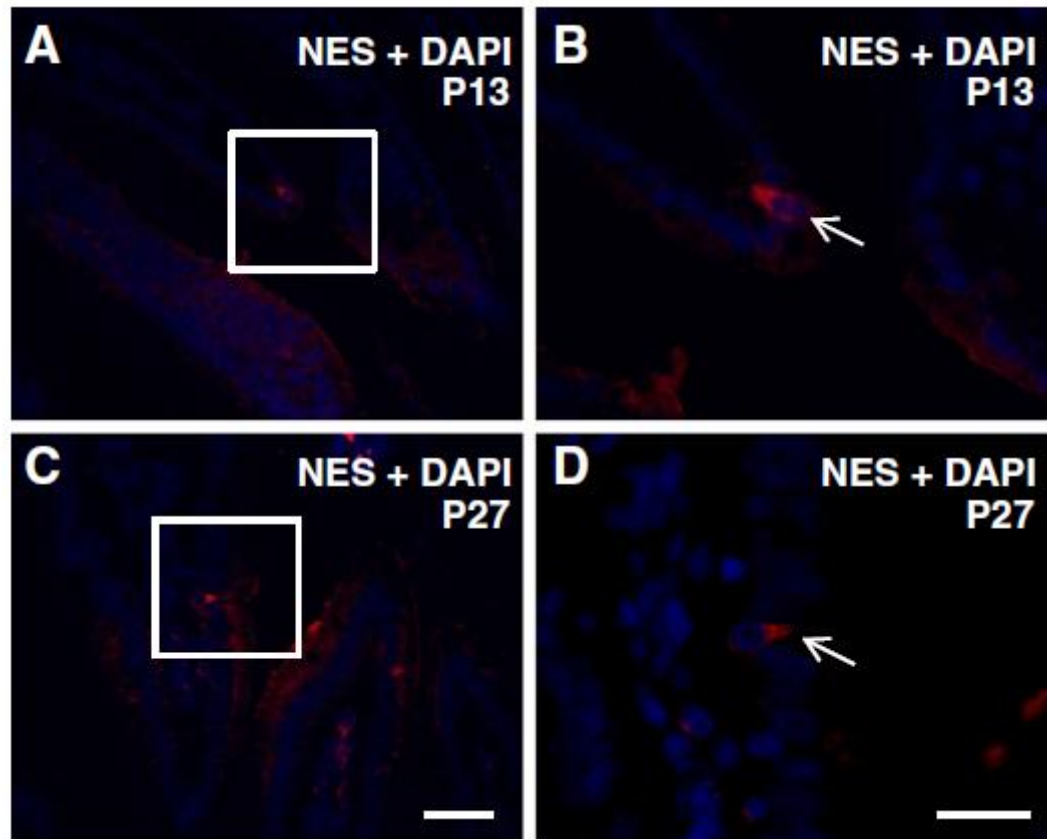


Figure 2.2 NUCB2/nesfatin-1 IR in the rat duodenum

Figure 2.2. NUCB2/nesfatin-1 immunohistochemical staining of the rat duodenum at postnatal days 13 (A and B) and 27 (C and D). Figures 2 displays a merged image of cells immunoreactive for NUCB2/nesfatin-1 (red), and DAPI (nuclei; blue). NUCB2/nesfatin-1 IR was detected in the enteroendocrine cells of the duodenal submucosa. Immunohistochemical images of enteroendocrine cells staining for NUCB2/nesfatin-1 at postnatal day 13 and postnatal day 27, (selected area) final magnification, 40 \times ; and higher power view of the selected area, final magnification, 100 \times . The open arrows point at enteroendocrine cells immunoreactive for NUCB2/nesfatin-1 in the villi of the rat duodenum. Representative images were taken of 8 slides (16 sections) from 2 neonatal duodenal tissues at postnatal days 13 and 27. Scale bar (A and C) = 50 μ m and (B and D) = 100 μ m. (E, embryonic day; P, postnatal).

2.3.3 Co-localization of NUCB2/nesfatin-1 and Chromogranin A (CgA) IR in the rat duodenum

Co-localization of NUCB2/nesfatin-1 and CgA was not observed at postnatal days 13 and 27 (data not shown), but co-expression was evident in the enteroendocrine cell present in the adult duodenal villi (**Figures 2.3A–F**).

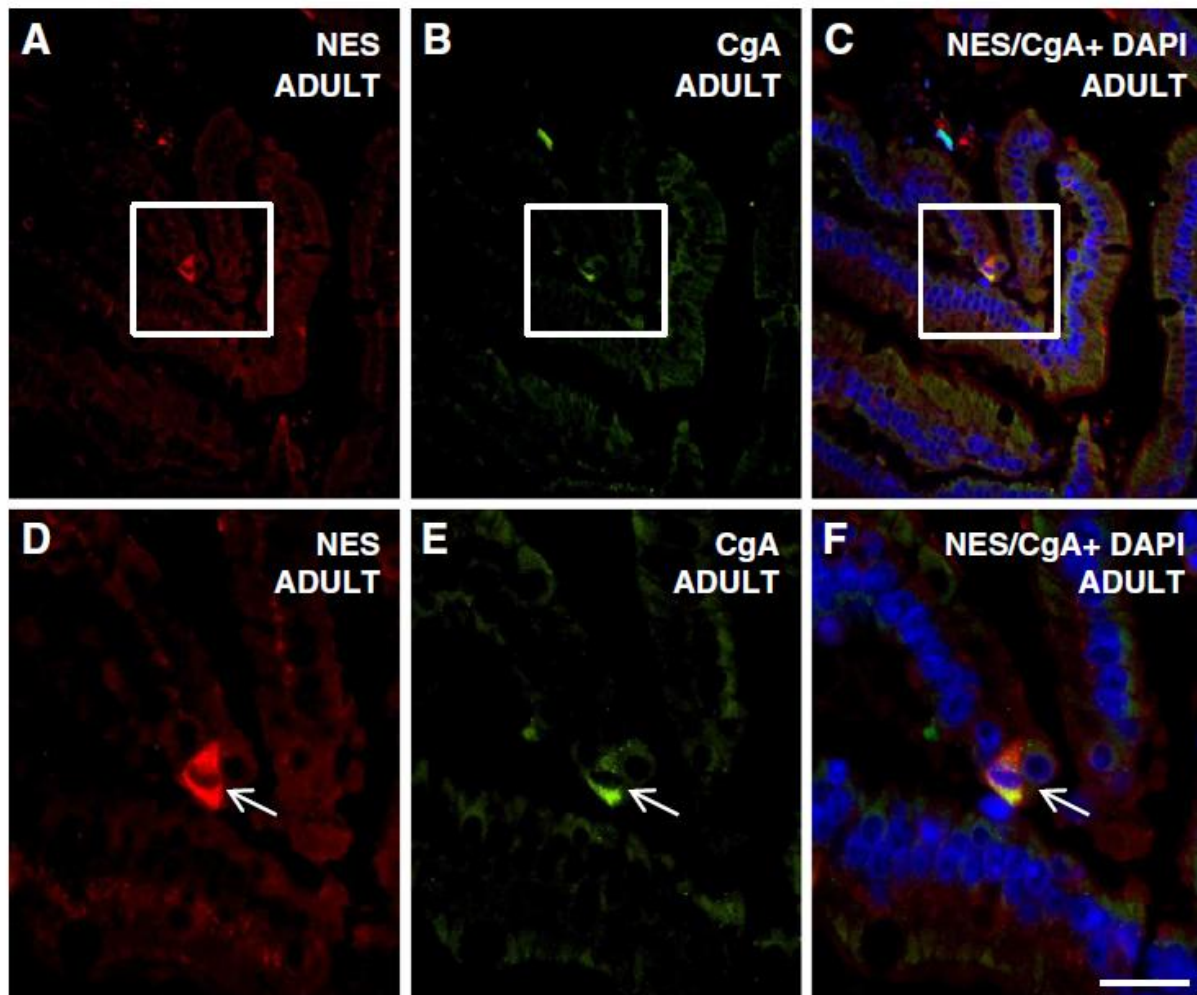


Figure 2.3 Co-localization of NUCB2/nesfatin-1 and Chromogranin A (CgA) IR in the rat duodenum

Figure 2.3. Co-localization of NUCB2/nesfatin-1 and chromogranin A (CgA) immunohistochemical staining of an adult rat duodenum. Figure 3 displays cells immunoreactive for NUCB2/nesfatin-1 (A, D; red), CgA (B, E; green) and the merged image of nesfatin-1, CgA and DAPI (C, F; yellow). NUCB2/nesfatin-1 and CgA IR was detected in the enteroendocrine cells of the adult duodenal submucosa. Immunohistochemical images of enteroendocrine cells staining for NUCB2/nesfatin-1, CgA at adult stage, (selected area) final magnification, 40x; and higher power view of the selected area, final magnification, 100x. The open arrows point at enteroendocrine cells immunoreactive for NUCB2/nesfatin-1 (D), CgA (E) and NUCB2/nesfatin-1 co-expressed with CgA (F) in the villi of the rat duodenum. Representative images were taken of 4 slides (8 sections) from adult duodenal tissues. Scale bar (A, B and C) = 50 μ m and (D, E and F) = 100 μ m.

2.3.4 NUCB2/nesfatin-1 IR in the rat pancreas

NUCB2/nesfatin-1 immunostaining was observed at all developmental stages in the rat endocrine pancreas. At embryonic day 21 (**Figure 2.4A**), NUCB2/nesfatin-1 immunoreactive islet cells were observed in the pancreatic tissue. These immunoreactive islet cells appear to be individual NUCB2/nesfatin-1 immunopositive endocrine cells. At postnatal day 1 (**Figure 2.4B**) and postnatal day 6 (**Figure 2.4C**), NUCB2/nesfatin-1 immunoreactive islet cells were identified in a number of regions where small clusters of islet-cell groups were observed in the pancreatic tissue. Clusters of endocrine cells immunopositive for NUCB2/nesfatin-1 were observed at postnatal day 13 (**Figure 2.4D**). At postnatal day 20 (**Figure 2.4E**), postnatal day 27 (**Figure 2.4F**), and adult (**Figure 2.4G**), there was an increase in NUCB2/nesfatin-1 IR, which was more abundant than what was detected in postnatal day 13.

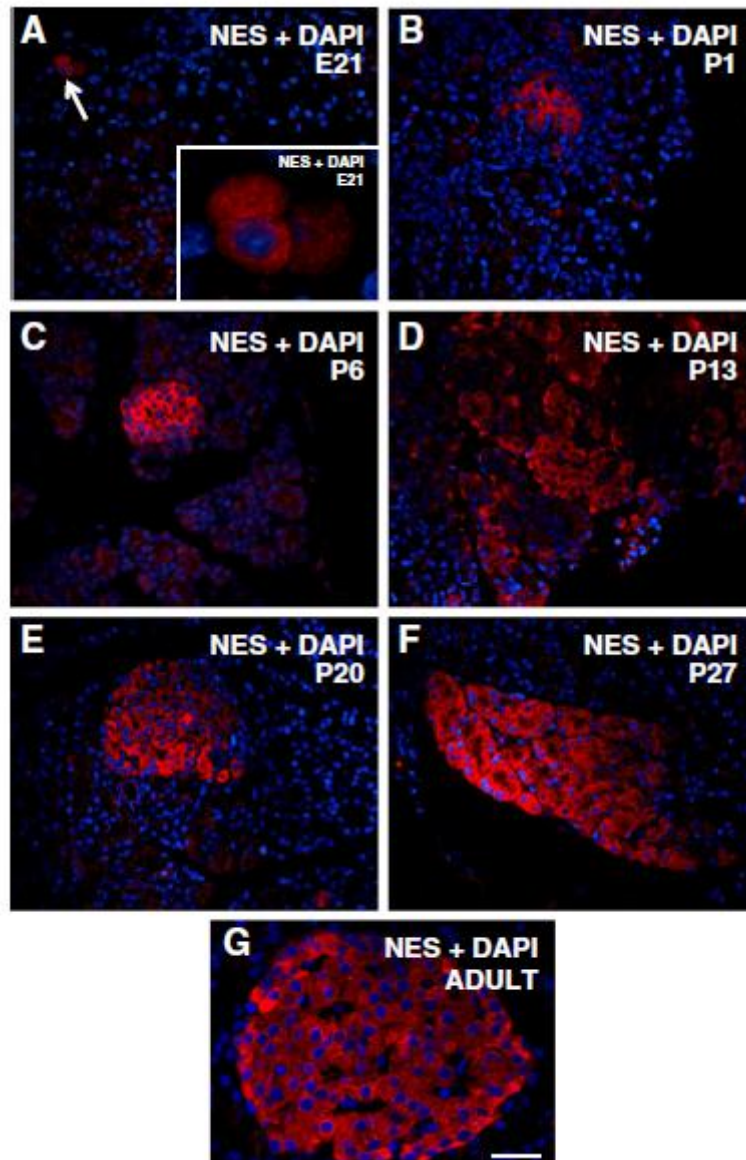


Figure 2.4 NUCB2/nesfatin-1 IR in the rat pancreas

Figure 2.4. NUCB2/nesfatin-1 immunohistochemical staining of the rat pancreas at embryonic day 21 (A) and postnatal days 1 (B), 6 (C), 13 (D), 20 (E), 27 (F) and adult (G). Pancreatic islet cells immunoreactive for NUCB2/nesfatin-1 (red) and DAPI (nuclei; blue) are shown in A–G. Image A displays a magnified image of a NUCB2/nesfatin-1 immunoreactive cell in the pancreatic tissue at embryonic day 21 represented by an (white) arrow. Representative images were taken of 8 slides (16 sections) from an adult, 3 embryonic and 5 neonatal pancreatic tissues at embryonic day 1 and postnatal days 1, 6, 13, 20 and 27. Scale bar = 50 μ m. (E, embryonic day; P, postnatal).

2.3.5 Co-localization of NUCB2/nesfatin-1 and insulin IR in the rat pancreas

Some, but not all islet cells immunopositive for insulin (**Figures 2.5B, E, H**) showed NUCB2/nesfatin-1 IR (**Figures 2.5A, D, G**), co-localizing both proteins on embryonic day 21 (**Figure 2.5C**), postnatal days 1 (**Figure 2.5F**) and 6 (**Figure 2.5I**). But all NUCB2/nesfatin-1 immunopositive islet cells were immunoreactive for insulin (**Figures 2.5C, F, I**). During development, on postnatal days 13, 20 and 27 all islet cells immunoreactive for insulin (**Figures 2.6B, E, H**) were immunopositive for NUCB2/nesfatin-1 (**Figures 2.6A, D, G**), showing co-localization of both proteins (**Figures 2.6C, F, I**).

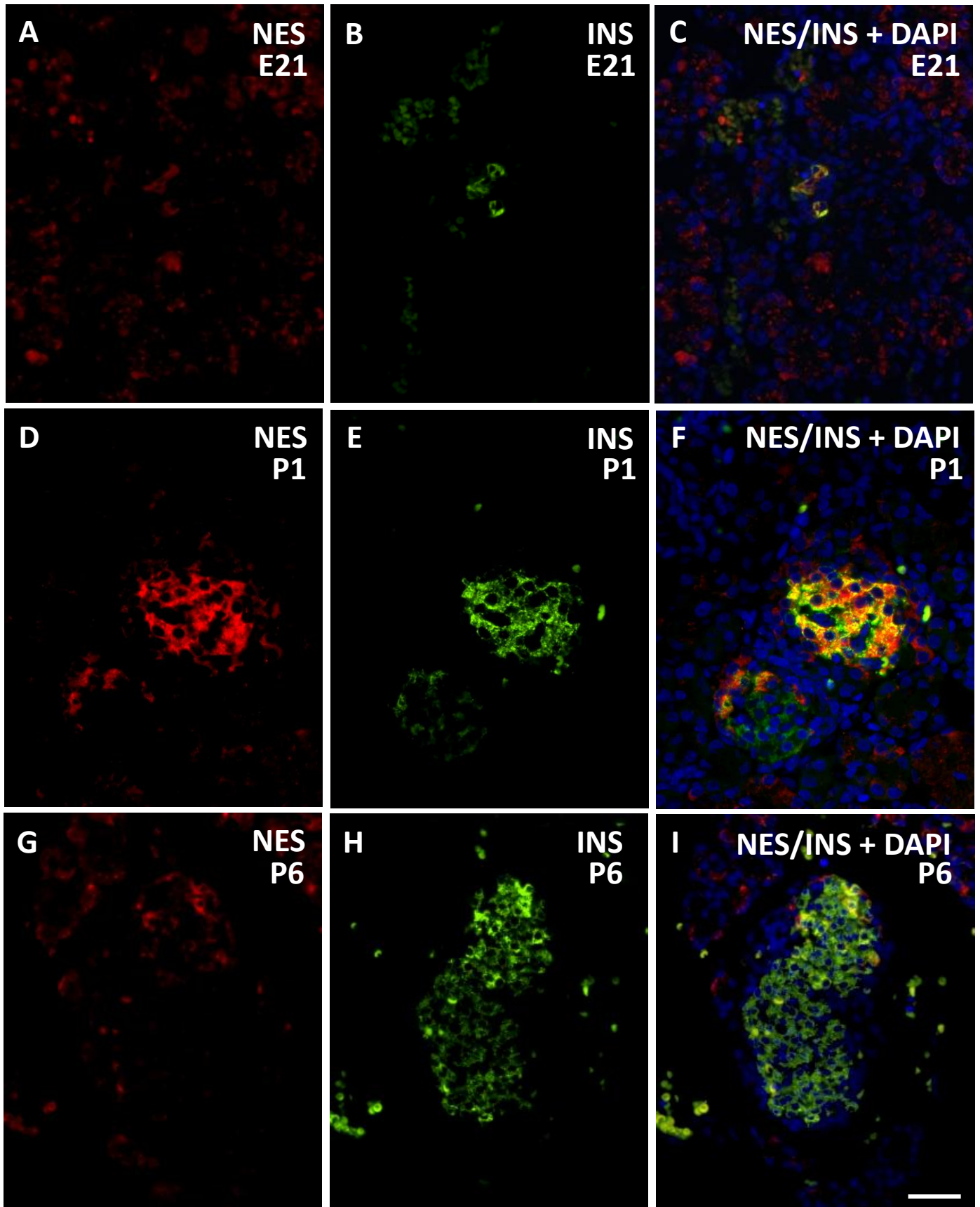


Figure 2.5 Co-localization of NUCB2/nesfatin-1 and insulin IR in the rat pancreas

Figure 2.5. Co-localization of NUCB2/nesfatin-1 and insulin immunohistochemical staining of the rat pancreas at embryonic day 21 (A, B, C) and postnatal days 1 (D, E, F) and 6 (G, H, I). Islet cells immunoreactive for NUCB2/nesfatin-1 (A, D, G; red), insulin (B, E, H; green), and the merged image of nesfatin-1, insulin and DAPI (C, F, I; yellow). Not all insulin immunopositive islet cells are positive for NUCB2/nesfatin-1 but all NUCB2/nesfatin-1 immunopositive cells are immunoreactive for insulin. Representative images were taken of 8 slides (16 sections) from 3 embryonic and 2 neonatal pancreatic tissues at embryonic day 1 and postnatal days 1 and 6. Scale bar = 50 μ m. (E, embryonic day; P, postnatal).

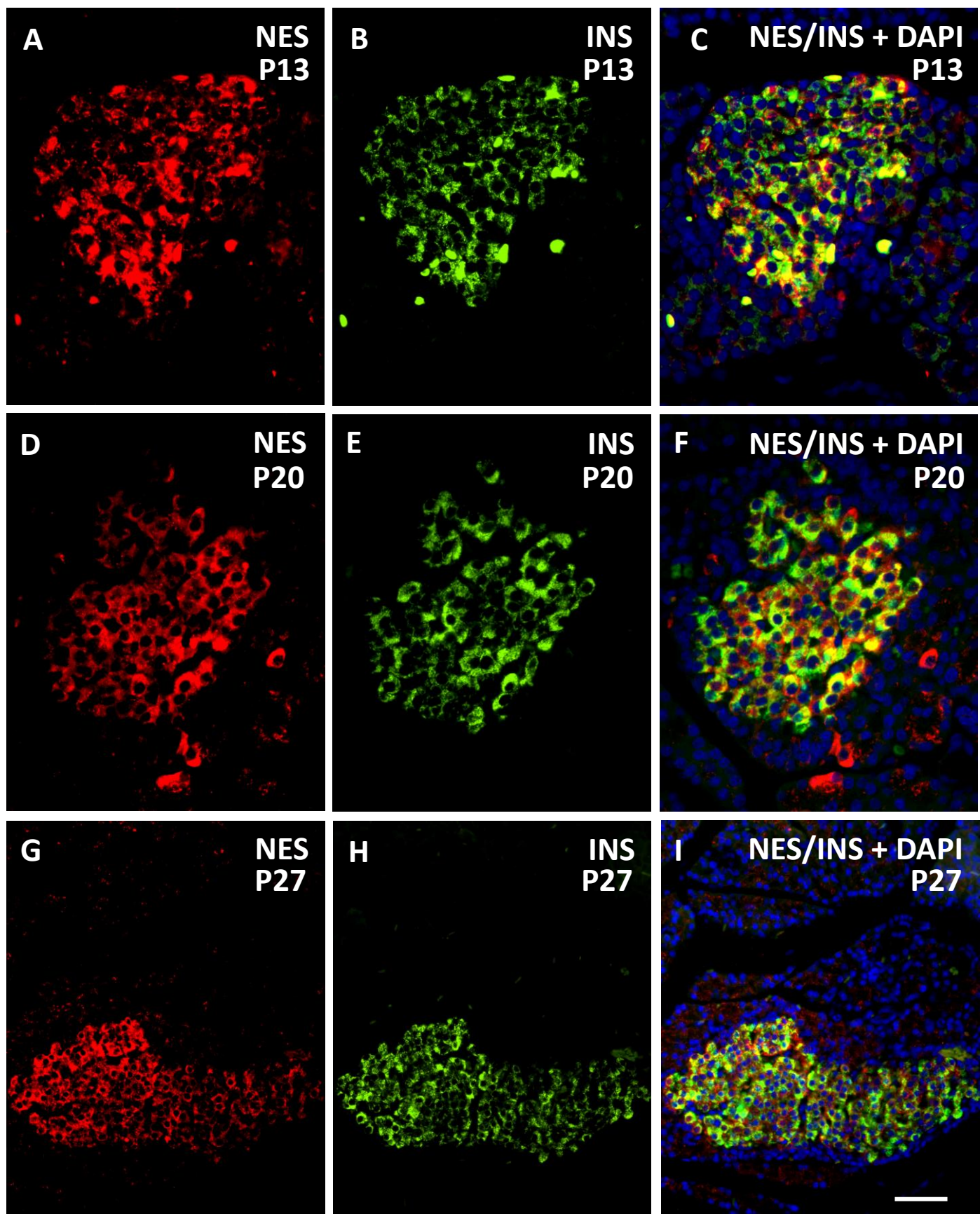


Figure 2.6 Co-localization of NUCB2/nesfatin-1 and insulin IR in the rat pancreas

Figure 2.6. Co-localization of NUCB2/nesfatin-1 and insulin immunohistochemical staining of the rat pancreas at postnatal days 13 (A, B, C), 20 (D, E, F) and 27 (G, H, I). Islet cells immunoreactive for NUCB2/nesfatin-1 (A, D, G; red), insulin (B, E, H; green), and the merged image of NUCB2/nesfatin-1, insulin and DAPI (C, F, I; yellow). A gradual increase in islet cells immunopositive for insulin are also immunoreactive for NUCB2/nesfatin-1 at postnatal days 13, 20 and 27 compared to embryonic day 1 and postnatal days 1 and 6 (Figures 5). Immunohistochemical images of the islet cells staining for NUCB2/nesfatin-1 at postnatal day 13 and postnatal day 20 are at final magnification, 40 ×; and lower final magnification, 20 ×, at postnatal day 27. All NUCB2/nesfatin-1 immunopositive cells are immunoreactive for insulin. Representative images were taken of 8 slides (16 sections) from 3 neonatal pancreatic tissues at postnatal days 13, 20 and 27. Scale bar = 50 μm. (E, embryonic day; P, postnatal).

2.3.6 Developmental expression of NUCB2 mRNA in the rat gastroenteropancreatic tissues

In the rat stomach, no significant differences were found in the expression of NUCB2 mRNA at various stages of development (**Figure 2.7A**). In contrast, NUCB2 mRNA expression in the rat duodenum on postnatal day 27 was higher than the NUCB2 mRNA expression in the adult duodenum (**Figure 2.7B**). No significant difference in NUCB2 mRNA expression was detected in the pancreas during developmental stages tested (**Figure 2.7C**).

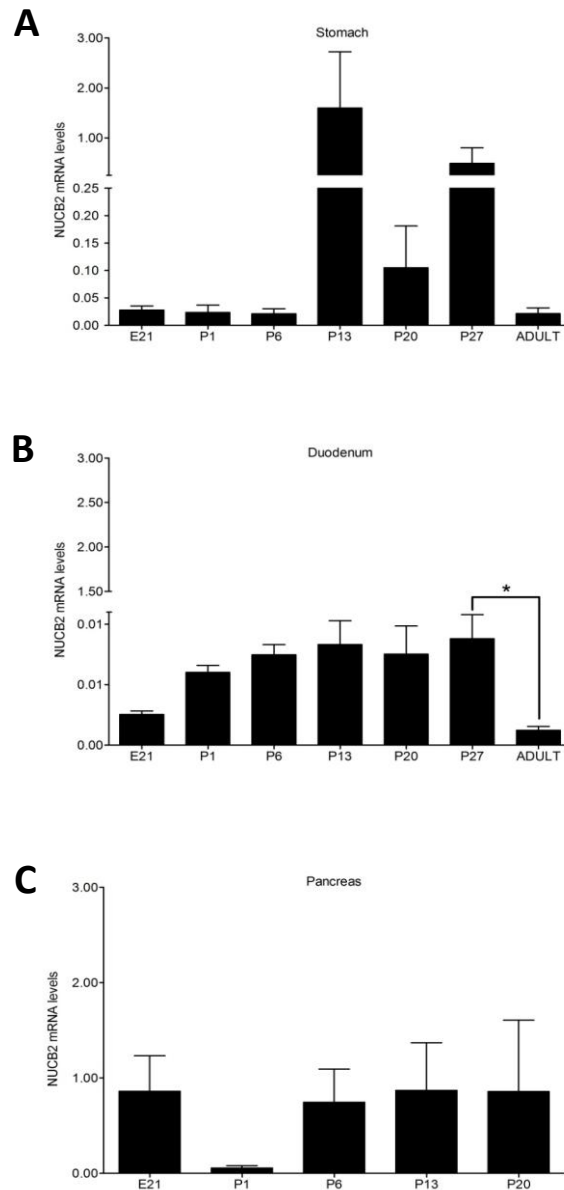


Figure 2.7 Developmental expression of NUCB2 mRNA in the rat gastroenteropancreatic tissues

Figure 2.7. Analysis of NUCB2 mRNA levels at different development stages in the stomach (A; E21 (n = 7), P1 (n = 7), P6 (n = 6), P13 (n = 7), P20 (n = 6), P27 (n = 6) and Adult (n = 4)), duodenum (B; E21 (n = 5), P1 (n = 7), P6 (n = 7), P13 (n = 7), P20 (n = 6), P27 (n = 6) and Adult (n = 4)) and the pancreas (C; E21 (n = 5), P1 (n = 7), P6 (n = 7), P13 (n = 7), and P20 (n = 3)) of Sprague Dawley (SD) Rats tissues. (E, embryonic day; P, postnatal). (*): The mRNA levels of NUCB2 determined by real-time PCR showed that NUCB2 mRNA expression in the duodenum at postnatal day 27 was higher than the NUCB2 mRNA expression in the adult ($p < 0.05$, ANOVA followed by Tukey's Multiple Comparison Test).

2.3.7 Serum NUCB2/nesfatin-1 levels during development

Serum NUCB2/nesfatin-1 levels on embryonic day 21 and postnatal day 1 were significantly lower than adults and levels found in postnatal days 6, 13, 20 and 27. No significant differences were found in serum NUCB2/nesfatin-1 levels in adults and postnatal days 6, 13, 20 and 27 (**Figure 2.8**).

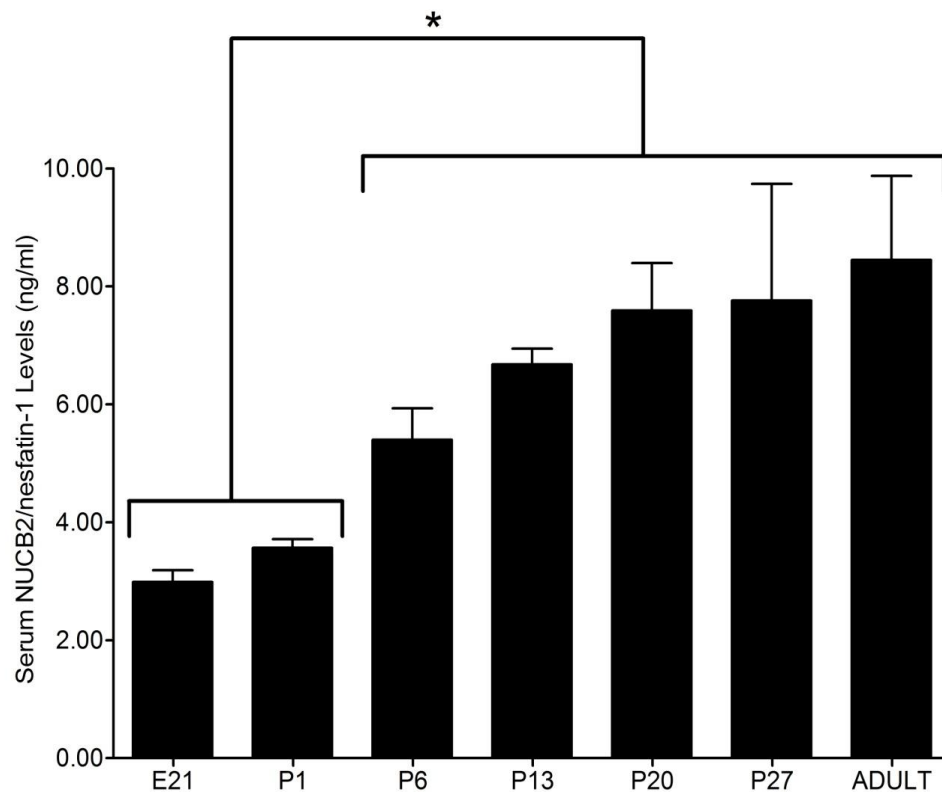


Figure 2.8 Serum NUCB2/nesfatin-1 levels during development

Figure 2.8. Circulating levels of serum NUCB2/nesfatin-1 in Sprague Dawley (SD) rats during various development stages (E21 (n = 8), P1 (n = 8), P6 (n = 5), P13 (n = 4), P20 (n = 4), P27 (n = 4) and Adult (n = 4)). (E, embryonic day; P, postnatal). (*): The serum NUCB2/nesfatin-1 levels pre-birth at embryonic day 21 and postnatal day 1 are lower than postnatal days 6, 13, 20, 27 and adult ($p < 0.05$, ANOVA followed by Tukey's Multiple Comparison Test).

2.4 Discussion

The results presented here is the first report on the developmental expression of NUCB2 mRNA and NUCB2/nesfatin-1 like immunoreactivity (IR) in the gastroenteropancreatic tissues and serum. The NUCB2/nesfatin-1 IR detected in the stomach is in agreement with previous reports that showed NUCB2/nesfatin-1 IR in the lower third and middle regions of the gastric oxyntic glands (Stengel et al., 2009b, Zhang et al., 2010). A large number of gastric endocrine cells displayed NUCB2/nesfatin-1 IR in the lower third regions of the gastric oxyntic glands in the Institute of Cancer Research (ICR) mice (Zhang et al., 2010). The distribution of NUCB2/nesfatin-1 IR cells changed with age: the gastric mucosa of suckling rats at postnatal day 13 displayed a few number of NUCB2/nesfatin-1 IR cells in the lower segments of the mucosa which was detected in the glandular base, but were gradually localized from the glandular base to the core of the gastric gland from postnatal day 20 to adult stage. It could be thus suggested that NUCB2/nesfatin-1 immunopositive cells extend with increasing age from the base to the middle portion of the gastric gland and correlates with high levels of NUCB2 mRNA at postnatal days 20 and 27. In the adult rat, NUCB2/nesfatin-1 IR was abundant, but NUCB2 mRNA was drastically reduced. This age-related variation of NUCB2/nesfatin-1 protein expression in the stomach during the perinatal period displays an ontogenic pattern of NUCB2/nesfatin-1 IR that could be closely related to the weaning period that is consistent with the change in diet from milk to rat chow.

Similar gastric expression profile for other metabolic hormones was also reported. For example, the gastric mucosa of Wistar rats on postnatal day 15 displayed increased leptin immunoreactivity in the basal part of the gastric glands but decreased immunoreactivity was evident in the superficial layer of the epithelium lining the mucosa (Oliver

et al., 2002). At postnatal day 21, leptin immunostaining in the gastric mucosa of weaned rats detected an increase in IR in many glandular endocrine cells of the mucosa. This reflects how increased amount of endogenous leptin is produced by the stomach coinciding with the transition from suckling to solid chow diet (Oliver et al., 2002), similar to what was observed in this study. Furthermore, studies on the ontogenic expression of ghrelin in SD rats showed that ghrelin immunoreactive cells were rare at embryonic day 21 and increased progressively until weaning (Walia et al., 2009). These findings on leptin and ghrelin are in general very similar to the stomach expression of NUCB2/nesfatin-1 determined in this study. An increase in NUCB2 mRNA expression was also observed at postnatal day 13 indicating the change of nutritional diet from milk to solid rat chow. In addition, remains of solid chow food were identified in the stomach lumen beginning from postnatal day 13, which is in coincident with the increase in NUCB2/nesfatin-1 expression suggesting that it would propose to be an ontogenically programmed period. These results suggest that macronutrients may affect the expression of NUCB2/nesfatin-1.

In the duodenum, NUCB2/nesfatin-1 IR was not detected at embryonic day 21 and postnatal days 1 and 6, but NUCB2/nesfatin-1 protein expression gradually increased during the second postnatal week. From postnatal days 13 to 27, NUCB2/nesfatin-1 IR was detected in the enteroendocrine cells of the duodenum. Co-localization of NUCB2/nesfatin-1 and chromogranin A (CgA) was not detected at postnatal days 13 and 27, but was co-expressed in the enteroendocrine cell found in the adult duodenal villi. Chromogranin A plays a major role in the secretion of peptide hormones and neurotransmitters of the trans-Golgi network and is expressed mostly in all endocrine and neuroendocrine cells (Hendy et al., 1995). Co-expression of NUCB2/nesfatin-1 and CgA in the intestinal cells of the adult duodenal villi suggests that the

NUCB2/nesfatin-1 IR cells are enteroendocrine cells. In addition, NUCB2 mRNA expression in the duodenum at postnatal day 27 was higher than adult NUCB2 mRNA expression. Although the function of NUCB2/nesfatin-1 in the duodenum is currently unknown, a gradual increase in the expression of NUCB2/nesfatin-1 IR and NUCB2 mRNA expression in the duodenum is observed, which suggests that NUCB2/nesfatin-1 protein expression in the duodenum may be involved in the absorption of nutrients (Zhang et al., 2010), as well as modulating the secretion of intestinal hormones. NUCB2/nesfatin-1IR is also observed in the Brunner's glands of SD rats and ICR mice (Zhang et al., 2010). These glands are involved in secreting alkaline products such as bicarbonate and mucus that aid in maintaining the structural and biological environment of the gastrointestinal tract (Krause, 2000). Further evaluation is required to elucidate the significance of NUCB2/nesfatin-1 expression in the enteroendocrine cells and Brunner's glands of the duodenal submucosa.

In fetuses, glucose metabolism depends on the mother (King, 2006), although these immature β -cells would synthesize and secrete less insulin than adults (Navarro et al., 2007) which was similar to the results of this study that detected less insulin IR during embryonic day 21. At birth, as the postnatal pups acquire glucose sensitivity, the endocrine islet cells of the pancreas begin to secrete insulin in order to modulate glucose metabolism. With development, response to glucose sensitivity increases reaching maturity after weaning (Asplund, 1973, Hole et al., 1988, Weinhaus et al., 1995). At postnatal day 20, as pups begin to wean, insulin secretion increases in order to accommodate their insatiable appetite (Navarro-Tableros et al., 2007). In this study, we observed age-related variation in insulin IR at all developmental stages. The day of birth (postnatal day 1) and postnatal day 20 are two important stages for pancreatic morphogenesis and glucose induced insulin secretion (Navarro-Tableros et

al., 2007, Ayuayo-Mazzucato et al., 2006). In this study, not all insulin immunopositive cells were immunoreactive for NUCB2/nesfatin-1 at embryonic day 21, postnatal day 1 and postnatal day 6. Gradually with age, all insulin immunopositive islet cells were immunoreactive for NUCB2/nesfatin-1 during the third and fourth week of development.

In adult SD rats, the pancreas, stomach and duodenum appear to be major sites of NUCB2/nesfatin-1 synthesis and secretion. There are also other tissues such as the esophagus, liver, small intestine and colon that may secrete nesfatin-1 (Zhang et al., 2009). The primary source of circulating NUCB2/nesfatin-1 levels is currently unknown. The abundant expression of NUCB2/nesfatin-1 in the gastroenteropancreatic tissues suggests a prominent role for these tissues in the synthesis and secretion of NUCB2/nesfatin-1. It was found that serum NUCB2/nesfatin-1 levels at embryonic day 21 and postnatal day 1 were significantly low in comparison to following postnatal days 13, 20 and 27, and adult. Overall, serum NUCB2/nesfatin-1 levels increased with age gradually reaching levels of adult at postnatal day 27 which is consistent, in part, with NUCB2/nesfatin-1 protein expression in the pancreas. In the gastroenteropancreatic tissues, the most abundant NUCB2/nesfatin-1 IR was detected in the later postnatal days and in adults. It is possible that NUCB2/nesfatin-1 secreted from the pancreatic tissue is released into circulation (Gonzalez et al., 2009) to regulate insulin secretion and glucose homeostasis. It is also possible that NUCB2/nesfatin-1 plays a role in the development of the tissue itself.

2.5 Conclusions

These findings demonstrate that circulating levels of serum nesfatin-1 increase with development. NUCB2/nesfatin-1 IR in the pancreas and gastrointestinal tract could possibly contribute to the gradual increase in serum NUCB2/nesfatin-1 levels. In addition, NUCB2/nesfatin-1 colocalizes with insulin in the islet β -cells at all developmental stages in an age-dependent manner suggesting that NUCB2/nesfatin-1 plays an important role in glucose metabolism during growth. NUCB2 mRNA levels in the duodenum at postnatal day 27 are higher than the adult NUCB2 mRNA expression, however metabolic effects of NUCB2 expression in the duodenum still remain elusive. This is the first study that has focused on the importance of NUCB2/nesfatin-1 expression in the developmental stages of rats. These results collectively suggest that NUCB2/nesfatin-1 has important age- and tissue-specific role in the developmental physiology of rats.

Transition

The next chapter focuses on my second objective: To elucidate the developmental expression of GOAT mRNA and colocalization of ghrelin, GOAT, NUCB2/nesfatin-1, PC 1/3 and PC 2 immunoreactivity in the pancreas during fetal and postnatal periods of Sprague Dawley rats. As discussed earlier, both ghrelin and nesfatin-1 are derived from their precursors by posttranslational processing by prohormone convertases (PC) 1/3 and 2. Ghrelin requires an acylation of its third serine residue to elicit many of its actions which is modified by an enzyme called ghrelin O-acyl transferase (GOAT). Both these peptides are expressed in the endocrine cells of the pancreatic islets. In addition, both ghrelin and nesfatin-1 are produced in the same endocrine cells, but are stored and secreted from distinct vesicles within the gastric mucosa. Most importantly both peptides have opposing actions in regulating glucose metabolism and whole body energy balance. Thus far, there is no research on the developmental expression of GOAT, and the co-expression of both NUCB2/nesfatin-1 and prohormone convertases in the pancreas. We found that ghrelin and GOAT, as well as NUCB2/nesfatin-1 and PCs are co-expressed in the endocrine cells of the pancreatic islets. ***This is the first study that provided information on GOAT mRNA and protein expression, and NUCB2 and PC immunoreactivity during development in the rat pancreas.*** Our findings suggest that ghrelin and nesfatin-1 expressed in the endocrine pancreas in an age-dependent manner during development of rats.

Publication: Mohan, H., Gasner, M., Unniappan, S. 2015. Ghrelin, Ghrelin-O-Acyl Transferase, Nucleobindin-2/Nesfatin-1 and Prohormone Convertases in the Pancreatic Islets of Sprague Dawley Rats During Development. Peptides. Manuscript Number: PEPTIDES-D-15-00119. Submission Status: Under Review.

Contributions: Michaela Gasner and Haneesha Mohan equally conducted all *in vivo* studies, collected and processed the tissue samples for RNA extraction, conducted immunohistochemistry and protein assays. I analysed the data and wrote the first draft of the manuscript. Suraj Unniappan helped with the experimental design, provided the research infrastructure, edited the manuscript and funded the project to completion.

Chapter 3

Ghrelin, Ghrelin-O-Acyl Transferase, Nucleobindin-2/Nesfatin-1 and Prohormone Convertases in the Pancreatic Islets of Sprague Dawley Rats During Development

3.1 Introduction

Hormones play a major role in the formation, growth and maintenance of an organ during development (Larsson, 1998, O'Dowd and Stocker, 2013). Tissue specific ontogenic expression of these hormones and its processing enzymes provide insight into their potential functional roles (Reddy et al., 1988). The islets of Langerhans in the endocrine pancreas of mammals are composed of cells that are a major source of glucoregulatory hormones that include insulin producing beta (β) cells and glucagon producing alpha (α) cells. Several additional peptides with endocrine actions have also been reported in the pancreatic islets of rodents and humans (Drucker, 2007, Reddy et al., 1988). Among these, ghrelin, mainly considered as an insulinostatic hormone (Dezaki et al., 2011), and nesfatin-1, an insulinotropic peptide (Gonzalez et al., 2011), are important regulators of metabolism and glucose homeostasis (Li et al., 2013, Su et al., 2010). The pancreatic islets are also ghrelin producing, in a cell named epsilon (ϵ) cells (Prado et al., 2004). Ghrelin is derived from preproghrelin after posttranslational processing by prohormone convertase (PC) 1/3. It was discovered as the first endogenous ligand of the growth hormone secretagogue receptor 1a (GHS-R1a) (Kojima et al., 1999). The amino acid sequence of ghrelin is highly conserved in humans (Kojima et al., 1999) and other species (Kojima et al., 2005, Stengel et al., 2012b). There is a unique acylation of the third serine residue (Ser 3) in ghrelin by n-octanoic acid (Kojima et al., 1999). This acylation is necessary for the binding of ghrelin to GHS-R1a and is critical for many of its biological functions. The enzyme responsible

for its acylation is ghrelin O-acyl transferase (GOAT) (Gutierrez et al., 2008, Mohan and Unniappan, 2013, Shlimun and Unniappan, 2011, Yang et al., 2008). GOAT belongs to the family of membrane-bound O-acyl transferase (MBOAT) that is localized within the membranes of the endoplasmic reticulum (Gutierrez et al., 2008, Yang et al., 2008). In contrast, GOAT proteins also share a high homology in the amino acid sequence from humans to zebrafish (Yang et al., 2008).

During fetal and postnatal development, ghrelin expression in the pancreas changes. In the developing mouse and rat pancreas, ghrelin immunoreactivity can be detected as early as embryonic day 9.5 and 15, peaking just before birth (Hill et al., 2009, Wierup et al., 2004). Ghrelin mRNA expression and total ghrelin concentration are elevated in the fetal pancreas, and is more abundant than in the fetal stomach (Hayashida et al., 2002). Immunohistochemical studies performed on pancreatic islets during embryonic day 21 to postnatal day 13 displayed few preproghrelin immunoreactive cells, at which they began to reduce and become untraceable with increase in age (Wali et al., 2009). Ghrelin is primarily expressed in ϵ -cells and glucagon (α -cells) producing cells produced in the fetal pancreatic islets (Hill et al. 2009, Prado et al., 2004). During pancreatic development, insulin and ghrelin were expressed in their specific cell types and were not co-localized at any postnatal period (Walia et al., 2009). The developmental expression of GOAT in the rodent pancreas is currently unknown.

Nesfatin-1 is an 82 amino acid peptide originally discovered from the rat hypothalamic extracts (Oh-I et al., 2006). PC1/3 and PC2 cause NUCB2 to be cleaved to nesfatin-1 (1-82 amino acids) (Oh-I et al., 2006). Nesfatin-1 is a meal responsive insulinotropic peptide playing a major role in glucose homeostasis (Li et al., 2013, Su et al., 2010] and insulin secretion (Gonzalez et al., 2011). Plasma nesfatin-1 concentrations are inversely correlated with glucose

levels in rats and diabetic humans (Li et al., 2010). NUCB2 mRNA expression and NUCB2/nesfatin-1 immunoreactivity was significantly increased in the pancreatic islets of diet induced obese, type 2 diabetic mice (Gonzalez et al., 2011). NUCB2 mRNA and NUCB2/nesfatin-1 immunoreactivity was attenuated, but still detectable in the pancreatic islets of STZ-induced type 1 diabetic mice (Gonzalez et al., 2011). We found that some, not all beta cells were immunoreactive for NUCB2/nesfatin-1 at embryonic day 21, postnatal day 1 and postnatal day 6. However, in post-natal day 27 and in adults all beta cells were immunopositive for NUCB2/nesfatin-1 (Mohan and Unniappan, 2012). The endocrine pancreas, especially the islet beta cells appears an abundant source of endogenous NUCB2/nesfatin-1. However, there is paucity of information on whether the prohormone processing enzymes PC1/3 and PC2, and NUCB2/nesfatin-1 are co-localized in the endocrine pancreas during development.

To date, the pancreatic islet specific ontogenic co-expression of prohormone convertases and ghrelin, and the expression of NUCB2/nesfatin-1 were studied separately. Developmental expression of GOAT in rodent pancreas is yet to be determined. Similarly, ontogenic patterns of co-expression of both prohormone convertases and NUCB2/nesfatin-1 are also unclear. It is important to understand how two metabolic peptides with opposing actions on insulin secretion and its processing enzymes that make them biologically active are locally produced within the pancreas. Therefore, the main objective of this research is to determine the expression of GOAT mRNA and colocalization of ghrelin, GOAT, NUCB2/nesfatin-1, PC 1/3 and PC 2 immunoreactivity in the pancreas during fetal and postnatal periods of Sprague Dawley rats. These findings indicate that the GOAT mRNA expression, as well as the islet cell specific immunolocalization of all proteins tested, are dependent on specific developmental stages. This

study, for the first time, shed light on the co-expression of NUCB2/nesfatin-1 and prohormone convertases, and GOAT and ghrelin in rat islets of Langerhans.

3.2 Material and Methods

3.2.1 Animals

Timed pregnant Sprague Dawley (SD) rats (Charles River Laboratories, St Constant, QU, Canada) were housed from day 13 of pregnancy in a 12h light:12h dark cycle (lights off at 7 PM and on at 7 AM), temperature and humidity controlled vivarium. Pregnant dams had *ad libitum* access to standard rat chow (60% carbohydrate, 27% protein, and 13 % fat; with energy density = 3.43 kcal/g; Lab Diets Inc., St. Louis, MO) and water. All animal experiments complied with the Canadian Council of Animal Care guidelines, and were approved by the institutional animal care committee.

3.2.2 Immunohistochemistry

Immunohistochemical studies were conducted as described in Chapter 2, section 1.2.2.2, with the following differences in procedures or antibodies used. These pancreatic sections were then incubated with mouse anti-ghrelin (Catalogue number ab 57222; 1:100 dilution; Abcam, Massachusetts) and with rabbit anti-GOAT (Catalogue number H-032-12; 1:100 dilution; Phoenix Pharmaceuticals, California) for 24 hours at room temperature. In addition, pancreatic sections were also incubated with goat anti-NUCB2 (Catalogue number sc-65160; 1:100 dilution; Santa Cruz Biotechnology, CA), and with either rabbit anti-PC 1/3 or rabbit anti-PC 2 (1:500 dilution; antibodies kindly donated by Dr. Iris Lindberg, University of Maryland, Baltimore, USA). All primary and secondary antibodies were diluted in antibody diluent reagent (DakoCytomation, Mississauga, Ontario). All slides were subsequently washed three times with 1x Phosphate Buffer Solution (PBS) and incubated with goat monoclonal anti-mouse FITC IgG (Heavy and Light Chain) (Green-Ghrelin; Catalogue number ab 6785; 1:100 dilution; Abcam, Massachusetts), goat anti-rabbit Texas Red® IgG (Red-Nesfatin-1; Catalogue number TI-1000;

1:100 dilution; Vector Laboratories, California), and/or Alexa Fluor 594 donkey anti-goat IgG (H+L) (Catalogue Number A11058; 1:100 dilution; Invitrogen Corporation Carlsbad, CA) secondary antibodies for 1 hour at room temperature. Slides were washed, mounted in DAPI and imaged as described earlier. Approximately 8 slides (from multiple rats) containing two sections of the pancreas from each developmental stage were stained using the above protocol and analyzed. Only representative images of tissues from each stage staining for ghrelin, GOAT, NUCB2/nesfatin-1, PC 1/3 and PC 2 are shown in the results section. Slides incubated with the secondary antibodies only were used as a negative control for NUCB2/nesfatin-1, PC 1/3, PC 2, ghrelin and GOAT (data not shown). NUCB2/nesfatin-1 antibody has been tested and validated in our lab. Preabsorption controls do not show any immunoreactivity (Kerbel and Unniappan, 2011, Gonzalez et al., 2010, Gonzalez et al., 2011). The primary antibody used in this study can bind to both the precursor NUCB2 and processed nesfatin-1. Therefore, the immunoreactivity detected is presented as NUCB2/nesfatin-1.

3.2.3 Real Time Quantitative PCR

For real time quantitative PCR analysis, 4 rats were housed in the vivarium from day 13 of pregnancy. Whole pancreatic tissues were harvested for total RNA extraction. Two pregnant dams were sacrificed on day 21 of pregnancy to gather the pancreatic tissue from the embryos on embryonic day 21. Pancreatic tissues were collected from neonatal pups born from the remaining 2 pregnant dams on postnatal days 1, 6, 13, 20 and 27. Pancreatic tissues were also collected from 4 adult male SD rats ($n = 4$, average weight = 200.35 grams and approximate age: 43-46 days) to analyze GOAT mRNA expression during each developmental stage and adulthood. Total RNA was extracted from the embryonic, postnatal and adult rat pancreas using the TRIzol RNA isolation reagent (Invitrogen, Canada). RNA purity was validated by optical density (OD)

absorption ratio (OD 260 nm/OD 280 nm) using a Multiskan® Spectrum spectrophotometer (Thermo, Vantaa, Finland). Only samples with an absorption ratio greater than 1.7 were used for cDNA synthesis. Synthesis of cDNAs was achieved using the iScript™ cDNA synthesis kit (BioRad, Canada), as directed by the manufacturer. The quantitative RT-PCR (qRT-PCR) protocol used for GOAT was 95° C for 3 minutes heat activation, followed by 95 cycles of 95° C for 30 seconds denaturation of double stranded DNA (dsDNA), 63° C for 30 seconds annealing of primers, and 73° C for 30 seconds elongation. The reaction for each sample was run in duplicates. For the analysis, GOAT mRNA expression was normalized using beta-actin as the housekeeping gene as described previously in our work using pancreatic samples (Mohan and Unniappan, 2012). The mRNA quantification was very precise, and the critical threshold values for beta-actin showed no variability. The gene expression data was obtained using the Pfaffl method (Pfaffl, 2001). The specificity of the amplified gene product was determined by analyzing the melting curve to limit the expression of non-specific gene products. All values were reported as mean \pm SEM. One-way ANOVA followed by Dunnett's multiple comparison test were performed to compare GOAT mRNA expression at each developmental stage. Data were analyzed with GraphPad Prism Version 5.0 for Windows (GraphPad Software, La Jolla California, USA).

3.3 Results

3.3.1 Ghrelin and GOAT Immunoreactivity in the Rat Pancreas

At postnatal day 20, 27 and the adult stage, some, but not all islet cells immunopositive for GOAT (**Figures 3.1B, 3.1E, 3.1H**) showed ghrelin immunoreactivity (**Figures 3.1A, 3.1D, 3.1G**), co-localizing both peptides (**Figures 3.1C, 3.1F, 3.1I**). No or very low staining for ghrelin and GOAT were observed in the pancreas selected from E21-P13 days (data not shown). No immunostaining was observed in the exocrine pancreas (**Figures 3.1A-I**).

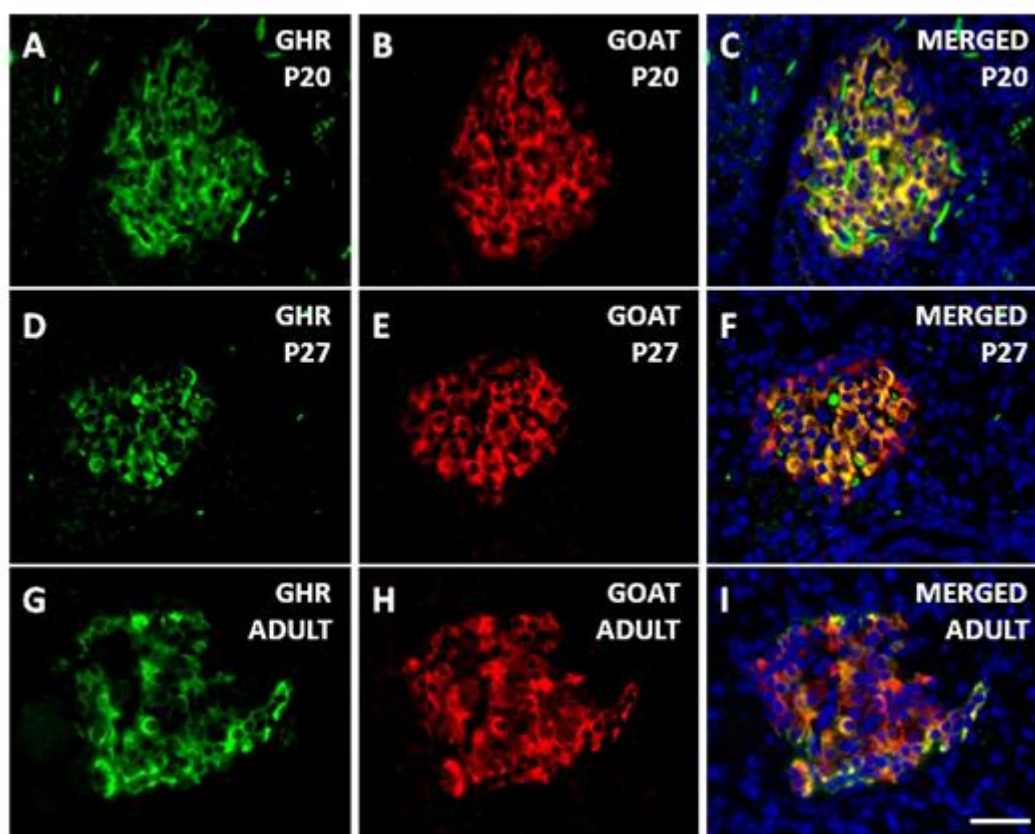


Figure 3.1 Co-localization of Ghrelin and GOAT in the Pancreatic Islets

Figure 3.1. Immunostaining displays that not all islet cells immunopositive for GOAT (Figure B, E and H; red) showed ghrelin immunoreactivity (Figure A, D and G; green) on postnatal day 20, 27 and adult, co-localizing for protein, enzyme and DAPI (Figure C, F and I; yellow). Representative images were taken of 8 slides (16 sections) from 2 neonatal pancreatic tissues at postnatal days 20, 27 and adult. Scale bar = 50 μ m. (P, Postnatal)³

3.3.2 NUCB2/nesfatin-1, PC1/3 and PC2 Immunoreactivity in the Rat Pancreas

At embryonic day 21, postnatal day 13, 20 and 27, a large number of islet cells immunopositive for NUCB2/nesfatin-1 (**Figures 3.2A, 3.2D, 3.2G, 3.2J**) showed PC1/3 immunoreactivity (**Figures 3.2B, 3.2E, 3.2H, 3.2K**), co-localizing for both protein and enzyme at these stages (**Figures 3.2C, 3.2F, 3.2I, 3.2L**). Majority of islets cells immunopositive for NUCB2/nesfatin-1 (**Figures 3.3A, 3.3D, 3.3G**) were also co-immunoreactive for PC2 (**Figures 3.3B, 3.3E, 3.3H**), at embryonic day 21, postnatal days 13 and 20 (**Figures 3.3C, 3.3F, 3.3I**). But at postnatal day 27, NUCB2/nesfatin-1 immunoreactivity was only observed in the core of pancreatic islets (**Figure 3.3J**), but PC2 staining was only observed in a ring of cells in the periphery (**Figure 3.3K**). No colocalization of NUCB2/nesfatin-1 and PC2 was observed at postnatal day 27 (**Figure 3.3L**). No immunostaining was observed in the exocrine pancreas (**Figures 3.2A-L and 3.3A-L**).

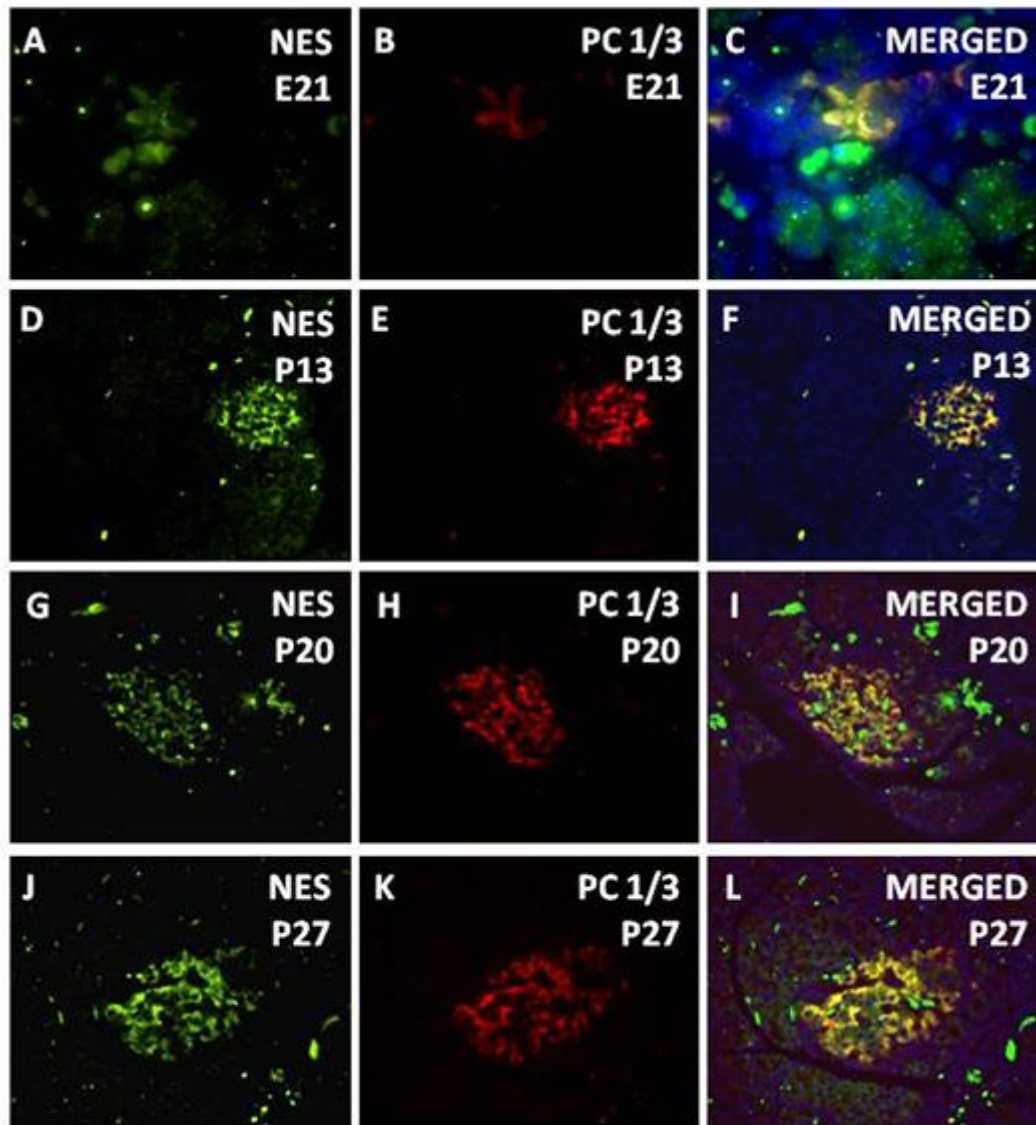


Figure 3.2 Co-localization of NUCB2/nesfatin-1 and PC 1/3 in the Pancreatic Islets

Figure 3.2. Co-localization of NUCB2/nesfatin-1 and PC 1/3 immunohistochemical staining of the rat pancreas at embryonic day 21 (A, B, C), postnatal day 13 (D, E, F), 20 (G, H, I) and 27 (J, K, L). Islet cells immunoreactive for NUCB2/nesfatin-1 (A, D, G, J; green), PC 1/3 (B, E, H, K; red), and the merged image of NUCB2/nesfatin-1, PC 1/3 and DAPI (C, F, I, L; yellow). Representative images were taken of 8 slides (16 sections) from 3 embryonic and 2 neonatal pancreatic tissues at embryonic day 21 and postnatal days 13, 20 and 27. Scale bar = 50 μ m. (E, Embryonic Day; P, Postnatal)

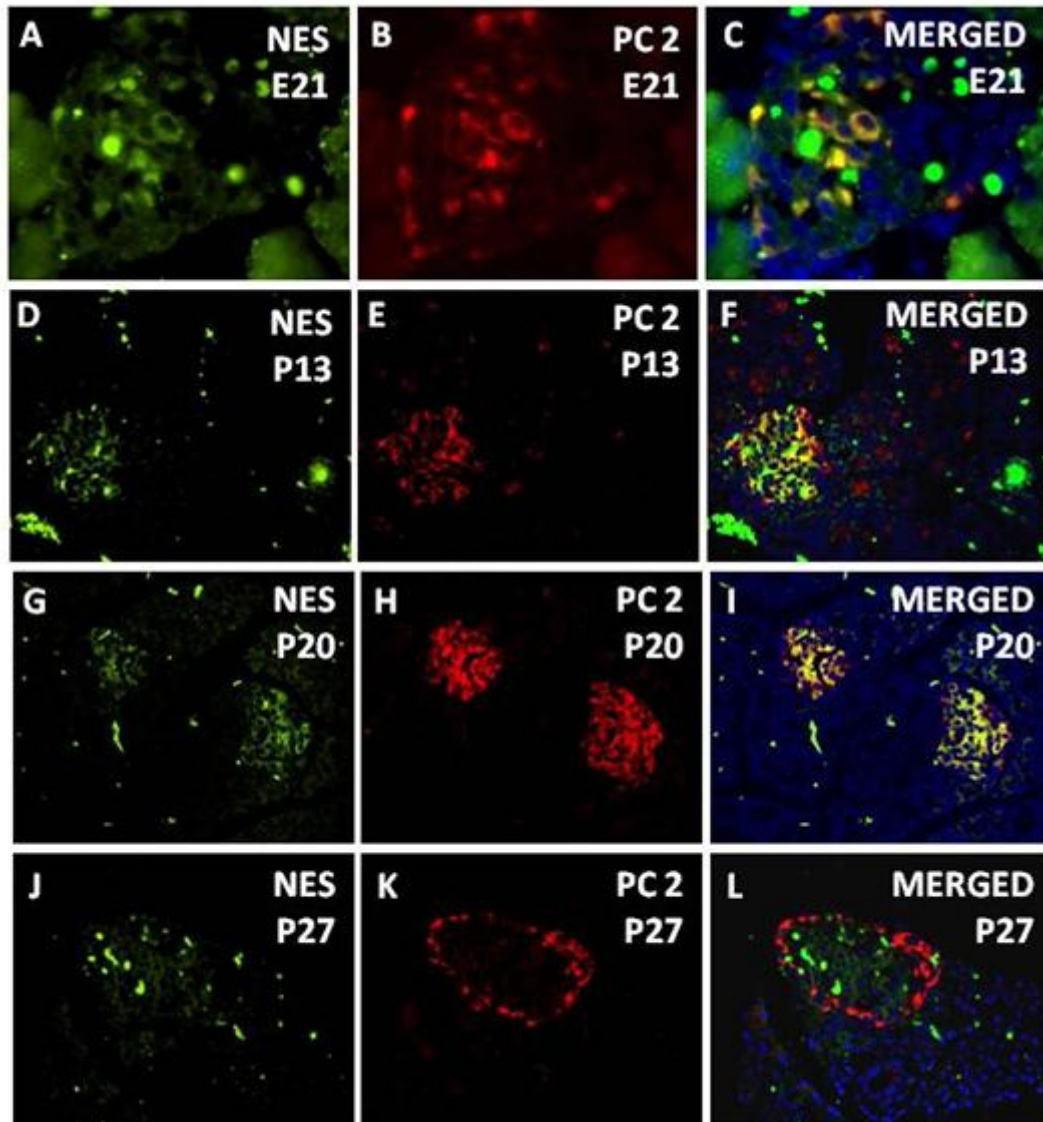


Figure 3.3 Localization of NUCB2/nesfatin-1 and PC 2 in the Pancreatic Islets

Figure 3.3. Co-localization of NUCB2/nesfatin-1 and PC 2 immunohistochemical staining of the rat pancreas at Embryonic day 21 (A, B, C), Postnatal day 13 (D, E, F) and 20 (G, H, I). At postnatal day 27 prohormone convertase 2 was only evident in the glucagon producing alpha-cells and NUCB2/nesfatin-1 was observed in the core expressed in the insulin producing beta-cells (J, K, L). Islet cells immunoreactive for NUCB2/nesfatin-1 (A, D, G, J; green), PC 2 (B, E, H, K; red), and the merged image of NUCB2/nesfatin-1, PC 2 and DAPI (C, F, I, L; yellow). . Representative images were taken of 8 slides (16 sections) from 3 embryonic and 2 neonatal pancreatic tissues at embryonic day 21 and postnatal days 13, 20 and 27. Scale bar = 50 μ m. (E, Embryonic Day; P, Postnatal)

3.3.3 Developmental Expression of GOAT mRNA in the Rat Pancreas

GOAT mRNA expression in the pancreas at postnatal day 27 is higher than its expression from embryonic day 21 to postnatal day 13 and adult stage (**Figure 3.4**).

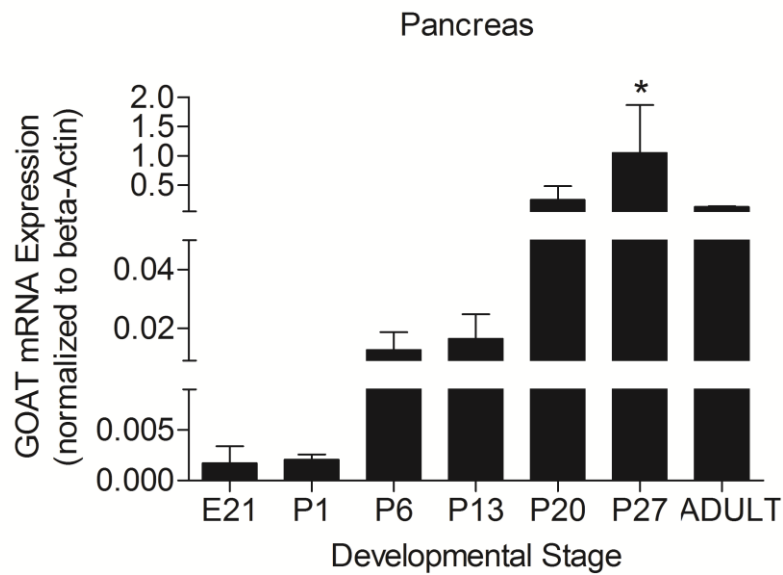


Figure 3.4 GOAT mRNA levels at different development stages

Figure 3.4. Analysis of GOAT mRNA levels at different development stages in pancreas (E21 (n=5), P1 (n=7), P6 (n=7), P13 (n=7), and P20 (n=3)) of Sprague Dawley (SD) Rats tissues. (E, Embryonic Day; P, Postnatal). In the pancreas, GOAT mRNA expression at postnatal day 27 is higher than mRNA expression levels from embryonic day 21 to postnatal day 13 and adult GOAT mRNA expression levels. (denoted by an asterisk; $p < 0.05$, ANOVA followed by Dunnett's multiple comparison test).

3.4 Discussion

The results presented here show the developmental stage-specific expression of ghrelin, NUCB2/nesfatin-1, GOAT, PC 1/3 and PC 2 in the pancreatic islets of rats. It is the first report on developmental stage specific co-expression of GOAT and ghrelin, and NUCB2/nesfatin-1 and prohormone convertases. In the pancreatic islet, both ghrelin and GOAT immunostaining was prominent from postnatal day 20 onwards. A major share of, but not all, islet cells in the pancreas that are immunopositive for GOAT showed ghrelin immunoreactivity on postnatal days 20 and 27 and in adults. Similar immunohistochemical studies found ghrelin immunoreactivity in islet cells of rat pancreas gradually increasing with development (Walia et al., 2009). It was reported that GOAT mRNA increases with age and body weight gain in male and female rats (Al-Massadi et al., 2010). Post birth, as neonates begin to gain glucose sensitivity, insulin is secreted in the islet cells in order to regulate glucose metabolism (Hole et al., 1988, Asplund, 1973, Weinhaus et al., 1995). The co-presence of both ghrelin and GOAT within the islets suggests the emergence of the ghrelinergic system in the pancreas around the same time the functional beta cells gain secretory activity. From a functional point of view, the presence of GOAT within the same cells enhances the chances for acylation of ghrelin to take place locally. It is likely that around the same time when insulin secretion begins, the ghrelin regulation of insulin release also commences. Ghrelin expression has been reported in the developing pancreas of rats (Walia et al., 2009). While ghrelin immunoreactivity decreased in post-natal days in this study ((Walia et al., 2009), our results indicate abundant expression of ghrelin and GOAT in post-natal days. This discrepancy is likely due to the difference in antibodies used. Similar to our results, ghrelin localization in islet beta cells was detected found before (Volante et al., 2002). We found that GOAT mRNA expression also follows a similar pattern, with the highest

expression found in P27. This result on GOAT mRNA expression is in line with our immunohistochemistry results, where most abundant expression of GOAT immunoreactivity was also detected in adults. This result provides further evidence for a gradual progression of GOAT synthesis in pancreatic islets. Considering that GOAT is essential for the acylation of ghrelin, which is critical for many of its biological activities, this new information about ghrelin and its modifying enzyme is significant.

While ghrelin is primarily considered insulinostatic (Dezaki et al., 2011), nesfatin-1 is insulinotropic (Gonzalez et al., 2011). We previously reported a developmental stage specific expression of NUCB2/nesfatin-1 in the gastroenteropancreatic tissues of rats (Mohan and Unniappan, 2012). However, whether the processing enzymes that produce nesfatin-1 from its precursor NUCB2 co-localizes with it is currently unknown. Here we report the co-localization of NUCB2/nesfatin-1 and PC1/3 and PC2 in rat pancreas. We found colocalization of NUCB2/nesfatin-1 with PC 1/3 at embryonic day 21 and postnatal day 13, 20 and 27. Similarly, colocalization of NUCB2 with PC2 was detected at embryonic day 21 and postnatal day 13 and 20. However, at postnatal day 27, PC2 was only evident in a ring of cells in the periphery of islets. This staining pattern is in agreement with our own (Gonzalez et al., 2009, Stengel et al., 2009b) and other findings (Foo et al., 2010) of nesfatin-1 exclusively in the islet beta cells, but not in the glucagon producing alpha-cells. Previous studies suggest that PC2 plays an important role in the development of β -cells (Vincent et al., 2003). Its major substrates are proglucagon and proinsulin (Rouille et al., 1995, Rouille et al., 1994) and thus, its immunoreactivity are detected in a population of islet cells expressing multiple hormones at early developmental stages dependent on growth. It appears that either PC2 or PC1/3, or both enzymes are available to process nesfatin-1 during development and in adulthood. Nesfatin-1 co-localizes PCs in the rat

hypothalamus (Oh-I et al., 2006), suggesting the processing of NUCB2 to nesfatin-1 in the brain. In fact, brain is the only tissue from which the processed nesfatin-1 was purified. The co-expression of PCs and NUCB2/nesfatin-1 in the pancreatic islets provides further evidence for endocrine pancreas as a source of endogenous nesfatin-1.

3.5 Conclusions

The outcome of this research for the first time demonstrates the relationships of GOAT and ghrelin, and nesfatin-1, and their processing enzymes in the pancreatic islets during developmental stages of rats. In the pancreas, GOAT mRNA expression at postnatal day 27 is higher than expression levels at rest of the developmental stages tested. These histological findings showing the local presence of processing enzymes for NUCB2 and ghrelin are suggestive of the endocrine pancreas as an endogenous source of these hormones with opposing metabolic actions. In conclusion, this article presented novel aspects of ghrelin, NUCB2/nesfatin-1 and its processing enzymes in fetal and postnatal periods. Further studies are required to gain a deeper understanding of the age- and tissue-specific roles of ghrelin and nesfatin-1 during development of rats.

Transition

Thus far, this thesis research focused on characterizing the developmental expression of NUCB2/nesfatin-1, and processing enzymes in gastroenteropancreatic tissues. These tissues appear predominant sources of meal responsive, endogenous nesfatin-1. However, the regulation of NUCB2/nesfatin-1 is poorly understood. The hypothesis is that macronutrients of diets differentially regulate endogenous NUCB2/nesfatin-1 in a tissue-specific manner. The aims of chapter 4 is to determine how different nutrients modulate NUCB2/nesfatin-1 secretion *in vitro* in cultured stomach ghrelinoma (MGN3-1) cells from mice and *in vivo* in male mice. As explained earlier, development and nutritional status can influence the transcriptional activity of genes tissue specifically regulating energy balance. First, we characterized MGN3-1 cells as nesfatin-1 secreting cells with the NUCB2 processing machinery, suggesting that this cell line is useful for studying nesfatin-1 biology. We found expression of NUCB2, ghrelin and prohormone convertases in MGN3-1 cells. We found that effects of diets on the expression of endogenous NUCB2/nesfatin-1 were myriad. Our results indicated that the synthesis and secretion of nesfatin-1 were altered by relative amounts of nutrients and such effects were dependent on the amount of nutrients, tissues and time of the day or duration of treatment. ***This was the first study that focused on nutrient regulation of NUCB2/nesfatin-1.*** Our results indicated that NUCB2/nesfatin-1 was modulated by nutrients in a tissue specific manner.

Publication: Mohan, H., Ramesh, N., Mortazavi, S., Le, A., Unniappan, S. 2014. Nutrients differentially regulate nucleobindin-2/nesfatin-1 *in vitro* in cultured stomach ghrelinoma (MGN3-1) cells and *in vivo* in male mice. PLoS One, 9, e115102.

Contributions: Haneesha Mohan conducted all *in vivo*, and *in vitro* studies, collected and processed the tissue samples for RNA extraction and performed protein assay. H. Mohan also performed protein assays, analyzed data and wrote the first draft of the manuscript. Naresh Ramesh helped with protein extraction and Western blot detection. Naresh Ramesh and Anthony Le conducted immunocytochemistry and microscopy on MGN3 cells. Sima Mortazavi processed

tissues for immunohistochemistry, conducted immunohistochemistry and microscopy. Suraj Unniappan helped with the experimental design, assisted with *in vivo* studies, provided the research infrastructure, edited the manuscript and funded the project to completion.

Chapter 4

Nutrients Differentially Regulate Nucleobindin-2/Nesfatin-1 *In Vitro* in Cultured Stomach Ghrelinoma (MGN3-1) Cells and *In Vivo* in Male Mice

4.1 Introduction

Nesfatin-1 [NEFA/NUCB2-encoded satiety and fat-influencing protein-1] is a potent anorexigenic peptide implicated in the regulation of energy balance and glucose homeostasis (Oh-I et al., 2006, Gonzalez et al., 2011). It is an 82 amino acid peptide derived from the precursor protein, nucleobindin-2 (NUCB2) (Oh-I et al., 2006). NUCB2 is composed of 396 amino acids, consisting of two EF hand motifs and a DNA binding domain (Oh-I et al., 2006, Barnikol-Watanabe et al., 1994). Post-translational processing by prohormone convertases (PC 1/3 and PC 2) causes NUCB2 to be cleaved into three peptides, nesfatin-1 (1-82 amino acids), nesfatin-2 (85-163 amino acids), and nesfatin-3 (166-396 amino acids). NUCB2/nesfatin-1 amino acid sequence is highly conserved across vertebrates (Gonzalez et al., 2010). NUCB2/nesfatin-1 is found in various hypothalamic nuclei that are involved in energy metabolism, such as the arcuate nucleus, paraventricular nucleus, supraoptic nucleus, lateral hypothalamic area and zona incerta (Kohno et al., 2008, Maejima et al., 2009). Insulin producing beta cells co-express nesfatin-1 in the pancreatic islets of rats and mice (Gonzalez et al., 2009, Gonzalez et al., 2011, Mohan and Unniappan, 2012), suggesting that nesfatin-1 could play an important role in insulin secretion and glucose homeostasis (Gonzalez et al., 2011). Ghrelin and NUCB/nesfatin-1 are colocalized in the gastric oxyntic mucosal glands in rodents (Stengel et al., 2009b) and humans (Stengel et al., 2013). NUCB2 mRNA expression in purified gastric mucosal endocrine cells was found to be higher than in the brain of rats (Stengel et al., 2009b). The full length NUCB2 protein was observed in the small and large intestines and liver of male rats, and

ICR mice (Zhang et al., 2010). The wide distribution of NUCB2/nesfatin-1 in central and peripheral tissues points to a role for nesfatin-1 in regulating metabolism.

Daily administration of nesfatin-1 caused extended reduction in food intake and body weight (Oh-I et al., 2006). Intracerebroventricular administration of NUCB2 suppresses food intake, body weight and subcutaneous, mesenteric and epididymal fat mass in adult rats in a dose dependent manner. In addition, NUCB2 knockdown in rats by infusing antisense morpholino oligonucleotide (as-MON) caused an increase in appetite and body weight (Oh-I et al., 2006). Intra-paraventricular nucleus injection of nesfatin-1 reduces cumulative food intake at 1 and 3 hours (Maejima et al., 2009). Intraperitoneal injections of nesfatin-1 resulted in a reduction in food intake in leptin resistant *db/db* mice and high fat diet fed mice (Kohno et al., 2008). Nesfatin-1 is composed of 3 structural fragments and only the mid-fragment (residues 24-53; M30) of nesfatin-1 is involved in producing anorectic responses (Shimizu et al., 2009, Stengel et al., 2012a). Together, these results provide clear evidence that support satiety effects of nesfatin-1.

Nesfatin-1 is a meal responsive glucoregulatory hormone (Stengel et al., 2009a, Stengel et al., 2009b), and pancreatic islets of rats release NUCB2 in response to glucose (Foo et al., 2010). In human studies, glucose treated subjects had higher basal nesfatin-1 levels compared to control subjects (Li et al., 2010). In MIN6 cells, a 4-fold increase in nesfatin-1 levels was observed when the cells were incubated in high glucose (16.7 mM) compared to low glucose (2.0 mM) (Gonzalez et al., 2011). Nesfatin-1 enhanced glucose stimulated insulin secretion from cultured MIN6 cells that were incubated in high glucose than in low glucose in a dose dependent manner (Gonzalez et al., 2011). In the pancreas of streptozotocin (STZ)-injected mice with Type 1 Diabetes, it was found that both NUCB2 and preproinsulin mRNA expression were

significantly lower (Gonzalez et al., 2011). In contrast, enhanced nesfatin-1 co-localization with insulin was found in the islet beta cells of high-fat diet-induced obese mice with Type 2 Diabetes. Nesfatin-1 has tissue specific effects on glucose uptake in rat adipocytes and muscle (Gonzalez et al., 2012a). Overall, nesfatin-1 exerts important roles in regulating whole body glucose and energy homeostasis.

While nesfatin-1 is emerging as an important meal responsive peptide (Oh et al., 2006, Stengel et al., 2009a, Stengel et al., 2009b, Gonzalez et al., 2011), what triggers its secretion remained unclear. What diet components trigger the post-meal secretion of nesfatin-1? This question remains unaddressed. The main focus of this study was to determine how different nutrients can modulate NUCB2/nesfatin-1 *in vitro* in cultured stomach ghrelinoma (MGN3-1) cells from mice and *in vivo* in male mice. The results from the *in vitro* studies indicate that MGN3-1 cells respond differently to nutrients in secreting NUCB2/nesfatin-1 and ghrelin. Similarly, acute or chronic intake of nutrients does influence NUCB2 mRNA expression and NUCB2/nesfatin-1 release in a diet specific manner.

4.2 Material and Methods

4.2.1 Ethics Statement

All studies using animals complied with the Canadian Council of Animal Care guidelines, and were approved by the Animal Research Ethics Board of the University of Saskatchewan (Protocol Number 2012-0033).

4.2.2 *In Vitro* Studies

Mouse stomach ghrelinoma (MGN3-1) cells (Iwakura et al., 2010) were cultured in DMEM (Invitrogen, Ontario, Canada; Catalogue # 11995-040) that was supplemented with 10% fetal bovine serum (Invitrogen; Catalogue # 12484) and 1% penicillin (100 U/mL) and streptomycin (100 µg/mL) (Invitrogen; Catalogue # 15140-122) at 37°C in 10% CO₂. At 80% confluency, MGN3-1 cells were seeded at 6×10^6 cells/well in a 12-well plate and the studies were performed when cells were 80-90% confluent. Each study was repeated thrice and the data from three studies were pooled to obtain an n = 9-12 wells/treatment. To determine whether glucose had an effect in a dose and time dependent manner, cells were incubated for 1 hour and 2 hours with 5.6, 25, 50, and 100 mM glucose DMEM media. The complete growth medium of MGN3-1 cells requires them to be growing at a high glucose level, which is 25 mM. In relation to the studies conducted with fatty acids and amino acids, we performed these studies using DMEM at low glucose levels (5.6 mM), since using a high glucose medium (25 mM) could mask the effect of the respective nutrients on NUCB2/nesfatin-1 secretion and synthesis. With respect to long chain fatty acids, we tested the effect of three different fatty acids using linolenic acid (Sigma-Aldrich, Ontario, Canada; Product # L2376), octanoic acid (Sigma-Aldrich; Product # C2875) and oleic acid (Sigma-Aldrich; Product # O1383). The cells were incubated for 4 hours with each fatty acids at 0, 1, 10, 100 µM. We used L-Tryptophan (Sigma-Aldrich; Product #

T8941) to test the effect of an amino acid on NUCB2 secretion and synthesis. The cells were incubated for 4 hours with L-tryptophan at 0.7, 1 and 10 mM. L-Tryptophan is present in the control medium (5.6 mM glucose DMEM) at a minimum dose of 0.7 mM, which is essential for their growth condition.

4.2.3 *In Vivo* Studies

For the chronic feeding of diets containing varying amounts of specific nutrients, age and weight-matched (5 weeks old, average body weight: 20 grams) male C57BL/6 mice (Charles River Laboratories, Quebec, Canada) were housed individually for 17 weeks in a 12 hours light: 12 hours dark cycle (lights off at 7 PM and on at 7 AM), temperature and humidity controlled vivarium. Mice were divided into four groups fed on a control (n = 6), high carbohydrate (n = 7), high protein (n = 7), and high fat (n = 7) diet with *ad libitum* access to water and their specific diet. All diets were purchased from Research Diets (New Brunswick, NJ). The calorie content of diets were: control (Product # D12451): 4.73 kcal/gm with 20% energy derived from protein, 35% energy derived from carbohydrate and 45% energy derived from fat; high carbohydrate (Product # D12450J) had 3.8 kcal/gm with 20% energy derived from protein, 70% energy derived from carbohydrate and 10% energy derived from fat; high protein (Product # D08091802) had 3.8 kcal/gm with 60% energy derived from protein, 30% energy derived from carbohydrate and 10% energy derived from fat, and high fat (Product # D12492) had 5.2 kcal/gm with 20% energy derived from protein, 20% energy derived from carbohydrate and 60% energy derived from fat. All mice were fed with the control diet for one week prior to starting their specific diets. Food intake, body weight, and blood glucose readings post 4 hours fast were measured once a week for 17 weeks.

For the acute administration of nutrients, age and weight-matched (5 weeks old, average body weight: 20 grams) male C57BL/6 Mice (Charles River Laboratories, St Constant, QU, Canada) were housed individually for 1 week and 2 days in a 12 h light:12 h dark cycle (lights off at 7 PM and on at 7 AM), temperature and humidity controlled vivarium. Mice were acclimatized for 1 week upon arrival and had ad libitum access to water and regular mouse chow for 11 days. Since we are performing an acute diet study, we needed the animals to acclimatize to the oral gavage procedure. We acclimatized the mice to this procedure by gavaging them with tap water for 2 days prior to the experimental day. On the 12th day, the mice were fasted for 4 hours and were gavaged with a specific liquid diet. The mice were divided into 4 groups: High protein (Isopure Protein Drink, Zero Carb - Mango peach flavor; Nature's Best, Clifton Park, New York; n=7), High fat (Splendido; Cold Pressed Extra Virgin Olive oil; President's Choice, Canada; n=7), High carbohydrate (D-Glucose; BioShop; Catalogue# GLU501.500; n=7), and Water (tap water; n=7). On the day of the study, 200 microliters of the above nutrients/water was administered to the mice by oral gavage. Blood glucose readings was taken at 0, 5, 10, 15, 20, 30, 60, 90 and 120 minutes, and blood was collected at 15, 30, 60, and 120 minutes for ELISA analysis to determine circulating levels of NUCB2/nesfatin-1. Tissues (stomach, small intestine [duodenum], large intestine and liver) were collected from each mouse upon termination of the study (deep isoflurane euthanasia followed by cervical dislocation). To maintain consistency, the timing and the duration of each experiment, surgeries and sample collection were kept constant for all studies.

4.2.4 Total RNA Extraction and cDNA Synthesis

Cells or tissues were collected from each study to compare NUCB2 mRNA expression. From the mice that underwent the chronic diet study, tissues (stomach, small intestine, large

intestine and liver) were harvested immediately after euthanasia. Total RNA was extracted from the MGN3-1 cells and tissues, using the TRIzol[®] RNA isolation reagent (Invitrogen). RNA purity was validated by optical density (OD) absorption ratio (OD 260 nm/OD 280 nm) using a NanoDrop 2000c (Thermo, Vantaa, Finland). Only samples with an absorption ratio greater than 1.8 were used for cDNA synthesis. Synthesis of cDNAs was conducted using iScript[™] cDNA synthesis kit as directed by the manufacturer (BioRad, Canada).

4.2.5 RT-PCR and Quantitative Real Time-PCR

RT-PCR and qRT-PCR for NUCB2, ghrelin, and RT-PCR for PC 1/3 and PC 2 were conducted as per conditions outlined in **Table 4.1**, using the CFX Connect Real-Time PCR Detection System (Bio-Rad). For the qRT-PCR analysis, mRNA expression of NUCB2 was normalized using beta-actin as a housekeeping gene. PCR products for NUCB2 in the stomach, liver and large intestine and these genes (NUCB2, ghrelin, PC 1/3 and PC 2) in the MGN3-1 cells were electrophoresed in 1% agarose gel to verify transcripts amplified. Based on previous studies (Gonzalez et al., 2011), we used beta-actin as an internal control to normalize the signal of NUCB2 mRNA. When using total RNA where mRNA quantification was very precise, the critical threshold values for beta-actin showed no variability. Relative NUCB2 mRNA expression was normalized with beta-actin from the same sample according to the Livak method (Schmittgen and Livak, 2008).

Table 4.1. Sequences of forward and reverse primers, and the conditions employed in PCR and qRT-PCR analyses of the expression of mRNAs of interest

Gene	Sequence (5' to 3')	PCR conditions [temperature (°C)/time (s)]
NUCB2	F: CCAGTGGAAAATGCAAGGAT	35 cycles of 95°/10; 60°/30; 73°/30
	R: GCTCATCCAGTCTCGTCCTC	
Ghrelin	F: GCATGCTCTGGATGGACATG	35 cycles of 95°/10; 50.5°/30; 73°/30
	R: CCTGATCTCCAGCTCCTC	
PC1/3	F: AGTGGAAAAGATGGTGAATG	35 cycles of 95°/10; 48.1°/30; 73°/30
	R: CTCCTCATTTAGGATGTCCA	
PC2	F: AATGGGAGGAAGAGGAATC	35 cycles of 95°/10; 50.5°/30; 73°/30
	R: TTGTTTTGAGGGTCAGTACC	

4.2.6 Immunocytochemistry and Microscopy

MGN3-1 cells were cultured in a Labtek™ Chamber Slide System™ (Nalge Nunc International, Rochester, NY) and were allowed to grow to near confluency. Cells were washed with 1X phosphate buffer solution (PBS; 2 x 5 minutes, 25°C) and fixed in a 4% paraformaldehyde (PFA) solution in 1X PBS for 10 minutes at 25°C, followed by another wash with 1X PBS (3 x 5 minutes, 25°C). The fixed cells were permeabilized in a solution of 0.3% Triton-X (Bioshop, Burlington, Ontario, Canada) in 1X PBS for 5 minutes at room temperature. Slides were incubated in blocking buffer containing 10% goat serum in 1X PBS for 1 hour at room temperature. Cells were then incubated in primary antibody (**Table 4.2**) at 4°C overnight. Slides were washed with PBS (3 x 5 minutes, 25°C) and incubated with secondary antibody (**Table 4.2**; the PC1/3 antibody was a generous gift from Dr. Iris Lindberg, University of Maryland School of Medicine) for 4 hours at room temperature. Finally, slides were washed with PBS (3 x 5 minutes, 25°C) and mounted with Vectashield® mounting medium containing 4', 6-diamidino-2-phenylindole (DAPI) (Vector Laboratories, Burlington, Ontario, Canada).

Cells were viewed using a Nikon Eclipse-Ti inverted fluorescence microscope (Nikon, Mississauga, Ontario, Canada) and images were captured using a Nikon DS-Qi1MC camera (Nikon). Images were analyzed using NIS-Elements basic research software (Nikon) on a Dell HP Workstation. Images shown are representative cells stained for ghrelin, NUCB2, PC 1/3 and PC2. For high resolution imaging, the cells were viewed, analysed and images captured using a Leica™ TCS SP5 confocal microscope.

Table 4.2. Antibodies used for immunofluorescence microscopy

Antibody	Dilution	Raised In	Manufacturer/Source
Ghrelin	1:100	Mouse	Abcam, Cambridge, MA, USA
Nesfatin-1	1:100	Rabbit	Phoenix Pharmaceuticals, Burlingame, CA, USA
PC1/3	1:100	Rabbit	Dr. Iris Lindberg, University of Maryland, USA
PC2	1:100	Rabbit	Abcam, Cambridge, MA, USA
Anti-Rabbit (Texas Red)	1:100	Goat	Vector Laboratories, Burlington, ON, Canada
Anti-Mouse (FITC)	1:100	Goat	Abcam, Cambridge, MA, USA

4.2.7 Western Blot Analysis, Immunohistochemistry and Fluorescence Microscopy

For confirming the presence of nucleobindin-2 (NUCB2) in the intestine and liver, 3 months old C57BL/6 male mice were used. Briefly, liver, and small and large intestines were collected, and separated for Western analysis or immunohistochemistry. Tissues for Western blot homogenized in T-PER® tissue protein extraction reagent (Thermo Scientific, #78510) followed protein concentration determination by Bradford assay. The samples were prepared in 1X Laemmli buffer containing 0.2% 2-mercaptoethanol (Bio-Rad, #161-0737 and -0710) and subsequently were boiled at 95°C for 5min followed by vortexing. The whole sample volume (20µL) each containing 50 µg protein or synthetic rat nesfatin-1 (ABGENT, 1µg/µL; previously used in 4, 29) was loaded on a gel, and run in a Mini-PROTEAN® TGX™ 8-16% gradient gel (Bio-Rad, #456-1104). After separation, the proteins were transferred to a 0.2 µm BioTrace™ nitrocellulose membrane (PALL Life Sciences, #27377-000) and then the membrane was blocked in 1X RapidBlock™ solution (AMRESCO, #M325). NUCB2 protein detection was performed using rabbit anti-nesfatin-1 (Catalogue number H-003-22; 1:500 dilution; Phoenix Pharmaceuticals, California) and GAPDH protein was detected by use of rabbit antiserum directed against mouse GAPDH (AbDSerotec®, #AHP1628) diluted 1:1000. As secondary antibody, goat anti-rabbit IgG (H+L) HRP conjugate (Bio-Rad, #170-6515) diluted 1:3000 was used. For protein visualization the membrane was incubated for 5 min in Clarity™ Western ECL substrate (Bio-Rad, #170-5061) and imaged using ChemiDoc™ MP imaging system (Bio-Rad, #170-8280) with chemiluminescence detection. Membrane stripping in between protein detection was conducted using Restore™ PLUS western blot stripping buffer (Thermo Scientific, #46430). Precision plus protein™ dual xtra standards (Bio-Rad, #161-0377) were used as molecular weight markers.

For immunohistochemical studies, the tissues collected were fixed in 4% formaldehyde for 24 hours at 4°C. Fixative was replaced with ethanol (three 70% ethanol), each followed by a 10 minute incubation at 4°C. Tissues were then stored in 70% ethanol at 4°C and were processed and sectioned at the Prairie Diagnostic Services Inc. (PDS Inc., Western College of Veterinary Medicine, University of Saskatchewan). Paraffin sections of 4 µm thickness were prepared for immunostaining. These sections were deparaffinized with xylene (incubated twice in 100% xylene; 5 minutes, 25°C) and rehydrated in a graded ethanol series (incubated twice in 100% ethanol, and once in each 95% ethanol, 70% ethanol, 50% ethanol; 2 minutes each, 25°C). The sections were then incubated with 3% hydrogen peroxide in distilled water to block endogenous peroxidase activity (30 minutes at room temperature). The sections were then blocked with serum-free protein block reagent (DAKO® Corporation, California) for 10 minutes before being incubated with primary antibodies. These sections were then incubated with rabbit anti-nesfatin-1 (Catalogue number H-003-22; 1:500 dilution; Phoenix Pharmaceuticals, California) for 24 hours at room temperature. All slides were subsequently washed three times with 1x PBS and incubated with goat anti-rabbit Texas Red® IgG (Red-Nesfatin-1; Catalogue number TI-1000; 1:100 dilution; Vector Laboratories, California) secondary antibody for 1 hour at room temperature. All primary and secondary antibodies were diluted in antibody diluent reagent (DakoCytomation®, Mississauga, Ontario). The slides were washed three times with 1x PBS and seven times with distilled water. Finally, the slides were mounted with Vectashield® medium that contain nuclear dye DAPI (Blue; Vector Laboratories, Burlingame, California). Sections were viewed under a Nikon Eclipse Ti-E inverted fluorescence microscope (Nikon Canada, Mississauga, Canada). Images were captured using a Nikon DS-QI1MC cooled monochrome camera connected to a Dell HP Workstation computer and NIS elements basic research imaging

software (Nikon Canada, Mississauga, Canada). Only representative images of small and large intestine staining for NUCB2/nesfatin-1 with DAPI are shown in the results section.

4.2.8 Nesfatin-1/NUCB2 Levels in Serum and Media

To investigate nutrient dependent changes in NUCB2/nesfatin-1 secretion from MGN3-1 cells, media was collected after specific incubation periods. In order to prevent cell debris, samples were centrifuged (13000 rpm for 10 minutes at 4°C) and the top 700 µL was stored at -20°C until nesfatin-1 measurement. For measuring circulating NUCB2/nesfatin-1, blood was collected at 7 a.m (soon after the light phase begins), 1 p.m. (middle of the light phase) and at 7 p.m (prior to the commencement of the dark phase). Blood samples were allowed to clot on ice, and serum was separated by centrifugation (7000 rpm for 9 minutes at 4°C) and stored at -20°C, until assays were conducted. NUCB2/Nesfatin-1 secretion levels in the media were measured using the Nesfatin-1 (1-82) (Rat) ELISA kit (Catalogue number EK-003-22, Phoenix Pharmaceuticals Inc., California). The limit of assay sensitivity was 1.2 ng/mL for nesfatin-1, with detectable range from 0.1-1000 ng/mL. The amount of immunoreactive material was determined using a non-linear regression curve-fit, which was used to quantify and compare the concentration of NUCB2/nesfatin-1 secretion in the serum and media samples.

4.2.9 NUCB2/Nesfatin-1 Levels in Serum and Media and Total Ghrelin levels In media

To investigate nutrient dependent changes in NUCB2/nesfatin-1 and total ghrelin secretion from MGN3-1 cells, media was collected after specific incubation periods. In order to prevent cell debris, samples were centrifuged (13000 rpm for 10 minutes at 4°C) and the top 700 µL was stored at -20°C until NUCB2/Nesfatin-1 and total ghrelin measurement. Blood samples were allowed to clot on ice, and serum was separated by centrifugation (7000 rpm for 9 minutes

at 4° C) and stored at -20° C, until assays were conducted. NUCB2/Nesfatin-1 secretion levels in the serum and media were measured using the Nesfatin-1 (1-82) (Rat) ELISA kit (Catalogue number EK-003-22, Phoenix Pharmaceuticals Inc., California). The limit of assay sensitivity was 1.2 ng/mL for nesfatin-1, with detectable range from 0.1-1000 ng/mL. Similarly, the total ghrelin secretion levels in the media was measured using the Ghrelin (Rat, Mouse) EIA kit (Catalogue number EK-031-31, Phoenix Pharmaceuticals Inc, California). The limit of assay sensitivity was 1.16 ng/mL for total ghrelin, with detectable range from 0-100 ng/mL. The amount of immunoreactive material was determined using a non-linear regression curve-fit, which was used to quantify and compare the concentration of NUCB2/nesfatin-1 secretion in the serum and media samples.

4.2.10 Statistical Analysis

Analyses of the quantified qRT-PCR and ELISA data were conducted using One-Way ANOVA followed by Tukey's multiple comparison test. GraphPad Prism[®] version 5 (GraphPad Software Incorporated, San Diego, CA, USA) was used for statistical analyses and graphs. Significance was assigned when $p < 0.05$. Data are expressed as mean \pm SEM.

4.3 Results

4.3.1 NUCB2, PC 1/3 and PC 2 mRNAs are expressed in MGN3-1 cells and NUCB2 mRNA is expressed in the stomach, liver, small intestine and large intestine of male mice

We identified expression of NUCB2 (202 bp), prohormone convertase 1/3 (400 bp), and prohormone convertase 2 (406 bp) mRNAs in MGN3-1 cells (**Figure 4.1A**). NUCB2 (202 bp) mRNA expression was also detected in the stomach, liver, small intestine and large intestine of male C57/BL6 mice (**Figure 4.1B**). Absolute levels of NUCB2 mRNA expression in the stomach was higher than NUCB2 mRNA expression in the liver, small intestine and large intestine (**Figure 4.1C**).

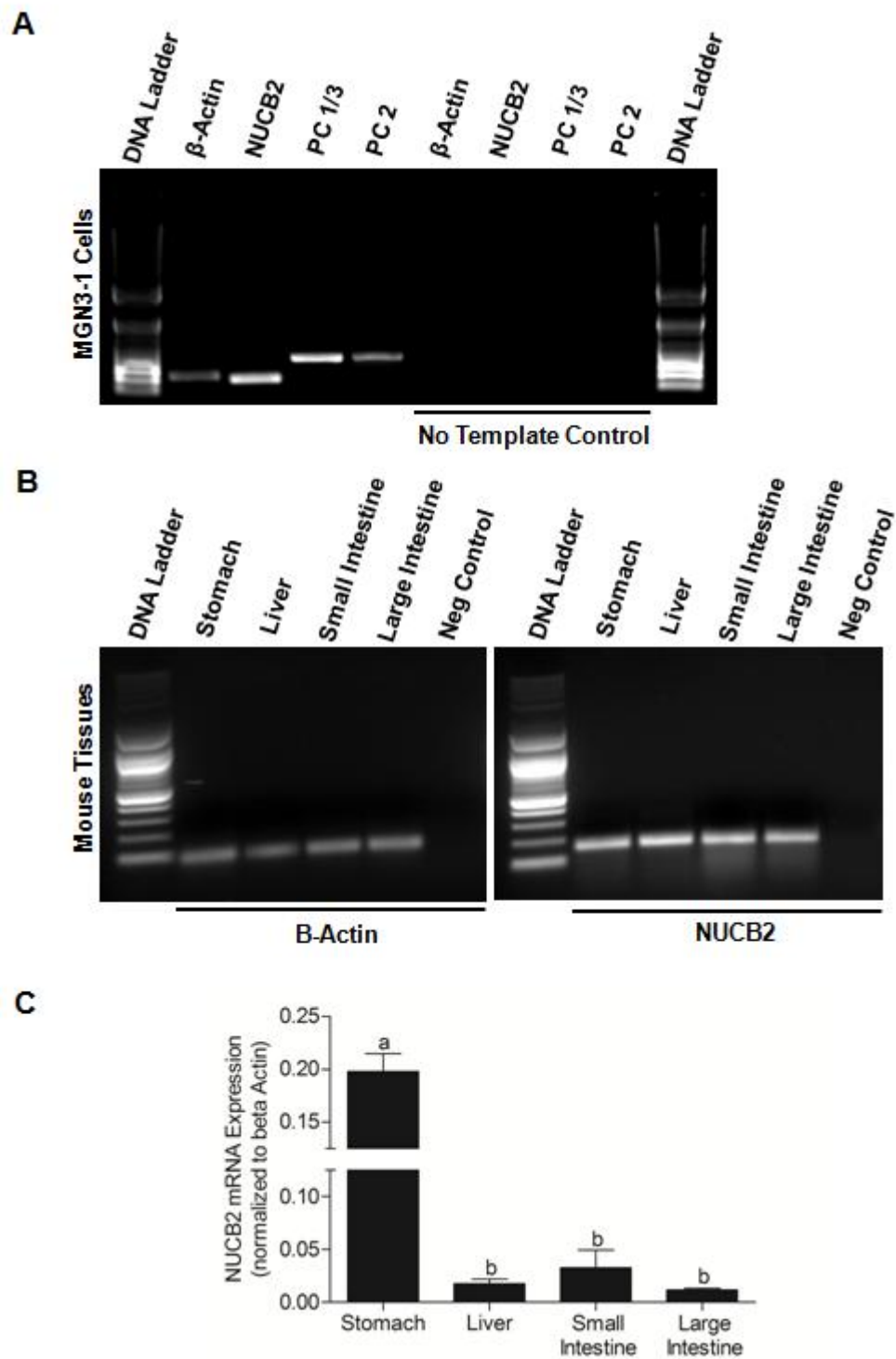


Figure 4.1 NUCB2, PC 1/3 and PC 2 mRNAs are expressed in MGN3-1 cells and NUCB2 mRNA is expressed in the stomach, liver, small intestine and large intestine of male mice

Figure 4.1. NUCB2, PC1/3 and PC2 mRNA Expression in MGN3-1 cells (A) and NUCB2 mRNA Expression in the Stomach, Liver, Small and Large Intestine from Male C57BL/6 Mice Tissues (B and C). Beta-Actin (β -Actin), nucleobindin-2 (NUCB2; 202 bp), prohormone convertase 1/3 (PC 1/3; 400 bp), and prohormone convertase 2 (PC 2; 406 bp) mRNAs were identified in MGN3-1 cells. No expression of these mRNAs was found in the RT-PCR reaction devoid of the cDNA template (A). Beta-Actin (β -Actin) and nucleobindin-2 (NUCB2; 202 bp) mRNAs expression were identified in the stomach, liver, small and large intestine from mice. No NUCB2 mRNA expression was found in PCR reactions devoid of the cDNA template (B). Relative abundance of NUCB2 mRNA expression normalized to β -Actin in the stomach, liver, small and large intestine is shown in (C). Letter “b” denotes significant difference from “a”, $p < 0.05$, One-Way ANOVA followed by Tukey’s multiple comparison test.

4.3.2 MGN3-1 cells are immunopositive for ghrelin, NUCB2/nesfatin-1, PC1/3 and PC2

Fluorescence microscopy displayed MGN3-1 cells stained with anti-nesfatin-1 antibody (Texas-Red; **Figure 4.2B**) and anti-ghrelin antibody (FITC-Green; **Figure 4.2A**) showed clear co-localization (Yellow; **Figure 4.2C**) of nesfatin-1 and ghrelin immunoreactivity. However, some ghrelin positive cells were not immunoreactive for nesfatin-1 (**Figure 4.2C**). MGN3-1 cells showed PC 1/3 immunoreactivity (Texas Red; **Figure 4.2D**) and PC 2 immunoreactivity (Texas Red, **Figure 4.2E**). DAPI (Blue) stained the nucleus of all cells including those cells not positive for the proteins studied. Control slides stained with secondary antibody alone (**Figure 4.2F**) had no immunoreactivity. Confocal imaging showed MGN3-1 cells stained with anti-nesfatin-1 antibody (Texas-Red; **Figure 4.3A**) and anti-ghrelin antibody (FITC-Green; **Figure 4.3B**) showed clear co-localization (Yellow; **Figure 4.3C**) of nesfatin-1 and ghrelin immunoreactivity. Negative control is stained with only secondary antibodies alone (**Figure 4.3D**).

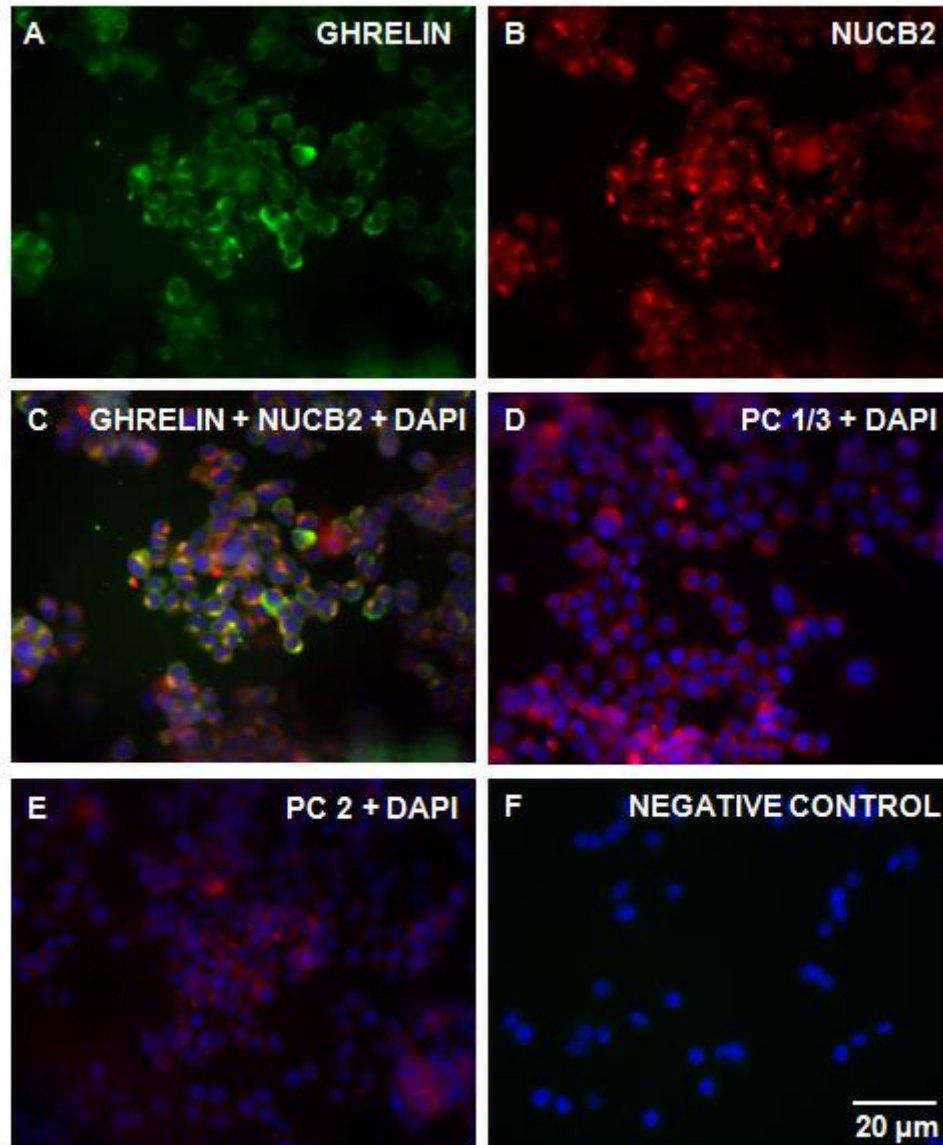


Figure 4.2 MGN3-1 cells are immunopositive for ghrelin, NUCB2/nesfatin-1, PC1/3 and PC2

Figure 4.2. MGN3-1 Cells are Immunopositive for NUCB2/Nesfatin-1, Ghrelin, PC 1/3 and PC 2. Immunocytochemical staining of MGN3-1 cells for ghrelin immunoreactivity (A; FITC-Green), nesfatin-1 immunoreactivity (B; Texas-Red) and the nuclear stain DAPI. A merged image showing co-localization of nesfatin-1 and ghrelin immunoreactivity is shown in (C; Yellow). Immunocytochemical staining of MGN3-1 cells for PC 1/3 immunoreactivity (D; Texas-red), PC 2 immunoreactivity (E; Texas-red) and the nuclear stain DAPI. No primary antibody controls are shown in (F) for nesfatin-1 and ghrelin, respectively. Images taken at 40X magnification. Scale bar = 20 μ m.

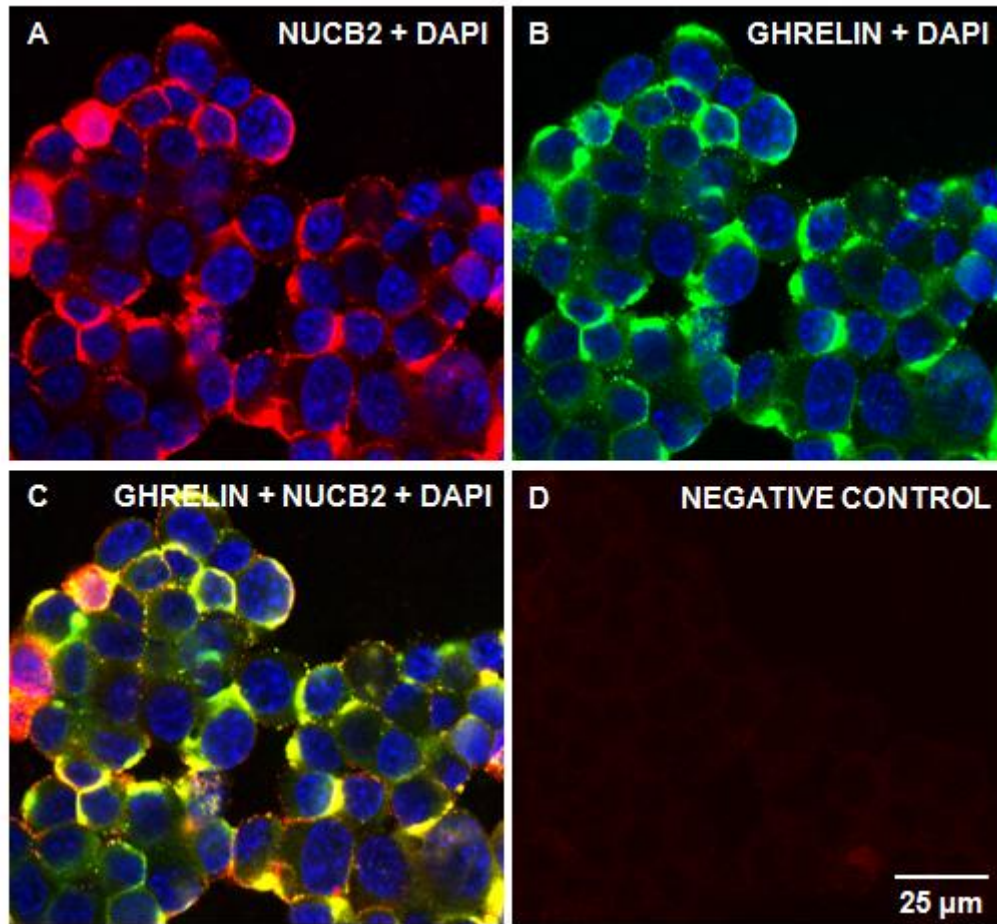


Figure 4.3 MGN3-1 cells are immunopositive for ghrelin, NUCB2/nesfatin-1, PC1/3 and PC2

Figure 4.3. NUCB2/Nesfatin-1 co-localizes with ghrelin in MGN-3 cells. Confocal micrographs of MGN-3 cells stained for NUCB2/nesfatin-1 (A; Texas-Red) and ghrelin (B; FITC-Green). Merged image of A and B showing co-localization of NUCB2/nesfatin-1 and ghrelin immunoreactive cells (C; Yellow). No primary antibody negative control labeled only with secondary antibodies (D). Nuclei are stained with DAPI (Blue; A, B and C). Images were merged using Image J™ PC-based software. Scale bar = 25 μm.

4.3.3 NUCB2 protein expression in large intestine, small intestine and liver from male mice

NUCB2 protein is expressed in the large intestine, small intestine and liver from male mice showing distinct band for NUCB2 corresponding to approximately 50 KDa. Rat nesfatin-1 peptide used as a positive control is shown as a distinct band corresponding to approximately 10 kDa (**Figure 4.4A; left image**). However, no bands showing the fully processed nesfatin-1 were visible at 10 kDa in the tissue samples (**Figure 4.4A; left image**). We also found bands of approximately 47 kDa underneath the 50 kDa band in the small intestine and liver, but not in the large intestine (**Figure 4.4A; left image**). A distinct band for GAPDH used as the control house-keeping gene is observed at 37 kDa shown in all tissues (**Figure 4.4A; right image**). NUCB2/nesfatin-1 immunoreactivity is found in the mucosal cells of small intestine (**Figure 4.4B; left image**) and large intestine (**Figure 4.4B; right image**).

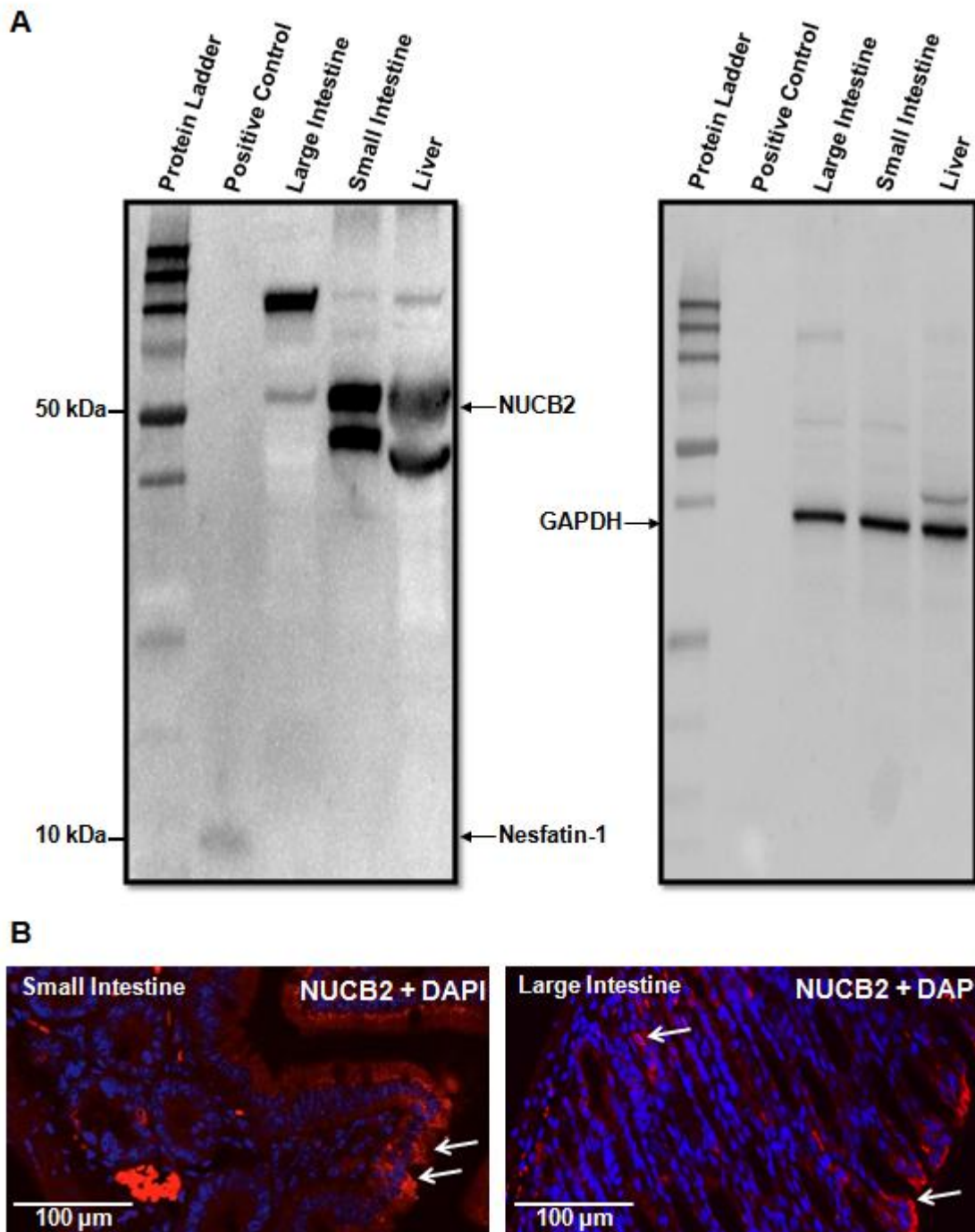


Figure 4.4 NUCB2 protein expression in large intestine, small intestine and liver from male mice

Figure 4.4. NUCB2 is expressed in the small intestine, large intestine and liver of male C57BL/6 mice. Tissues show distinct bands for NUCB2/nesfatin-1 corresponding to 50 kDa. Rat nesfatin-1 (Custom synthesized, ABGENT, 1 μ g/ μ L) was used as a positive control which is shown as a distinct band corresponding to 10 kDa (A; Left Image). Mouse glyceraldehyde 3-phosphate dehydrogenase (GAPDH) is uniformly expressed in liver, small and large intestine. The blots that were loaded with 50 μ g of total protein/well previously for NUCB2 protein detection were stripped and re-blocked with mouse GAPDH primary antibody. Representative blot (n = 4 independent experiments) showing distinct bands for GAPDH corresponding to 37 kDa (A; Right Image). Mucosal cells showing NUCB2/nesfatin-1 (Texas-Red) immunoreactivity, and DAPI are found in the small intestine (B; left image) and large intestine (B; right image) from male mice. Arrows point to cells that are immunopositive for NUCB2/nesfatin-1 and shows distinct DAPI-stained nuclei. Representative images were taken of 4 slides (8 sections/tissue) from three adult male mice. Scale bar = 100 μ m.

4.3.4 Effects of glucose and L-Tryptophan on NUCB2 mRNA expression in, and NUCB2/nesfatin-1 secretion from MGN3-1 cells

Cells incubated at 100 mM glucose DMEM had a higher NUCB2 mRNA expression than cells incubated at 5.6, 25 and 50 mM DMEM glucose concentrations at 1 hour post-incubation (**Figure 4.5A**). At 2 hours post-incubation, cells incubated at 100 mM DMEM were significantly higher in NUCB2 mRNA expression than cells incubated at 5.6 and 50 mM glucose DMEM (**Figure 4.5C**). At 1 hour (**Figure 4.5B**) and 2 hours (**Figure 4.5D**), there were no significant differences in NUCB2/nesfatin-1 secretion. NUCB2 mRNA expression was significantly higher in cells incubated at 10 mM L-Tryptophan (**Figure 4.5E**) in comparison to cells incubated at 0.07 and 1.0 mM L-Tryptophan. NUCB2/nesfatin-1 secretion from cells incubated at 1.0 and 10.0 mM L-Tryptophan were significantly higher than cells incubated at 0.7 mM L-Tryptophan (**Figure 4.5F**).

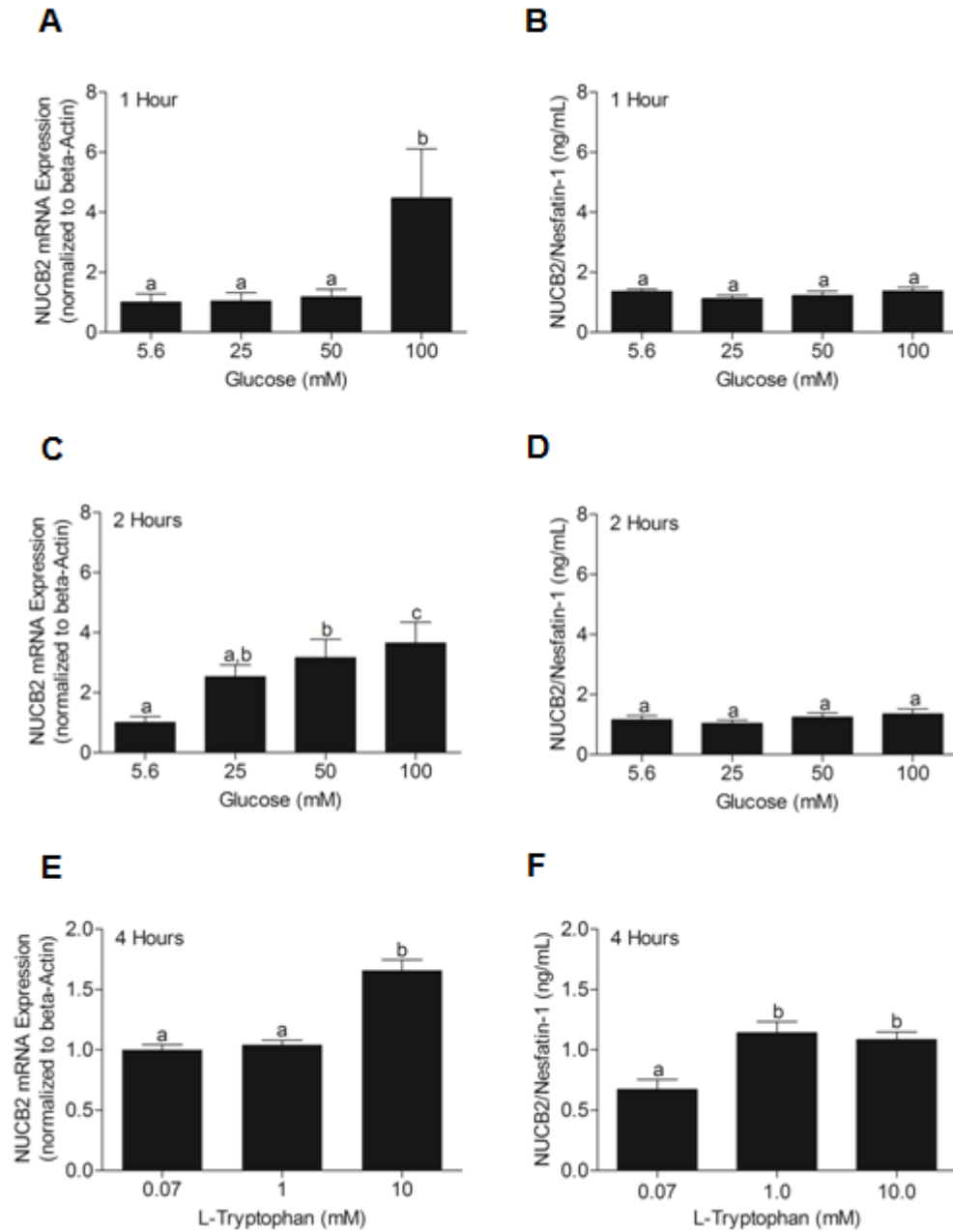


Figure 4.5 Effects of glucose and L-Tryptophan on NUCB2 mRNA expression in, and NUCB2/nesfatin-1 secretion from MGN3-1 cells

Figure 4.5. NUCB2 mRNA Expression (A, C, E) and NUCB2/nesfatin-1 Secretion (B, D, F) from MGN3-1 Cells Incubated with Different Concentrations of Glucose (5.6 mM, 25 mM, 50 mM and 100 mM) at Various Incubation Periods (1 Hour and 2 Hours), and with Different Concentrations of L-Tryptophan (0.07 mM, 1 mM, 10 mM; 4 Hours). MGN3-1 cells incubated at 100 mM glucose had a significant increase in NUCB2 mRNA expression at 1 hour post-incubation (A; $p < 0.05$), but no significant differences was found in nesfatin-1 secreted into the media from the same cells (B). Similarly, glucose caused a dose dependent increase in NUCB2 mRNA expression at 2 hours post-incubation (C; $p < 0.5$) without causing any changes in nesfatin-1 secretion (D). $n = 9$ wells/concentration pooled from 3 different studies. MGN3-1 cells incubated at 10 mM L-Tryptophan had a significant increase in NUCB2 mRNA expression than cells incubated at 0.07 mM and 1 mM L-Tryptophan (E; $p < 0.05$). Nesfatin-1 secretion significantly increased from cells incubated at 1 mM and 10 mM L-Tryptophan than 0.07 mM L-Tryptophan (F; $p < 0.05$). $n = 12$ wells/concentration pooled from 3 different studies. Letters b and c denote significant differences found between control (a) and various treatment groups, using One Way ANOVA followed by Tukey's Multiple Comparison Test. There are no significant differences between groups marked by same letters.

4.3.5 Effect of linolenic acid, octanoic acid and oleic acid on NUCB2 mRNA expression in, and NUCB2/nesfatin-1 secretion from MGN3-1 cells

We found NUCB2 mRNA expression significantly reduced in cells treated with 1, 10, and 100 μ M oleic acid (**Figure 4.6E**) in comparison to the control. No changes in NUCB2 mRNA were observed in cells treated with linolenic (**Figure 4.6A**) and octanoic acid (**Figure 4.6C**). Further, NUCB2/nesfatin-1 secretion was unaltered in cells treated with different doses of linolenic acid (**Figure 4.6B**), octanoic acid (**Figure 4.6D**), and oleic acid (**Figure 4.6F**).

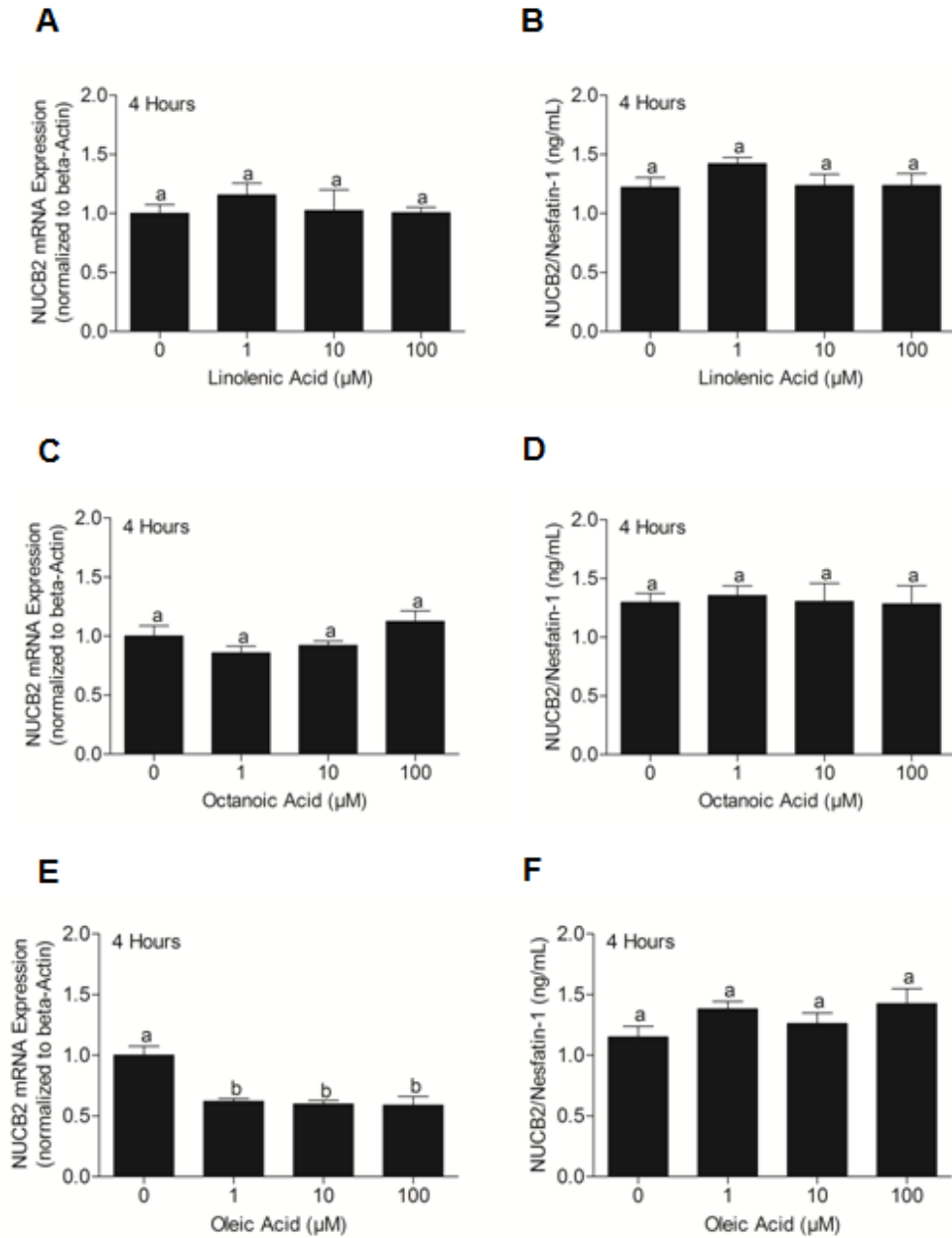
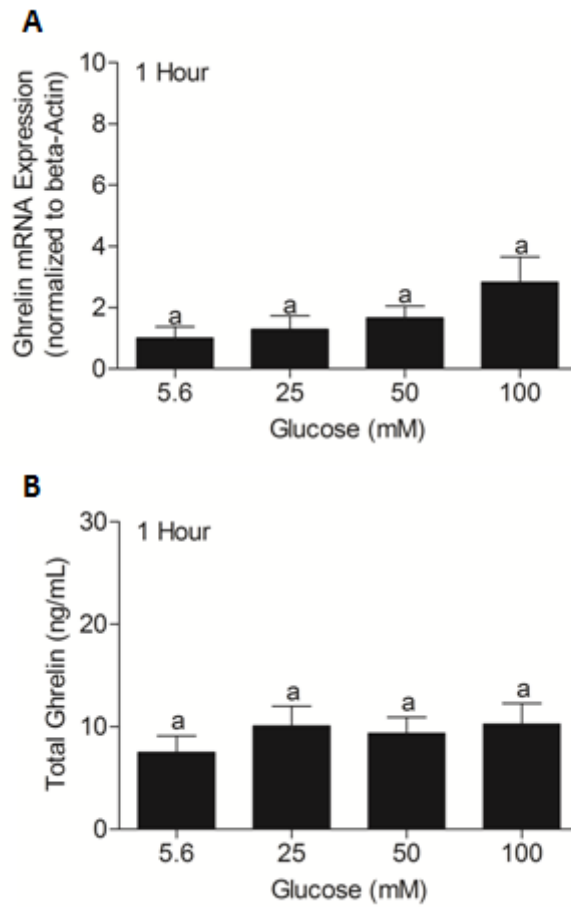


Figure 4.6 Effect of linolenic acid, octanoic acid and oleic acid on NUCB2 mRNA expression in, and NUCB2/nesfatin-1 secretion from MGN3-1 cells

Figure 4.6. NUCB2 mRNA Expression (A, C, E) and NUCB2/nesfatin-1 Secretion (B, D, F) from MGN3-1 Cells Incubated for 4 Hours with Different Concentrations of Linolenic Acid, Octanoic Acid and Oleic Acid (0 μ M, 1 μ M, 10 μ M, 100 μ M). No change in NUCB2 mRNA expression (A, C) and nesfatin-1 secretion (B, D) when MGN3-1 cells were incubated with different concentrations of linolenic acid and octanoic acid. MGN3-1 cells incubated at 1, 10, 100 μ M oleic acid had a significant decrease in NUCB2 mRNA expression (E; $p < 0.05$), but no significant difference was found in nesfatin-1 secretion at 4 hours post-incubation (F; $p < 0.05$). $n = 9$ wells/concentration pooled from 3 different studies. Different letters (a and b) shows significant differences found between control and various treatment groups, using One Way ANOVA followed by Tukey's Multiple Comparison Test. There are no significant differences between groups marked by same letters.

4.3.6 Effect of L-tryptophan, linolenic acid, octanoic acid and oleic acid independently on ghrelin mRNA expression in, and total ghrelin secretion from MGN3-1 cells

No changes in ghrelin mRNA (**Supporting Figure S4.1A**) and total ghrelin secretion (**Supporting Figure S4.1B**) were found when cells were treated with different doses of glucose post 1 hour incubation. Ghrelin mRNA expression was significantly higher in cells incubated at 1 mM L-Tryptophan (**Figure 4.7A**) in comparison to cells incubated at 0.07 and 10 mM L-Tryptophan. No significant difference in total ghrelin secretion from cells treated with different doses of L-Tryptophan (**Figure 4.7B**). We found no change in ghrelin mRNA expression (**Figure 4.7C**), but total ghrelin secretion was high from cells incubated at 100 μ M linolenic acid (**Figure 4.7D**) in comparison to control, 1 and 10 μ M doses. No changes in ghrelin mRNA (**Figure 4.7E**) and total ghrelin secretion (**Figure 4.7F**) were found when cells were treated with different doses of octanoic acid. Meanwhile, ghrelin mRNA (**Figure 4.7H**), and total ghrelin secretion (**Figure 4.7I**) were significantly higher in cells treated with 100 μ M oleic acid, compared to the control, 1 and 10 μ M oleic acid.



Supporting Figure S4.1

Ghrelin mRNA Expression (A) and Total Ghrelin Secretion (B) from MGN3-1 Cells Incubated for 1 Hour with Different Concentrations of Glucose (5.6 mM, 25 mM, 50 mM and 100 mM). No changes in ghrelin mRNA and total ghrelin secretion were found when cells were treated with different doses of glucose post 1 hour incubation.

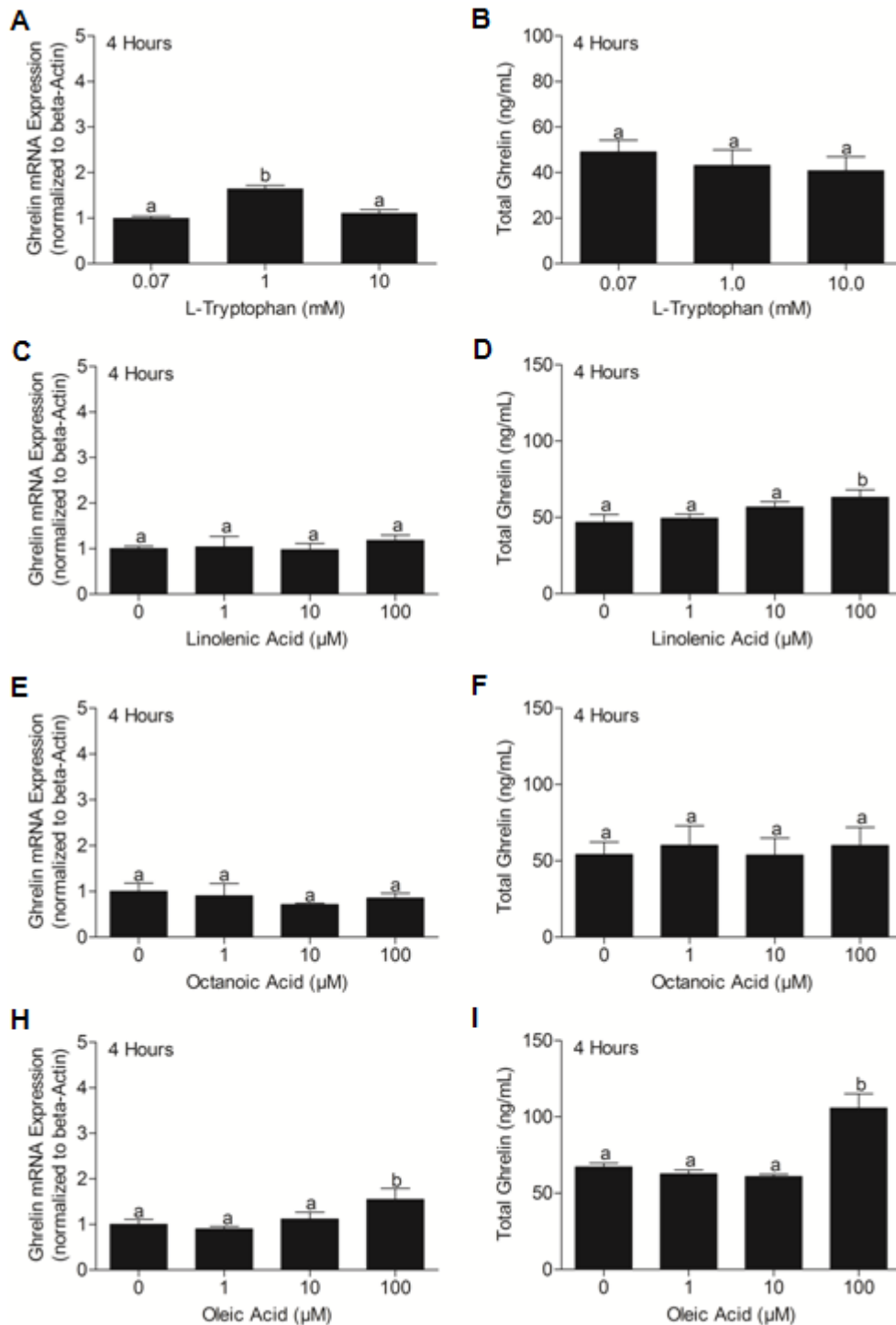
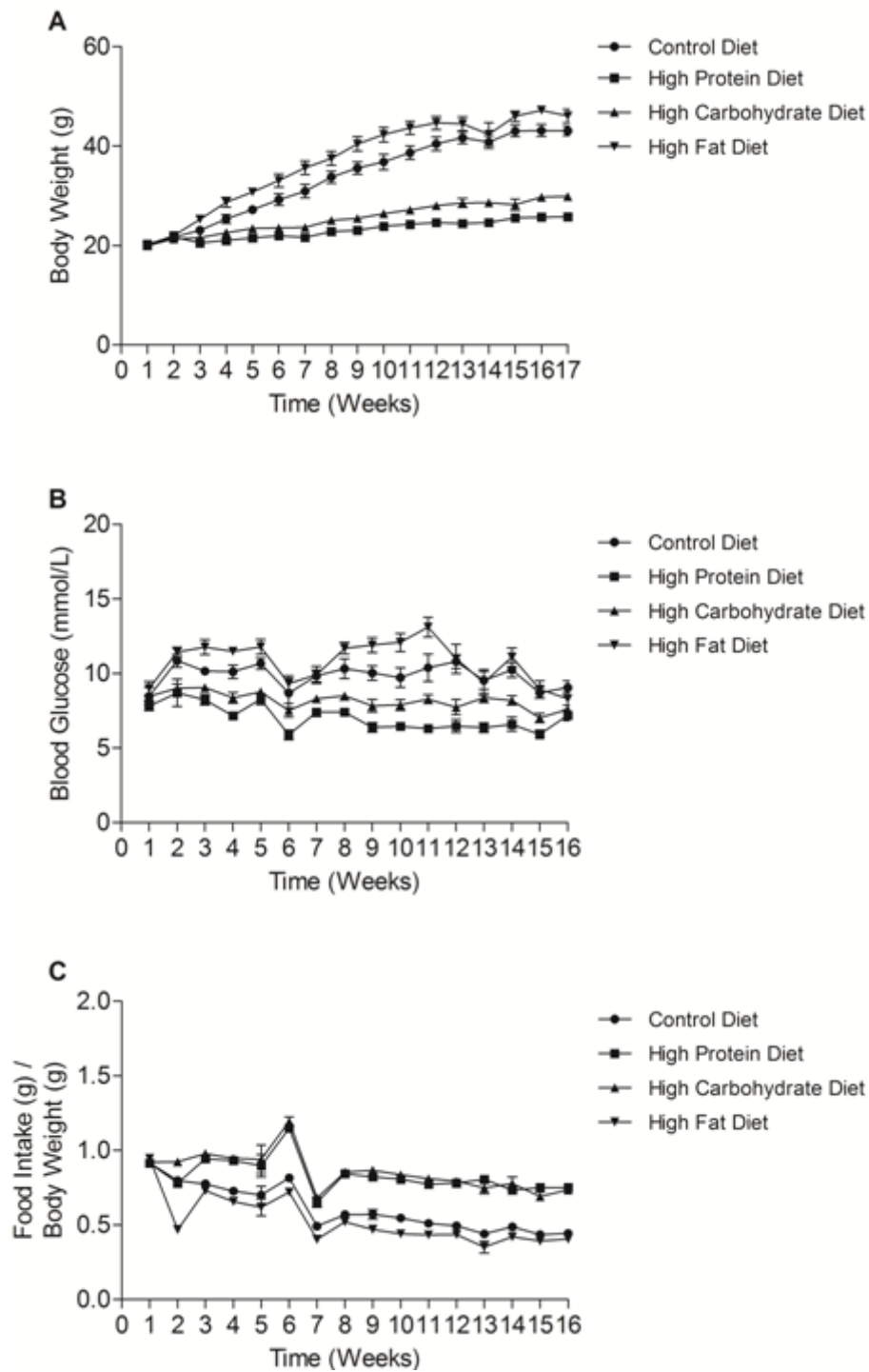


Figure 4.7 Effect of L-tryptophan, linolenic acid, octanoic acid and oleic acid independently on ghrelin mRNA expression in, and total ghrelin secretion from MGN3-1 cells

Figure 4.7. Ghrelin mRNA Expression (A, C, E, H) and Total Ghrelin Secretion (B, D, F, I) from MGN3-1 Cells Incubated for 4 Hours with Different Concentrations of L-Tryptophan (0.07 mM, 1 mM, 10 mM) and with Different Concentrations of Linolenic Acid, Octanoic Acid and Oleic Acid (0 μ M, 1 μ M, 10 μ M, 100 μ M). MGN3-1 cells incubated at 1 mM L-Tryptophan had a significant increase in Ghrelin mRNA expression than cells incubated at 0.07 mM and 10 mM L-Tryptophan (A; $p < 0.05$). No change in total ghrelin secretion (B) when MGN3-1 cells were incubated with different concentrations of L-Tryptophan. $n = 12$ wells/concentration pooled from 3 different studies. No change in ghrelin mRNA expression (C), but a significant increase in total ghrelin secreted into the media from the same cells incubated at 100 μ M linolenic acid (D; $p < 0.05$). No change in ghrelin mRNA expression (E) and total ghrelin secretion (F) when MGN3-1 cells were incubated with different concentrations of octanoic acid. A significant increase in ghrelin mRNA expression (H; $p < 0.05$) and total ghrelin secreted into the media from the same cells incubated at 100 μ M oleic acid (I; $p < 0.05$). $n = 9$ wells/concentration pooled from 3 different studies. Different letters shows significant differences found between control and various treatment groups, using One Way ANOVA followed by Tukey's Multiple Comparison Test. There are no significant differences between groups marked by same letters.

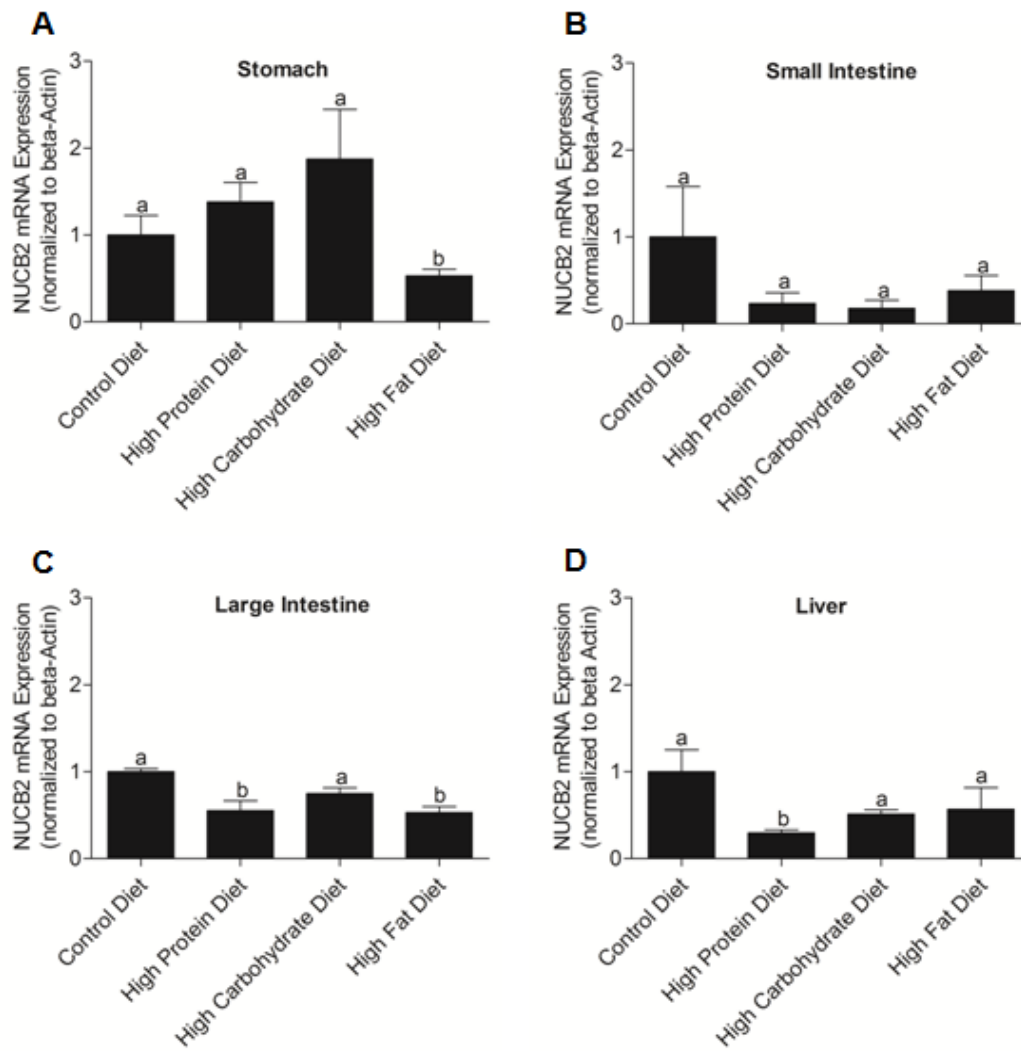
4.3.7 Chronic effects of nutrients on NUCB2 mRNA expression and serum NUCB2/nesfatin-1 in mice

The body weight, food intake and blood glucose profile of mice fed on various diets are shown in **Supporting Figure S4.2**. Mice fed on a high fat diet had significantly low expression of NUCB2 mRNA in the stomach compared to those fed on a control, high protein or high carbohydrate diets (**Figure 4.8A**). There was no significant difference in the expression of NUCB2 mRNA in the small intestine between mice fed on a control, high protein, high carbohydrate or high fat diets (**Figure 4.8B**). Mice fed on the high protein and high fat diets have comparatively low expression of NUCB2 mRNA in the large intestine than mice fed on control or high carbohydrate diets (**Figure 4.8C**). Mice fed on a high protein diet had a significant low expression of NUCB2 mRNA in the liver than mice fed on the other diets (**Figure 4.8D**). At 7 a.m, there were no differences in serum nesfatin-1/NUCB2 levels in mice fed different diets (**Figure 4.9A**). At 1 p.m, the high carbohydrate diet fed mice had significantly higher serum nesfatin-1/NUCB2 in circulation (**Figure 4.9B**). Serum nesfatin-1/NUCB2 was significantly lower in mice fed high carbohydrate, high protein or high fat, compared to control diet fed mice at 7 p.m (**Figure 4.9C**).



Supporting Figure S4.2

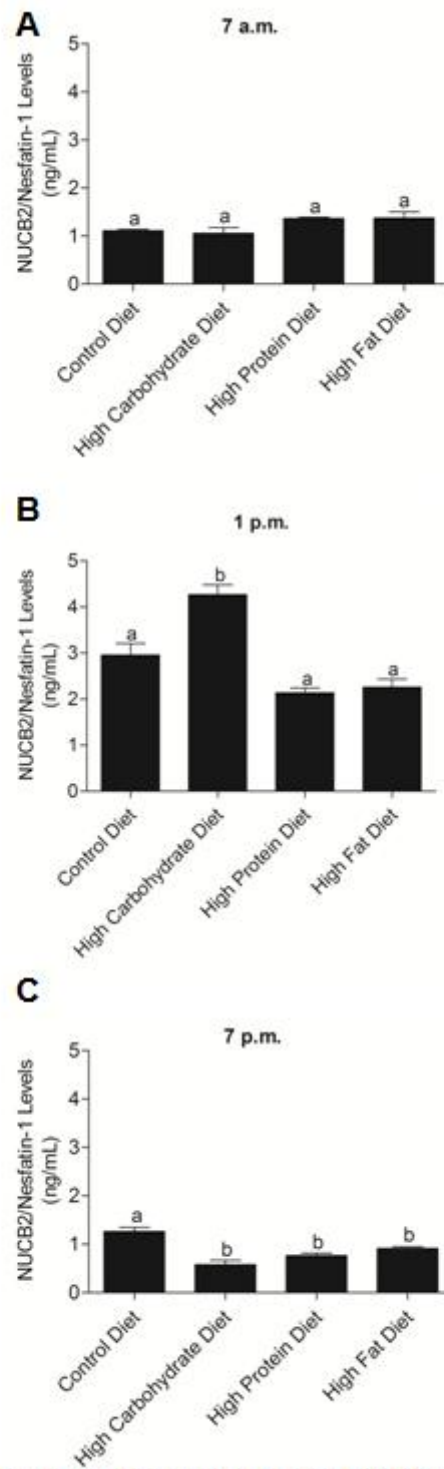
Weekly Body Weight (A), Blood Glucose (B) and Food Intake to Body Weight Ratio (C) on Mice Fed Chronically on Various Nutrient Diets for 17 Weeks. Mice fed on a control diet and a high fat diet had an increase in the body weight compared to mice fed with a high protein and a high carbohydrate diet (A; $p < 0.05$). Mice fed on a high protein diet and high carbohydrate diet had lower weekly blood levels than mice fed a control and high fat diet (B; $p < 0.05$). Mice fed on a control diet and a high fat diet was had an increase in the ratio of food intake to body weight than mice fed with a high protein and a high carbohydrate diet (C; $p < 0.05$). Mice ($n = 6-7$ mice/group) had *ad libitum* access to water and their specific diet, control diet, high carbohydrate diet, high protein diet, and high fat diet. Significant difference was found between the various fed groups, using One Way ANOVA followed by Tukey's Multiple Comparison Test.



CD: Control Diet; HP: High Protein Diet; HC: High Carbohydrate Diet; HF: High Fat Diet

Figure 4.8 Chronic effects of nutrients on NUCB2 mRNA expression in mice

Figure 4.8. NUCB2 mRNA Expression in the Stomach (A), Small Intestine (Duodenum; B), Large Intestine (C) and Liver (D) of Mice Fed Various Diets. NUCB2 mRNA was significantly reduced in the stomach (A; $p < 0.05$) from mice fed on a high fat diet than mice fed on the control, high protein and high carbohydrate diet ($n=5-6$ mice/group). No significant difference were found in NUCB2 mRNA expression in the small intestine from mice fed on various diets [B; (CD; $n=5$), (HP; $n=7$), (HC; $n=7$), (HF; $n=7$)]. Mice fed on high protein and high fat diets had significantly low expression of NUCB2 mRNA in the large intestine (C; $p < 0.05$) than mice fed on the control and high carbohydrate diet [(CD; $n=6$), (HP; $n=7$), (HC; $n=6$), (HF; $n=7$)]. Mice fed on a high protein diet had low expression of NUCB2 mRNA in the liver (D; $p < 0.05$) than mice fed on other diets [(CD; $n=6$), (HP; $n=7$), (HC; $n=7$), (HF; $n=7$)]. Different letters (a and b) shows significant differences found between the various fed groups, using One Way ANOVA followed by Tukey's Multiple Comparison Test. There are no significant differences between groups marked by same letters.



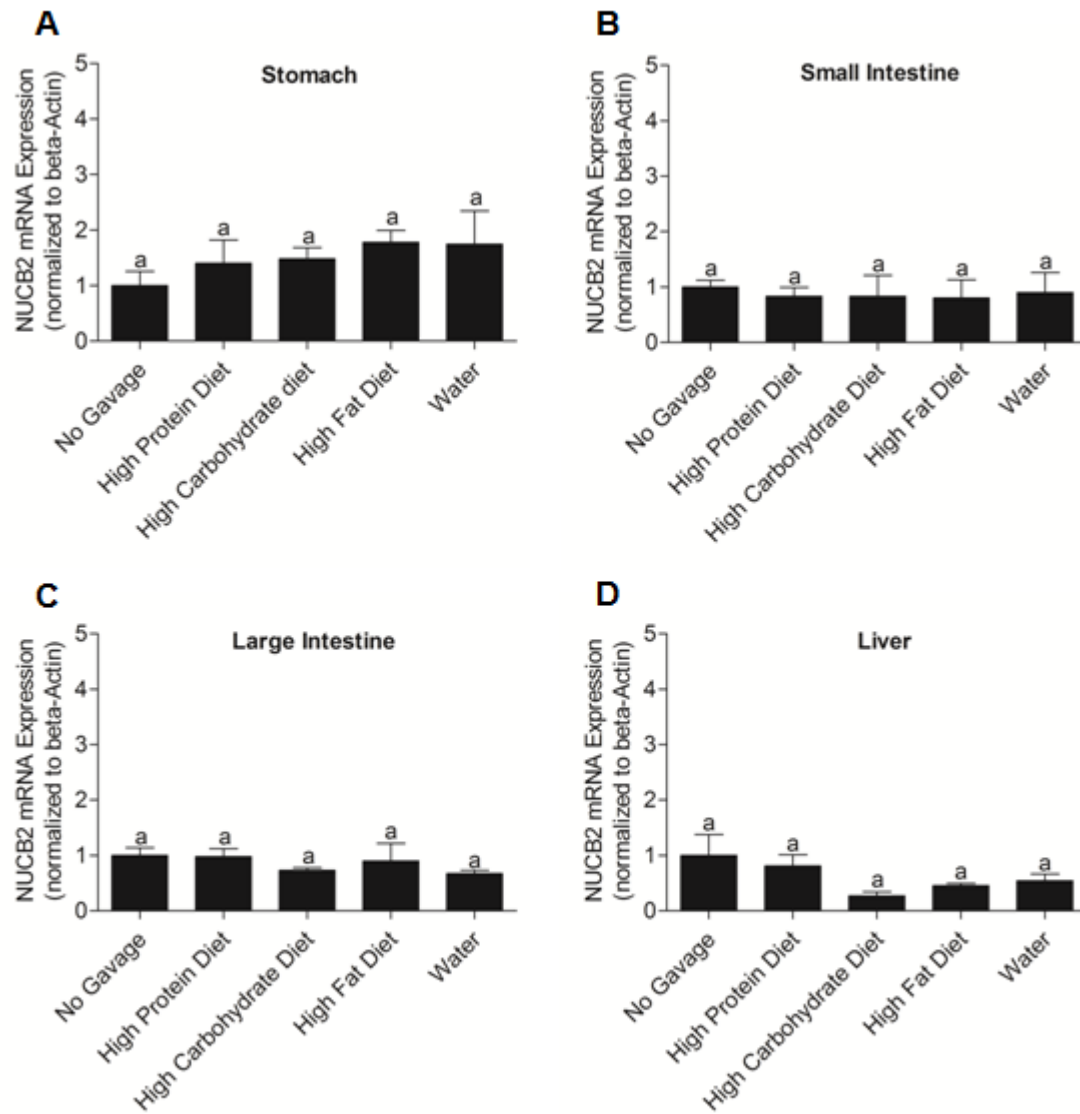
CD: Control Diet; HP: High Protein Diet; HC: High Carbohydrate Diet; HF: High Fat Diet

Figure 4.9 Chronic effects of nutrients on serum NUCB2/nesfatin-1 in mice

Figure 4.9. Serum NUCB2/Nesfatin-1 Levels at 7 a.m., 1 p.m., and 7 p.m. in Mice Fed Various Diets. Mice were chronically fed on a control diet (n=6), high carbohydrate diet (n=7), high protein diet (n=7), and high fat diet (n=7). No significant difference in serum NUCB2/nesatin-1 levels was found in mice fed on different diets at 7 a.m. (A). High carbohydrate diet fed mice had significantly higher serum NUCB2/nesatin-1 in circulation at 1 p.m. (B; $p<0.05$). Serum NUCB2/nesatin-1 was significantly lower in mice fed high carbohydrate, high protein or high fat, compared to control diet fed mice at 7 p.m. (C; $p<0.05$). Different letters (a and b) shows significant differences found between the various fed groups, using One Way ANOVA followed by Tukey's Multiple Comparison Test. There are no significant differences between groups marked by same letters.

4.3.8 Acute effects of nutrients on NUCB2 mRNA expression, blood glucose and serum NUCB2/nesfatin-1 in mice

There were no significant changes in the expression of NUCB2 mRNA in the stomach (**Figure 4.10A**), small intestine (**Figure 4.10B**), large intestine (**Figure 4.10C**) and liver (**Figure 4.10D**) between mice fed on a high protein, high carbohydrate, high fat or water. We found that the group gavaged with the glucose diet had significant high blood glucose levels compared to the groups gavaged with water, high protein and high fat liquid diets (**Figure 4.11A**). In order to validate blood glucose tolerance in each group during the oral gavage study, we analyzed the area under the curve from 0- 30 minutes. We found that the group gavaged with glucose had a significant increase in the concentration of blood glucose levels in the initial 30 minutes post-gavage. During the intra-peritoneal glucose tolerance test, NUCB2/nesfatin-1 levels in the high fat diet gavaged mice at 15, 30, 60, 120 minutes were significantly higher compared to mice fed with water, high protein and high carbohydrate diet, at all four time points tested (**Figure 4.11B**).



NG: No Gavage; HP: High Protein Diet; HC: High Carbohydrate Diet; HF: High Fat Diet; W: Water

Figure 4.10 Acute effects of nutrients on NUCB2 mRNA expression NUCB2/nesfatin-1 in mice

Figure 4.10. NUCB2 mRNA Expression in the Stomach (A), Small Intestine (Duodenum; B), Large Intestine (C) and Liver (D) of Mice gavaged with water, high protein, high carbohydrate, high fat and the No Gavage Group (n=7 mice/group). No significant differences were found in NUCB2 mRNA in the stomach of mice gavaged with various liquid diets and no gavage group. Same letters (a) indicate no significant differences found between the various groups, using One Way ANOVA followed by Tukey's Multiple Comparison Test.

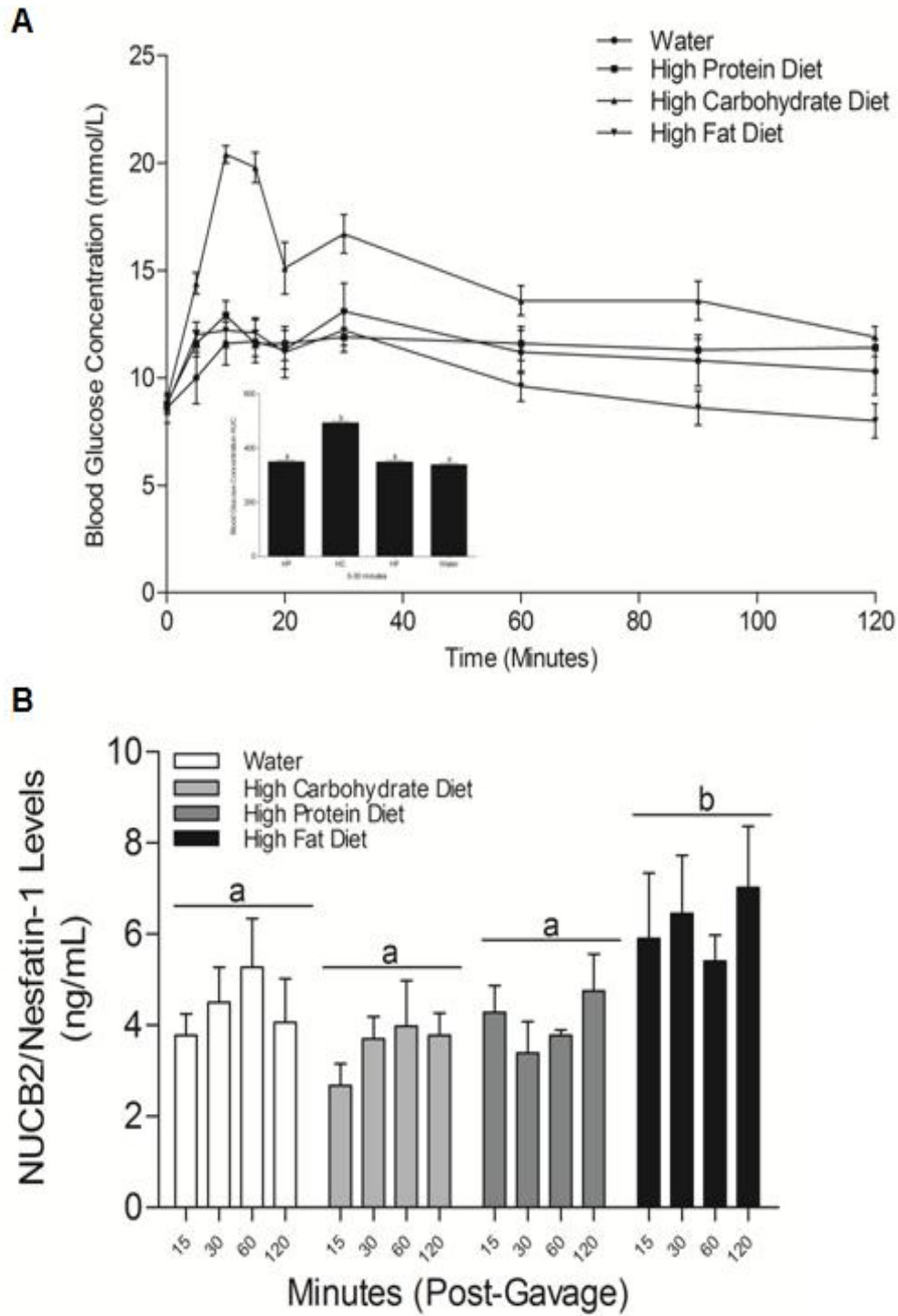


Figure 4.11 Acute effects of nutrients on blood glucose and serum NUCB2/nesfatin-1 in mice

Figure 4.11. Blood Glucose and Serum NUCB2/Nesfatin-1 in mice during acute administration of various liquid diets and in no-gavage group. (A) Fold change in blood glucose measured during an oral gavage study in mice gavaged with a specific liquid diet, divided into 5 groups: high protein (n=7), High fat (n=7), High carbohydrate (n=7), water (n=7) and a no gavage group (n=7). Mice gavaged with the high carbohydrate liquid diet had high concentrations of blood glucose compared to the no-gavage group and the groups gavaged with water, high protein and high fat liquid diets ($p < 0.05$, ANOVA followed by Tukey's Multiple Comparison Test). Blood glucose concentration - Area under the Curve from 0-30 measured during an oral gavage study in mice gavaged with a specific liquid diet, divided into 4 groups: high protein, high fat, high carbohydrate, and water (n= 7 mice/group). Letter *a* denotes no difference between the groups gavaged with water, high protein and high fat liquid diet. Letter *b* denotes that the high carbohydrate group had significantly elevated glucose levels compared to high protein, high carbohydrate, high fat and water gavaged mice during 0-30 minutes post-administration ($p < 0.05$, One-Way ANOVA followed by Tukey's Multiple Comparison Test). (B) Secretion profile representing circulating levels of NUCB2/Nesfatin-1 in mice gavaged with a specific liquid diet, divided into 4 groups: high protein, high fat, high carbohydrate, and water (n= 7 mice/group). Letter *a* denotes no difference in serum NUCB2/Nesfatin-1 levels between mice gavaged with water, high protein, high carbohydrate, high fat liquid diets and the no-gavage group within the four time points tested. Letter *b* denotes that the serum nesfatin-1/NUCB2 levels in the high fat diet fed group was significantly higher to the levels in the control mice or mice fed other diets at all time points ($p < 0.05$, One-Way ANOVA followed by Tukey's Multiple Comparison Test).

4.4 Discussion

The first main contribution of this work was the characterization of MGN3-1 cells as a source of nesfatin-1 and a tool for studying the regulation of nesfatin-1 secretion. mRNAs encoded for NUCB2, and its processing enzymes PC 1/3 and PC 2 in MGN3-1 cells. These findings are supported by NUCB2, PC 1/3 and PC 2 immunoreactivity detected in the same cells. Further, it was determined that MGN3-1 cells colocalize both nesfatin-1 and ghrelin, an observation that confirmed previous findings of nesfatin-1 in the X/A ghrelin cells in the stomach (Stengel et al., 2009b). The cell line MGN3-1 used in this research is a pure population of ghrelinoma cells, and it has been characterized that these cells express prohormone convertases and ghrelin-O-acyl transferase (Iwakura et al., 2010). Current results, together with previous findings indicate that the enzyme machinery required to process NUCB2 to nesfatin-1 is present in MGN3-1 cells. MGN3-1 cells were then used to identify how nutrients modulate NUCB2 synthesis and secretion. Cells incubated for 2 hours at 100 mM glucose containing DMEM had significantly higher NUCB2 mRNA expression than cells incubated at lower glucose concentrations. However, it was found that NUCB2/nesfatin-1 secretion was not influenced by changes in glucose concentrations introduced. Meanwhile, both NUCB2 mRNA expression and NUCB2/nesfatin-1 secretion were enhanced by L-Tryptophan. Since previous studies on nutrient regulation of hormones looked at the effects of fatty acids on protein secretion (Janssen et al., 2012, Hirasawa et al., 2005, Hara et al., 2009, Briscoe et al., 2003), three fatty acids, oleic acid, linoleic acid and octanoic acid were tested individually. Only oleic acid was found to inhibit NUCB2 mRNA expression, while the other two fatty acids were ineffective in modulating NUCB2 mRNA and NUCB2/nesfatin-1 secretion. Both in the glucose and oleic acid treatments, changes were found in NUCB2 mRNA expression, with no effects on nesfatin-1

secretion. It is possible that the NUCB2 mRNA expression and secretion in response to these nutrients are uncoupled in ghrelinoma cells. Further studies are required to elucidate the specific effectors in the transcriptional, translational and post-translational regulation of NUCB2/nesfatin-1 synthesis and secretion.

Glucose inhibits ghrelin secretion from stomach endocrine cells (Sakata et al., 2012, Brogilo et al., 2004). In current studies using MGN3 cells, glucose was ineffective in causing any changes on ghrelin. Meanwhile, glucose elicited stimulatory effect on NUCB2 mRNA expression. The difference in our results is possibly due many differences in the experimental protocols, types of cells (primary cells versus cell lines) and doses used. Here, effects of amino acids and fatty acids on ghrelin mRNA expression and secretion were also explored. As in the case of NUCB2 mRNA, the expression of ghrelin mRNA expression was also significantly higher in cells incubated with L-Tryptophan, but at a different dose (1 mM). Meanwhile, the effects of some fatty acids on ghrelin appear to be the opposite of what was seen on NUCB2 mRNA expression. Total ghrelin secretion from MGN3-1 cells incubated at 100 μ M linolenic acid was significantly higher. In addition, ghrelin mRNA and total ghrelin secretion was significantly increased from cells incubated at 100 μ M oleic acid. This data showed that oleic acid stimulated ghrelin, while suppressed nesfatin-1. While nesfatin-1 is produced in stomach ghrelin cells, it has been shown that nesfatin-1 is present in distinct secretory vesicles (Stengel et al., 2009b). Nutrient regulation of ghrelin secretion is also complex, with diverse effects in a tissues specific manner (Al Massadi et al., 2010, Greenman et al., 2004) In general, proteins and lipids decreases ghrelin secretion (Koliaki et al., 2010). Although the mechanisms by which nutrients are sensed by MGN3-1 cells are yet to be identified, at least in the case of fatty acids, that it may involve free fatty acid receptors. Other studies have identified that medium and long

chain fatty acids bind to G-protein coupled receptors such as GPR40 and GPR120 (Tanaka et al., 2008, Edfalk et al., 2008). GPR40 is expressed in the brain and in the pancreatic β -cells and binds to free fatty acids stimulating the secretion of insulin (Liou et al., 2011). Dietary fat has shown to stimulate cholecystokinin (CCK) by binding to GPR40 (Tanaka et al., 2008). In contrast, GPR120 is expressed in the distal intestine, binding to long chain fatty acids such as α -linolenic acid (Hara et al., 2009). Previous studies on the effects of free fatty acids in the enterendocrine cell line STC-1 have shown that fatty acids stimulate glucagon-like peptide-1 (GLP-1) and CCK (Hara et al., 2009, Krause, 2000). Further studies are required to unravel the mechanism of nutrient regulation of nesfatin-1 in gut cells.

A second major contribution of this work was the determination of NUCB2/nesfatin-1 mRNA, and protein (immunoreactivity) in the liver and small and large intestines of mice. The quantification of NUCB2 mRNA indicated that the relative abundance of NUCB2 was much lower in the intestine and liver, when compared to the stomach of mice. Approximately 50 kDa bands representing NUCB2 was present in total protein collected from the liver, and small and large intestines. However, no bands of the expected 10 kDa size representing the processed nesfatin-1 was detected in any of the tissues tested. This result concurs with previous findings of a full length NUCB2 protein in the liver, and small and large intestine of male rats and ICR mice (Zhang et al., 2010). Meanwhile, Stengel and colleagues (2009b) were unable to find NUCB2/nesfatin-1 in the liver and intestinal samples collected from male Sprague Dawley rats. This inability to detect NUCB2 in Sprague Dawley rats is unclear. Possible reasons include species differences in NUCB2 expression and/or differences in the physiological status of the rats used in that study. Similar to both (Zhang et al., 2010, Stengel et al., 2009b) studies discussed above, we were unable to find the processed nesfatin-1 in any of the tissues tested.

Stengel and colleagues (2009b) also found a processed band of approximately 47 kDa in their Western blot. Similar to this, we also detected second band 3 kDa less in molecular weight (approximately 47 kDa) in the small intestine and liver, but not in the large intestine. As concluded by Stengel and colleagues (2009b), the 47 kDa band suggests that the signal peptide in the NUCB2 from liver and small intestine could be cleaved, and the precursor released into circulation. The mucosal cells of both small and large intestine showed sparsely distributed cells that were immunopositive for NUCB2/nesfatin-1. Whether the nesfatin-1 positive cells were indeed intestinal enteroendocrine cells, and nesfatin-1 actions on intestinal physiology require further assessment.

Mice fed on a high fat diet had significantly lower expression of NUCB2 mRNA in the stomach compared to mice fed on the other diets. This was also evident in the present *in vitro* studies where MGN3-1 gastric cells had low NUCB2 mRNA expression levels when treated with oleic acid. The difference in the levels of NUCB2 mRNA expression could be a result of how various gastric cells absorb nutrients in response to chronic intake of carbohydrate and fats. The process by which how fats and carbohydrates are processed by gastric mucosal cells likely also affects endogenous nesfatin-1. Central administration of nesfatin-1 inhibits gastric acid secretion (Xia et al., 2012). It would be interesting to investigate enzymes that are involved in the digestion of carbohydrates and fat including pancreatic amylase and lipase to determine whether they are modulated simultaneously with NUCB2 mRNA expression in the stomach. No significant difference was observed in NUCB2 mRNA expression in the small intestine of different diet fed groups. But in the large intestine, it was found that mice fed on the high protein and high fat diet had comparatively lower expression of NUCB2 mRNA than mice fed on the control and high carbohydrate diet. NUCB2/nesfatin-1 may be involved in the absorption of

nutrients as well as controlling the secretion of intestinal hormones (Zhang et al., 2010). Other studies report NUCB2/nesfatin-1 immunoreactivity is also observed in the Brunner's glands of SD rats and ICR mice (Zhang et al., 2010). These glands are involved in secreting alkaline products such as bicarbonate, mucus containing intestinal lipase, peptidase that could be influenced by nutrient absorption (Stengel et al., 2012) affecting NUCB2 gene expression.

It was revealed that high protein fed mice had significantly lower NUCB2 mRNA expression in the liver, compared to mice fed other diets. Previous studies have shown that nesfatin-1 is a glucose dependent insulintropic peptide (Gonzalez et al., 2011). Liver is a major insulin responsive tissue involved in glucose homeostasis. It has been shown that peripheral infusion of nesfatin-1 upregulates mRNAs encoding phosphoenolpyruvate carboxykinase 1 and glucose-6-phosphatase, two enzymes that are critical in hepatic gluconeogenesis in the liver (Gonzalez et al., 2012a). The endogenous changes in nesfatin-1 due to nutrient abundance might result in local changes in other liver proteins involved implicated in glucose metabolism. No changes in NUCB2/nesfatin-1 levels in mice were found, when sampled at 7 a.m, the onset of light phase. However, at 1 p.m, the mice fed high carbohydrate had the highest levels of nesfatin-1. At 7 p.m, all mice, except the ones in the control group had significantly lower nesfatin-1 levels. Such suppression of an anorexigen prior to the onset of feeding time is also supportive of the satiety role of endogenous nesfatin-1. This difference in circulating NUCB2/nesfatin-1 levels could be attributed to a possible circadian pattern of NUCB2/nesfatin-1 release. In the acute diet study, nutrients had no significant differential effects in the expression of NUCB2 mRNA in the stomach, small intestine, large intestine and liver of mice. As expected, the acute administration of a high carbohydrate diet increased blood glucose levels within the initial 30 minutes. However, no significant increase in NUCB2/nesfatin-1 levels in the glucose gavaged group was

found. Meanwhile, NUCB2/nesfatin-1 levels at 15, 30, 60, and 120 minutes post-gavage were significantly increased in mice fed on a high fat liquid diet. In addition, in this acute study to determine whether gastric distention would cause a release in NUCB2/nesfatin-1 in circulation, we had a no-gavage group and the group that was gavaged with water only. There was no difference in NUCB2/nesfatin-1 in circulation in these two control groups. This suggests that NUCB2/nesfatin-1 changes in circulation indeed require nutrient sensing, as water ingestion alone and resulting distension of gut wall did not elicit the same results. On the other hand, a recent study has revealed that gastric distention results to the activation of NUCB2/nesfatin-1 expressing neurons in the nucleus of the solitary tract of rats (Bonnet et al., 2013). Overall, these results indicate that the nutrient elicited changes in NUCB2 expression varies depending on the mode of treatment and the duration of experiment.

4.5 Conclusion

The study provided the first set of information on nutrient regulation of nesfatin-1. Present findings suggested that the effects of diets on the expression of endogenous NUCB2/nesfatin-1 were myriad, with specific effects on mRNA expression versus secretion, in a dose and time dependent manner. MGN3-1 cells were characterized as nesfatin-1 secreting cells with the NUCB2 processing machinery, suggesting that this cell line is useful for studying nesfatin-1 biology. Glucose simulated NUCB2 mRNA expression in a dose and time-dependent manner in MGN3-1 cells. L-Tryptophan stimulated NUCB2 mRNA expression and nesfatin-1 secretion. From the *in vivo* studies, NUCB2 mRNA expression was significantly lower in the liver of mice fed on a high protein diet compared to mice fed other diets. High fat fed mice had a significant reduction in NUCB2 mRNA expression in the stomach, while high protein and high fat diet resulted in the attenuation of NUCB2 mRNA in the large intestine. Mice fed on the high protein, high carbohydrate and high fat demonstrated a post-prandial increase in NUCB2/nesfatin-1 secretion. These results indicated that the synthesis and secretion of nesfatin-1 were altered by the relative amount of nutrients and such effects are dependent on the amount of nutrients, tissues and time of the day or duration of treatment. While such variations exist, these data in general support that fat is inhibitory, while carbohydrate and protein are NUCB2/nesfatin-1 stimulatory. Nesfatin-1 is explored as an anti-obesity compound. Nutrient dependent changes in endogenous NUCB2/nesfatin-1 should also be considered, especially when developing diet or exogenous nesfatin-1 based potential therapies for obesity and related metabolic diseases.

Transition

The final data chapter focuses on my fourth objective: To study whether the genetic loss of nesfatin-1 alters whole body energy homeostasis, islet morphology, islet hormone release and glucose and whole body energy homeostasis in NUCB2 knockout (NKO) mice. My research on developmental expression of NUCB2/nesfatin-1 (Chapter 2 and 3) and nutrient regulation of NUCB2/nesfatin-1 (Chapter 4) provided significant new information on endogenous nesfatin-1. Our research, and data from several other researchers independently determined several actions of nesfatin-1 in regulating energy balance. However, whether endogenous NUCB2/nesfatin-1 is critical in regulating metabolic homeostasis remain unknown. Using a NUCB2/nesfatin-1 knockout mouse model, we determined whether NUCB2/nesfatin-1 is critical for maintaining energy balance. Our preliminary data on the phenotype characterization of NKO mice demonstrates a sexually dimorphic effect of NUCB2/nesfatin-1 disruption in mice: an increase in body weight, food intake, attenuated glucose stimulated insulin secretion and altered energy homeostasis.

Publication: Mohan, H., Tsushima, R., Ceddia, R., Pasupuleti, V., Mortazavi, S., Unniappan, S., 2015. Preliminary Characterization of Nucleobindin-2 Knockout Mice: Sexually Dimorphic Defects in Whole Body Energy Homeostasis, Glucose Tolerance and Insulin Secretion. Manuscript in Preparation.

Contributions: Haneesha Mohan conducted *in vivo* and *in vitro* studies, collected and processed the tissue samples for various experimental analyses, and prepared the manuscript. Haneesha Mohan. processed tissues for immunohistochemistry, conducted immunohistochemistry analysis and microscopy. Robert Tsushima helped with *in vitro* studies with respect to pancreatic islet isolation and protein assays. Rolando Ceddia shared equipment to conduct *in vivo* studies using CLAMS. Sima Mortazavi and Venkat Pasupulletti helped with several *in vitro* and *in vivo* studies. Suraj Unniappan. helped with the research, secured funding for the project and edited the manuscript.

Chapter 5

Preliminary Characterization of Nucleobindin-2 Knockout Mice: Sexually Dimorphic Defects in Whole Body Energy Homeostasis, Glucose Tolerance and Insulin Secretion

5.1 Introduction

Nesfatin-1 is co-expressed with insulin in rodent and human pancreatic β -cells, and has glucoregulatory functions (Gonzalez et al., 2012b, Gonzalez et al., 2011, Gonzalez et al., 2009). Nesfatin-1 is a novel metabolic protein implicated in the regulation of energy balance. It is derived from the precursor, nucleobindin-2 (NUCB2) that is cleaved by prohormone convertases 1/3 and 2 (Gonzalez et al., 2011, Oh-I et al., 2006). It is actively being explored as a potential anti-obesity and anti-diabetic molecule (Li et al., 2010, Shimizu et al., 2009). It was initially discovered by subtraction cloning from both neuronal and adipocytic cell lines (Oh-I et al., 2006). NUCB2/nesfatin-1 is highly conserved across vertebrates (Gonzalez et al., 2010, Mohan and Unniappan, 2013, Zhang et al., 2010) with functions that are species- and tissue-specific (**Chapter 1**). Nesfatin-1 regulates food intake, energy balance, glucose metabolism and insulin secretion, reproduction, gastric emptying, development, stress modulation, thermogenesis, and cardiovascular functions (Mohan and Unniappan, 2013) as detailed in **Chapter 1**. Our knowledge on NUCB2/nesfatin-1 control of various physiological systems evolved since its discovery in 2006. However, a key question remains unanswered: Is endogenous nesfatin-1 critical for the regulation of all physiological processes it is involved with? In order to address this, a NUCB2 knockout (NKO) mouse model was generated. This model allowed us to gain further insights on the metabolic significance of NUCB2 gene and nesfatin-1. The hypothesis is that the genetic disruption of NUCB2, which leads to the absence of nesfatin-1, results in an alteration in whole body energy homeostasis. This chapter focuses on the phenotype

characterization of NKO mice, with a special emphasis on insulin secretion, glucose regulation, metabolic hormone milieu and whole body energy homeostasis.

5.2 Materials and Methods

5.2.1 Generation of the NKO mice

To study NUCB2 gene function in mice, a random mutagenesis approach called, ‘gene trapping,’ where insertion of a synthetic DNA element into an endogenous gene leads to transcriptional disruption was implemented. The gene trapping vector construct used was VICTR 48 Ominobank Vector. This construct mainly consists of 2 long terminal repeats (LTR), splice acceptor (SA), restriction enzymes (*Bgl*II and *Hind*III), a selectable marker gene (neomycin phosphotransferase; NEO) and polyadenylation signals (pA and SV40tpA). This construct was then placed within a retroviral genome that was used to infect a mutant cell line. The insertion of the vector occurred within the transcriptionally active regions. The marker gene NEO was expressed and translated, allowing selection of mutant clones (OST287865). 129SvEv^{Brd}-derived parent embryonic stem cells (Lex-1) were cultured with the mutant clone consisting of the vector and subsequently NUCB2 gene in the Lex-1 cells was disrupted by the mutant clone. Gene disruption was achieved through the capture of the endogenous NUCB2 gene transcription via retroviral insertion of the trapping vector within the intron between the first and second non-coding exons of the NUCB2 gene (**Figure 5.1**; Accession Number: NM_016773). Following, transcription tagging or 3’ RACE (**r**apid **a**mplification of **c**DNA **e**nds) method was used to identify whether NUCB2 gene was disrupted by gene trapping in the cells. It was found that NUCB2 gene was trapped by the mutant vector in chromosome number 7 (Tag ID: OST287865; Tag Location: 116509455-116509600 base pairs). The gene trapping method repressed the transcription of NUCB2 gene and therefore no translation of protein will occur. Transgenic Lex-1 cells were selected and then injected into the early stage of a host mouse embryo. These cells integrated with the host’s embryonic stem cells. The embryos were then placed into the uterus of

pregnant mice, where they developed into chimeric mice. The chimeric mice were bred to C57BL/6-^{Tyrc-Brd} mice to generate F1 heterozygous animals. These progeny were intercrossed to generate F2 wild type, heterozygous, and homozygous mutant (NKO) progeny. These mice are viable and their preliminary phenotypic characterization was posted at the Mouse Genome Informatics site. Lexicon Genetics conducted the above gene manipulations and generated the NKO mice. However, these mice were not maintained as a live colony, but frozen sperm and cryopreserved embryos were available through a NIH funded repository at the Texas Genome Research Institute (TGRI). We purchased the cryopreserved sperm and re-derived the NKO line at the Jackson labs under the auspices of the TGRI. The MGI and TGRI preliminary data suggests that the NKO mice show an increased heart rate, increased levels of serum alkaline phosphatase and decreased insulin levels and impaired glucose tolerance during oral glucose load.

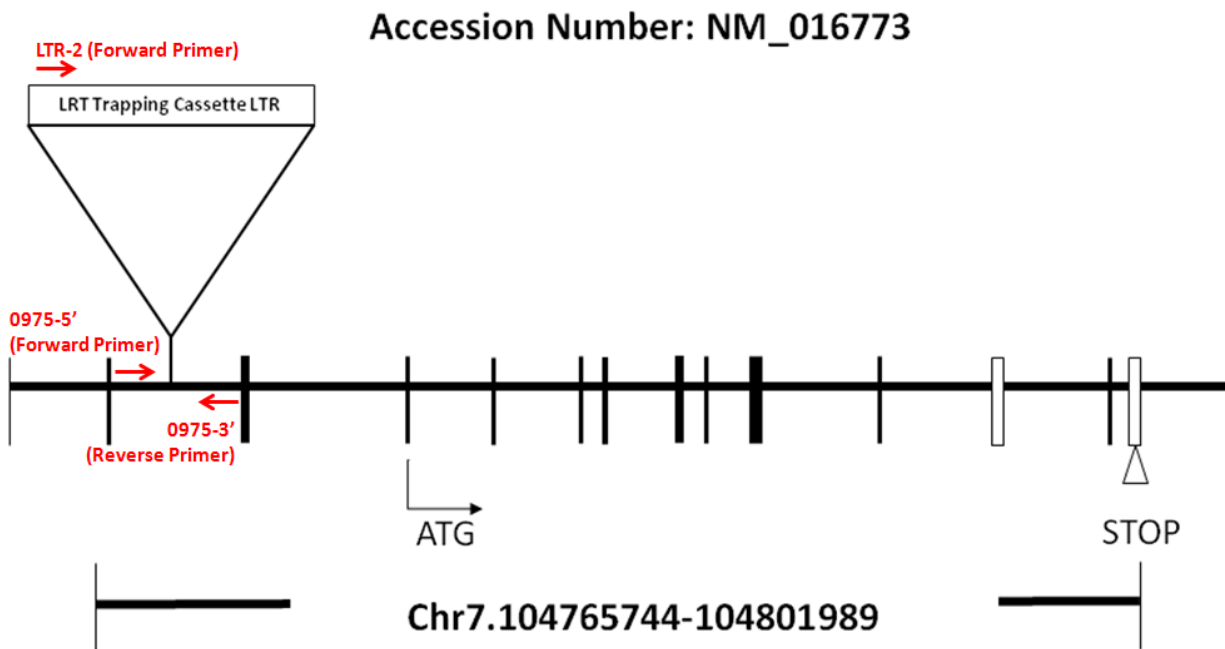


Figure 5.1 Creation of the NUCB2 KO Model

Figure 5.1. A graphical representation depicting a trapping vector facilitated insertion; a retroviral insertion made within the intron between the first and second non-coding exons of the NUCB2 gene in chromosome 7, which was used to create the NKO mouse.

5.2.2 Genotyping

Mouse genomic DNA was isolated from NKO and wildtype (C57BL/6; WT) male and females tail biopsies. Tail snip were suspended in a 1.5 mL tube containing 250 µl Direct PCR Lysis Reagent (Catalogue Number 102-T, Viagen Biotech, Inc., Los Angeles, California) containing 0.05-0.1 mg/mL Proteinase K (Catalogue Number p6556, Sigma-Aldrich, Ontario, Canada). Tubes were incubated at 55° C in a rotating hybridizing oven until complete lysis was achieved (16-24 hrs). Lysates were incubated at 85°C for 45 min by floating the whole rack (containing tubes) on water bath. Ten microliters of the crude lysate per 100 µl PCR reaction was used. Qiagen HotStar Taq DNA polymerase (Catalogue Number 203203, Valencia, California) was used for PCR according to the manufacturer's instructions. PCR was performed using the primer pairs to distinguish the wild type (WT; Amplicon size: 439 Base pairs; oligo F (0975-5'); 5'-TCTACATCATGCTGGATCAACAGG-3' and oligo R (0975-3'); 5' TCTGCCTGCCTGATACCATGCTCCC-3') and gene trapped-mutant (NKO; Amplicon size: 441 Base pairs; oligo F (LTR-2); 5'-AAATGGCGTTACTTAAAGCTAGCTTGC-3' and oligo R (0975-3'); 5'- TCTGCCTGCCTGATACCATGCTCCC -3') (**Figure 5.1**). Negative control PCR reactions consisted only of primers and required reagents, but no template DNA.

5.2.3 Western Blot Analysis

Tissues (liver, stomach, duodenum, pancreas) from age-matched male and female WT and NKO mice were lysed with lysis buffer (0.5mM sodium orthovanadate, 1µM pepstatin A, 20M phenylmethylsulfonyl fluoride, protease inhibitor, phosphatase inhibitor) followed by periodic vortexing for 30-40 minutes. In addition we used five positive control cell lysates - COS cells (American Type Culture Collection (ATCC), CRL-1561 Cell Lines, Manassas, VA) that were transfected with/without NUCB2, either NUCB2 with PC 1/3, NUCB1 (Miura et al., 1992)

with PC 1/3 or NUCB2 with Furin and MGN3-1 cells (Source: Refer to Chapter 4) that were lysed by scraping with lysis buffer. We used COS cells as they are easy to maintain in culture and several cloning vectors are available to transfect them.

COS 7 cells were maintained in growth medium which consisted of Dulbecco's Modified Eagle Medium high glucose, containing pyruvate, L-glutamine (DMEM, Catalogue Number 319-005-CL; Wisent, St. Bruno, QC, Canada) supplemented with 10% fetal bovine serum (Fetal Bovine Serum; Catalogue Number 080-150; Wisent, St. Bruno, QC, Canada) and penicillin/streptomycin (Catalogue Number 450-201-EL; Wisent, St. Bruno, QC, Canada). Cells for transfection were seeded in 6-well cell culture plates (Greiner; Sigma-Aldrich, Ontario, Canada) at least 2 days prior to the start of transfection. When cells were 80% confluent, they were refed with 1.5 mLs of growth medium three hours before the start of transfection. Plasmid DNA was transfected using TurboFect (Fermentas; Catalogue Number R0531; Thermo Fischer Scientific, Mississauga, ON, Canada) as per manufacturer instructions. Briefly, 200 µl of serum free DMEM was aliquoted into autoclaved eppendorf tubes. A total of 2 µg of plasmid DNA was added and 6 µl of TurboFect reagent. Mixtures were immediately vortexed and incubated for 18 minutes at room temperature. To each of 2 wells, 100 µl of this DNA mixture was added (for duplicate wells) and cells were returned to incubator overnight. The next morning, transfection medium was aspirated, cells were washed twice with 2 mL of phosphate buffered saline (Phosphate Bovine Serum; Catalogue Number 311-010-CL; Wisent, St. Bruno, QC, Canada) and refed with 2 mL/well of growth medium. Expression of GFP and DsRed were examined to determine approximate efficiency which was typically 70% of cells being positive for GFP expression. For transfections, each well received 0.5 µg of NUCB1, NUCB2, PC1/3 or Furin plasmids, 0.25 µg pcGFP, 0.25 µg pBlueDsRed, 0.5 µg pGEM9Z and empty pcDNA3 if only

one expression plasmid was examined (NUCB1, NUCB2, PC1/3 and Furin were in CMV-based expression plasmids identical or near-identical to the pcDNA3 plasmid backbone). Cells were returned to the incubator for 30-48 hours and then harvested for Western Blotting. Briefly, medium was removed and cells were washed twice with cold PBS and extracted on ice with an NP-40 lysis buffer (0.5% NP-40, 50 mM Tris-HCl [pH 8.0], 150 mM NaCl, 10 mM sodium pyrophosphate, 1 mM EDTA [pH 8.0], 0.1 M sodium fluoride) containing 10 µg/mL leupeptin and aprotinin, 5 µg/mL pepstatin A, 0.2 mM PMSF and 0.5 mM sodium orthovanadate. Lysates were extracted on ice for 30 minutes with periodic vortexing. Cleared lysates were transferred to new eppendorf tubes (combined duplicate wells) and protein concentrations were determined using the Bradford method (BioRad) with bovine serum albumin (BSA) as a standard. Extracts used for immunoblotting were diluted in sample buffer containing SDS/β-mercaptoethanol and boiled. For Western Blotting, equal µg amounts of cell lysates were examined. These cells allow us to clone genes and enzymes to study gene expression and test mammalian expression vector constructs. For endogenous control specificity rat nesfatin-1(1-82) [VPIDVDKTKVHNVEPVESARIEPPDTGLYYDEYLKQVIEVLETDPHFREKLQKA

DIEEIRSGRLSQELDLVSHKVRTRLDEL] was synthesized by Abgent Technologies (San Diego, CA). Synthetic nesfatin-1 was purified using HPLC to more than or equal to 95% purity. The mass and purity were confirmed by mass spectrometry.

The lysate of tissue or cells was centrifuged and the supernatant containing soluble protein was extracted. Protein concentration was determined by the Bradford method (Bio-Rad Laboratories). Laemmli buffer (0.5 M Tris-HCl, glycerol, 10% SDS, 0.5% Bromophenol Blue, 5% β-mercaptoethanol) was added to the samples and stored at -80° C until needed. Prior to use, samples were boiled at 95° C for 4 minutes. Equal quantities of protein were

electrophoresed on a 10% or 15% SDS-polyacrylamide gel, followed by electroblotting onto a polyvinylidene fluoride (PVDF) membrane overnight at room temperature. Membranes were washed in 1X TBSTN wash buffer (Tris-buffered saline, 0.05% Tween-20, 0.05% NP-40) (30 min, 25°C) and blocked in a solution of 3% BSA in 1X TBSTN for 4-6 hours. Membranes were then probed with Rabbit anti-nesfatin-1 primary antibody (Catalogue Number H-003-22; 1:1000 dilution, Phoenix Pharmaceuticals) or Rabbit anti-preproghrelin primary antibody (Catalogue Number SC-50297; 1:1000 dilution; Santa Cruz Biotechnology, Santa Cruz, CA, USA) overnight at 4°C. Membranes were then washed in 1X TBSTN (3 × 10 min, 25°C) and incubated with goat anti-rabbit IgG (H+L)-HRP secondary antibody (Bio-Rad, 1:3000 dilution) for 2 hours at room temperature. Membranes were washed in 1X TBSTN 5-7 times over 1.5 hours. Immune complexes were viewed on CL-Xposure™ film (Thermo-Scientific, Waltham, MA, USA) and developed using Immobilon™ Western Chemiluminescent HRP Substrate (Millipore, Billerica, MA, USA) according to the manufacturer's instructions.

5.2.4 Immunohistochemistry

For immunohistochemical studies, 2 male and 2 female NKO and WT mice were used. All dissections and tissue collection were conducted at the same time of the day (13:00-14:00 hours) to provide consistency. The pancreatic tissues were processed and slides were obtained for staining (Refer to **Chapter 2** for details on fixation, paraffin embedding, sectioning, staining, viewing and capturing of tissue image). These pancreatic sections were incubated with Mouse anti-nesfatin-1 primary antibody (Catalogue Number ALX-804-854-C100; 1:100 dilution, Enzo Life Science, Inc.) and guinea pig anti-insulin (Catalogue number ab 7842; 1:100 dilution; Abcam, Massachusetts) for 24 hours at room temperature. The slides were incubated with goat monoclonal anti-mouse FITC IgG (Heavy and Light Chain) (Green-Ghrelin; Catalogue number

ab 6785; 1:100 dilution; Abcam, Massachusetts) and goat anti-guinea pig TEXAS RED IgG (Heavy and Light Chain) (TEXAS Red-NUCB2/Nesfatin-1; Catalogue number ab 6906; 1:100 dilution; Abcam, Massachusetts) secondary antibodies for 1 hour at room temperature. Approximately 8 slides containing two sections of the pancreas from each mouse were stained using the above protocol and analyzed. Only representative images of the pancreas from each mouse are shown in the results section.

5.2.5 Weekly Body Weight and Food Intake Measurement

To determine the preliminary phenotypic changes in male (C57BL/6; n=4 and NKO; n=5) and female (C57BL/6; n=5 and NKO; n=4) age-matched mice, weekly measurements on body weight and food intake were recorded 4 hours post-fast using a digital weighing scale (VWR, Mississauga, Ontario) once a week for 18 weeks. Mice were age-matched and their body weight and food intake measurements commenced from 16 weeks of age in both genders. In a separate study, for 17 weeks, male and female age-matched mice (from 13 to 29 weeks of age) were fed on a low fat diet (Product # D12450i; Research Diets, New Brunswick, NJ) that had 3.8 kcal/gm with 20% energy derived from protein, 70% energy derived from carbohydrate and 10% energy derived from fat, and high fat diet (Product # D12451i; Research Diets, New Brunswick, NJ) that had 4.73 kcal/gm with 20% energy derived from protein, 35% energy derived from carbohydrate and 45% energy derived from fat. Similarly, weekly measurements on body weight and food intake were recorded 4 hours post-fast. The numbers of mice in each group are provided in the respective figure legend. We used the Mann-Whitney test of a non-Gaussian distribution or one-way ANOVA followed by Tukey's Multiple Comparison Test or Student-Newman Keuls multiple comparisons test to compare the mean \pm SEM of body weight and/or food intake to body weight ratio between the two groups of male and female mice.

5.2.6 *In Vitro* Effects on Glucose Stimulated Insulin Secretion (GSIS) from Isolated Islets

In order to determine whether glucose has direct effects on islets to stimulate insulin secretion, a GSIS assay was conducted. There were two studies performed. For the first study islets were gathered from three male and female NKO mice. For the second study, islets were gathered from three C57BL/6 and NKO female mice. We made 1 mg/mL of collagenase (Cat# C7657-500MG, Lot# SLBD3783V, Sigma-Aldrich, Ontario, Canada) solution in 1X Hank's Balanced Salt Solution (HBSS) and diluted it to 0.05 mg/mL. Once the mouse was anesthetized, a cervical dislocation was performed. An incision was made above the abdomen. Once the location of the ampulla was identified, it was blocked with surgical clamps on the duodenum wall to restrict the collagenase flow from the bile pathway into the duodenum. In a 5 mL syringe, 3 mL of the collagenase was filled with a 30 G1/2-G needle (Becton Dickinson and Company, Mississauga, Ontario, Canada). By viewing under the microscope, the needle was inserted into the common bile duct. The pancreas distends slowly as the collagenase is perfused. The pancreas was then excised from the stomach and the duodenum and placed in a 15 mL falcon tube containing 500 μ L of 0.05 mg/mL collagenase. The tube was then placed in a water bath set at 37°C for 10 minutes. The tube was shaken and then placed in the water bath at 37°C for 2 minutes. After pancreatic digestion, 1XHBSS was added to the tube to stop the digestion and kept on ice. After termination of digestion was completed using 1X HBSS, the tube was centrifuged at 1200 rpm (13.9 x G) for 2 minutes. After centrifugation, the supernatant above the pellet was then removed and discarded. Using an electronic pipetter, 5 mL of Histopaque was slowly added. Using the method of suction and ejection, the pellet was broken for the Histopaque to mix with pellet. After this step, using an electronic pipetter, 5 mL of 1XHBSS was slowly

added on the top layer. Spin at 1800 rpm for 10 minutes. Since Histopaque is toxic to islets, the top supernatant is poured off into a new falcon tube (50 mL) and cold 1X HBSS was added over the top. The islets were handpicked using a microscope from one culture dish to another culture dish which contained the 1X HBSS. Once all islets were handpicked, the islets were transferred to a dish containing 5.5 mM RPMI. The islets were washed twice and then transferred into a dish containing 5.5 mM RPMI for overnight incubation at 5% CO₂. Keeping islets in a sterile environment at 37° C at 5% CO₂ limits exposure to contamination and changes in pH.

The following morning, the culturing medium was replaced with 2 mL of 2.0 mM RPMI glucose and incubated for 2 hours. When performing a GSIS, it is essential that the islets are cultured in Krebs-Ringer Bicarbonate Buffer (KRB) solution. The KRB solution consists of salts that play an important role in cell culture experiment. It consists of basic salts that help in maintaining the pH and osmotic balance in the medium. It provides the cells with an environment that is rich in inorganic ions and basic solutions that are essential for survival during an *in-vitro* assay. Different glucose concentrations of KRB were made which include 2.0 mM and 16.7 mM KRB to represent hypoglycemic and hyperglycemic condition. After incubating the islets at 2.0 mM RPMI, the medium was removed and the islets were washed twice with 2 mL of 2.0 mM KRB. For the GSIS study, an 8 well plate was used. Each well consisted of 1 mL of 2.0 mM KRB. The islets were removed from the 35 mm dish and then 20 islets were counted and placed into each well. The plate was kept in a sterile incubator in 37°C at 5% CO₂ for 30 minutes. After 30 minutes, the supernatant was discarded, and the islets were incubated with 1 mL of 2.0 mM KRB for 1 hour. The supernatant was collected into a 1.5 mL tube and 1 mL of 5.5 mM KRB was added in each well and was kept at 37°C at 5% CO₂ for 1 hour. After an hour, the supernatant was collected into a 1.5 mL tube and 1 mL of 16.7 mM KRB

was added in each well and was kept at 37°C at 5% CO₂ for 1 hour. After 1 hour, the supernatant was collected into a 1.5 mL tube. The islets were washed by adding 1 mL of phosphate buffer solution into each well and the solution was discarded. Potassium chloride (KCL; 1 mL) was added to each well and the islets were collected with the KCL. Potassium Chloride (KCl) induces β -cell depolarization in the islet cells allowing for calcium influx which activates exocytotic insulin release. The islets in each tube were sonicated for 10 seconds and were kept on ice. The tubes were spun at 15000 rpm for 5 minutes and the top 500 μ L of the supernatant were transferred into new tubes. The tubes were stored at -20°C. Meanwhile the supernatant collected during incubation periods of 2.0 mM, 5.6 mM and 16.7 mM KRB media were spun at 1500 rpm and the top 700 μ L supernatant was collected into new pre-labelled 1.5 mL microcentrifuge tubes. The supernatant collected was used to measure insulin secreted from the islets extracted from wildtype and NKO female mice. We used an in-house mouse radioimmunoassay (Robert Tsushima Lab, York University) to measure secretion of insulin induced by glucose. ANOVA followed by a post-hoc Bonferroni test was used to compare the mean \pm SEM of insulin levels secreted into media between the two groups in the study.

5.2.7 Assessment of Whole-Body Energy Homeostasis Using Comprehensive Laboratory Animals Monitoring System (CLAMS)

To assess whole-body metabolic homeostasis in C57BL/6 and NKO male mice, they were housed in the CLAMS (Columbus Instruments, OH) for three days for automatic monitoring of multiple metabolic parameters. Four age-matched male mice in each group were used. The CLAMS is equipped with an open-circuit calorimeter for measuring accumulative oxygen (O₂), O₂ consumption (VO₂), carbon dioxide production (VCO₂), and respiratory exchange ratio (RER). RER was calculated by dividing VCO₂ by VO₂ with values ranging from

0.7 to 1.0. A shift of RER values toward 0.7 indicates that fatty acids contribute the most to energy production, while a shift towards 1.0 indicates the carbohydrates are the main substrates used. The percent of fatty acids and carbohydrates utilized at every time point for each animal was determined from the RER. Each cage is also equipped with a system of infrared (IR) beams that detects animal movement in the X (the length of the cage) and Z (the height of the cage) axes. We measured the total number of X-axis IR beam breaks (X-TOT), number of ambulatory X-axis IR-beam breaks (X-AMB) and total number of vertical rearing motions (Z-TOT). The data was analyzed using Graphpad Prism® version 5. The CLAMS system was calibrated according to manufacturer's instructions prior to beginning the experiments. We used the Mann-Whitney test of a non-Gaussian distribution to compare the mean \pm SEM of various metabolic parameters between the two groups of male mice.

5.2.8 Intraperitoneal Glucose Tolerance Test (IPGTT)

To elucidate the effects of the loss of NUCB2 gene on intraperitoneally injected glucose clearance, we conducted an IPGTT. It will help us detect whether loss of NUCB2 gene has an influence in glucose metabolism during glucose administration. IPGTT was conducted in male (C57BL/6; n=4 and NKO; n=5) and female (C57BL/6; n=5 and NKO; n=4) age-matched mice. After a tail snip, blood was collected to the One-Touch® Ultra Glucometer strip (LifeScan, Canada) for measurement of blood glucose using the One-Touch® Ultra Glucometer (LifeScan, Canada). Blood glucose was measured 6 hours post-fast. D-Glucose (Catalogue number GLU501.500; Bioshop; Canada) dissolved in saline was then injected intraperitoneally (1 gram/kilogram Body Weight of mice) and blood glucose was measured again at time points of 5, 10, 20, 30, 60, 90, 120, and 150 minutes, post injection. In addition to blood glucose monitoring, blood was collected from the tail into capillary tubes (100 μ L) at 5 and 30 minutes to

measure insulin levels during the IPGTT. Circulating insulin levels in the serum were measured using the Mouse Ultrasensitive Insulin ELISA kit (Catalogue number 80-UNSMU-E01, ALPCO, Salem, New Hampshire). The limit of the assay sensitivity was 0.115 ng/mL (5 μ L) for insulin, with a detectable range from 0.025 – 6.9 ng/mL. The amount of immunoreactive material was determined using a sigmoidal relationship curve. In a separate study, IPGTT (as described above) was also performed on male and female age-matched mice fed on a low fat diet and high fat diet (Details on diet and mice number in each group are described above). We measured the area under the curve (AUC) of blood glucose (0-150 minutes) and insulin (5-30 minutes) profile. The data was analyzed using an Unpaired t-test to measure the difference in AUC of blood glucose and insulin profile between the groups.

5.2.9 Insulin Tolerance Test (ITT)

In order to determine the effects of loss of NUCB2 gene on insulin sensitivity, an ITT was performed. ITT helps monitor glucose concentration over time, but in response to insulin administration rather than of glucose as in IPGTT. The degree to which glucose falls following insulin administration is indicative of whole body insulin action. Insulin tolerance test was conducted in male (C57BL/6; n=4 and NKO; n=5) and female (C57BL/6; n=5 and NKO; n=4) age-matched mice. After a tail snip, blood was collected to the One-Touch® Ultra Glucometer strip (LifeScan, Canada) for measurement of blood glucose using the One-Touch® Ultra Glucometer (LifeScan, Canada). Fasting blood glucose was measured 6 hours post-fast. Insulin (1 Unit/kilogram body weight) was then injected intraperitoneally and blood glucose was measured again at time points of 5, 10, 20, 30, 60, 90, 120, and 150 minutes, post injection. In a separate study, ITT (as described above) was also performed on male and female age-matched mice fed on a low fat diet and high fat diet (Details on diet and mice number in each group are

described above). One-way ANOVA followed by Student-Newman Keuls multiple comparisons test. Data are expressed as mean \pm SEM of blood glucose levels between the two groups in each gender.

5.2.10 Absolute Terminal Organ/Tissue Weight

Male (C57BL/6; n=3 and NKO; n=5) and female (C57BL/6; n=5 and NKO; n=4) age-matched mice were dissected at 40 weeks of age and weight of their organs/tissue (Heart, Spleen, Brown Adipose Tissue (BAT), Epididymal/Perigonadal Fat, Soleus Muscle) were measured using a digital weighing scale (VWR, Mississauga, Ontario). An Unpaired t-test was used to measure the difference in organs/tissue weight between the groups.

5.2.11 Serum Insulin, Glucagon, Ghrelin and Leptin Levels

Enzyme-linked immunosorbent assay (ELISA) was used to measure the circulating levels of insulin, glucagon, ghrelin and leptin in the blood. As these NKO mice are derived in a mixed background of 2 strains (C57BL/6 and 129Sv), we had gender specific comparative control strain groups for each group of NKO mice. Blood was collected from male and female C57BL/6, 129Sv and NKO mice. Blood samples were allowed to clot on ice, and serum was separated by centrifugation (7000 rpm for 9 minutes at 4°C) and stored at -20°C, until assay was conducted.

Insulin secretion levels in the serum was measured using the mouse ultrasensitive insulin ELISA kit (Catalogue number 80-UNSMU-E01, ALPCO, Salem, New Hampshire) according to the manufacturer's instructions to measure serum insulin levels in each group (Mouse Ultrasensitive Insulin ELISA kit specification details are described in the above IPGTT section). Glucagon secretion levels in the serum was measured using the Glucagon (Human, Mouse, Rat) ELISA kit (Catalogue number 48-GLUHU-E01, ALPCO, Salem, New Hampshire). The limit of the assay sensitivity was 10000 pg/mL (5 μ L) against the C-terminal (19-29 amino acids) of

glucagon, with a detectable range from 41 - 10000 pg/mL. The amount of immunoreactive material was determined using a standard relationship curve-fit. Ghrelin secretion levels in the serum were measured using the Rat/Mouse ghrelin (Active) ELISA kit (Catalogue number EZRGRA-90K, EMD Millipore, Darmstadt, Germany). The minimal limit of the assay sensitivity was 8 pg/mL for active ghrelin, with a detectable range from 25 – 2000 pg/mL. The amount of immunoreactive material was determined using a linear standard curve. Leptin secretion levels in the serum was measured using the leptin (Mouse/Rat) ELISA kit (Catalogue number EK-003-17, Phoenix Pharmaceuticals Inc., California). The limit of the assay sensitivity was 4000 pg/mL for leptin, with a detectable range from 62.5 – 4000 ng/mL. The amount of immunoreactive material was determined using a linear standard curve. For each assay, the amount of immunoreactive material was measured using the correlation or linear regression model recommended to quantify and compare the concentration of protein in the serum samples between the various groups of mice in both genders. All values were reported as mean \pm SEM. Unpaired t-test or Two way ANOVA followed by a post-hoc Bonferroni multiple comparison test to compare between each strain (C57BL6 or 129Sv) and NKO in both genders was used.

5.2.12 Statistical Software

Statistical analyses on the data were analyzed using the GraphPad Prism Version 4.0 (GraphPad Software Inc.)

5.3 Results

5.3.1 Confirmation of NUCB2 Gene Disruption in NKO Male and Female Mice

The insertion of a vector disabled the NUCB2 gene in the NKO male and female mice. Mutant primers created are specific to the retroviral insertion. **Figure 5.2A, 5.2B** display wildtype NUCB2 male and female mice gene that binds specifically to the wildtype primers (WT; 439 bp). No bands representing the NUCB2 mRNA were observed in the NKO male and female mice samples. **Figure 5.3A, 5.3B** displays amplicon bands only in the NKO male and female gene lanes that are specific to the retroviral insertion present and not in the wildtype mice lanes (MT; 441 bp).

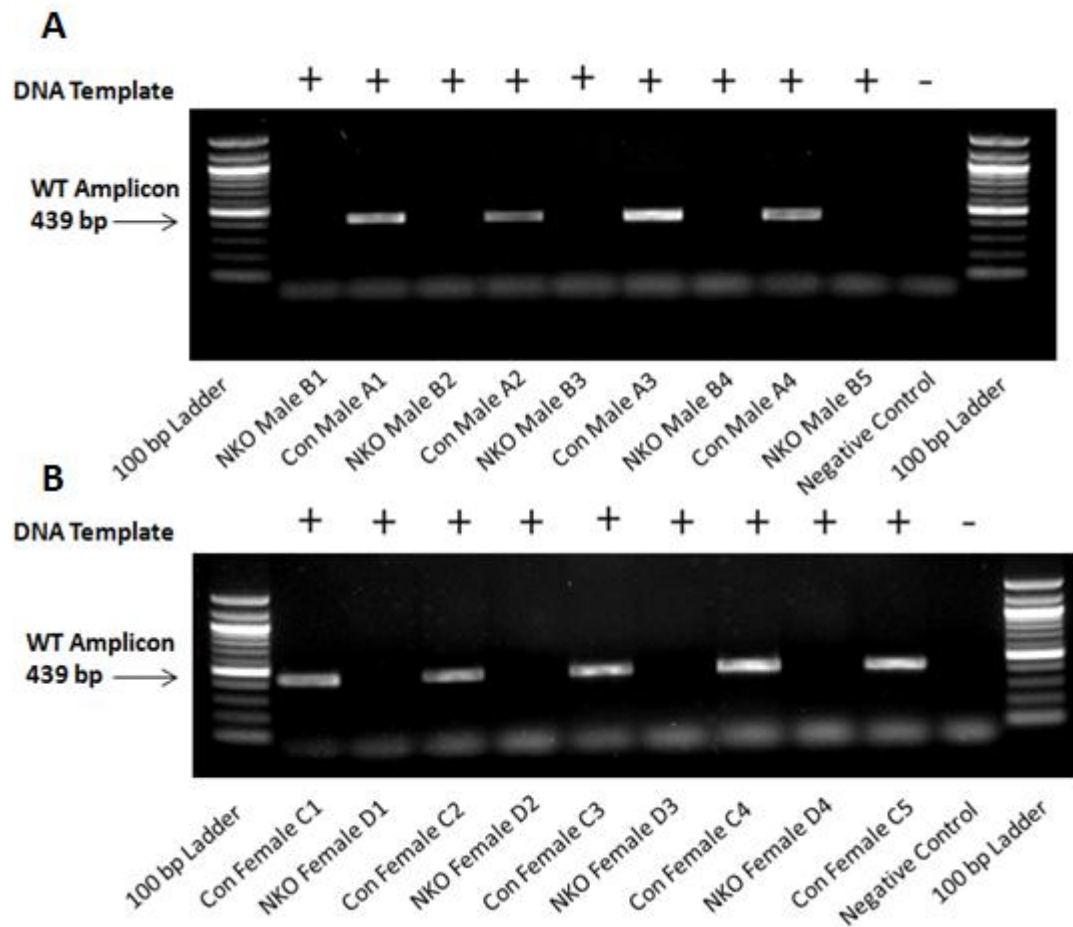


Figure 5.2 Confirmation of NUCB2 Gene Presence in WT Male and Female Mice

Figure 5.2. Wildtype (Strain: C57BL/6), NUCB2 gene in the male (2A) and female (2B) mice binds specifically to wildtype primers (439 bp). No bands are observed in the NKO male and female mice lanes as primers are specific to the wildtype (WT) mice which do not bind to the NUCB2 knock out male and female mice gene.

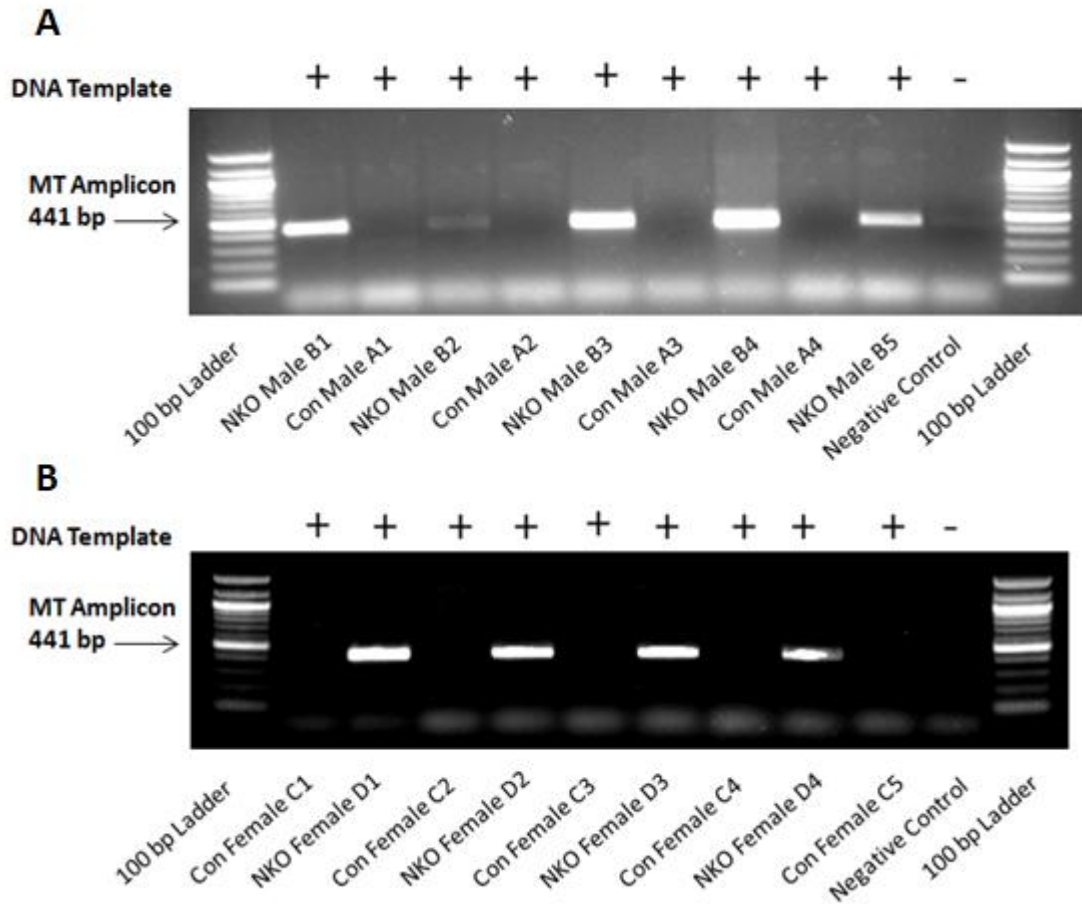


Figure 5.3 Confirmation of NUCB2 Gene Disruption in NKO Male and Female Mice

Figure 5.3. NKO mice display a band for the mutant primers (MT) created specific to the retroviral insertion. The band is observed in the NKO male (3A) and female (3B) mice gene lanes that are specific to the insertion present (441 bp). No bands of NUCB2 are observed in the wildtype (Strain: C57BL/6) male mice and female gene lanes.

5.3.2 Loss of NUCB2/nesfatin-1 protein expression in the Liver, Stomach, Duodenum, Pancreas from NKO Male and Female Mice

NUCB2 protein is expressed in the liver (**Figure 5.4; Lanes 2 and 4**), stomach (**Figure 5.5; Lanes 2 and 4**), duodenum (**Figure 5.6; Lanes 2 and 4**) and pancreas (**Figure 5.7; Lanes 2 and 4**) of male and female WT mice, showing distinct band for NUCB2 corresponding at 50 kDa. No NUCB2 protein expression was observed in the liver (**Figure 5.4; Lanes 3 and 5**), stomach (**Figure 5.5; Lanes 3 and 5**), duodenum (**Figure 5.6; Lanes 3 and 5**) and pancreas (**Figure 5.7; Lanes 3 and 5**) from males and female NKO mice. No bands showing the fully processed nesfatin-1 was visible at 10 kDa in any of the tissue sample from both the groups in either genders. Controls used were COS cells transfected with/without NUCB2, NUCB2 and PC 1/3, NUCB1 and PC 1/3 and NUCB2 and furin, MGN-3 cell lines which displayed specific expression of the genes transfected into the cells. Rat nesfatin-1 peptide used as a positive control is shown as a distinct band corresponding to 10 kDa (**Figure 5.4; Lane 10, Figure 5.5; Lane 9, Figure 5.6; Lane 9, Figure 5.7; Lane 9**).

Preproghrelin protein expression appears reduced in the stomach of NKO male and female mice (Lanes 3 and 5) compared to WT mice (Lanes 2 and 4), showing a distinct band for preproghrelin corresponding at 13 kDa (**Supporting Figure S5.1**).

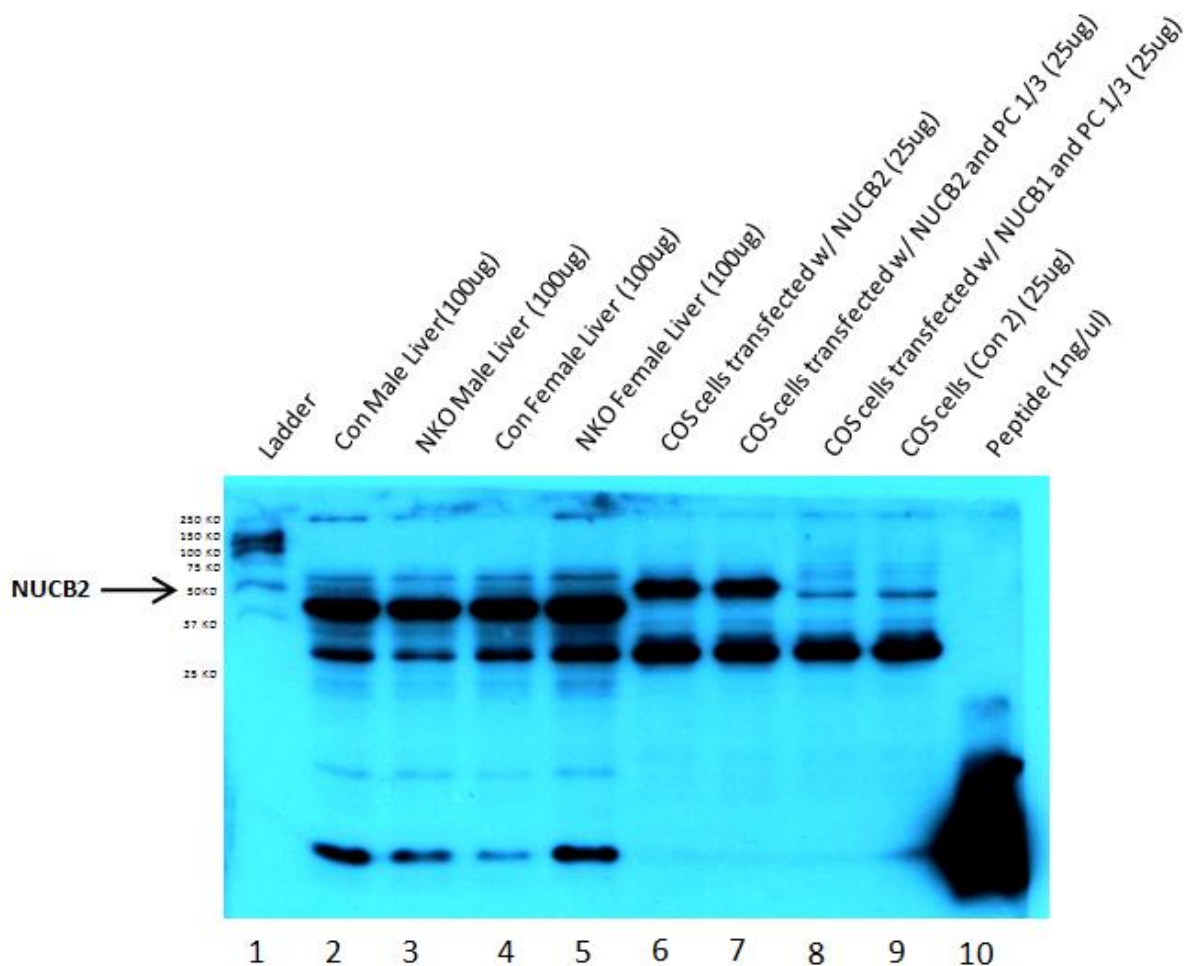


Figure 5.4 Western Blot Display the Loss of NUCB2 Protein Expression in the Liver from NKO Male and Female Mice

Figure 5.4. Western Blot display the loss of NUCB2 protein expression in Lanes 3 and 5 observed in male and female liver tissue of NKO mice in comparison to wildtype male and female mice shown in lane 2 and 4 observed at 50 kDa. Controls used were COS cells transfected with NUCB2, NUCB2 and PC 1/3, NUCB1 and PC 1/3, COS cell line and the nesfatin-1 peptide.

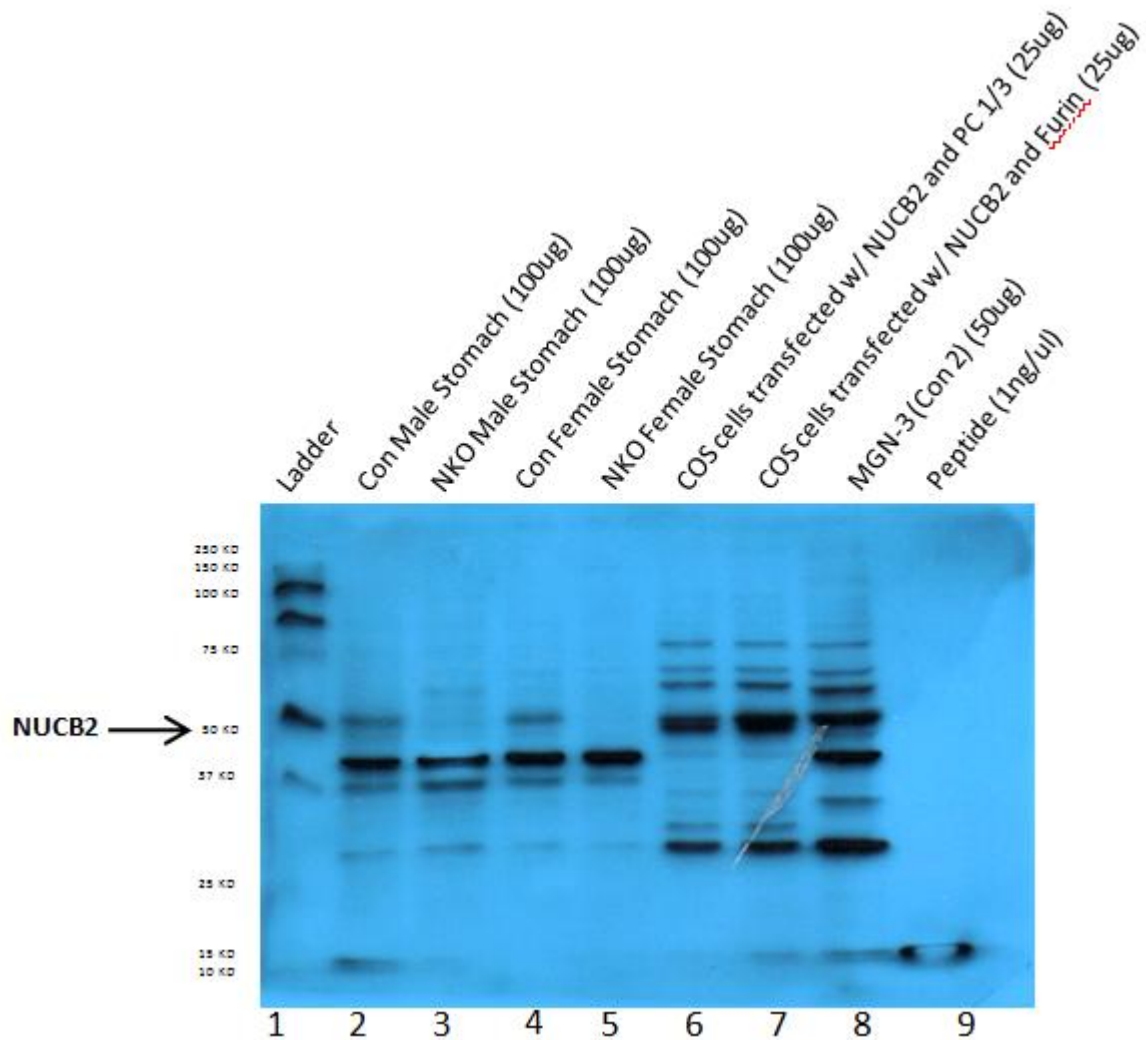


Figure 5.5 Western Blot Display the Loss of NUCB2 Protein Expression in the Stomach from NKO Male and Female Mice

Figure 5.5. Western Blot display the loss of NUCB2 protein expression in Lanes 3 and 5 observed in male and female stomach tissue of NKO mice in comparison to wildtype male and female mice shown in lane 2 and 4 observed at 50 kDa. Controls used were COS cells transfected with NUCB2 and PC 1/3, NUCB2 and furin, MGN-3 cell line and the nesfatin-1 peptide.

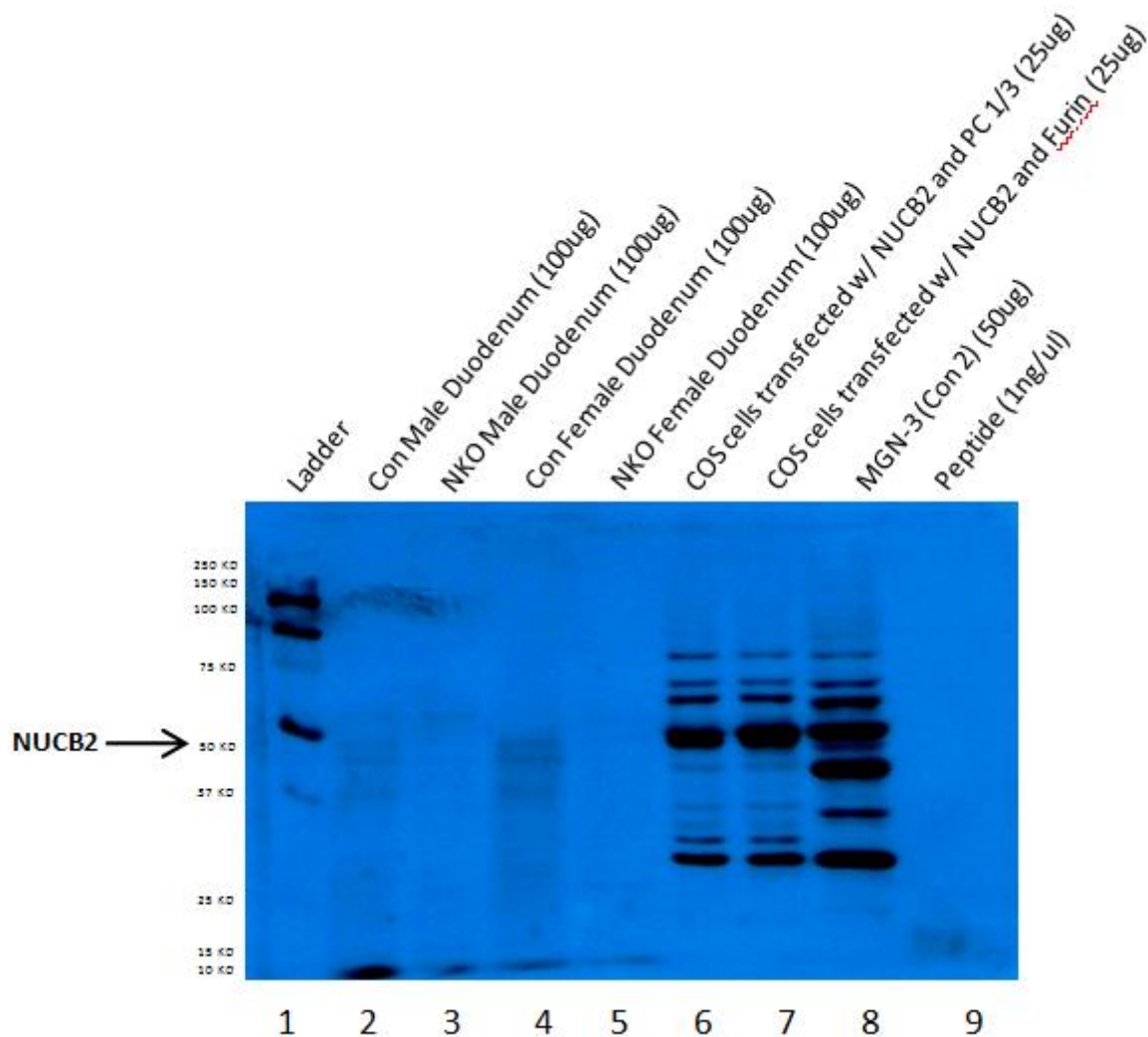


Figure 5.6 Western Blot Display the Loss of NUCB2 Protein Expression in the Duodenum from NKO Male and Female Mice

Figure 5.6. Western Blot display the loss of NUCB2 protein expression in Lanes 3 and 5 observed in male and female duodenum tissue of NKO mice in comparison to wildtype male and female mice shown in lane 2 and 4 observed at 50 kDa. Controls used were COS cells transfected with NUCB2 and PC 1/3, NUCB2 and furin, MGN-3 cell line and the nesfatin-1 peptide.

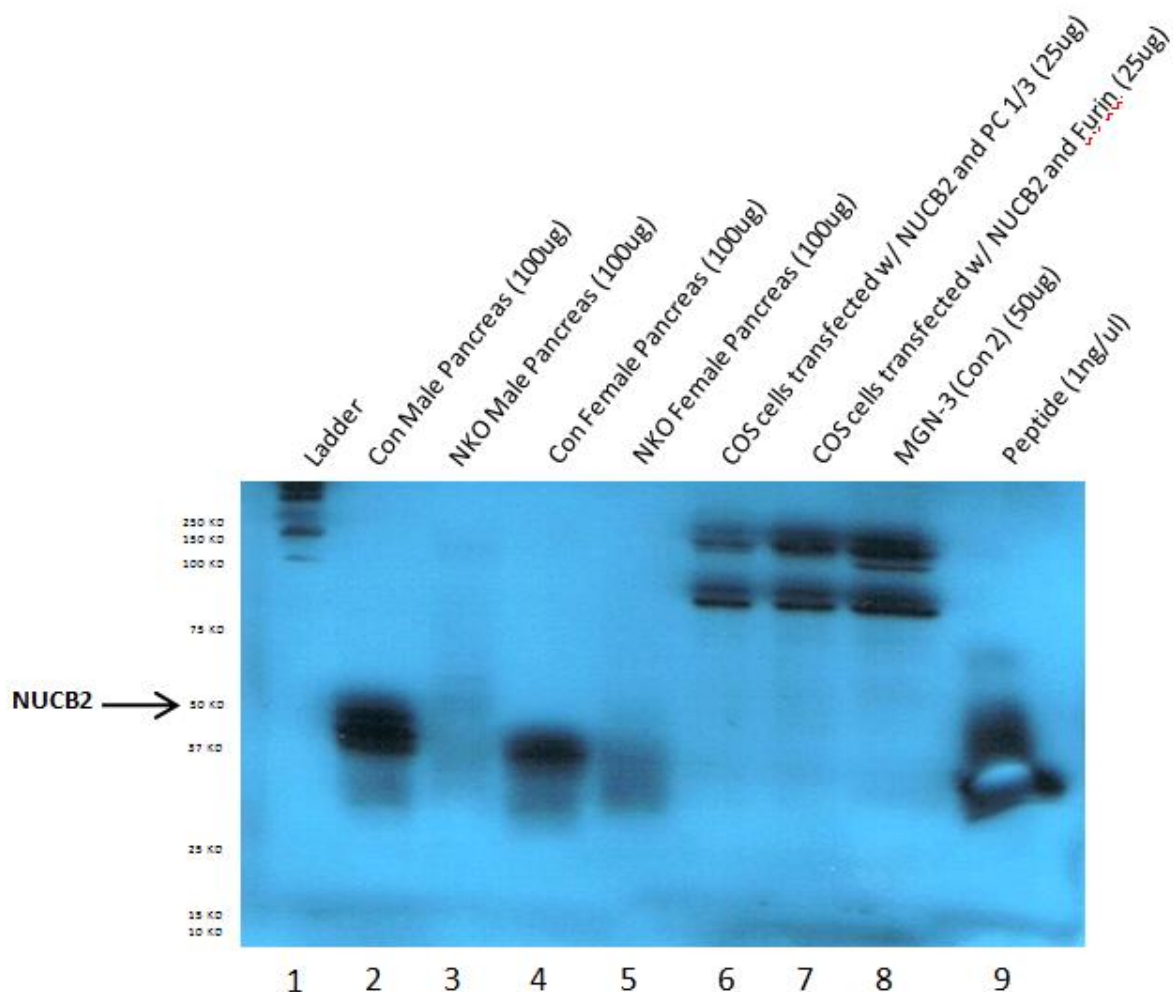
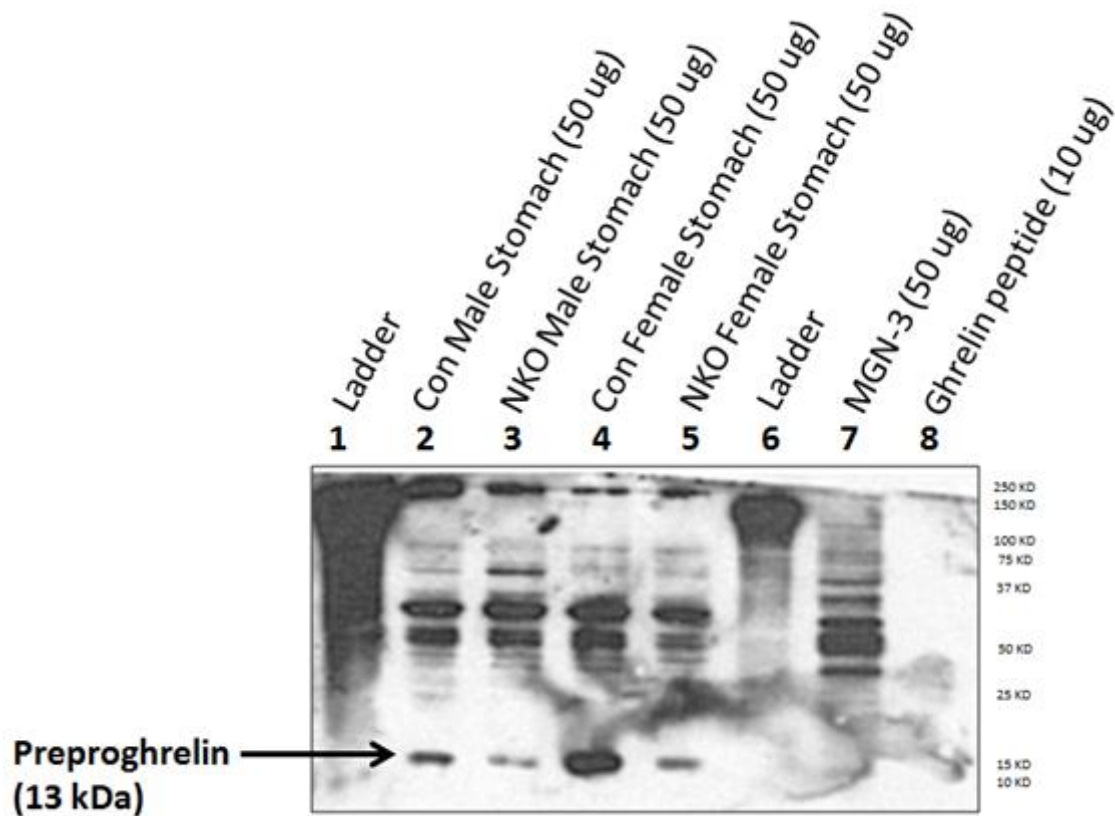


Figure 5.7 Western Blot Display the Loss of NUCB2 Protein Expression in the Pancreas from NKO Male and Female Mice

Figure 5.7. Western Blot display the loss of NUCB2 protein expression in Lanes 3 and 5 observed in male and female pancreatic tissue of NKO mice in comparison to wildtype male and female mice shown in lane 2 and 4 observed at 50 kDa. Controls used were COS cells transfected with NUCB2 and PC 1/3, NUCB2 and furin, MGN-3 cell line and the nesfatin-1 peptide.



Supporting Figure S5.1

Western Blot Display the Attenuation of Preproghrelin Protein Expression in the Stomach from NKO Male and Female Mice

Supporting Figure S5.1. Western Blot displays the attenuation of perproghrelin protein expression in Lanes 3 and 5 observed in male and female stomach tissues of NKO mice in comparison to wildtype male and female mice shown in lane 2 and 4 observed at 13 kDa. Controls used were MGN-3 cell line and ghrelin peptide.

5.3.3 Insulin producing β -cells are immunonegative for NUCB2/nesfatin-1 but Not for Insulin in NKO Male and Female Pancreatic Islets

There was no NUCB2/nesfatin-1 immunoreactivity (FITC-Green; **Figure 5.8F, 5.8J**) in the insulin producing β -cells from NKO male and female pancreatic islets which depicts staining for insulin (TEXAS-Red; **Figure 5.8G, 5.8K**). Merged image displays NKO pancreatic male and female islet cells immunopositive for insulin and not for NUCB2 (**Figure 5.8H, 5.8L**). Control used was a wildtype male pancreatic islet that displayed co-immunoreactivity for insulin (TEXAS-Red; **Figure 5.8C**) and NUCB2/nesfatin-1 (FITC-Green; **Figure 5.8B**) in the insulin producing β -cells shown in the merged image immunopositive for both proteins (Yellow; **Figure 5.8D**). DAPI stained for nuclei in the cells of the pancreatic tissue are shown in blue (**Figure 5.8A, 5.8E, 5.8I**).

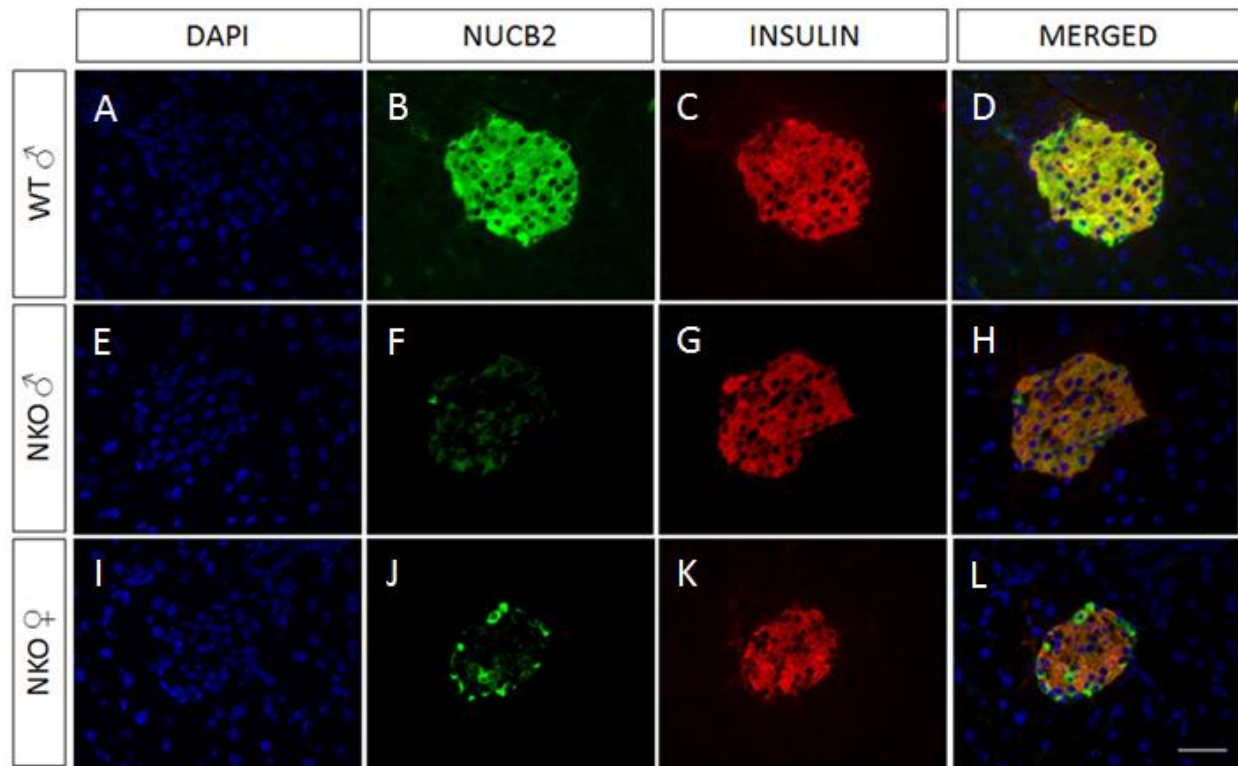


Figure 5.8 Insulin producing β -cells are immunonegative for NUCB2/nesfatin-1 but Not for Insulin in NKO Male and Female Pancreatic Islets

Figure 5.8. Immunohistochemical analysis displays the co-presence of insulin and NUCB2/nesfatin-1 in the wildtype (WT) male pancreatic islets (β -cells) used as a control. Insulin positive β -cells display the lack of NUCB2/nesfatin-1 staining in a NKO male and female pancreatic islets. Nuclei is stained with DAPI; blue. NUCB2/nesfatin-1 is stained with FITC-Grn. Insulin is stained with TEXAS-Red. Scale bar = 25 μ m.

5.3.4 Body weight of NKO Male and Female Mice

NKO male (**Figure 5.9A**) and female (**Figure 5.9B**) mice had significantly higher body weight compared to wildtype (C57BL/6) male and female mice fed *ad libitum* on regular chow. NKO male mice (**Figure 5.10A**) fed on 45% kcal fat diet had significantly increased body weight compared to NKO male fed *ad libitum* on 10% kcal fat diet and wildtype male mice fed on 10% and 45% kcal fat diet. NKO female mice (**Figure 5.10B**) fed *ad libitum* on 10% kcal and 45% kcal fat diet had significantly increased body weight than wildtype female mice fed on 10% and 45% kcal fat diet.

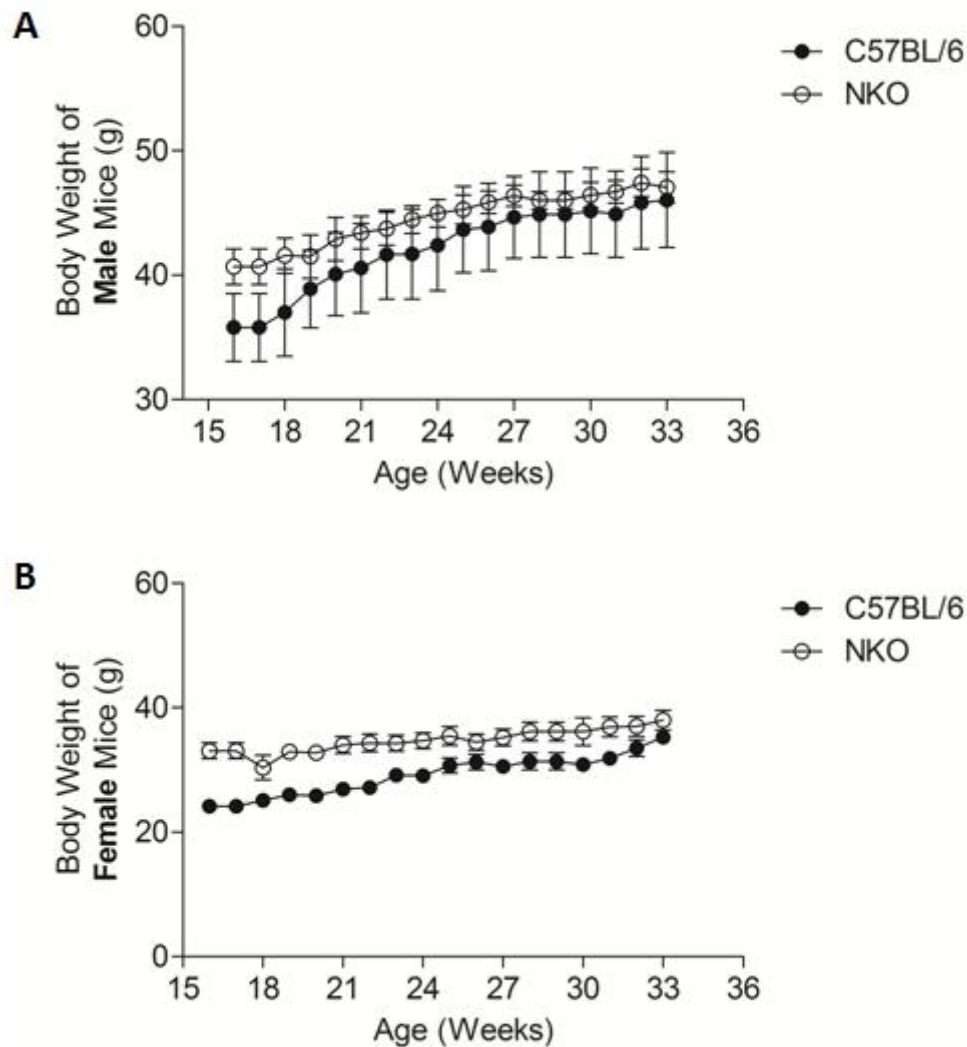


Figure 5.9 Body Weight of NKO and WT Mice fed *Ad Libitum* on Regular Chow

Figure 5.9. Line graph represents body weight measured in C57BL/6 (●; wildtype) and NKO (○) male (A) and female (B) mice recorded over a period of 17 weeks fed *ad libitum* on regular chow. NKO male and female mice have increased body weight compared to wildtype male and female mice fed *ad libitum* on regular chow. Mann-Whitney test of a non-Gaussian distribution to compare the mean \pm SEM of body weight between the two groups of male and female mice

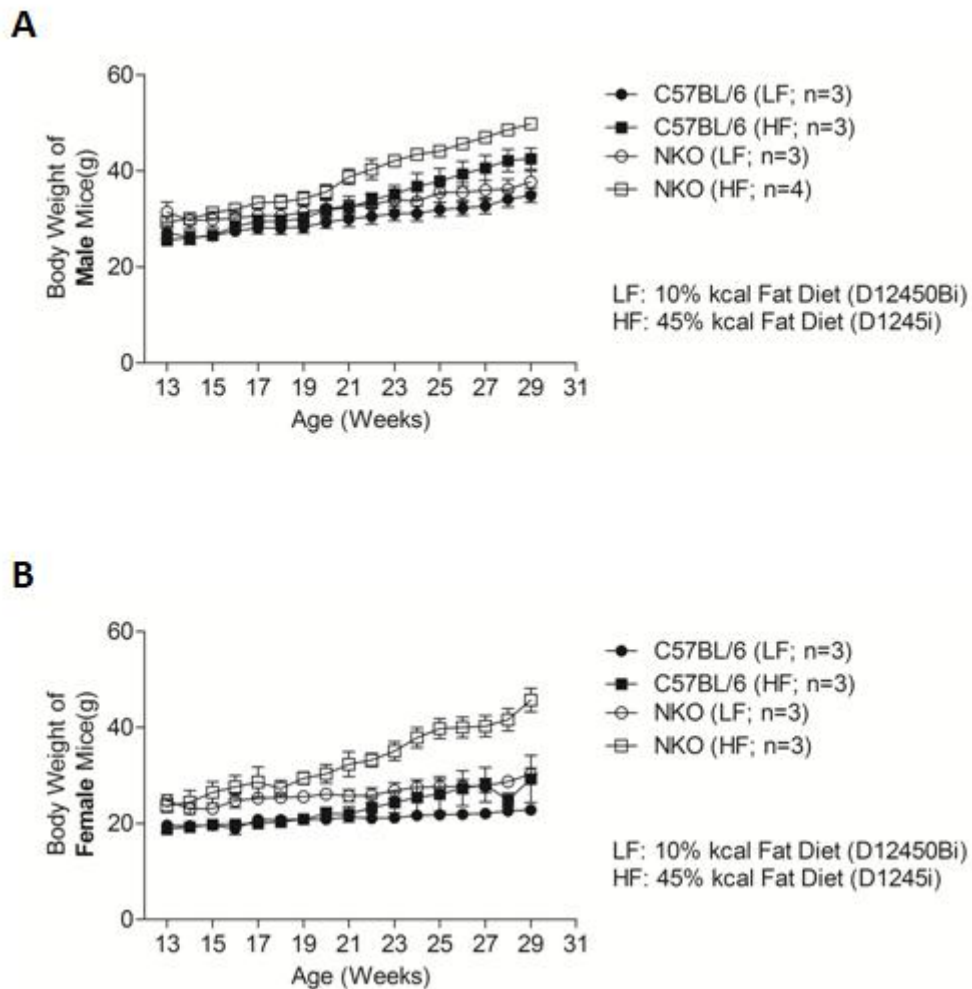


Figure 5.10 Body Weight of NKO and WT Mice fed *Ad Libitum* on 10% and 45% kcal Fat Diet

Figure 5.10. Line graph represents body weight measured in C57BL/6 (wildtype) and NKO male (A) and female (B) mice recorded over a period of 17 weeks fed *ad libitum* on 10% and 45% kcal fat diet. NKO male mice fed on 45% kcal fat diet (\square ; $p < 0.05$) have increased body weight compared to NKO male fed on 10% kcal fat diet (\circ) and wildtype male mice fed on 10% (\bullet) and 45% kcal fat diet. (\blacksquare). NKO female mice fed on 10% kcal fat diet (\circ ; $p < 0.05$) have increased body weight than wildtype female mice fed on 10% (\bullet) and 45% kcal fat diet (\blacksquare). NKO female mice fed on 45% kcal fat diet (\square ; $p < 0.05$) have increased body weight compared to NKO female fed on 10% kcal fat diet and wildtype female mice fed on 10% and 45% kcal fat diet. We used one-way ANOVA followed by Student-Newman Keuls multiple comparisons test to compare the mean \pm SEM of body weight between the two groups of male and female mice.

5.3.5 Food Intake of NKO Male and Female Mice

NKO male (**Figure 5.11A**) mice have increased food intake compared to wildtype (C57BL/6) male mice fed *ad libitum* on regular chow. No significant difference in food intake was found between NKO female (**Figure 5.11B**) mice and wildtype female mice. NKO male mice (**Figure 5.12A**) fed on 45% kcal fat diet have increased food intake compared to NKO male fed *ad libitum* on 10% kcal fat diet and wildtype male mice fed on 45% kcal fat diet. No significant difference was found in food intake between wildtype male mice fed on 10% kcal and 45% kcal fat diet and NKO male mice fed on 10% kcal fat. No significant difference was found in food intake between wildtype and NKO female mice fed on 10% kcal and 45% kcal fat diet (**Figure 5.12B**).

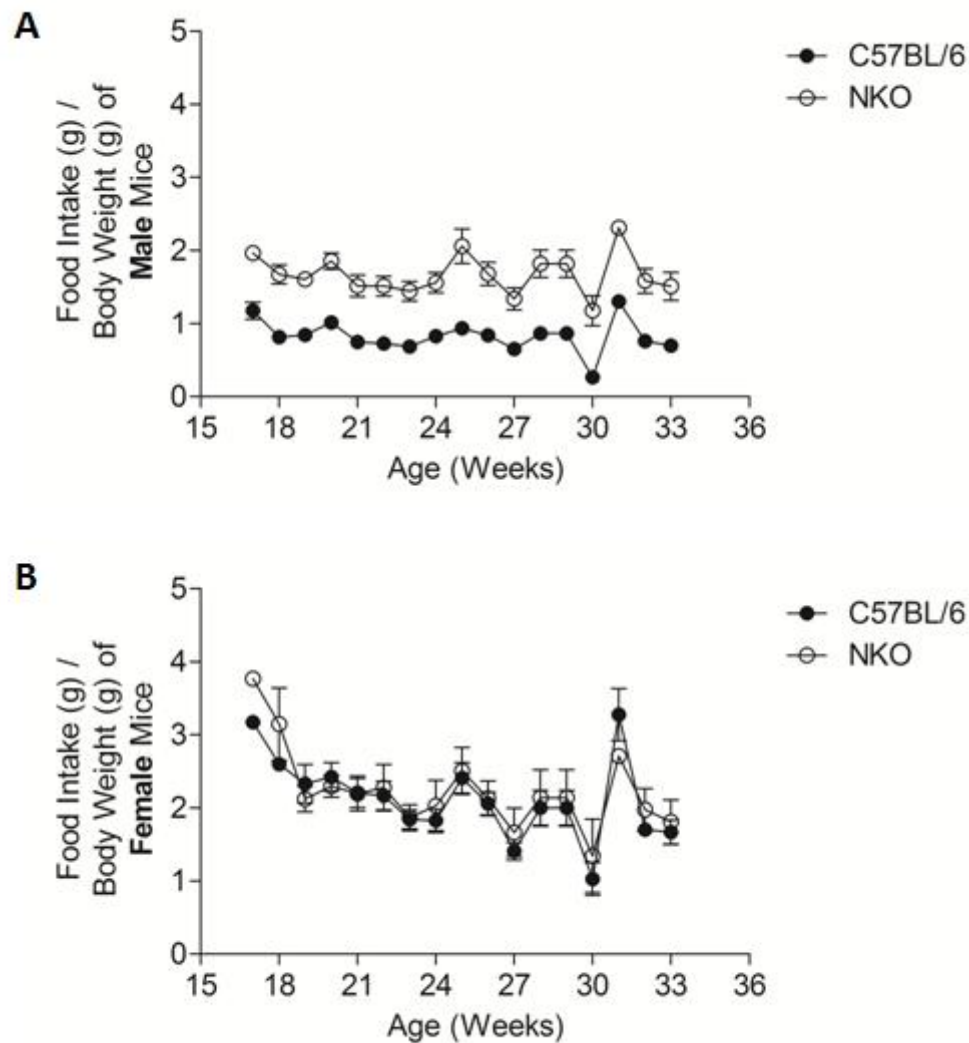


Figure 5.11 Food Intake of NKO Mice and WT Mice fed *Ad Libitum* on Regular Chow

Figure 5.11. Line graph represents food intake (food intake to body weight ratio) measured in C57BL/6 (●; wildtype) and NKO (○) male (A) and female (B) mice recorded over a period of 17 weeks fed *ad libitum* on regular chow. NKO male mice have increased food intake compared to wildtype male mice fed *ad libitum* on regular chow ($p < 0.05$). Mann-Whitney test of a non-Gaussian distribution to compare the mean \pm SEM of food intake between the two groups of male and female mice

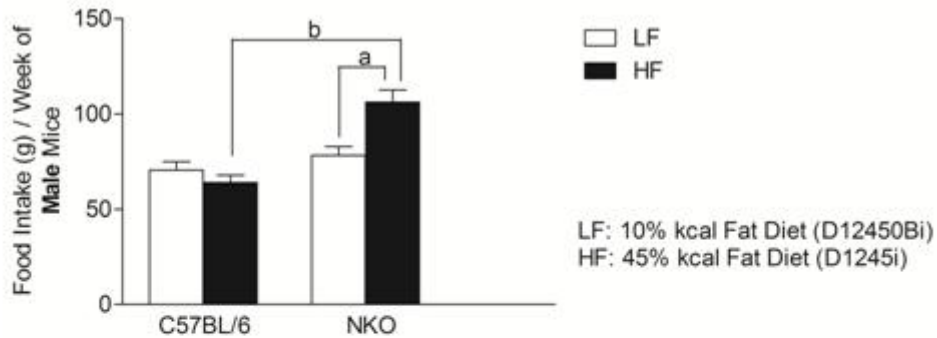
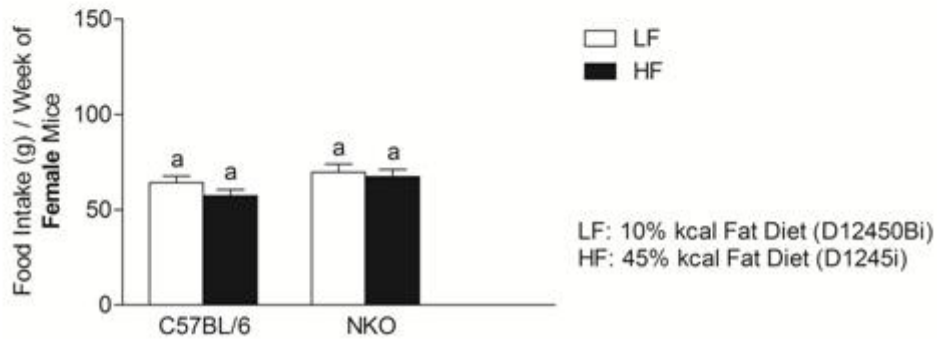
A**B**

Figure 5.12 Food Intake of NKO and WT Mice fed *Ad Libitum* on 10% and 45% kcal Fat Diet

Figure 5.12. Bar graph represents food intake (food intake / week) measured in C57BL/6 (wildtype) and NKO male (A) and female (B) mice recorded over a period of 17 weeks fed *ad libitum* on 10% and 45% kcal fat diet. NKO male mice fed on 45% kcal fat diet ($p < 0.05$) have increased food intake compared to NKO male fed on 10% kcal fat diet and wildtype male mice fed on 45% kcal fat diet but not 10% kcal fat diet. No significant difference was found in food intake between wildtype (10% kcal and 45% kcal fat diet) and NKO female mice (10% kcal and 45% kcal fat diet). We used one-way ANOVA followed by Tukey's multiple comparisons test to compare the mean \pm SEM in food intake between the two groups of male and female mice.

5.3.6 GSIS from Wildtype and NKO Female Mice Pancreatic Islets

NKO female pancreatic islets present at 16.7 mM glucose KRB buffer solution and 16.7 mM glucose KRB buffer solution + KCl had a significantly lower insulin level than to that of female wildtype mice pancreatic islets (**Figure 5.13**). There was no significant difference in glucose stimulated insulin secretion from female pancreatic islets gathered from NKO and wildtype mice present in 2.0 mM and 5.6 mM glucose KRB buffer solution.

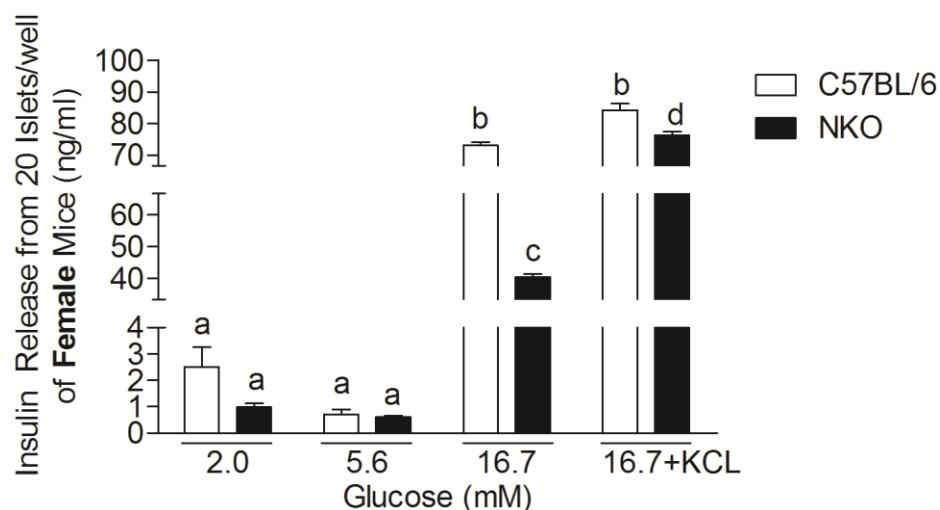


Figure 5.13 GSIS on Pancreatic Islets Isolated from Wildtype (C57BL/6) and NKO Female Mice

Figure 5.13. Bar graph representing glucose stimulated insulin secretion (GSIS) on pancreatic islets gathered from wildtype (C57BL/6) and NKO female mice present in 2.0 mM glucose, 5.6 mM glucose, 16.7 mM glucose and 16.7 mM glucose + KCL. NKO female pancreatic islets present at 16.7 mM glucose KRB buffer solution and 16.7 mM glucose KRB buffer solution + KCL had a significantly lower insulin level than to that of female wildtype mice pancreatic islets ($P < 0.001$). An in house radioimmunoassay was used to determine the insulin levels. We used a post test following two-way ANOVA using the Bonferroni method to compare the mean \pm SEM of insulin levels secreted into media between the two groups in each study.

5.3.7 Organ/Tissue Weight of NKO Male and Female Mice

Organs/Tissue were dissected from the wildtype (C57BL/6) and NKO male (**Figure 5.14**) and female (**Figure 5.15**) mice. No significant difference was found in the weight of the heart (**Figures 5.14A, 5.15A**), spleen (**Figures 5.14B, 5.15B**), brown fat (**Figures 5.14C, 5.15C**), epididymal fat (**Figures 5.14D**), perigonadal fat (**Figures 5.15D**) and soleus muscle (**Figures 5.14E, 5.15E**) in two groups of male and female mice.

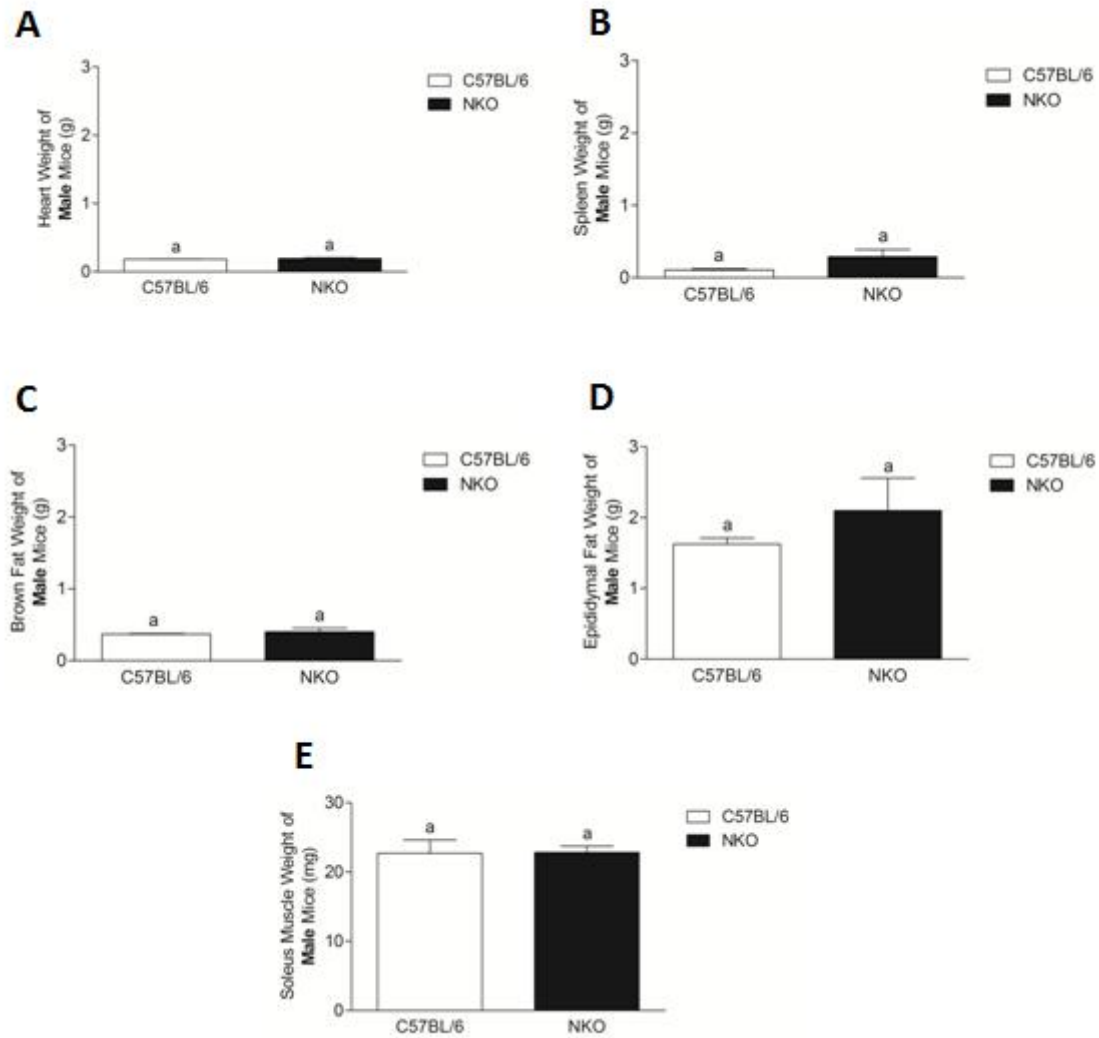


Figure 5.14 Organ/tissue Weight of WT and NKO Male Mice

Figure 5.14. Bar graph displays the organ/tissue weight of WT (C57BL/6) and NKO male mice. No significant difference was found in the weight of the heart (A), spleen (B), brown fat (C), epididymal fat (D) and soleus muscle (E) between the two groups of male mice. We used an Unpaired t-test to measure the difference in organs/tissue weight between the two groups of male mice.

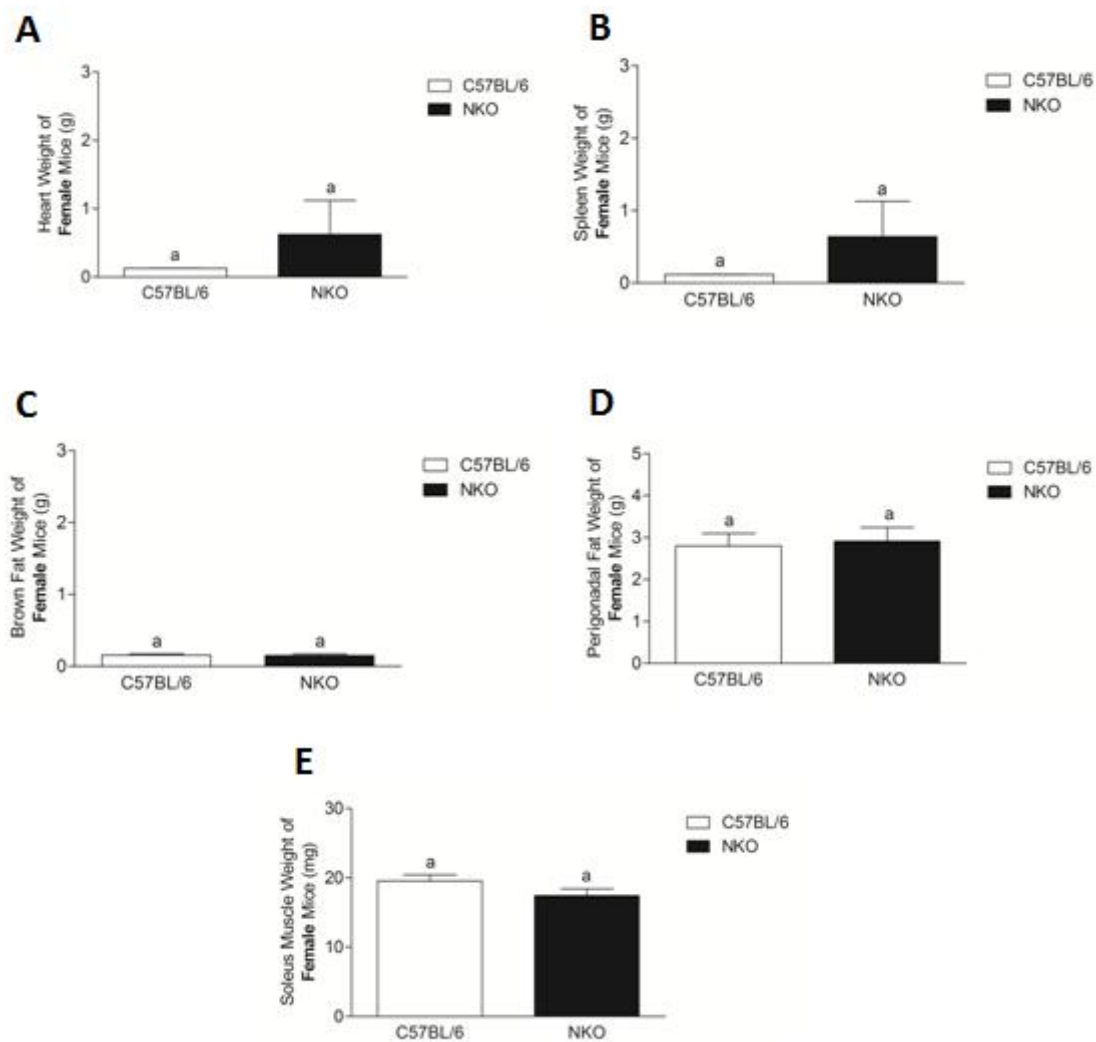


Figure 5.15 Organ/tissue Weight of WT and NKO Female Mice

Figure 5.15. Bar graph displays the organ/tissue weight of wildtype (C57BL/6) and NKO female mice. No significant difference was found in the weight of the heart (A), spleen (B), brown fat (C), epididymal fat (D) and soleus muscle (E) between the two groups of female mice. We used an Unpaired t-test to measure the difference in organs/tissue weight between the two groups of female mice.

5.3.8 Whole-Body Energy Homeostasis in NKO Male Mice Using CLAMS

The volume of oxygen consumption (**Figure 5.16B**) and Z-TOT (**Figure 5.16G**) of NKO was significantly higher than wildtype male mice. In contrast, the respiratory exchange ratio (**Figure 5.16D**) of NKO was significantly lower than wildtype male mice. No significant difference in accumulative oxygen (**Figure 5.16A**), carbon dioxide consumption (**Figure 5.16C**), X-TOT (**Figure 5.16E**) and X-AMB (**Figure 5.16F**) was found between male C57BL/6 and NKO mice.

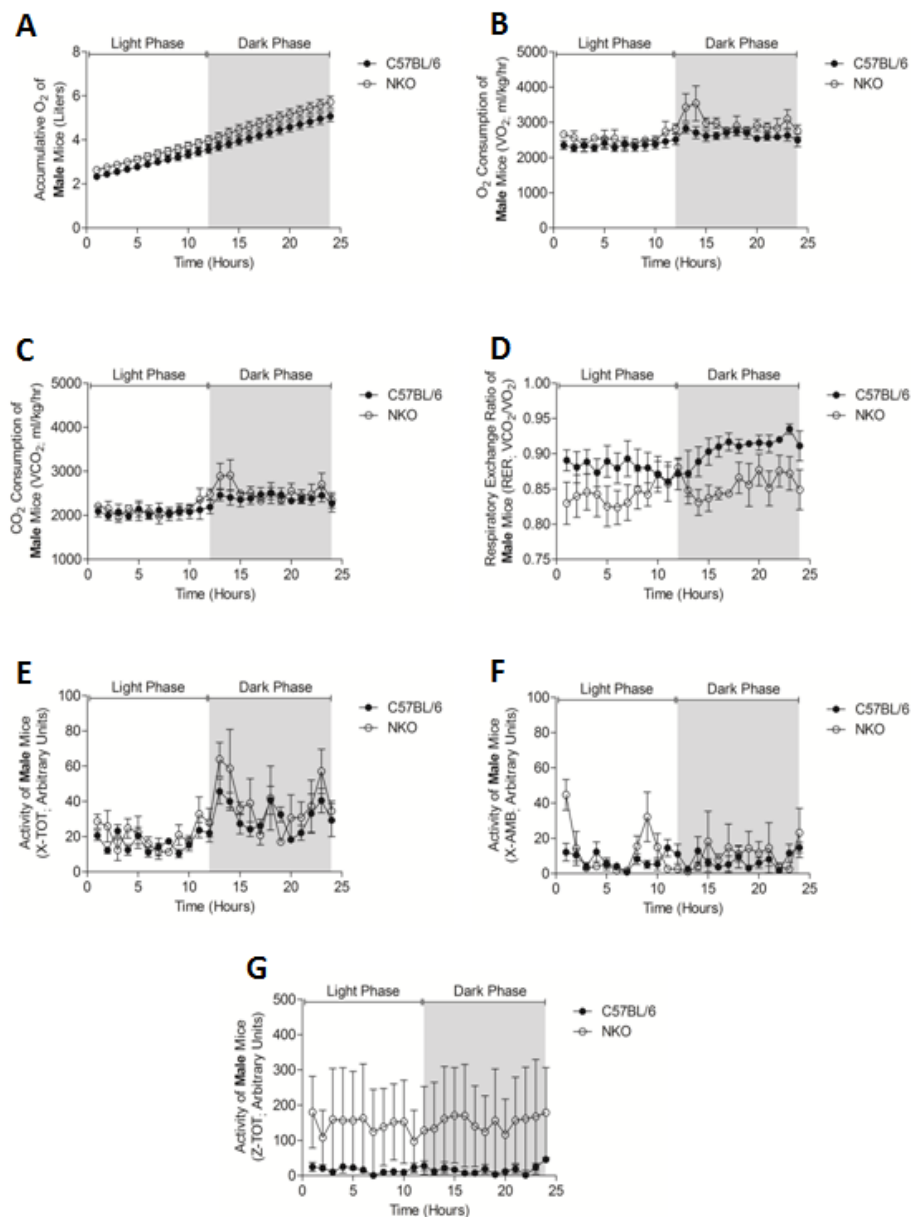


Figure 5.16 Whole-Body Energy Homeostasis in NKO Male Mice Using CLAMS

Figure 5.16. Line graph represents metabolic parameter [Accumulative oxygen (A; O_2), O_2 consumption (B; VO_2) carbon dioxide production (C; VCO_2), respiratory exchange ratio (D; RER), total number of X-axis IR beam breaks (E; X-TOT), number of ambulatory x-axis IR-beam breaks (F; X-AMB), total number of vertical rearing motions (G; Z-TOT)] measured in C57BL/6 (●; wildtype) and NKO (○) male mice. The volume of oxygen consumption and Z-TOT of NKO was significant higher than wildtype male mice ($p < 0.0001$). In contrast, the respiratory exchange ratio of NKO was significantly lower than wildtype male mice ($p < 0.0001$). We used the Mann-Whitney test of a non-Gaussian distribution to compare the mean \pm SEM of various metabolic parameters between the two groups of male mice.

5.3.9 Blood Glucose and Insulin Levels in NKO Male and Female Mice during an IPGTT

Area under the curve (AUC) of glucose profile (0-150 minutes) shows NKO was significantly lower than WT male mice (**Figure 5.17A**) fed on regular chow. No significant difference in the AUC of glucose profile (0-150 minutes) was found between the NKO and WT female mice (**Figure 5.18A**). Similarly, no significant difference in the AUC of insulin profile (5-30 minutes) was found between NKO and wildtype male (**Figure 5.17B**) and female (**Figure 5.18B**) mice fed on regular chow. No significant difference in the AUC of glucose profile (0-150 minutes) was found between NKO and wildtype male (**Figure 5.19A**) and female (**Figure 5.19B**) mice fed on different fat diets.

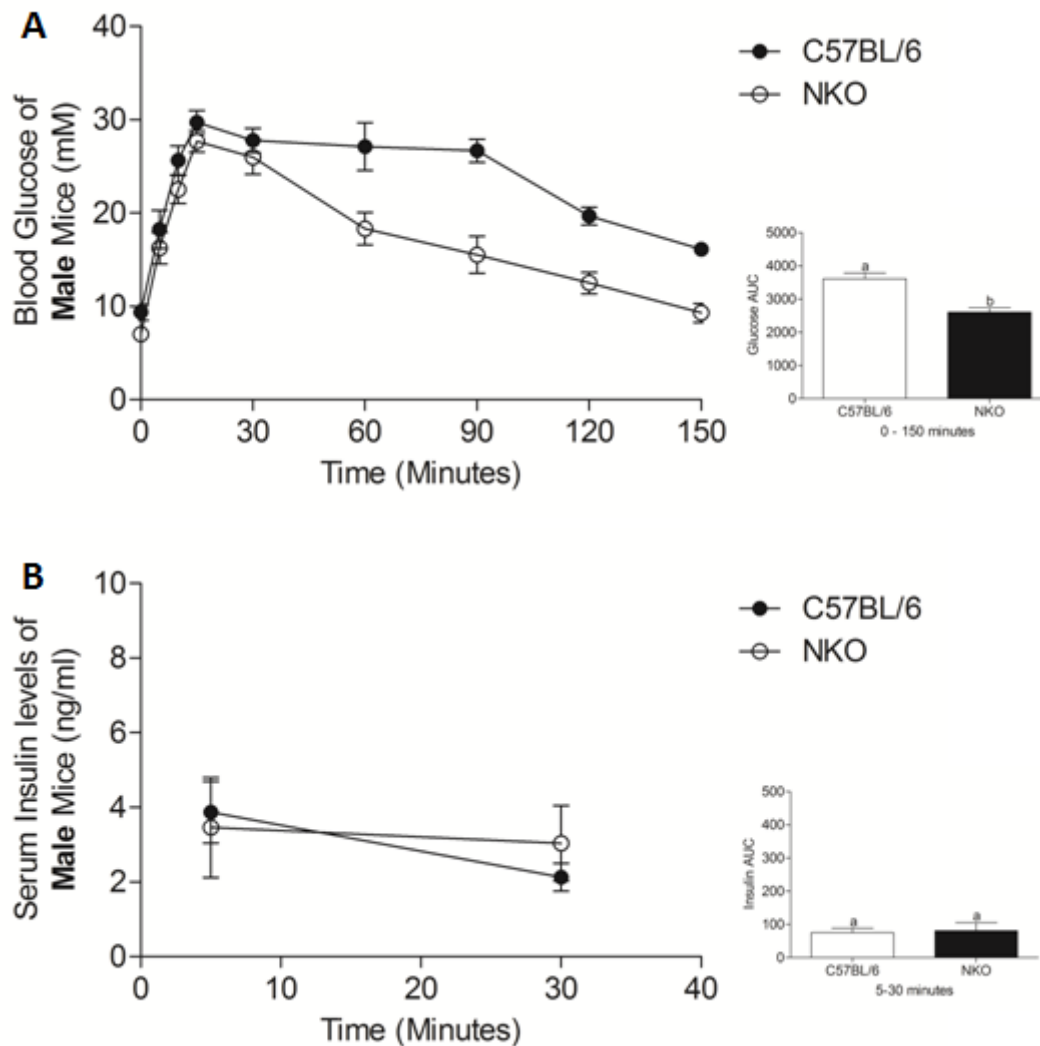


Figure 5.17 IPGTT in NKO and WT Male Mice fed *Ad Libitum* on Regular Chow

Figure 5.17. Line graph represents blood glucose levels (A) measured at 0, 5, 10, 20, 30, 60, 90, 120, and 150 minutes and insulin secretion levels (B) measured at 5 and 30 minutes during an intraperitoneal glucose tolerance test (IPGTT) measured in C57BL/6 (●; wildtype) and NKO (○) male mice. An inset in each figure shows the area under the curve for glucose (A) and insulin (B) profiles. AUC of glucose profile shows NKO was significantly lower than WT male mice. No significant difference in the AUC of insulin profile was found between the NKO and WT male mice. We used an Unpaired t-test to measure the difference in AUC of glucose and insulin profiles between the two groups of male mice.

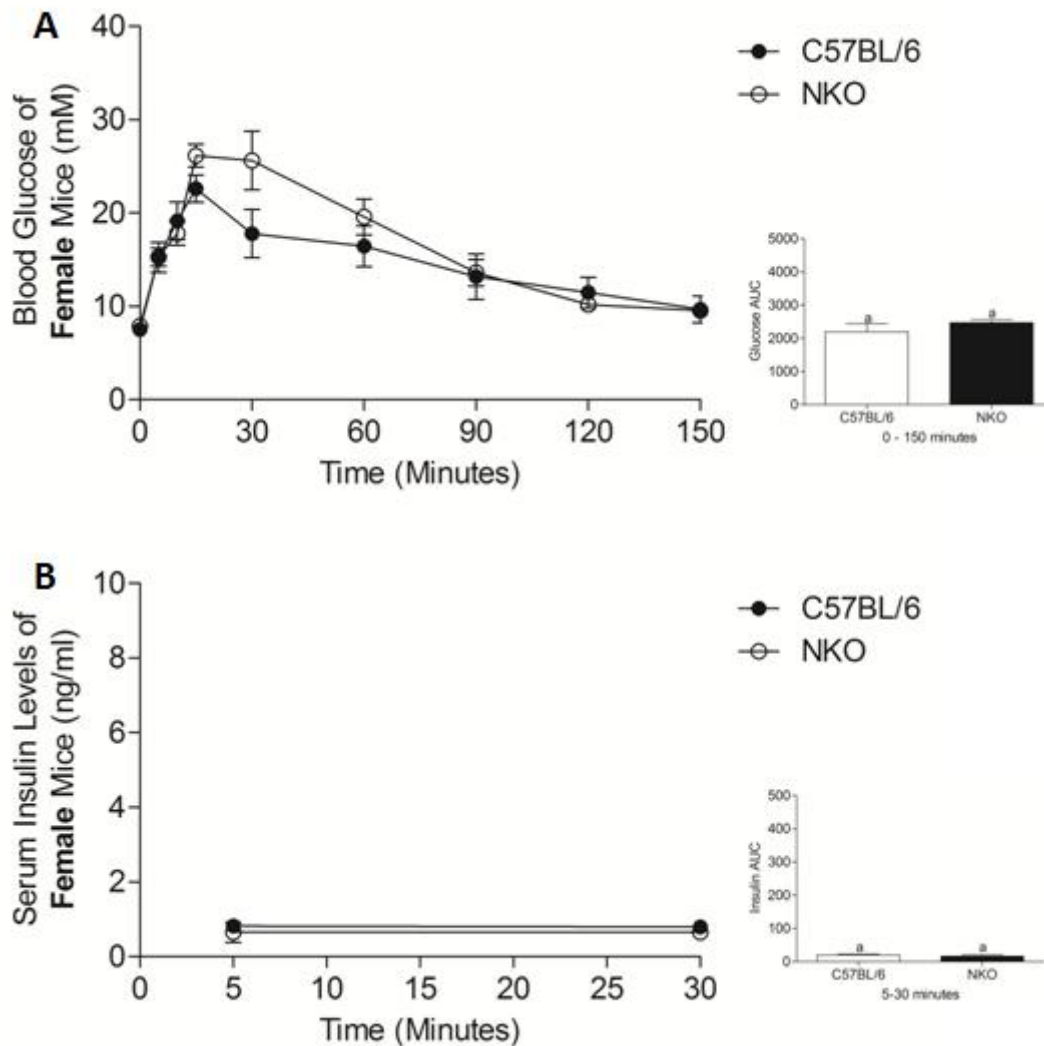


Figure 5.18 IPGTT in NKO and WT Female Mice fed *Ad Libitum* on Regular Chow

Figure 5.18. Line graph represents blood glucose levels (A) measured at 0, 5, 10, 20, 30, 60, 90, 120, and 150 minutes and insulin secretion levels (B) measured at 5 and 30 minutes during an intraperitoneal glucose tolerance test (IPGTT) measured in C57BL/6 (●; wildtype) and NKO (○) female mice. An inset in each figure shows the area under the curve for glucose (A) and insulin (B) profiles. No significant difference in the AUC of glucose and insulin profile was found between the NKO and WT female mice. We used an unpaired t-test to measure the difference in AUC of glucose and insulin profiles between the two groups of female mice.

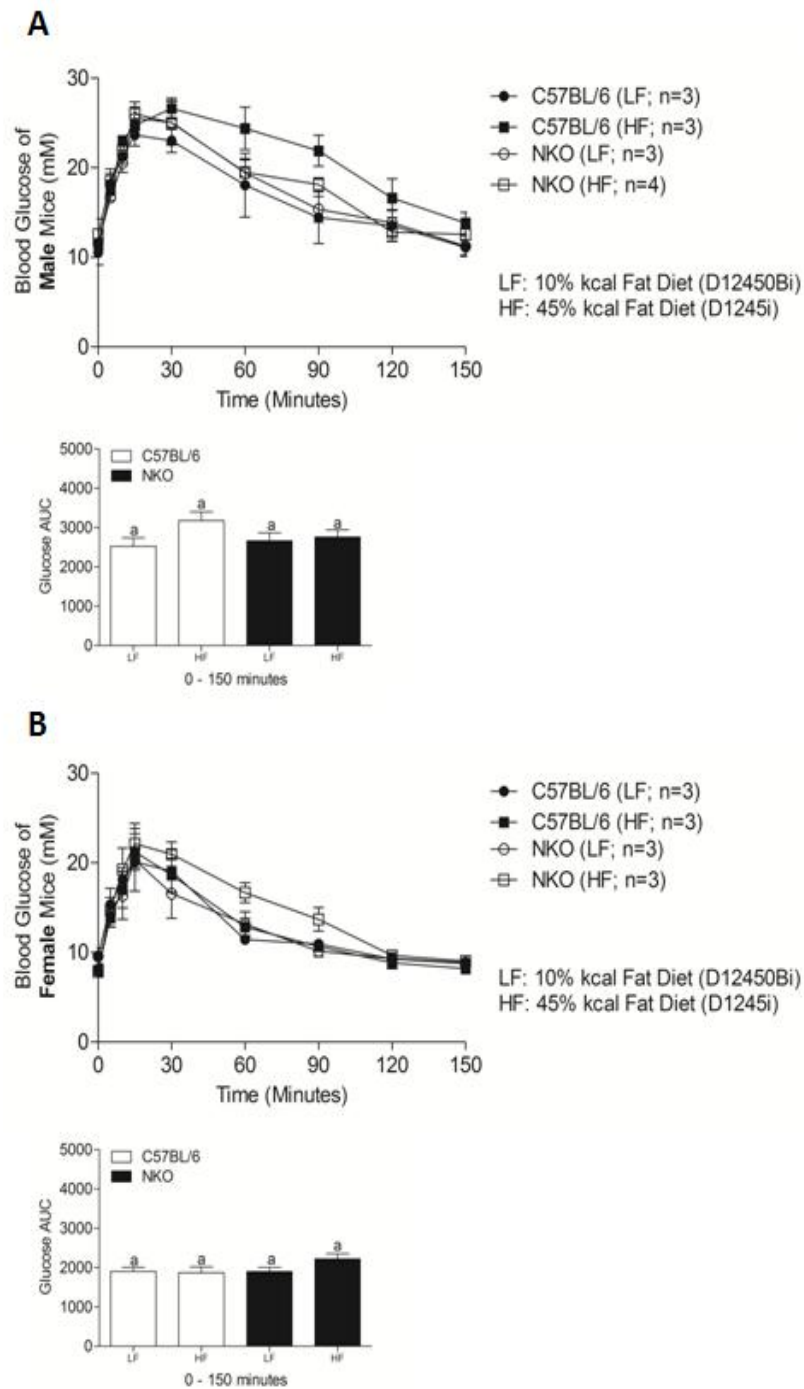


Figure 5.19 IPGTT in NKO and WT Mice fed *Ad Libitum* on 10% and 45% kcal Fat Diet

Figure 5.19. Line graph represents blood glucose levels measured at 0, 5, 10, 20, 30, 60, 90, 120, and 150 minutes during an intraperitoneal glucose tolerance test (IPGTT) measured in C57BL/6 (wildtype; 10% (●) and 45% (■) kcal fat diet) and NKO (10% (○) and 45% (□) kcal fat diet male (A) and female (B) mice. An inset in each figure shows the area under the curve for glucose profiles. No significant difference in the AUC of glucose profile was found between the NKO and WT female mice in both diet fed groups. We used one-way ANOVA followed by Tukey's multiple comparisons test to compare the mean \pm SEM to the measure the difference in AUC of glucose profile.

5.3.10 ITT and Blood Glucose Levels in NKO Male and Female Mice

No significant difference in the AUC of glucose profile was found between NKO and WT male (**Figure 5.20A**) and female (**Figure 5.20B**) mice fed on regular chow. No significant differences in the AUC of glucose profile were found between NKO and WT male mice fed on the different fat diets (**Figure 5.21**).

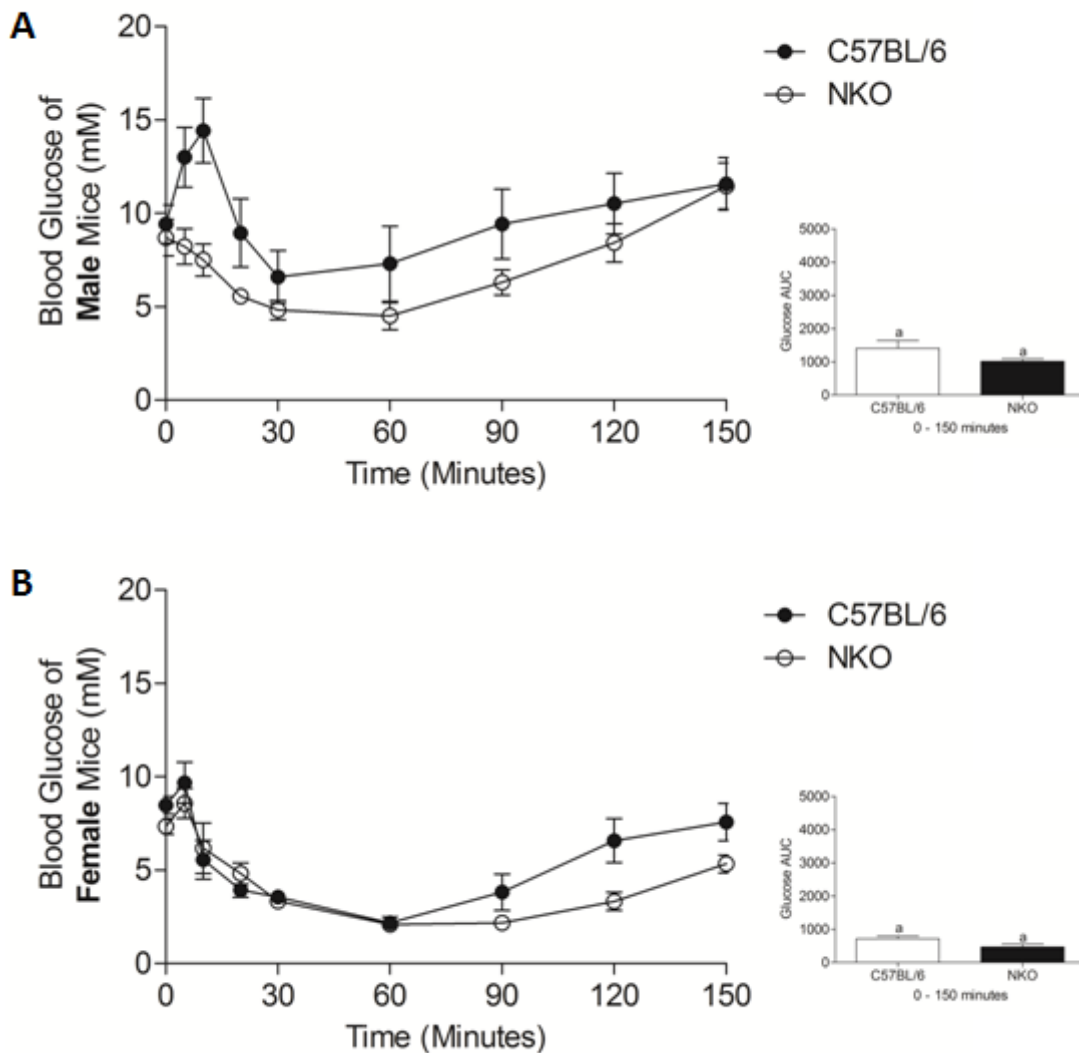


Figure 5.20 ITT in NKO and WT Mice fed *Ad Libitum* on Regular Chow

Figure 5.20. Line graph represents blood glucose levels measured at 0, 5, 10, 20, 30, 60, 90, 120, and 150 minutes during an insulin tolerance test (ITT) measured in C57BL/6 (●; wildtype) and NKO (○) male and female mice. No significant difference in the AUC of glucose profile was found between the NKO and WT male and female mice fed *ad libitum*. We used an Unpaired t-test to measure the difference in AUC of glucose profiles between the two groups mice.

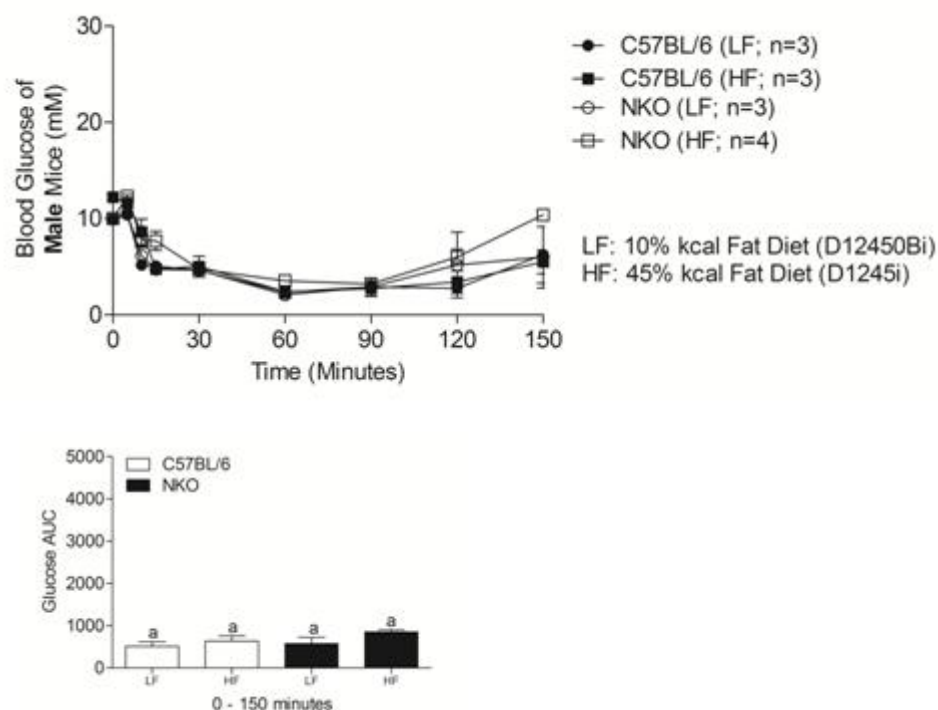


Figure 5.21 ITT in NKO and WT Male Mice fed *Ad Libitum* on 10% and 45% kcal Fat Diet

Figure 5.21. Line graph represents blood glucose levels measured at 0, 5, 10, 20, 30, 60, 90, 120, and 150 minutes during an insulin tolerance test (ITT) measured in C57BL/6 (wildtype; 10% (●) and 45% (■) kcal fat diet) and NKO (10% (○) and 45% (□) kcal fat diet) male mice. No significant difference in the AUC of glucose profile was found between the NKO and WT male mice in both diet fed groups. We used one-way ANOVA followed by Tukey's multiple comparisons test to compare the mean \pm SEM to the measure the difference in AUC of glucose profile.

5.3.11 Serum Insulin, Glucagon, Ghrelin and Leptin in NKO Male and Female Mice

Serum insulin levels of male NKO mice were significantly lower than wildtype (C57BL/6) mice (**Figure 5.22A**). Serum leptin levels of male NKO mice were significantly higher than wildtype (C57BL/6) mice (**Figure 5.22B**). No significant difference in serum leptin and insulin levels was found between female wildtype (C57BL/6) and NKO mice. No significant difference in serum insulin levels (**Figure 5.23A**) and leptin (**Figure 5.23B**) was found between NKO and wildtype (129sv) male and female mice. No significant difference in serum glucagon levels was found between NKO and wildtype (C57BL/6; **Figure 5.22C** and 129sv; **Figure 5.23C**) male and female mice. No significant difference in serum ghrelin levels was found between NKO and wildtype (C57BL/6; **Figure 5.22D** and 129sv; **Figure 5.23D**) male and female mice.

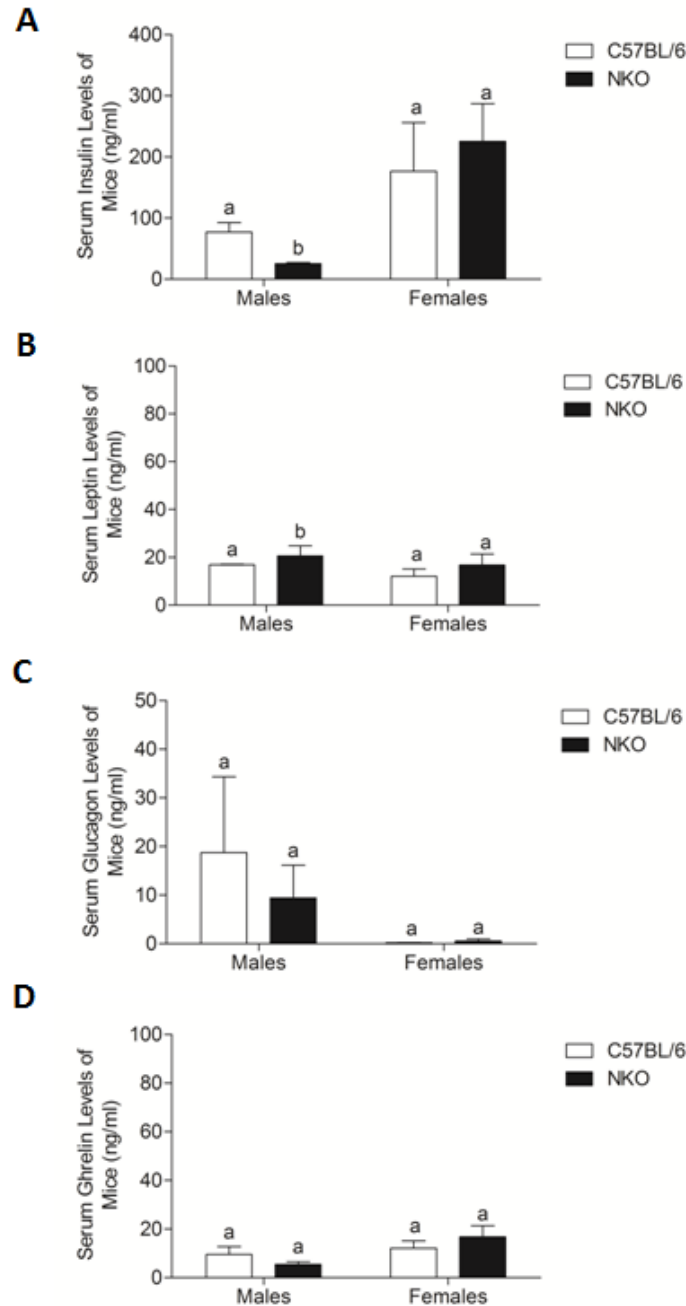


Figure 5.22 Serum Protein Levels in NKO and WT (C57BL/6) Mice fed *Ad Libitum* on Regular Chow

Figure 5.22. Bar graph represents serum insulin (A), leptin (B), glucagon (C) and ghrelin (D) levels in wildtype (C57BL/6) and NKO male and female mice. Serum insulin levels of male NKO mice were significantly lower than wildtype and NKO mice. Serum leptin levels of male NKO mice were significantly higher than wildtype mice ($p < 0.05$). We used an Unpaired t-test to measure the difference in serum protein levels between the two groups of male and female mice.

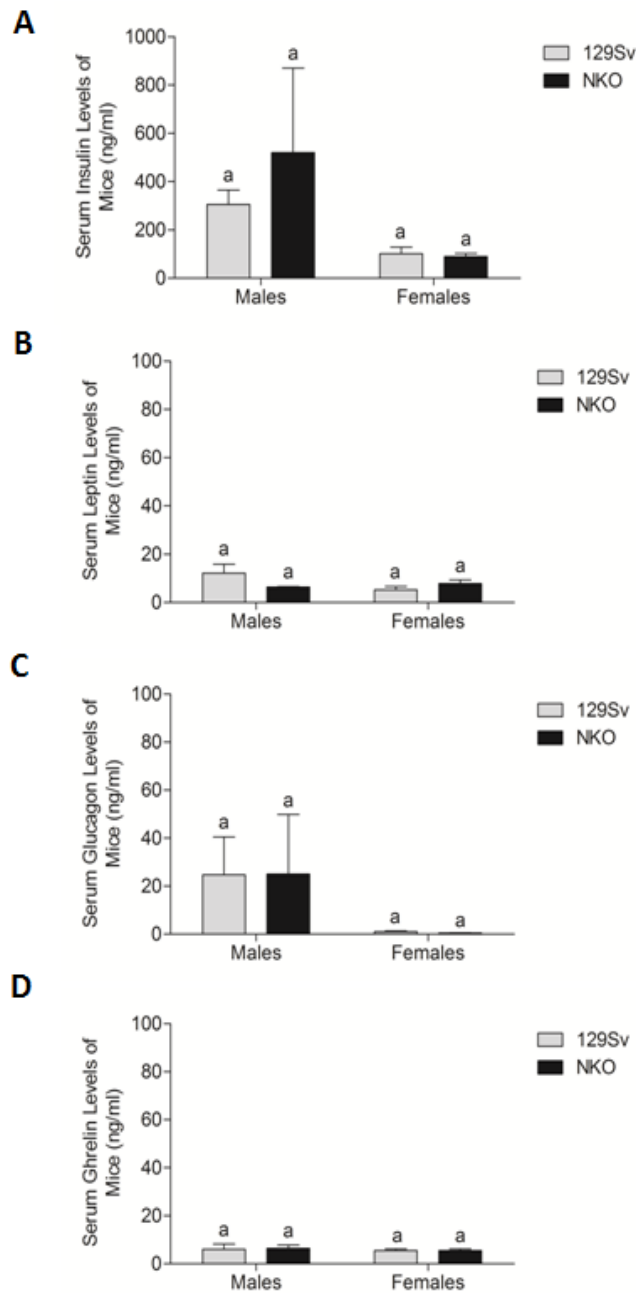


Figure 5.23 Serum Protein Levels in NKO and WT (129Sv) Mice fed *Ad Libitum* on Regular Chow

Figure 5.23. Bar graph represents serum insulin (A), leptin (B), glucagon (C) and ghrelin (D) levels in wildtype (129Sv) and NKO male and female mice. No change in serum insulin, glucagon, ghrelin and leptin levels between WT and NKO male and female mice. We used an Unpaired t-test to measure the difference in serum protein levels between the two groups of male and female mice.

5.4 Discussion

Several laboratories studied the anorexigenic effects of nesfatin-1, modulation of endogenous nesfatin-1 under different metabolic conditions (Nakata et al., 2013, Cao et al., 2013), and its interaction with other proteins (Nakata et al., 2013). This chapter reports that the deletion of endogenous NUCB2 affects body weight, food intake, insulin secretion and glucose levels, and whole body energy homeostasis, in a sexually dimorphic manner. NUCB2 ablation caused an increase in body weight in both male and female NKO mice fed *ad libitum* on regular chow and fed on a high fat diet, when compared to WT mice. The increase in food intake was only observed in NKO male mice fed *ad libitum* on regular mouse chow or on a high fat diet versus low fat diet compared to female NKO mice. These results are in agreement with previously published studies where they created a NUCB2 knockdown rat via adenoviral-mediated RNA interference and observed an increase in food intake (Wu et al., 2014).

Nesfatin-1 is anorexigenic and it influences fat mass by decreasing depot specific fat weight (Oh I et al., 2006). This research shows that the absence of NUCB2 and nesfatin-1 causes an increase in bodyweight, and a male specific increase in food intake. Several contributing factors likely exist for this increase in bodyweight. These include altered food intake, increased fat mass, lean mass, reduced physical activity and a decrease in energy expenditure. Preliminary visual observations provided an impression of increased fat depots in NKO mice, but this was not substantiated when we weighed the fat contents from several depots. Nesfatin-1 plays a role in adipogenesis (Osaki et al., 2012, Ramanjaneya et al., 2013, Ramanjaneya et al., 2010) and has an effect in reducing fat mass (Oh-I et al., 2006, Ramanjaneya et al., 2013, Ramanjaneya et al., 2010). This could partly suggest why an increase in the fat depots was observed in NKO mouse. Other factors such as weight of internal organs, bone density, free fluid content (collectively

referred to as the lean mass) that were not measured in this study could have also attributed to the increase in body weight in addition to fat mass. Imaging techniques, especially MRI scans are being considered to quantify the lean versus lipid mass of these mice.

In order to determine the whole body energy homeostasis, the CLAMS was used. It was found that the respiratory exchange ratio was lower in the NKO male compared to the wildtype mice suggesting one reason for increased body weight. However, an increase in total activity was also observed in NKO mice. Although some leads to the increase in body weight is deductible from these data, the low sample numbers and the fact that this study was only conducted in male mice restricts our ability in making solid conclusions. Moreover, in NKO male mice, there is a decrease in serum insulin and an increase in leptin levels. This altered metabolic hormone milieu might also contribute to the increased body weight. Gender and body weight are known to significantly affect serum leptin levels in circulation (Frederich et al., 1995, Niskanen et al., 1997). Also studies have shown that leptin and insulin together regulate food intake and body weight in rats (Air et al., 2002). An increase in food intake is associated with an increase in adipocyte stores and can contribute to an increase in plasma leptin levels (Muzumdar et al., 2003). Circulating leptin levels are directly proportional to fat mass (Rosenbaun et al., 1996, Racussin et al., 2014). The observed increase in circulating leptin levels could be attributed to increase in fat depots observed in the NKO male mice. Increased leptin levels can cause a decrease in glucose stimulated insulin secretion by activating melanocortin receptors in the brain (Muzumdar et al., 2003). Therefore, it could be suggested that increase in circulating leptin could result in a decrease in insulin levels found in male NKO mice. Both insulin and leptin are known to produce adiposity signals to maintain long-term regulation of body weight sending to the brain. Studies have found that when changes in insulin and leptin levels occur, energy

homeostasis and adiposity is altered. Accordingly, we found that NKO male mice display changes in insulin and leptin levels and it could be suggested that the brain responds by adjusting food intake to regulate adipose tissue mass in the body (Air et al., 2002). An interesting observation is the more noticeable changes observed in the metabolic phenotype of male mice only. There appears to be a sexually dimorphic effect for nesfatin-1 loss.

Other knockout studies (Ramanathan et al., 2014) have also reported gender-specific variation in food intake and body weight which is attributed to the functional roles of hormones that are gender dependent. Hypothalamic neuropeptide, hypocretin (Hcrt), also known as orexin is known to be involved in the regulation of body weight and energy metabolism (Tsuneki et al., 2008) and has shown to regulate gender specific effects. Research on HcrtKO mice revealed that only female HcrtKO mice displayed an increase in body weight, body fat, muscle, free fluid levels and circulating serum levels compared to age matched controls. No difference was observed between male HcrtKO and wildtype controls (Ramanathan et al., 2014). In addition, kisspeptin receptor knockout studies have revealed that kisspeptin is not only involved in reproduction, but also has a sexual dimorphic role on body weight, energy expenditure, and glucose homeostasis (Seminara et al., 2003, Topaloglu et al., 2012). Thus far, research has shown that kisspeptin is involved in regulating the reproductive axis by stimulating the gonadotropin-releasing hormone neurons by binding to its receptor (Kiss1r). As kiss1r is found in many central (Lehman et al., 2013) and peripheral tissues (Brown et al., 2008, Hauge-Evans et al., 2006) involved in metabolism raises the curiosity to unravel other physiological roles in addition to reproduction. Studies on Kiss1r knockouts have shown that Kiss1rKO females have higher body weight, leptin levels, and adiposity, with impaired glucose tolerance compared to wildtype controls (Tolson et al., 2014). Kiss1rKO females also displayed reduced locomotor

activity, respiratory rate, and energy expenditure. Males displayed normal body weight and glucose regulation (Tolson et al., 2014). Sexual dimorphic role is also observed in other receptor knockout models, which include the vasopressin V1a receptor knockout (V1aRKO) mouse model. It was found that reduced anxiety-like behavior was only observed in V1aRKO males compared to females (Bielsky et al., 2005). Reduced anxiety like behavior is also found in male oxytocin KO (OTKO) males compared to female mice (Winslow et al., 2000). These studies reveal that ablation of a hormone or its receptor can induce sexual dimorphic changes in physiology. Research suggests that differences in body weight, food intake, hormone secretion manifest after puberty, indicating the importance and activation of gonadal hormones and therefore it is important to perform phenotypic characterization in a gender dependent manner (Arnold et al., 2012). One study identified that multiple genes are expressed at different levels in the liver of male and female mice (Van Nas et al., 2009). After the gonads were removed, the difference in gene expression between the sexes was attenuated (Van Nas et al., 2009), suggesting that genetic differences are dependent on the production of gonadal hormones. Also, hormonal and non-hormonal mechanisms are known to alter the epigenome and regulate sex differences via epigenetic mechanisms (Arnold et al., 2012).

Previous research described in chapters 2-3 found that NUCB2 is expressed in the β -cells and plays an important role in glucose stimulated insulin secretion (Gonzalez et al., 2012a, Gonzalez et al., 2011). NKO male and female pancreatic β -cells and pancreatic tissue displayed a loss of NUCB2/nesfatin-1 protein expression compared to wildtype controls. Paraffin sections of pancreatic tissue from NKO female mice had comparatively larger islets than male mice. Although preliminary in nature, it was observed that the NKO male mice have fewer numbers of pancreatic islets. Glucose stimulated insulin secretion from the NKO mice islets was attenuated

compared to WT pancreatic islets. In agreement with this reduced number of islets, male mice appear to have less GSIS compared to female mice. In addition, glucose and KCl stimulated insulin secretion was also attenuated in female mice. While the mechanisms of this defect still remain unclear, NUCB2 ablation disrupts glucose stimulated insulin production from islets. These results suggest that NKO pancreatic islets have decreased insulin production and/or impaired secretion and glucose responsiveness. The results of this research show that NUCB2/nesfatin-1 is important for normal islet function and islet formation: in the absence of NUCB2, males have smaller islets and are fewer in number, with decrease in insulin production compared to female NKO mice. Other KO studies have also emphasized the importance of hormones in islet structure and function. For instance, neuroligin-2 KO mice have shown that absence of neuroligin-2 resulted in smaller, fewer and decreased insulin content in beta cells (Zhang et al., 2013). Now, to determine whether the effects of NUCB2 deletion on islet formation in males were due solely to the loss of NUCB2 gene in the islets, future studies using a conditional, islet-specific NKO mouse would be necessary. Overall, these results are in agreement with the *in vitro* insulinitropic effects of nesfatin-1 reported before (Gonzalez et al., 2011, Nakata et al., 2011). Interestingly, we did not see any defects in serum insulin levels *in vivo* in *ad libitum* fed mice before or after a glucose load. This result is in contrast to the preliminary findings gathered from TGRI.

Sex specific differences in glucose homeostasis in male and female NKO mice were observed during an IPGTT and ITT. IPGTT found an improvement in glucose handling in chow fed male NKO mice during 60-150 minutes post-glucose administration. Meanwhile, in chow fed female NKO mice, blood glucose was significantly higher at 30 minutes, but no differences were found at other time points. This pattern was also visible in NKO mice fed a high fat diet. Further,

in an ITT, NKO mice displayed persistent decrease in blood glucose compared to the WT controls, while in females a decrease was observed at the later stages of sampling. This shows that the absence of NUCB2 and/or nesfatin-1 enhances glucose handling, even when there are no changes in insulin levels *in vivo*. This could be due to an increase in glucose uptake in target tissues and change in insulin sensitivity as a result of NUCB2 ablation. Previous studies showed that nesfatin-1 treated *ad libitum* rats had normal blood glucose levels with higher insulin and lower glucagon levels during an oral glucose tolerance test (Gonzalez et al., 2012a). Nesfatin-1 altered insulin sensitivity without a change in glucose suggesting that insulin mediated glucose uptake is altered in the peripheral tissue. Decrease in glucose levels by nesfatin-1 treatment was prevented as gluconeogenesis in the liver along with inhibition of glucose uptake in the skeletal muscle would have occurred (Gonzalez et al., 2012a). This suggests that presence of nesfatin-1 controls insulin mediated glucose uptake in peripheral tissue to main glucose homeostasis. Removing nesfatin-1 demonstrates an increase in insulin sensitivity, thus enhancing glucose homeostasis. It is likely that glucose uptake in peripheral tissues is improved. In contrast, another study demonstrated that intravenous injections of nesfatin-1 significantly reduced blood glucose levels in *db/db* mice compared to *ad libitum* mice (Su et al., 2010). Also, peripheral infusion of nesfatin-1 showed reduction in blood glucose levels in mice fed regular chow and high fat diet (Li et al., 2013). Both of the studies discussed above suggest that nesfatin-1 enhances insulin sensitivity regulating glucose metabolism. The difference in results obtained among studies warrants that additional studies on nesfatin-1 effect on insulin mediated glucose uptake in peripheral tissues must be performed. In the NKO male and female liver, stomach, duodenum, and pancreatic tissues, NUCB2 protein expression was absent. The loss of NUCB2 protein expression in the NKO male and female stomach tissues coincides with a decrease in

preproghrelin (**See Supplementary Figure S5.1**) protein expression in the stomach of NKO male and female mice supporting the knowledge that the loss of NUCB2 can affect the production of other hormones co-expressed in the same tissue, in this case, ghrelin. NUCB2 and ghrelin are known to be expressed in the gastric X/A-endocrine like cells of the stomach (Mohan et al., 2014, Stengel et al., 2013, Stengel et al., 2012b). The absence of NUCB2/nesfatin-1 could cause gender-specific fluctuations in the secretion of other metabolic hormones it interacts or is co-expressed with, modulating whole body energy metabolism and regulating glucose homeostasis.

5.6 Limitations of the Study and Reasons for the Lack of Complete Characterization

A major limitation in this study is that it is not complete, and sample sizes are low. This stems from the mixed background of the NKO mice used. Once the question about the background was raised, TGRI was contacted and based on the genome scan data, they confirmed that the NKO mice used here are 75% C57BL/6 or 25% 129Sv strain. Variability in backgrounds might lead to altered metabolic phenotype and reflect in food intake, body weight, and whole body energy homeostasis. In order to limit these confounding factors, it was necessary to generate the NKO mice on a pure genetic background. This can be achieved by consistently breeding the genetically modified mice on a pure genetic background. Therefore, the phenotype characterization was terminated in 2012, and all efforts were focused on generating the NKO on pure C57BL/6 background.

Briefly, an outcross, backcross and intercross to obtain pure genetically modified NKO mice on a pure C57BL/6 background. In the first step, we performed an outcross by breeding a wild type C57BL/6 from Charles River with a homozygous NKO mouse to obtain genetically modified NKO mice that is 75% of pure genetic background (C57BL/6). We observed that all the progenies were heterozygous. Next we performed step 2, where we mated the heterozygous male pups from step 1 with wildtype Charles River female C57BL/6 mice to get N1 progenies. We repeated this step three times (N2-N4). For each cross in N2-N4, the male heterozygous pups obtained from the previous N cross were mated with a wildtype female. By N2 they should be pure C57BL/6 background (0% 129 Sv), but we repeated it for two more crosses to ensure they are indeed pure C57BL/6. In step 3, the pure male and female heterozygous mice were crossed to obtain homozygous NKO mice. The homozygous NKO mice obtained in step 3 were

then crossed to generate more homozygous progenies for studies to be repeated. By performing these crosses, we benefited in having a genetically modified mice on a pure genetic background that will help interpretation of results with confidence. Finally, to ensure that the breeding strategy provided desired results, a genome scan was conducted at Jackson Labs on these homozygous mice. The results of the genome scan confirmed that the mice are indeed 99% pure C57BL/6 background.

5.7 Ongoing Studies on NKO Mice Characterization and Future Directions

Currently, the phenotype characterization of this newly generated homozygous NKO mice in pure C57BL/6 background is in progress. We aim to perform quantitative analysis (qRT-PCR and Western Blot) on islet derived endocrine factors. We will also perform a simultaneous multiparameter assessment of NKO mice and their wild type controls by using metabolic cages (Comprehensive Laboratory Animal Monitoring System; CLAMS) that will measure their food intake, feeding bouts, and food eaten per bout, water intake, activity, VO_2 , VCO_2 , respiratory exchange ratio, heart rate and body temperature for 24 hours. In addition, *in vitro* studies will be performed to determine the glucose responsive insulin release from islets of NKO mice and their wild type controls. We will also repeat the above studies in mice fed high fat diet to see whether/how the NKO mice develop high fat diet induced obesity and diabetes. Overall, all studies presented in this chapter, and more, with an increased “n” are being conducted. The results of these studies will be available by the time of the thesis defense.

Transition

The final chapter focuses on my general discussion with respect to the findings detailed in chapters 2-5. This chapter summarizes and discusses the collective contributions of this research specifically to the nesfatin-1 field, and in general to the body of literature on the neuroendocrine regulation of energy balance. It highlights shortfalls of this research, and some possible logical future directions arising from the current findings.

Chapter 6

General Discussion

Since 2006, the year nesfatin-1 discovery was first reported, just over 250 articles on nesfatin-1 were published in PubMed. From these publications, we already know that nesfatin-1 is an important meal responsive multifunctional hormone with metabolic effects. This thesis, by providing some novel information, also contributes significantly to the growing knowledge base on nesfatin-1. The main contributions of this research, some limitations and future considerations are outlined in this chapter.

6.1 Contribution 1: Tissue Specific Expression of NUCB2/Nesfatin-1-PCs, and Ghrelin-GOAT – Developmental Perspectives

The research outlined in chapters 2 and 3 presents the findings on the developmental expression of NUCB2/nesfatin-1 in the gastroenteropancreatic tissues and serum of rats. We found that NUCB2/nesfatin-1 colocalizes with insulin in the islet β -cells at all developmental stages in an age-dependent manner suggesting that NUCB2/nesfatin-1 plays an important role in glucose metabolism during growth (Mohan and Unniappan, 2012). NUCB2 is processed by PC 1/3 and/or PC 2 to nesfatin-1. PC 2 is present only in the pancreatic alpha cells at postnatal day 27, but at all other stages, both PC 1/3 and PC 2 colocalize with NUCB2/nesfatin-1 in β -cells. NUCB2 mRNA levels in the duodenum at postnatal day 27 are higher than the adult NUCB2 mRNA expression, however metabolic effects of NUCB2 expression in the duodenum still remain elusive (Mohan and Unniappan, 2012). Circulating levels of serum nesfatin-1 increased with development. NUCB2/nesfatin-1 IR in the pancreas and gastrointestinal tract could possibly contribute to the gradual increase in serum NUCB2/nesfatin-1 levels (Mohan

and Unniappan, 2012). This was the first study that has focused on NUCB2/nesfatin-1 expression in the developmental stages of rats suggesting it has an age- and tissue-specific role in the developmental physiology of rats (Mohan and Unniappan, 2012). It is known that hormones exert tissue- and age-specific effects during development (Dauncey et al. 2001). Hormones can be growth stimulatory and growth inhibitory during fetal and postnatal periods (Dauncey et al., 2001, Fowden and Forhead, 2009). The hormones act as environmental and maturational signals to regulate the accretion and differentiation of tissue pre- and post-birth ensuring proper development based on the nutrient supply available (Fowden and Forhead, 2009). From the results outlined in this thesis, it could be suggested that NUCB2/nesfatin-1 is a growth regulatory peptide. The identification of intra- and extra-islet nesfatin-1 specific roles in the pancreas requires further studies.

6.2 Contribution 2: MGN3 Cells as a Tool to Study Regulation of NUCB2/Nesfatin-1

Some experiments in Chapter 4 determined whether stomach ghrelinoma cells, MGN3-1, express NUCB2/nesfatin-1. One of the major contributions to nesfatin-1 research is that we characterized MGN3-1 cells as a source of nesfatin-1. This provided us a tool for studying the regulation of nesfatin-1 secretion *in vitro*. mRNAs encoding NUCB2, and its processing enzymes PC 1/3 and PC 2 in MGN3-1 cells were detected in MGN3 cells. These findings are further supported by the identification of NUCB2, PC 1/3 and PC 2 immunoreactivity in the same cells. It was also found that MGN3-1 cells co-localize both nesfatin-1 and ghrelin, an observation that confirms previous findings (Stengel et al., 2009b). This now enables researchers to use MGN3-1 cells as a tool to study the regulation of nesfatin-1.

6.3 Contribution 3: NUCB2/Nesfatin-1 in the Small Intestine

The expression of nesfatin-1 in the intestine was a contentious issue, with some reports finding nesfatin-1 in the intestine (Zhang et al., 2010), while some others not (Stengel et al., 2009b). A relatively small, yet significant finding reported in chapter 2 and in chapter 4 is the identification of NUCB2 mRNA and nesfatin-1 immunoreactivity in the intestine of both rats (chapter 2) and mice (chapter 3). Using RT-PCR, qRT-PCR, Western blot analysis and immunohistochemistry, confirmed that NUCB2/nesfatin-1 exists within the enteric tissues. The intestinal roles of nesfatin-1 are yet to be identified.

6.4 Contribution 4: Nutrient Regulation of NUCB2/Nesfatin-1

Availability of nutrients is profoundly important for fetal and postnatal development and expression of genes encoding proteins of importance (Dauncey et al., 2001). Intake of nutrients can affect numerous genes involved in differentiation, growth and metabolism (Dauncey et al., 2001, Hall et al., 2012). To date, there is no information available on the regulation of NUCB2 mRNA expression or nesfatin-1 secretion, other than some reports that found that meal intake (Oh-I et al., 2006, Stengel et al., 2009a, Stengel et al., 2009b, Gonzalez et al., 2012a) or glucose (Gonzalez et al., 2011) stimulated nesfatin-1 release into circulation. Are meal contents or individual nutrients modulators of NUCB2/nesfatin-1 synthesis and expression? Studies in chapter 4 addressed this, where acute (liquid) and chronic (solid) feeding of mice with a high fat, high carbohydrate and high protein diet was achieved. It was determined that nesfatin-1 is regulated by macronutrients in a tissue specific manner. These effects were again found to be different between acute and chronic exposure. While the above studies elucidated the regulation of NUCB2/nesfatin-1 in vivo, another approach using MGN3-1 cells

explored how components of macronutrients tested influence NUCB2 mRNA and NUCB2/nesfatin-1 secretion in stomach cells, a major source of this peptide. Collectively, the results from this research, for the first time indicate that nesfatin-1/NUCB2 is modulated by nutrients and these effects are specific to the nutrients and the tissues and cells it is produced from.

6.5 Contribution 5: Is NUCB2/Nesfatin-1 Critical for Energy Homeostasis?

Gene deletion in mice is a widely used approach to determine the biological necessity of an endogenous protein. A NUCB2 knockout (NKO) mice model was generated. This provides a valuable tool to gather additional information on the importance of nesfatin-1. It was found that deletion of NUCB2 affects body weight, food intake, insulin secretion and glucose metabolism, and whole body energy homeostasis (**Table 6.1**). An increase in body weight in both genders of NKO mice fed *ad libitum* on regular chow and fed on a high fat diet compared to WT mice was observed. The increase in food intake was only observed in NKO male mice fed *ad libitum* on regular mouse chow or on a high fat diet versus low fat diet compared to female NKO mice. NKO male and female pancreatic β -cells and pancreatic tissue displayed a loss of NUCB2/nesfatin-1 protein expression compared to wildtype controls. Insulin secretion was attenuated from NKO versus WT pancreatic islets when incubated in high glucose suggesting that NUCB2 ablation disrupted glucose stimulated insulin production from islets. In the NKO male and female liver, stomach, duodenum, and pancreatic tissues, NUCB2 protein expression was absent. The loss of NUCB2 protein expression in the NKO male and female stomach tissues coincides with a decrease in preproghrelin. Moreover, in NKO male mice, we observed a decrease in serum insulin and increase in leptin levels in

circulation suggesting impairment in protein secretion in NKO males mice only. We believe that absence of NUCB2/nesfatin-1 can cause gender-specific fluctuations in the secretion of other metabolic hormones, modulating whole body energy metabolism. The respiratory exchange ratio was lower in NKO males compared to wildtype mice suggesting a mix of fat and carbohydrate utilizations. An increase in oxygen consumption and total activity was also observed. NUCB2 knockdown in rats causes an increase in food intake and body weight (Wu et al., 2014), similar to what we found in the NKO mice. Together, the data presented in chapter 5 provide important information supporting a metabolic role for nesfatin-1. **Table 6.1** provides a summary on the preliminary characterization of NKO male and female mice. While the NKO mice are fertile and viable, it appears that an intact NUCB2 gene producing the nesfatin-1 protein is important for maintaining energy balance and metabolic hormonal milieu. Although this research is conducted in mice, the findings significantly enhance our knowledge, and are extendable to human health and disease. For example, both NUCB2 mutations are reported in obese children (Zegers et al., 2012) and in obesity in men (Zegers et al., 2011). Altered body weight and glucose homeostasis appear to be the most striking and common phenotype resulting from NUCB2/nesfatin-1 disruption in mice (chapter 5 and preliminary results using NKO mice in pure C57BL/6 background) and in children and adults in the human population (Zegers et al., 2011, Zegers et al., 2012).

Table 6.1: Preliminary Characterization of NKO Male and Female Mice

Findings	Male	Female
Body Weight	↑	↑
Food Intake	↑	↔
NUCB2 Protein Expression	☒	☒
Preproghrelin Protein Expression	↓	↓
Blood Glucose Levels	↓	↔
Insulin Secretion	ND	↓
Insulin Sensitivity	↑	↔
Serum Insulin Levels	↓	↔
Serum Leptin Levels	↑	↔
Respiratory Exchange Ratio	↓	ND
Oxygen Consumption	↑	ND
Total Activity	↑	ND

↑ - Increase, ↓ - Decrease, ↔ - No Change, ND - Not Determined, ☒ - Absent

6.6 Nesfatin-1 and the Neuroendocrine Regulation of Energy Balance

As indicated in chapter 1, the endocrine regulation of metabolism is achieved by multiple, redundant factors secreted from central and peripheral tissues. The brain, gut, pancreas and adipose tissue are major sources of metabolic hormones, and are also sites of their action. How does nesfatin-1 fit in with this system? The research outlined in chapters 2-4 provides important new information on the tissue sources of nesfatin-1. It is now clear that the endocrine pancreas and the gastrointestinal tract are major sources of endogenous nesfatin-1. Nesfatin-1 is also meal dependent, but its tissue-specific expression and secretion appear to vary and is dependent on the nature of the nutrient and the duration of exposure to the nutrient. While several pharmacological and tissue knockdown strategies were used to elucidate the physiological functions, to date, no results on the complete absence of nesfatin-1 has been studied. Our results clearly indicate that the lack of nesfatin-1 disrupts energy homeostasis in multiple ways. The developmental expression, meal related expression and secretion as well the results of complete absence of nesfatin-1 – all provide strong support to the existing notion that nesfatin-1 is also a key player in the already existing multifactorial system that regulates energy balance (**Figure 6.1**). In addition to the defects in whole body energy homeostasis, the lack of nesfatin-1 also caused alterations in leptin and insulin, two long-term satiety signals. Thus, it is likely that the metabolic phenotype of NKO mice is due to abnormalities in other hormones, including leptin and insulin.

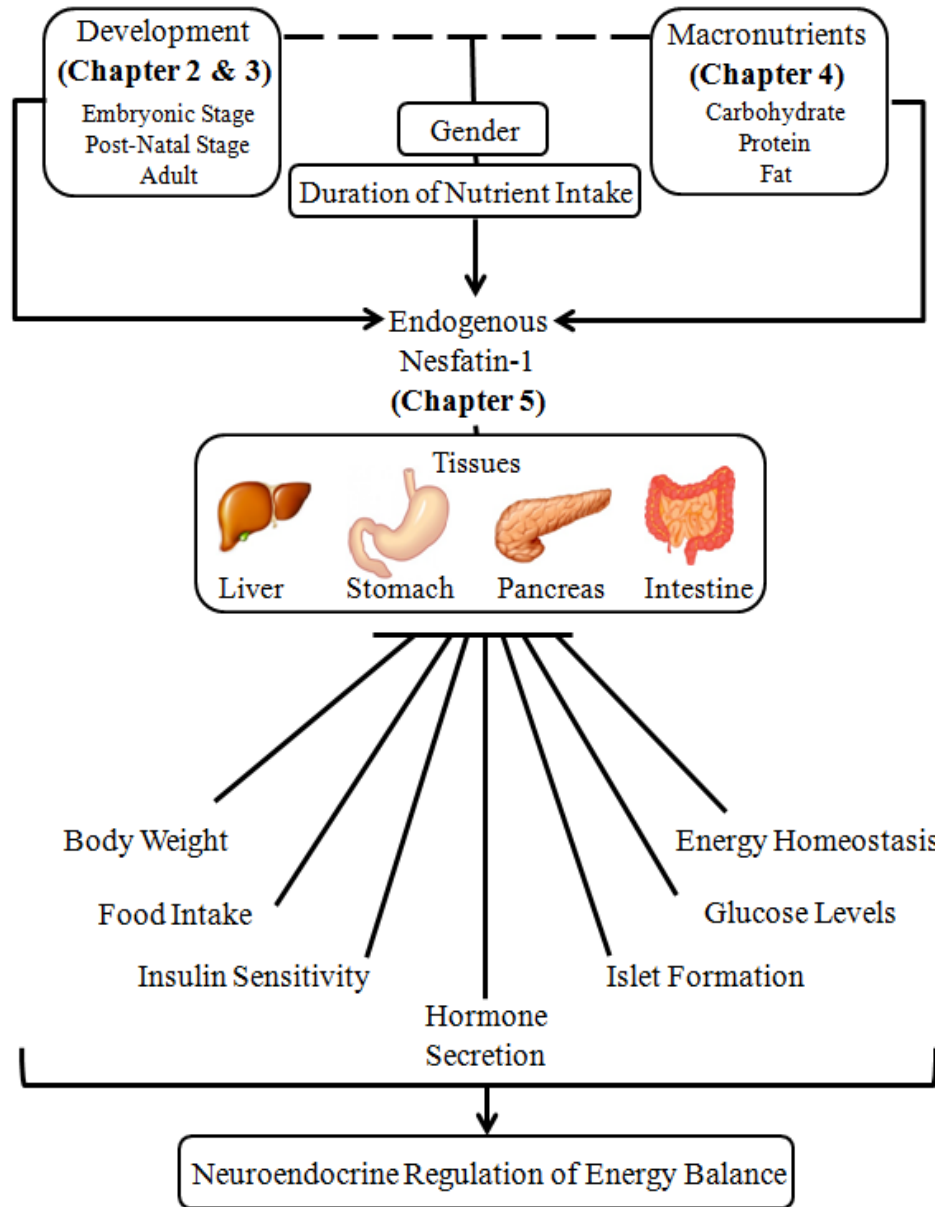


Figure 6.1 Summary of Thesis Findings

Figure 6.1. The development stage (embryonic, post-natal, adult) and the intake of macronutrients (carbohydrates, protein, fat) affect endogenous production of nesfatin-1. Development and macronutrients are dependent on gender and duration of specific macronutrient intake, which modulate the synthesis and secretion of nesfatin-1 in important metabolic tissues that include the liver, stomach, pancreas and intestine. Endogenous nesfatin-1, mainly produced from the gastroenteropancreatic tissues and liver, affect body weight, food intake, insulin sensitivity, islet formation, glucose levels, RER and hormone secretion, thereby contributing to the neuroendocrine regulation of energy homeostasis.

6.7 Limitations of this Research

6.7.1 Antibody Specificity

For immunohistochemistry, immunoassays and Western blot analysis, the NUCB2 antibody (Phoenix) used by several studies, including this research, binds to both NUCB2 and nesfatin-1. We found out that the nesfatin-1 region in NUCB2 shares similar amino acid sequence to a nesfatin-1 like region in NUCB1. In our NKO mice (which could be considered as a negative control), this antibody is not effective in detecting any signals, although smearing in Western gels and isolated immunopositive cells in immunohistochemistry were detected. It is likely that the antibody used here, to some extent, also binds to NUCB1 and/or its processed peptides. Therefore, it would be beneficial to use an antibody that binds specifically to nesfatin-1 region of NUCB2, not NUCB1. It was recently made in our laboratory, and we commenced using this antibody to further enrich our data from immunohistochemical studies and Western blot analysis.

6.7.2 Gender Specific Expression of NUCB2/Nesfatin-1

From chapter 5, it appears that the lack of NUCB/nesfatin-1 results in sexually dimorphic phenotypes. There was a lack of gender specific mRNA quantification in peripheral tissues of rats during development. In Chapter 2 and 3, embryonic and postnatal tissues extracted for RNA extraction and quantified data presented were a mixed pool of male and female tissues. Similarly, in chapter 4 also only male mice were used. These studies must be repeated in future where we separate male and female tissues and quantify NUCB2 mRNA expression tissue- and gender-specifically. During puberty, sex hormones can also play a major role in influencing the production of metabolic hormones in tissues of male and female rats important for development. Therefore, it

would be interesting to determine whether NUCB2/nesfatin-1 synthesis and secretion are divergent in males and females.

6.7.3 Lack of Protein Determination

Although secreted milieu of nesfatin-1 was measured, tissue-specific protein expression in peripheral tissues from mice fed on different nutrient diets was missing in Chapter 4. Only mRNA expression was used to determine NUCB2. It would have been beneficial to perform protein extraction on tissues dissected from mice fed on different diets to detect the nesfatin-1 protein levels in each tissue using Western blot techniques. Future studies should consider how chronic intake of nutrients modulates nesfatin-1 protein in specific tissues.

6.7.4 NKO = NUCB2 knockout or Nesfatin-1 knockout?

In addition to the mixed background issue discussed in chapter 5, another topic worth considering is the absence of both NUCB2 and nesfatin-1 in NKO mice. NUCB2 is also a secreted protein, which could elicit cellular functions. In the NKO mice, both precursor and the processed peptide are absent. Therefore, the phenotype observed in these mice could be due to the absence of either nesfatin-1 or NUCB2 alone or both peptides. To determine whether the NKO metabolic phenotype is exclusively due to the absence of nesfatin-1, it is possible to reintroduce nesfatin-1 into the system by pharmacological or genetic approaches. If the metabolic defects in NKO mice are masked by the administration of nesfatin-1, then it will be clear that the lack of nesfatin-1 is indeed the reason for defects in NKO mice.

6.8 Ongoing Research and Future Directions

As several pilot studies were conducted for the preliminary characterization of NKO mice in Chapter 5, the number of mice used in each study was limited. We did not expand the colony as it was found that the mice used were of mixed background. Therefore, instead of increasing the “n” and repeating the studies, we decided to pursue backcrossing to generate mice in pure C57BL/6 background. This was partly done to limit wastage of funds, and to focus in obtaining more meaningful data. It is important to note that we were able to perform statistical analysis on all data obtained in the pilot study. However, in order to account for multiple factors that include age, diet and gender, we require an increase in subject numbers in each study. These aspects, including a higher “n” and more appropriate statistical analyses will be considered in future studies using the pure bred mice. Currently all experiments in chapter 5 are being repeated in NKO mice that are of 99% C57BL/6 strain obtained after repeated backcrossing. This approach limits the possible variability of results (qualitative and quantitative) due to the mixed background of mice used. When analyzing data obtained from our new studies, factorial and repeated measures ANOVA will be used. Each study will have at least 6-8 mice per group.

The mouse mutagenesis approach used here has focused on a global NUCB2 gene deletion. Mutations to achieve cell- and tissue-specific gene modification provide a more valuable and accurate strategy. Such a strategy would help delineate the specific effects of NUCB2/nesfatin-1 absence on individual tissues. Efforts are currently underway in our lab to generate tissue specific NKO mice using the *cre-lox* technology. Research in our lab now also focuses to determine whether nesfatin-1 modulates gastric hormones

including ghrelin, and enteric hormones including GLP-1, GIP, CCK and PYY. There is very limited evidence that suggest that the neuronal and islet beta cell effects of nesfatin-1 are mediated via a G-protein coupled receptor (Nakata et al., 2011, Brailoiu et al., 2007, Iwasaki et al., 2009). Preliminary findings suggest that GPR3, GPR6 and/or GPR12 are potential receptors for nesfatin-1 (Mori et al., 2008, Osei-Hyiaman et al., 2011), although further research is required. As previous studies discovered that the stomach, pancreas and liver are tissues where endogenous expression of NUCB2 is found regulating glucose and energy homeostasis, we further investigated whether these receptors are found in these tissues of mice. All three receptors are present in the stomach, pancreas and liver of mice (**Appendix, Figure A**). Moreover, it was found that GPR12 colocalizes with insulin in islets β -cells (**Appendix, Figure B**), but not glucagon producing α -cells (**Appendix, Figure C**). This result suggests a possible direct action of the ligands of these GPR12 on islet beta cells. Further studies must be conducted to learn the receptor-mediated mechanism of action of nesfatin-1.

6.9 Conclusions

The aim of this thesis research was to better understand NUCB2/nesfatin-1 as an endogenous bioactive peptide. Since NUCB2/nesfatin-1 is implicated in both metabolic physiology and pathophysiology, it is a vital contributor to whole-body energy homeostasis. This research identified or provided novel and conclusive evidences to support nesfatin-1 as a metabolic regulator. In conclusion, it was determined that NUCB2/nesfatin-1 is indeed a meal regulated metabolic factor predominantly produced from the gastroenteropancreatic tissues. The data obtained here supports all of the hypotheses that led to this research. It further supports nesfatin-1 as a prospective candidate molecule for the treatment of metabolic diseases.

Appendix

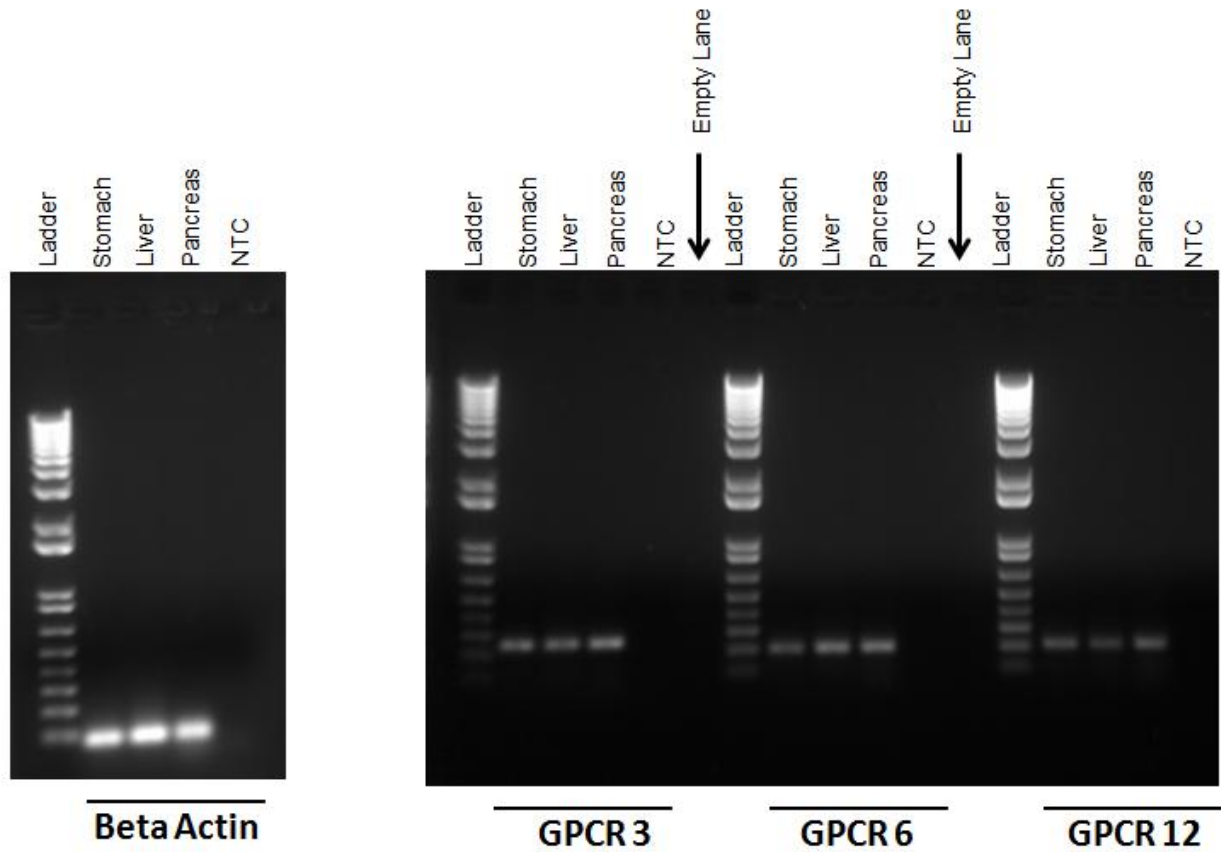


Figure A GPR3, GPR6 and GPR12 mRNAs are expressed in the stomach, liver, pancreas of male mice

Figure A. GPR3 (Amplicon Size: 187 base pairs), GPR6 (Amplicon Size: 214 base pairs) and GPR12 mRNAs (Amplicon Size: 232 base pairs) are expressed in the stomach, liver, and pancreas of male mice. Beta-Actin (β -Actin; Amplicon Size: 123 base pairs) mRNAs expressions were identified in the stomach, liver and pancreas from mice. No GPR3, GPR6 and GPR12 and β -Actin mRNA expression was found in PCR reactions devoid of the cDNA template.

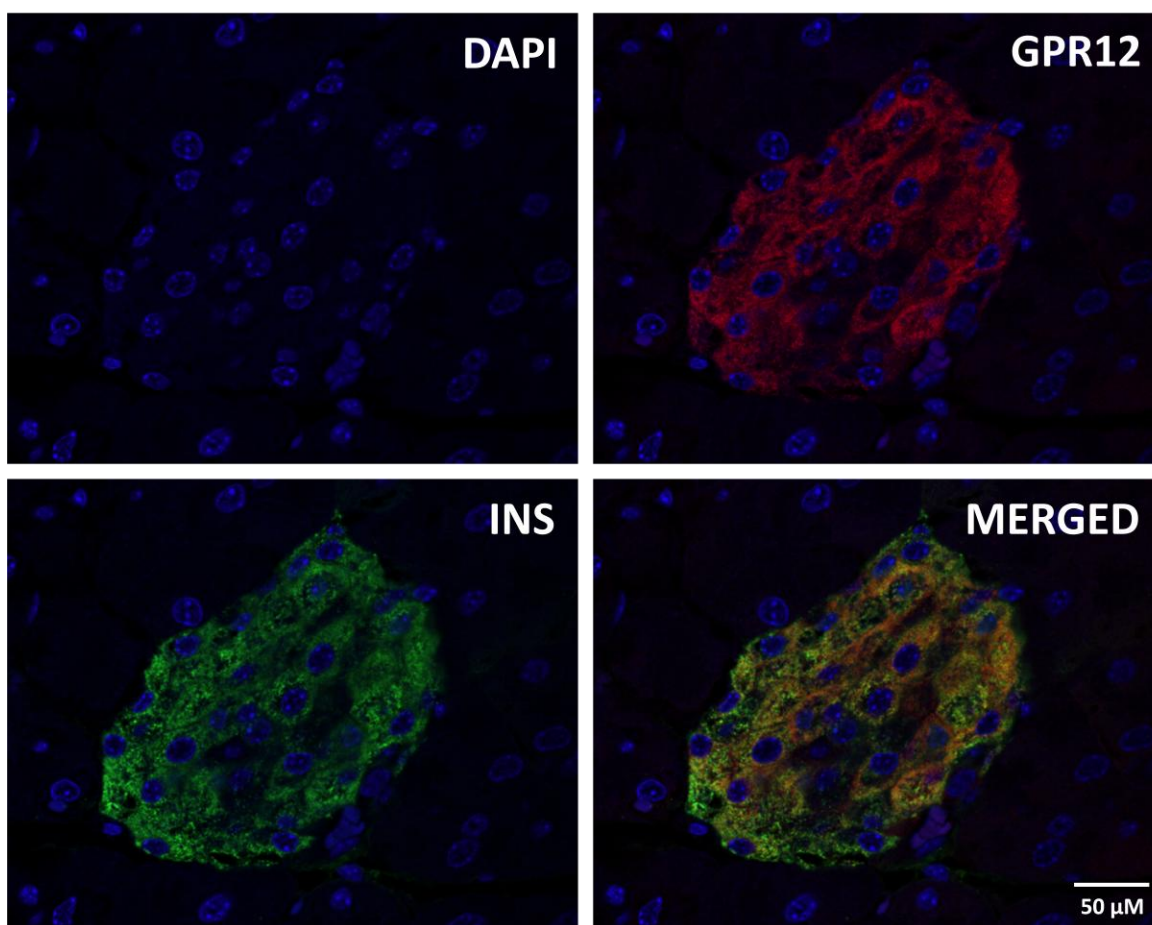


Figure B Co-localization of GPR12 and insulin IR in the mouse pancreas

Figure B. Co-localization of GPR12 and insulin immunohistochemical staining of the mouse pancreas was evident in the insulin producing beta-cells. Islet cells immunoreactive for GPR12 (red), insulin (green), nuclei (blue) and the merged image of GPR12, insulin and DAPI (yellow). Representative images were taken of 4 slides. Scale bar = 50 μ m.

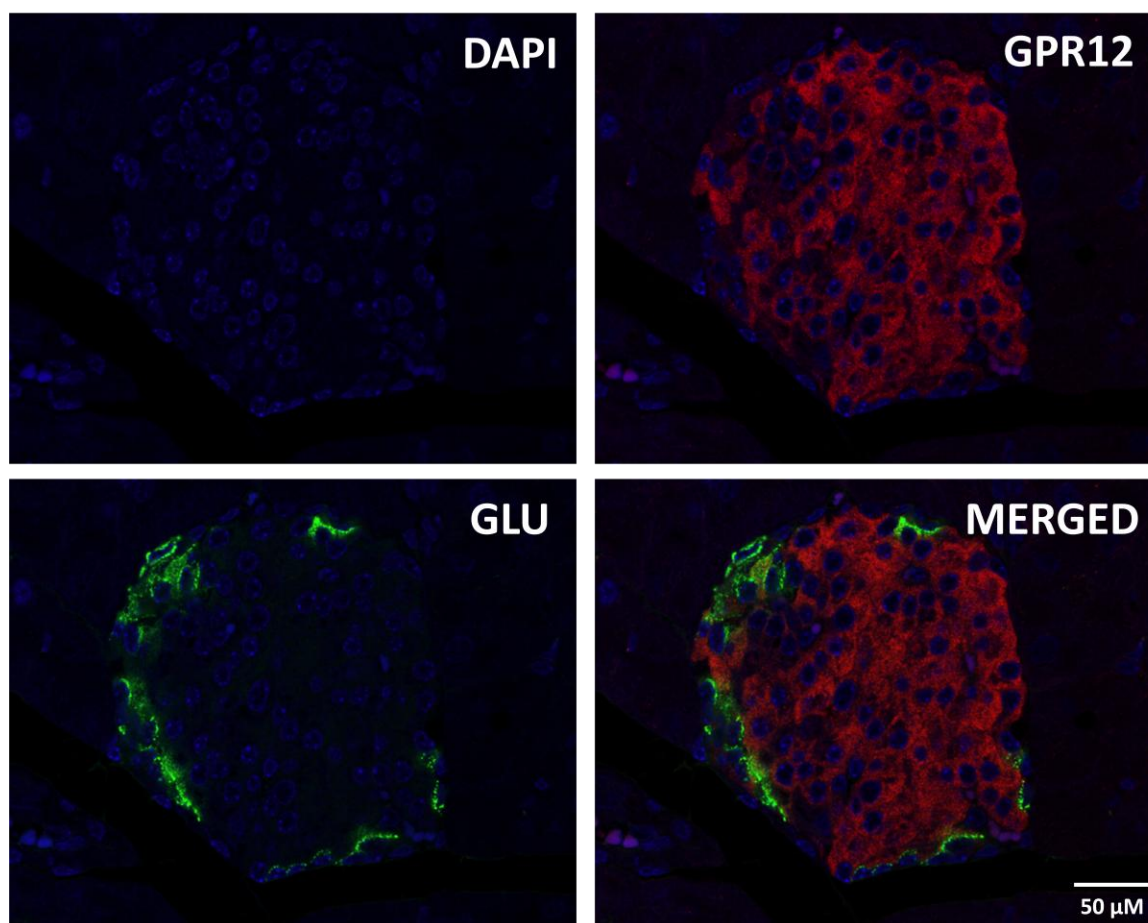


Figure C Localization of GPR12 and glucagon IR in the mouse pancreas

Figure C. Localization of GPR12 and glucagon immunohistochemical staining of the mouse pancreas. No-colocalization was found as GPR12 was evident in the insulin producing beta-cells and glucagon was evident in the glucagon producing alpha-cell. Islet cells immunoreactive for GPR12 (red), glucagon (green), nuclei (blue) and the merged image of GPR12, glucagon and DAPI (yellow). Representative images were taken of 4 slides. Scale bar = 50 μ m.

References

- Adeghate E, Ponery AS. Ghrelin stimulates insulin secretion from the pancreas of normal and diabetic rats. *J Neuroendocrinol.* 2002; 14: 555–560
- Ademoglu EN, Gorar S, Carliloglu A, Yazıcı H, Dellal FD, Berberoglu Z, Akdeniz D, Uysal S, Karakurt F. Plasma nesfatin-1 levels are increased in patients with polycystic ovary syndrome. *J Endocrinol Invest.* 2014; 37: 715-9
- Aguayo-Mazzucato C, Sanchez-Soto C, Godinez-Puig V, Gutierrez-Ospina G, Hiriant M. Restructuring of pancreatic islets and insulin secretion in a postnatal critical window. *PloS One* 2006; 1: e35
- Air EL, Benoit S, Clegg DJ, Seeley RJ, Woods SC. Insulin and leptin combine additively to reduce food intake and body weight in rats. *Endocrinology.* 2002; 143: 2449-52
- Al Massadi O, Pardo M, Roca-Rivada A, Castelao C, Casanueva FF, Seoane LM. Macronutrients act directly on the stomach to regulate gastric ghrelin release. *J Endocrinol Invest.* 2010; 33: 599-602
- Al-Massadi O, Crujeiras AB, González RC, Pardo M, Diéguez C, Casanueva FF, Seoane LM. Age, sex, and lactating status regulate ghrelin secretion and GOAT mRNA levels from isolated rat stomach. *American Journal of Physiology - Endocrinology and Metabolism.* 2010; 299: E341-E50
- An W, Li Y, Xu G, Zhao J, Xiang X, Ding L, Li J, Guan Y, Wang X, Tang C, Li X, Mulholland M, Zhang W. Modulation of ghrelin o-acyltransferase expression in pancreatic islets. *Cell Physiol Biochem.* 2010; 26: 707–716
- Angelone T, Filice E, Pasqua T, Amodio N, Galluccio M, Montesanti G, Quintieri AM, Cerra MC. Nesfatin-1 as a novel cardiac peptide: identification, functional characterization, and protection against ischemia/reperfusion injury. *Cell Mol Life Sci.* 2012; 70(3): 495-509
- Aradhyam GK, Balivada LM, Kanuru M, Vadivel P, Vidhya BS. Calnuc: Emerging roles in calcium signaling and human diseases. *IUBMB Life.* 2010; 62: 436–46
- Ariyasu H, Takaya K, Tagami T, Ogawa Y, Hosoda K, Akamizu T, Suda M, Koh T, Natsui K, Toyooka S, Shirakami G, Usui T, Shimatsu A, Doi K, Hosoda H, Kojima M, Kangawa K, and Nakao K. Stomach is a major source of circulating ghrelin, and feeding state determines plasma ghrelin-like immunoreactivity levels in humans. *J Clin Endocrinol Metab.* 2001; 86: 4753–4758
- Arnold AP, Chen X, Itoh Y. What a difference an X or Y makes: sex chromosomes, gene dose, and epigenetics in sexual differentiation. *Handb Exp Pharmacol.* 2012; 214: 67-88
- Arvat E, Di Vito L, Broglio F, Papotti M, Muccioli G, Dieguez C, Casanueva FF, Deghenghi R, Camanni F, and Ghigo E. Preliminary evidence that Ghrelin, the natural GH secretagogue

(GHS)-receptor ligand, strongly stimulates GH secretion in humans. *J Endocrinol Invest.* 2000; 23: 493–495

Arvat E, Maccario M, Di Vito L, Broglio F, Benso A, Gottero C, Papotti M, Muccioli G, Dieguez C, Casanueva FF, Deghenghi R, Camanni F, and Ghigo E. Endocrine activities of ghrelin, a natural growth hormone secretagogue (GHS), in humans: comparison and interactions with hexarelin, a nonnatural peptidyl GHS, and GH-releasing hormone. *J Clin Endocrinol Metab.* 2001; 86: 1169–1174

Asakawa A, Inui A, Kaga T, Yuzuriha H, Nagata T, Ueno N, Makino S, Fujimiya M, Nijima A, Fujino MA, and Kasuga M. Ghrelin is an appetite-stimulatory signal from stomach with structural resemblance to motilin. *Gastroenterology.* 2001; 120: 337–345

Asplund K. Dynamics of insulin release from the foetal and neonatal rat pancreas. *Eur J Clin Invest.* 1973; 3: 338-44

Atsuchi K, Asakawa A, Ushikai M, Ataka K, Tsai M, Koyama K, Sato Y, Kato I, Fujimiya M, Inui A. Centrally administered nesfatin-1 inhibits feeding behaviour and gastroduodenal motility in mice. *Neuroreport* 2010; 21: 1008–11

Baldanzi G, Filigheddu N, Cutrupi S, Catapano F, Bonisconi S, Fubini A, Malan D, Baj G, Granata R, Broglio F, Papotti M, Surico N, Bussolino F, Isgaard J, Deghenghi R, Sinigaglia F, Prat M, Muccioli G, Ghigo E, and Graziani A. Ghrelin and des-acyl ghrelin inhibit cell death in cardiomyocytes and endothelial cells through ERK1/2 and PI 3-kinase/AKT. *J Cell Biol.* 2002; 159: 1029–1037.

Balthasar N, Dalgaard LT, Lee CE, Yu J, Funahashi H, Williams T, Ferreira M, Tang V, McGovern RA, Kenny CD, Christiansen LM, Edelstein E, Choi B, Boss O, Aschkenasi C, Zhang CY, Mountjoy K, Kishi T, Elmquist JK, Lowell BB. Divergence of melanocortin pathways in the control of food intake and energy expenditure. *Cell.* 2005; 123: 493-505

Bando M, Iwakura H, Ariyasu H, Hosoda H, Yamada G, Hosoda K, Adachi S, Nakao K, Kangawa K, Akamizu T. Transgenic overexpression of intraislet ghrelin does not affect insulin secretion or glucose metabolism in vivo. *Am J Physiol Endocrinol Metab.* 2012; 302: E403-8

Barnett BP, Hwang Y, Taylor MS, Kirchner H, Pfluger PT, Bernard V, Lin YY, Bowers EM, Mukherjee C, Song WJ, Longo PA, Leahy DJ, Hussain MA, Tschöp MH, Boeke JD, Cole PA. Glucose and weight control in mice with a designed ghrelin O-acyltransferase inhibitor. *Science* 2010; 330: 1689–1692

Barnikol-Watanabe S, Gross NA, Gotz H, Henkel T, Karabinos S, Kratzin H, Barnikol HU, Hilschmann N. Human protein NEFA, a novel DNA-binding/EF-hand/leucine zipper protein. Molecular cloning and sequence analysis of the cDNA, isolation and characterization of the protein. *Biol Chem Hoppe Seyler.* 1994; 375: 497–512

Barreiro ML, Gaytan F, Caminos JE, Pinilla L, Casanueva FF, Aguilar E, Dieguez C, and Tena-Sempere M. Cellular location and hormonal regulation of ghrelin expression in rat testis. *Biol Reprod.* 2002; 67: 1768–1776

Beaumont NJ, Skinner VO, Tan TM, Ramesh BS, Byrne DJ, MacColl GS, Keen JN, Bouloux PM, Mikhailidis DP, Bruckdorfer KR, Vanderpump MP, and Srai KS. Ghrelin can bind to a species of high density lipoprotein associated with paraoxonase. *J Biol Chem.* 2003; 278: 8877–8880

Bielsky IF, Hu SB, Ren X, Terwilliger EF, Young LJ. The V1a vasopressin receptor is necessary and sufficient for normal social recognition: a gene replacement study. *Neuron.* 2005. 18; 47(4): 503-13

Boguszewski CL, Van der Lely AJ. The role of the gastrointestinal tract in the control of energy balance. *Translational Gastrointestinal Cancer.* 2015; 4(1): 3-13

Bonnet MS, Ouelaa W, Tillement V, Trouslard J, Jean A, Gonzalez BJ, Gourcerol G, Dallaporta M, Troadec JD, Mounien L. Gastric distension activates NUCB2/nesfatin-1-expressing neurons in the nucleus of the solitary tract. *Regul Pept.* 2013; 187:17-23

Bowers CY, Reynolds GA, Momany FA. New advances on the regulation of growth hormone (GH) secretion. *Int J Neurol.* 1984; 18: 188-205

Boyanton Jr BL, Blick KE. Stability Studies of Twenty-Four Analytes in Human Plasma and Serum. *Clinical Chemistry.* 2002; 48:2242–7

Brailoiu GC, Dun SL, Brailoiu E, Inan S, Yang J, Chang JK, Dun NJ. Nesfatin-1: distribution and interaction with a G protein-coupled receptor in the rat brain. *Endocrinology.* 2007; 148: 5088-94

Brailoiu GC, Deliu E, Tica AA, Rabinowitz JE, Tilley DG, Benamar K, Koch WJ, Brailoiu E. Nesfatin-1 activates cardiac vagal neurons of nucleus ambiguus and elicits bradycardia in conscious rats. *J Neurochem.* 2013; 126(6): 739-48

Briscoe CP, Tadayyon M, Andrews JL, Benson WG, Chambers JK, Eilert MM, Ellis C, Elshourbagy NA, Goetz AS, Minnick DT, Murdock PR, Sauls HR Jr, Shabon U, Spinage LD, Strum JC, Szekeres PG, Tan KB, Way JM, Ignar DM, Wilson S, Muir AI. The orphan G protein-coupled receptor GPR40 is activated by medium and long chain fatty acids. *J Biol Chem.* 2003; 278: 11303-11311

Broglia F, Arvat E, Benso A, Gottero C, Muccioli G, Papotti M, van der Lely AJ, Deghenghi R, and Ghigo E. Ghrelin, a natural GH secretagogue produced by the stomach, induces hyperglycemia and reduces insulin secretion in humans. *J Clin Endocrinol Metab.* 2001; 86: 5083–5086

Broglia F, Gottero C, Prodam F, Destefanis S, Gauna C, Me E, Riganti F, Vivenza D, Rapa A, Martina V, Arvat E, Bona G, van der Lely AJ, Ghigo E. Ghrelin secretion is inhibited by glucose

load and insulin-induced hypoglycemia but unaffected by glucagon and arginine in humans. *Clin Endocrinol (Oxf)*. 2004; 61: 503-9

Brown RE, Imran SA, Ur E, Wilkinson M. KiSS-1 mRNA in adipose tissue is regulated by sex hormones and food intake. *Mol Cell Endocrinol*. 2008; 281(1–2): 64–72

Caldwell LK, Pierce AL, Riley LG, Duncan CA, Nagler JJ. Plasma nesfatin-1 is not affected by long-term food restriction and does not predict rematuration among iteroparous female rainbow trout (*Oncorhynchus mykiss*). *PLoS One*. 2014; 9(1): e85700

Cao X, Liu XM, Zhou LH. Recent progress in research on the distribution and function of NUCB2/nesfatin-1 in peripheral tissues. *Endocr J*. 2013; 60(9): 1021-7

Çatli G, Abaci A, Anik A, Böber E Low serum nesfatin-1 levels may be a contributing factor for monogenic obesity due to prohormone convertase 1 deficiency. *Med Hypotheses*. 2013; 81(2): 172-4

Celio MR, Heizmann CW. Calcium-binding protein parvalbumin as a neuronal marker. *Nature*. 1981; 293: 300-2

Cerdá-Reverter JM, Ling MK, Schiöth HB, Peter RE. Molecular cloning, characterization and brain mapping of the melanocortin 5 receptor in the goldfish. *J Neurochem*. 2003; 87(6): 1354-67

Cerdá-Reverter JM, Peter RE. Endogenous melanocortin antagonist in fish: structure, brain mapping, and regulation by fasting of the goldfish agouti-related protein gene. *Endocrinology*. 2003; 144: 4552-61

Cerda-Reverter JM, Schioth HB, Peter RE. The central melanocortin system regulates food intake in goldfish. *Regul Pept*. 2003; 115: 101–13

Chanoine JP, Wong ACK. Ghrelin Gene Expression Is Markedly Higher in Fetal Pancreas Compared with Fetal Stomach: Effect of Maternal Fasting. *Endocrinology*. 2004; 145: 3813–20

Chen X, Dong J, Jiang ZY. Nesfatin-1 influences the excitability of glucosensing neurons in the hypothalamic nuclei and inhibits the food intake. *Regul Pept*. 2012; 177(1-3): 21-6

Christoffels A, Koh EG, Chia JM, Brenner S, Aparicio S, Venkatesh B. Fugu genome analysis provides evidence for a whole-genome duplication early during the evolution of ray-finned fishes. *Mol Biol Evol*. 2004; 21: 1146–51

Chung Y, Kim J, Im E, Kim H, Yang H. Progesterone and 17 β -estradiol regulate expression of nesfatin-1/NUCB2 in mouse pituitary gland. *Peptides*. 2014; 63C: 4-9

Cowley MA, Grove K. To be or NUCB2, is nesfatin the answer? *Cell Metab* 2006; 4: 421-2

- Cunha DA, Amaral MEC, Carvalho CPF, Collares-Buzato CB, Carneiro EM, Boschero AC. Increased expression of SNARE proteins and synaptotagmin IV in islets from pregnant rats and in vitro prolactin-treated neonatal islets. *Biol Res* 2006; 39: 555-6
- Darambazar G, Nakata M, Okada T, Wang L, Li E, Shinozaki A, Motoshima M, Mori M, Yada T. Paraventricular NUCB2/nesfatin-1 is directly targeted by leptin and mediates its anorexigenic effect. *Biochem Biophys Res Commun*. 2015; 456(4): 913-8
- Date Y, Kojima M, Hosoda H, Sawaguchi A, Mondal MS, Suganuma T, Matsukura S, Kangawa K, and Nakazato M. Ghrelin, a novel growth hormone-releasing acylated peptide, is synthesized in a distinct endocrine cell type in the gastrointestinal tracts of rats and humans. *Endocrinology*. 2000; 141: 4255–4261
- Date Y, Murakami N, Kojima M, Kuroiwa T, Matsukura S, Kangawa K, and Nakazato M. Central effects of a novel acylated peptide, ghrelin, on growth hormone release in rats. *Biochem Biophys Res Commun*. 2000; 275: 477–480
- Date Y, Nakazato M, Hashiguchi S, Dezaki K, Mondal MS, Hosoda H, Kojima M, Kangawa K, Arima T, Matsuo H, Yada T, and Matsukura S. Ghrelin is present in pancreatic alpha-cells of humans and rats and stimulates insulin secretion. *Diabetes*. 2002; 51: 124–129
- Dauncey MJ WP, Burton KA, Katsumata M. Nutrition-hormone receptor-gene interactions: implications for development and disease. *Proc Nutr Soc*. 2001; 60: 63-72
- Dezaki K, Damdindorj B, Sone H, Dyachok O, Tengholm A, Gylfe E, Kurashina T, Yoshida M, Kakei M, Yada T. Ghrelin attenuates cAMP-PKA signaling to evoke insulinostatic cascade in islet β -cells. *Diabetes*. 2011; 60: 2315-24
- Dong J, Guan HZ, Jiang ZY, Chen X. Nesfatin-1 influences the excitability of glucosensing neurons in the dorsal vagal complex and inhibits food intake. *PLoS One*. 2014; 9(6): e98967
- Drucker DJ. The role of gut hormones in glucose homeostasis. *J Clin Invest*. 2007; 117: 24-32
- Edfalk S, Steneberg P, Edlund H. Gpr40 is expressed in enteroendocrine cells and mediates free fatty acid stimulation of incretin secretion. *Diabetes*. 2008; 57: 2280-2287
- Fan W, Voss-Andreae A, Cao WH, Morrison SF. Regulation of thermogenesis by the central melanocortin system. *Peptides*. 2005; 26: 1800-13
- Ferré P, Decaux JF, Issad T, Girard J. Changes in energy metabolism during the suckling and weaning period in the newborn. *Reproduction Nutrition D'éveloppement*. 1986; 26 (2B): 619-631
- Ferré P, Pegorier JP, Girard J. The effects of inhibition of gluconeogenesis in suckling newborn rats. *Biochemical Journal*. 1977; 162(1): 209-212
- Foo K, Brimar H, Broberger C. Distribution and neuropeptide coexistence of nucleobindin-2 mRNA/nesfatin-like immunoreactivity in the rat CNS. *Neuroscience*. 2008; 156: 563-79

- Foo KS, Brauner H, Ostenson CG, Broberger C. Nucleobindin-2/nesfatin in the endocrine pancreas: distribution and relationship to glycaemic state. *J Endocrinol.* 2010; 204: 255-63
- Fort P, Salvert D, Hanriot L, Jegu S, Shimizu H, Hashimoto K, Mori M, Luppi PH. The satiety molecule nesfatin-1 is co-expressed with melanin concentrating hormone in tuberal hypothalamic neurons of the rat. *Neuroscience.* 2008; 155(1): 174-81
- Fowden AL, Forhead AJ. Hormones as epigenetic signals in developmental programming. *Exp Physiol.* 2009; 94: 607-25
- Frederich RC, Hamann A, Anderson S, Löllmann B, Lowell BB, Flier JS. Leptin levels reflect body lipid content in mice: evidence for diet-induced resistance to leptin action. *Nat Med.* 1995; 1(12): 1311-4
- Gahete MD, Córdoba-Chacón J, Salvatori R, Castaño JP, Kineman RD, Luque RM: Metabolic regulation of ghrelin O-acyl transferase (GOAT) expression in the mouse hypothalamus, pituitary, and stomach. *Mol Cell Endocrinol.* 2010; 317: 154–160
- Gaigé S, Bonnet MS, Tardivel C, Pinton P, Trouslard J, Jean A, Guzylack L, Troadec JD, Dallaporta M. c-Fos immunoreactivity in the pig brain following deoxynivalenol intoxication: focus on NUCB2/nesfatin-1 expressing neurons. *Neurotoxicology.* 2013; 34: 135-49
- Gantulga D, Maejima Y, Nakata M, Yada T. Glucose and insulin induce Ca²⁺ signaling in nesfatin-1 neurons in the hypothalamic paraventricular nucleus. *Biochem Biophys Res Commun.* 2012; 420(4): 811-5
- Garcés MF, Poveda NE, Sanchez E, Sánchez ÁY, Bravo SB, Vázquez MJ, Diéguez C, Nogueiras R, Caminos JE. Regulation of NucB2/Nesfatin-1 throughout rat pregnancy. *Physiol Behav.* 2014; 133: 216-22
- García-Galiano D, Navarro VM, Roa J, Ruiz-Pino F, Sánchez-Garrido MA, Pineda R, Castellano JM, Romero M, Aguilar E, Gaytán F, Diéguez C, Pinilla L, Tena-Sempere M. The anorexigenic neuropeptide, nesfatin-1, is indispensable for normal puberty onset in the female rat. *J Neurosci* 2010; 30: 7783-92
- García-Galiano D, Pineda R, Ilhan T, Castellano JM, Ruiz-Pino F, Sánchez-Garrido MA, Vazquez MJ, Sangiao-Alvarellos S, Romero-Ruiz A, Pinilla L, Diéguez C, Gaytán F, Tena-Sempere M. Cellular distribution, regulated expression, and functional role of the anorexigenic peptide, NUCB2/nesfatin-1, in the testis. *Endocrinology.* 2012; 153(4): 1959-71
- García-Galiano D, Tena-Sempere M. Emerging roles of NUCB2/nesfatin-1 in the metabolic control of reproduction. *Curr Pharm Des.* 2013; 19(39): 6966-72
- Gnanapavan S, Kola B, Bustin SA, Morris DG, McGee P, Fairclough P, Bhattacharya S, Carpenter R, Grossman AB, and Korbonits M. The tissue distribution of the mRNA of ghrelin and subtypes of its receptor, GHS-R, in humans. *J Clin Endocrinol Metab.* 2002; 87: 2988

- Goebel M, Stengel A, Wang L, Lambrecht NW, Taché Y. Nesfatin-1 immunoreactivity in rat brain and spinal cord autonomic nuclei. *Neurosci Lett*. 2009; 452: 241-6
- Goebel M, Stengel A, Wang L, Tache Y. Central nesfatin-1 reduces the nocturnal food intake in mice by reducing meal size and increasing inter-meal intervals. *Peptides*. 2010; 32: 36–43
- Goebel M, Stengel A, Wang L, Taché Y. Restraint stress activates nesfatin-1-immunoreactive brain nuclei in rats. *Brain Res*. 2009; 1300: 114-24
- Goebel-Stengel M, Wang L, Stengel A, Taché Y. Localization of nesfatin-1 neurons in the mouse brain and functional implication. *Brain Res*. 2011; 1396: 20-34
- González CR, Vázquez MJ, López M, Diéguez C. Influence of chronic undernutrition and leptin on GOAT mRNA levels in rat stomach mucosa. *J Mol Endocrinol*. 2008; 41: 415–421
- Gonzalez R, Kerbel B, Chun A, Unniappan S. Molecular, Cellular and Physiological Evidences for the Anorexigenic Actions of Nesfatin-1 in Goldfish. *PLoS One*. 2010; 5: e15201
- Gonzalez R, Perry RL, Gao X, Gaidhu MP, Tsushima RG, Ceddia RB, Unniappan S. Nutrient responsive nesfatin-1 regulates energy balance and induces glucose-stimulated insulin secretion in rats. *Endocrinology*. 2012a; 152: 3628-37
- Gonzalez R, Reingold B, Gao X, Gaidhu MP, Tsushima RG, Unniappan S. Nesfatin-1 exerts a direct, glucose-dependent insulintropic action on mouse islet beta- and MIN6 cells. *J Endocrinol*. 2011; 208: R9-R16
- Gonzalez R, Shepperd E, Thiruppugazh V, Lohan S, Grey CL, Chang JP, Unniappan S. Nesfatin-1 regulates the hypothalamo-pituitary-ovarian axis of fish. *Biol Reprod*. 2012b; 87: 84
- Gonzalez R, Tiwari A, Unniappan S. Pancreatic beta cells colocalize insulin and pronesfatin immunoreactivity in rodents. *Biochem Biophys Res Commun*. 2009; 381: 643-648
- Gotoh K, Masaki T, Chiba S, Ando H, Shimasaki T, Mitsutomi K, Fujiwara K, Katsuragi I, Kakuma T, Sakata T, Yoshimatsu H. Nesfatin-1, corticotropin-releasing hormone, thyrotropin-releasing hormone, and neuronal histamine interact in the hypothalamus to regulate feeding behavior. *J Neurochem*. 2013; 124(1): 90-9
- Greenman Y, Golani N, Gilad S, Yaron M, Limor R, Stern N. Ghrelin secretion is modulated in a nutrient- and gender-specific manner. *Clin Endocrinol (Oxf)*. 2004; 60: 382-388
- Gualillo O, Caminos J, Blanco M, Garcia-Caballero T, Kojima M, Kangawa K, Dieguez C, and Casanueva F. Ghrelin, a novel placental-derived hormone. *Endocrinology*. 2001; 142: 788–794
- Guo AY, Zhu QH, Chen X, Luo JC. GSDS: a gene structure display server. *Yi Chuan*. 2007; 29: 1023–6

Gutierrez JA, Solenberg PJ, Perkins DR, Willency JA, Knierman MD, Jin Z, Witcher DR, Luo S, Onyia JE, Hale JE. Ghrelin octanoylation mediated by an orphan lipid transferase. *Proc Natl Acad Sci USA*. 2008; 105: 6320–5

Hall KD, Heymsfield SB, Kemnitz JW, Klein S, Schoeller DA, Speakman JR. Energy balance and its components: implications for body weight regulation. *Am J Clin Nutr*. 2012; 95: 989-94

Hanash SM. Biomedical applications of two-dimensional electrophoresis using immobilized pH gradients: current status. *Electrophoresis*. 2000; 21: 1202-120

Hara T, Hirasawa A, Sun Q, Sadakane K, Itsubo C, Iga T, Adachi T, Koshimizu TA, Hashimoto T, Asakawa Y, Tsujimoto G. Novel selective ligands for free fatty acid receptors GPR120 and GPR40. *Naunyn Schmiedebergs Arch Pharmacol*. 2009; 380: 247-255

Hatef A, Shajan S, Unniappan S. Nutrient status modulates the expression of nesfatin-1 encoding nucleobindin 2A and 2B mRNAs in zebrafish gut, liver and brain. *Gen Comp Endocrinol*. 2014; S0016-6480(14): 00366-9

Hauge-Evans AC, Richardson CC, Milne HM, Christie MR, Persaud SJ, Jones PM. A role for kisspeptin in islet function. *Diabetologia*. 2006; 49(9): 2131–2135

Hayashida T, Nakahara K, Mondal MS, Date Y, Nakazato M, Kojima M, Kangawa K, and Murakami N. Ghrelin in neonatal rats: distribution in stomach and its possible role. *J Endocrinol*. 2002; 173: 239–45

Hendy GN, Bevan S, Mattei MG, Mouland AJ. Chromogranin A. *Clin Invest Med*. 1995; 18: 47-65.

Henrotte JG. A crystalline constituent from myogen of carp muscles. *Nature*. 1952; 169: 968-9

Hill JT, Mastracci TL, Vinton C, Doyle ML, Anderson KR, Loomis ZL, Schrunck JM, Minic AD, Prabakar KR, Pugliese A, Sun Y, Smith RG, Sussel L. Ghrelin is dispensable for embryonic pancreatic islet development and differentiation. *Regul Pept*. 2009; 157: 51-6

Hiller-Sturmhöfel S, Bartke A. The Endocrine System. *Alcohol Health and Research World*. 1999, 22: 153-64

Hirasawa A, Tsumaya K, Awaji T, Katsuma S, Adachi T, Yamada M, Sugimoto Y, Miyazaki S, Tsujimoto G. Free fatty acids regulate gut incretin glucagon-like peptide-1 secretion through GPR120. *Nat Med*. 2005; 11: 90-94

Hofmann K. A superfamily of membrane-bound O-acyltransferases with implications for Wnt signaling. *Trends Biochem. Sci*. 2000; 25:111–112

Hole R, Smith MP, Sharp G. Development of the biphasic response to glucose in fetal and neonatal rat pancreas. *American Journal of Physiology*. 1988; 254: E167-E74

Horvath TL, Bruning JC. Developmental programming of the hypothalamus: a matter of fat. *Nat Med*. 2006; 12: 52-3

Hosoda H, Kojima M, Matsuo H, and Kangawa K. Ghrelin and des-acyl ghrelin: two major forms of rat ghrelin peptide in gastrointestinal tissue. *Biochem Biophys Res Commun*. 2000; 279: 909–913

Howard AD, Feighner SD, Cully DF, Arena JP, Liberators PA, Rosenblum CI, Hamelin M, Hreniuk DL, Palyha OC, Anderson J, Paress PS, Diaz C, Chou M, Liu KK, McKee KK, Pong SS, Chaung LY, Elbrecht A, Dashkevich M, Heavens R, Rigby M, Sirinathsinghji DJ, Dean DC, Melillo DG, Patchett AA, Nargund R, Griffin PR, DeMartino JA, Gupta SK, Schaeffer JM, Smith RG, Van der Ploeg LH. A receptor in pituitary and hypothalamus that functions in growth hormone release. *Science*. 1996; 273: 974-7

Iglesias MJ, Pineiro R, Blanco M, Gallego R, Dieguez C, Gualillo O, Gonzalez-Juanatey JR, and Lago F. Growth hormone releasing peptide (ghrelin) is synthesized and secreted by cardiomyocytes. *Cardiovasc Res*. 2004; 62: 481–488

Iwakura H, Li Y, Ariyasu H, Hosoda H, Kanamoto N, Bando M, Yamada G, Hosoda K, Nakao K, Kangawa K, Akamizu T. Establishment of a novel ghrelin-producing cell line. *Endocrinology*. 2010; 151: 2940-2945

Iwasaki Y, Nakabayashi H, Kakei M, Shimizu H, Mori M, Yada T. Nesfatin-1 evokes Ca²⁺ signaling in isolated vagal afferent neurons via Ca²⁺ influx through N-type channels. *Biochemical and Biophysical Research Communications*. 2009; 390: 958–62

Iwasaki Y, Nakabayashi H, Kakei M, Shimizu H, Mori M, Yada T. Nesfatin-1 evokes Ca²⁺ signaling in isolated vagal afferent neurons via Ca²⁺ influx through N-type channels. *Biochem Biophys Res Commun*. 2009; 390(3): 958-62

Jaillon O, Aury JM, Brunet F, Petit JL, Stange-Thomann N, Mauceli E, Bouneau L, Fischer C, Ozouf-Costaz C, Bernot A, Nicaud S, Jaffe D, Fisher S, Lutfalla G, Dossat C, Segurens B, Dasilva C, Salanoubat M, Levy M, Boudet N, Castellano S, Anthouard V, Jubin C, Castelli V, Katinka M, Vacherie B, Biémont C, Skalli Z, Cattolico L, Poulain J, De Berardinis V, Cruaud C, Duprat S, Brottier P, Coutanceau JP, Gouzy J, Parra G, Lardier G, Chapple C, McKernan KJ, McEwan P, Bosak S, Kellis M, Volff JN, Guigó R, Zody MC, Mesirov J, Lindblad-Toh K, Birren B, Nusbaum C, Kahn D, Robinson-Rechavi M, Laudet V, Schachter V, Quétier F, Saurin W, Scarpelli C, Wincker P, Lander ES, Weissenbach J, Roest Crollius H. Genome duplication in the teleost fish *Tetraodon nigroviridis* reveals the early vertebrate proto-karyotype. *Nature*. 2004; 431: 946–57

Janssen S, Laermans J, Iwakura H, Tack J, Depoortere I. Sensing of fatty acids for octanoylation of ghrelin involves a gustatory G-protein. *PLoS One*. 2012; 7: e40168

- Jia FY, Li XL, Li TN, Wu J, Xie BY, Lin L. Role of nesfatin-1 in a rat model of visceral hypersensitivity. *World J Gastroenterol*. 2013; 19(22): 3487-93
- Kadowaki T, Wilder E, Klingensmith J, Zachary K, Perrimon N. The segment polarity gene porcupine encodes a putative multitrans-membrane protein involved in Wingless processing. *Genes Dev*. 1996; 10: 3116–3128
- Kamegai J, Tamura H, Shimizu T, Ishii S, Sugihara H, Wakabayashi I. Chronic central infusion of ghrelin increases hypothalamic neuropeptide Y and Agouti-related protein mRNA levels and body weight in rats. *Diabetes*. 2001; 50: 2438–2443
- Kanai Y, Isonishi S, Katagiri T, Koizumi T, Miura K, Kurosawa Y. Early induction of anti-double-stranded DNA antibodies in lupus-prone MRL mice inoculated with Ly-24+ cells cloned from lymph node cells of an MRL/Mp-lpr/lpr mouse: possible effect of putative cytokines produced by cloned Ly-24+ cells. *Immunol Lett*. 1990; 24: 49-55
- Kanai Y, Katagiri T, Mori S, Kubota T. An established MRL/Mp-lpr/lpr cell line with null cell properties produces a B cell differentiation factor(s) that promotes anti-single-stranded DNA antibody production in MRL spleen cell culture. *Int Arch Allergy Appl Immunol*. 1986; 81(1): 92-4
- Kanai Y, Miura K, Uehara T, Amagai M, Takeda O, Tanuma S, Kurosawa Y. Natural occurrence of Nuc in the sera of autoimmune-prone MRL/lpr mice. *Biochem Biophys Res Commun*. 1993; 196: 729-36
- Kanai Y, Tanuma S. Purification of a novel B cell growth and differentiation factor associated with lupus syndrome. *Immunol Lett*. 1992; 32: 43-8
- Kanamoto N, Akamizu T, Hosoda H, Hataya Y, Ariyasu H, Takaya K, Hosoda K, Saijo M, Moriyama K, Shimatsu A, Kojima M, Kangawa K, and Nakao K. Substantial production of ghrelin by a human medullary thyroid carcinoma cell line. *J Clin Endocrinol Metab*. 2001; 86: 4984–4990
- Kang K, Schmahl J, Lee JM, Garcia K, Patil K, Chen A, Keene M, Murphy A, Sleeman MW. Mouse ghrelin-O-acyltransferase (GOAT) plays a critical role in bile acid reabsorption. *FASEB J*. 2012; 26: 259-71
- Kanuru M, Samuel JJ, Balivada LM, Aradhyam GK. Ion-binding properties of Calnuc, Ca21 versus Mg21-Calnuc adopts additional and unusual Ca21-binding sites upon interaction with G-protein. *FEBS J*. 2009; 276: 2529–46
- Karabinos A, Bhattacharya D, Morys-Wortmann C, Kroll K, Hirschfeld G, Kratzin HD, Barnikol-Watanabe S, Hilschmann N. The divergent domains of the NEFA and nucleobindin proteins are derived from an EF-hand ancestor. *Mol Biol Evol*. 1996; 13: 990–8

Kerbel B, Unniappan S. Nesfatin-1 Suppresses Energy Intake, Co-localises Ghrelin in the Brain and Gut, and Alters Ghrelin, Cholecystokinin and Orexin mRNA Expression in Goldfish. *J Neuroendocrinol.* 2011; 24: 366-77

Kim MS, Yoon CY, Park KH, Shin CS, Park KS, Kim SY, Cho BY, and Lee HK. Changes in ghrelin and ghrelin receptor expression according to feeding status. *Neuroreport.* 2003; 14: 1317–1320

King JC. Maternal obesity, metabolism and pregnancy outcomes. *Annu Rev Nutr.* 2006; 26: 271-91

Kirchner H, Gutierrez JA, Solenberg PJ, Pfluger PT, Czyzyk TA, Willency JA, Schürmann A, Joost HG, Jandacek RJ, Hale JE, Heiman ML, Tschöp MH. GOAT links dietary lipids with the endocrine control of energy balance. *Nat Med.* 2009; 15: 741–745

Kishimoto M, Okimura Y, Nakata H, Kudo T, Iguchi G, Takahashi Y, Kaji H, and Chihara K. Cloning and characterization of the 5'(-)-flanking region of the human ghrelin gene. *Biochem Biophys Res Commun.* 2003; 305: 186–192

Kitamura K, Kato J, Kawamoto M, Tanaka M, Chino N, Kangawa K, and Eto T. The intermediate form of glycine-extended adrenomedullin is the major circulating molecular form in human plasma. *Biochem Biophys Res Commun.* 1998; 244: 551–555

Kohno D, Nakata M, Maejima Y, Shimizu H, Sedbazar U, Yoshida N, Dezaki K, Onaka T, Mori M, Yada T. Nesfatin-1 neurons in paraventricular and supraoptic nuclei of the rat hypothalamus coexpress oxytocin and vasopressin and are activated by refeeding. *Endocrinology.* 2008; 149(3): 1295-301

Kojima M, Hosoda H, Date Y, Nakazato M, Matsuo H, Kangawa K. Ghrelin is a growth-hormone-releasing acylated peptide from stomach. *Nature.* 1999; 402: 656–60

Kojima M, Kangawa K. Ghrelin: structure and function. *Physiol Rev.* 2005; 85: 495–522

Koliaki C, Kokkinos A, Tentolouris N, Katsilambros N. The effect of ingested macronutrients on postprandial ghrelin response: a critical review of existing literature data. *Int J Pept.* 2010; doi: 10.1155/2010/710852.

Könczöl K, Pintér O, Ferenczi S, Varga J, Kovács K, Palkovits M, Zelena D, Tóth ZE. Nesfatin-1 exerts long-term effect on food intake and body temperature. *Int J Obes (Lond).* 2012; 36(12): 1514-21

Korbonits M, Bustin SA, Kojima M, Jordan S, Adams EF, Lowe DG, Kangawa K, Grossman AB. The expression of the growth hormone secretagogue receptor ligand ghrelin in normal and abnormal human pituitary and other neuroendocrine tumors. *J Clin Endocrinol Metab.* 2001a; 86: 881–887

- Korbonits M, Kojima M, Kangawa K, and Grossman AB. Presence of ghrelin in normal and adenomatous human pituitary. *Endocrine*. 2001b; 14: 101–104
- Krause WJ. Brunner's glands: a structural, histochemical and pathological profile. *Progress in histochemistry and cytochemistry*. 2000; 35: 259-367
- Kretsinger RH, Nockolds CE. Carp muscle calcium-binding protein. II. Structure determination and general description. *J Biol Chem*. 1973; 248: 3313-26
- Larsson LI. On the development of the islets of Langerhans. *Microsc Res Tech*. 1998; 43: 284-91
- Lee HM, Wang G, Englander EW, Kojima M, and Greeley GH Jr. Ghrelin, a new gastrointestinal endocrine peptide that stimulates insulin secretion. enteric distribution, ontogeny, influence of endocrine, and dietary manipulations. *Endocrinology*. 2002; 143: 185–190
- Lee VD, Stapleton M, Huang B. Genomic structure of *Chlamydomonas caltractin*. Evidence for intron insertion suggests a probable genealogy for the EF-hand superfamily of proteins. *J Mol Biol*. 1991; 221: 175-91
- Lee YC, Damholt AB, Billestrup N, Kisbye T, Galante P, Michelsen B, Kofod H, Nielsen JH. Developmental expression of proprotein convertase 1/3 in the rat. *Mol Cell Endocrinol*. 1999; 155: 27-35
- Lehman MN, Hileman SM, Goodman RL. Neuroanatomy of the kisspeptin signaling system in mammals: comparative and developmental aspects. *Adv Exp Med Biol*. 2013; 784: 27–62
- Lents CA, Barb CR, Hausman GJ, Nonneman D, Heidorn NL, Cisse RS, Azain MJ. Effects of nesfatin-1 on food intake and LH secretion in prepubertal gilts and genomic association of the porcine NUCB2 gene with growth traits. *Domest Anim Endocrinol*. 2013; 45(2): 89-97
- Li QC, Wang HY, Chen X, Guan HZ, Jiang ZY. Fasting plasma levels of nesfatin-1 in patients with type 1 and type 2 diabetes mellitus and the nutrient-related fluctuation of nesfatin-1 level in normal humans. *Regul Pept*. 2010;159: 72-7
- Li R, Wu Q, Zhao Y, Jin W, Yuan X, Wu X, Tang Y, Zhang J, Tan X, Bi F, Liu JN. The novel pro-osteogenic activity of NUCB2(1-83.). *PLoS One*. 2013; 8(4): e61619
- Li Z, Gao L, Tang H, Yin Y, Xiang X, Li Y, Zhao J, Mulholland M, Zhang W. Peripheral effects of nesfatin-1 on glucose homeostasis. *PLoS One*. 2013; 8: e71513
- Li Z, Xu G, Li Y, Zhao J, Mulholland MW, Zhang W. mTOR-dependent modulation of gastric nesfatin-1/NUCB2. *Cell Physiol Biochem*. 2012; 29(3-4): 493-500
- Lin F, Zhou C, Chen H, Wu H, Xin Z, Liu J, Gao Y, Yuan D, Wang T, Wei R, Chen D, Yang S, Wang Y, Pu Y, Li Z. Molecular characterization, tissue distribution and feeding related changes of NUCB2A/nesfatin-1 in Ya-fish. *Gene*. 2015; 536(2): 238-46

- Liou AP, Lu X, Sei Y, Zhao X, Pechhold S, Carrero RJ, Raybould HE, Wank S. The G-protein-coupled receptor GPR40 directly mediates long-chain fatty acid-induced secretion of cholecystokinin. *Gastroenterology*. 2011; 140: 903-912
- Lorenz, D. N., Ellis, S. B. and Epstein, A. N. Differential effects of upper gastrointestinal fill on milk ingestion and nipple attachment in the suckling rat. *Dev. Psychobiol*. 1982; 15: 309–330
- Lu S, Guan JL, Wang QP, Uehara K, Yamada S, Goto N, Date Y, Nakazato M, Kojima M, Kangawa K, and Shioda S. Immunocytochemical observation of ghrelin-containing neurons in the rat arcuate nucleus. *Neurosci Lett*. 2002; 321: 157–160
- Maejima Y, Sedbazar U, Suyama S, Kohno D, Onaka T, Takano E, Yoshida N, Koike M, Uchiyama Y, Fujiwara K, Yashiro T, Horvath TL, Dietrich MO, Tanaka S, Dezaki K, Oh-I S, Hashimoto K, Shimizu H, Nakata M, Mori M, Yada T. Nesfatin-1-regulated oxytocinergic signaling in the paraventricular nucleus causes anorexia through a leptin-independent melanocortin pathway. *Cell Metab*. 2009; 10: 355-65
- Maejima Y, Shimomura K, Sakuma K, Yang Y, Arai T, Mori M, Yada T. Paraventricular nucleus nesfatin-1 neurons are regulated by pituitary adenylate cyclase-activating polypeptide (PACAP). *Neurosci Lett*. 2013; 551: 39-42
- Miura K, Kurosawa Y, Kanai Y. Calcium-binding activity of nucleobindin mediated by an EF-hand moiety. *Biochem Biophys Res Commun*. 1994; 199: 1388–93
- Miura K, Titani K, Kurosawa Y, and Kanai Y. Molecular cloning of nucleobindin, a novel DNA-binding protein that contains both a signal peptide and a leucine zipper structure. *Biochem Biophys Res Commun*. 1992; 187: 375–80
- Miyata S, Yamada N, Kawada T. Possible involvement of hypothalamic nucleobindin-2 in hyperphagic feeding in Tsumura Suzuki obese diabetes mice. *Biol Pharm Bull*. 2012; 35(10): 1784-93
- Mohan H, Ramesh N, Mortazavi S, Le A, Iwakura H, Unniappan S. Nutrients Differentially Regulate Nucleobindin-2/Nesfatin-1 In Vitro in Cultured Stomach Ghrelinoma (MGN3-1) Cells and In Vivo in Male Mice. *PLoS One*. 2014; 9: e115102
- Mohan H, Unniappan S. Phylogenetic aspects of nucleobindin-2/nesfatin-1. *Curr Pharm Des*. 2013; 19: 6929-34
- Mohan H, Unniappan S. Ontogenic pattern of nucleobindin-2/nesfatin-1 expression in the gastroenteropancreatic tissues and serum of Sprague Dawley rats. *Regul Pept*. 2012; 175(1-3): 61-9
- Mohan H, Unniappan S. Discovery of ghrelin o-acyltransferase. *Endocr Dev*. 2013; 25: 16-24

- Moncrief ND, Kretsinger RH, Goodman M. Evolution of EF-hand calciummodulated proteins. I. Relationships based on amino acid sequences. *J Mol Evol.* 1990; 30: 522-62
- Mori K, Yoshimoto A, Takaya K, Hosoda K, Ariyasu H, Yahata K, Mukoyama M, Sugawara A, Hosoda H, Kojima M, Kangawa K, and Nakao K. Kidney produces a novel acylated peptide, ghrelin. *FEBS Lett.* 2000; 486: 213–216
- Mori M, Eguchi H. US Patent # US 2009/0155833 A1. 2008. Screening method for nesfatin-1 action regulating substance or nesfatin-1 like action substance with the use of receptor protein selected from the group consisting of GPR3, GPR6 and GPR9
- Morton GJ, Cummings DE, Baskin DG, Barsh GS, Schwartz MW. Central nervous system control of food intake and body weight. *Nature.* 2006; 443: 289-95
- Murphy KG, Bloom SR. Gut Hormones and the Regulation of Energy Homeostasis. *Nature.* 2006; 444 (7121): 854-59
- Muzumdar R, Ma X, Yang X, Atzmon G, Bernstein J, Karkanias G, Barzilai N. Physiologic effect of leptin on insulin secretion is mediated mainly through central mechanisms. *FASEB J.* 2003; 17(9): 1130-2
- Myers Jr MG. Keeping the fat off with nesfatin. *Nature medicine.* 2006; 12: 1248-9
- Nakata M, Manaka K, Yamamoto S, Mori M, Yada T. Nesfatin-1 enhances glucose-induced insulin secretion by promoting Ca(2+) influx through L-type channels in mouse islet beta-cells. *Endocr J.* 2011; 58: 305-13
- Nakata M, Yada T. Role of NUCB2/nesfatin-1 in glucose control: diverse functions in islets, adipocytes and brain. *Curr Pharm Des.* 2013; 19(39): 6960-5
- Nakayama S, Moncrief ND, Kretsinger RH. Evolution of EF-hand calciummodulated proteins. II. Domains of several subfamilies have diverse evolutionary histories. *J Mol Evol.* 1992; 34: 416-48
- Nakazato M, Murakami N, Date Y, Kojima M, Matsuo H, Kangawa K, Matsukura S. A role for ghrelin in the central regulation of feeding. *Nature.* 2001; 409: 194–198
- Navarro-Tableros V, Fiordelisio T, Hernandez-Cruz A, Hiriart M. Physiological development of insulin secretion, calcium channels, and GLUT2 expression of pancreatic rat beta-cells. *Am J Physiol Endocrinol Metab.* 2007; 292: E1018-E29
- Niskanen LK, Haffner S, Karhunen LJ, Turpeinen AK, Miettinen H, Uusitupa MI. Serum leptin in obesity is related to gender and body fat topography but does not predict successful weight loss. *Eur J Endocrinol.* 1997; 137(1): 61-7
- Nussey S, Saffron A. Whitehead. *Endocrinology: An Integrated Approach.* Oxford, UK: Bios, 2001. Print.

O'Dowd JF, Stocker CJ. Endocrine pancreatic development: impact of obesity and diet. *Front Physiol.* 2013; 4: 170

Oh I S, Shimizu H, Satoh T, Okada S, Adachi S, Inoue K, Eguchi H, Yamamoto M, Imaki T, Hashimoto K, Tsuchiya T, Monden T, Horiguchi K, Yamada M, Mori M. Identification of nesfatin-1 as a satiety molecule in the hypothalamus. *Nature.* 2006; 443: 709-12

Ohgusu H, Shirouzu K, Nakamura Y, Nakashima Y, Ida T, Sato T, Kojima M. Ghrelin Oacyltransferase (GOAT) has a preference for n-hexanoyl-CoA over n-octanoyl-CoA as an acyl donor. *Biochem Biophys Res Commun.* 2009; 386: 153–158

Oliver P, Pico C, De Matteis R, Cinti S, Palou A. Perinatal expression of leptin in rat stomach. *Developmental dynamics: an official publication of the American Association of Anatomists.* 2002; 223: 148-54

Osaki A, Shimizu H, Ishizuka N, Suzuki Y, Mori M, Inoue S. Enhanced expression of nesfatin/nucleobindin-2 in white adipose tissue of ventromedial hypothalamus-lesioned rats. *Neurosci Lett.* 2012; 521: 46-51

Osei-Hyiaman D, Sophie-Dreher L, Nishimura S, Encinas J. Fasting Co-Suppresses Nesfatin-1 and GPR12 in Mouse Hypothalamic Appetite Center: Implications for Energy Metabolism. *Endocr Rev.* 2011; 32: P2-300

Pan W, Hsueh H, Kastin AJ. Nesfatin-1 crosses the blood-brain barrier without saturation. *Peptides.* 2007; 28: 2223-8

Peino R, Baldelli R, Rodriguez-Garcia J, Rodriguez-Segade S, Kojima M, Kangawa K, Arvat E, Ghigo E, Dieguez C, and Casanueva FF. Ghrelin-induced growth hormone secretion in humans. *Eur J Endocrinol.* 2000; 143: R11–R14

Peng C, Gallin W, Peter RE, Blomqvist AG, Larhammar D. Neuropeptide-Y gene expression in the goldfish brain: distribution and regulation by ovarian steroids. *Endocrinology.* 1994; 134: 1095–103

Pfaffl MW. A new mathematical model for relative quantification in real-time RT-PCR. *Nucleic Acids Res.* 2001; 29: e45

Pickavance LC, Staines WA, Fryer JN. Distributions and colocalization of neuropeptide Y and somatostatin in the goldfish brain. *J Chem Neuroanat.* 1992; 5: 221-33

Prado CL, Pugh-Bernard AE, Elghazi L, Sosa-Pineda B, Sussel L. Ghrelin cells replace insulin-producing beta cells in two mouse models of pancreas development. *Proc Natl Acad Sci USA.* 2004; 101: 2924–9

- Price CJ, Samson WK, Ferguson AV. Nesfatin-1 inhibits NPY neurons in the arcuate nucleus. *Brain Res.* 2008; 1230: 99-106
- Price TO, Samson WK, Niehoff ML, Banks WA. Permeability of the blood-brain barrier to a novel satiety molecule nesfatin-1. *Peptides.* 2007; 28: 2372-81
- Ramanathan L, Siegel JM. Gender differences between hypocretin/orexin knockout and wild type mice: age, body weight, body composition, metabolic markers, leptin and insulin resistance. *J Neurochem.* 2014; 131: 615-24
- Ramanjaneya M, Addison M, Randeve HS. Possible role of NUCB2/nesfatin-1 in adipogenesis. *Curr Pharm Des.* 2013; 19: 6976-80
- Ramanjaneya M, Chen J, Brown JE, Tripathi G, Hallschmid M, Patel S, Kern W, Hillhouse EW, Lehnert H, Tan BK, Randeve HS. Identification of Nesfatin-1 in Human and Murine Adipose Tissue: A Novel Depot-Specific Adipokine with Increased Levels in Obesity. *Endocrinology.* 2010; 151(7): 3169-80
- Ravussin Y, LeDuc CA, Watanabe K, Mueller BR, Skowronski A, Rosenbaum M, Leibel RL. Effects of chronic leptin infusion on subsequent body weight and composition in mice: Can body weight set point be reset? *Mol Metab.* 2014; 3(4): 432-40
- Reddy S, Elliott RB. Ontogenic development of peptide hormones in the mammalian fetal pancreas. *Experientia.* 1988; 44: 1-9
- Reimer MK, Pacini G, and Ahren B. Dose-dependent inhibition by ghrelin of insulin secretion in the mouse. *Endocrinology.* 2003; 144: 916–921
- Reimer RA, Maurer AD, Lau DC, Auer RN: Long-term dietary restriction influences plasma ghrelin and GOAT mRNA level in rats. *Physiol Behav.* 2010; 99: 605–610
- Rindi G, Necchi V, Savio A, Torsello A, Zoli M, Locatelli V, Raimondo F, Cocchi D, and Solcia E. Characterisation of gastric ghrelin cells in man and other mammals: studies in adult and fetal tissues. *Histochem Cell Biol.* 2002; 117: 511–519
- Rosenbaum M1, Nicolson M, Hirsch J, Heymsfield SB, Gallagher D, Chu F, Leibel R. Effects of gender, body composition, and menopause on plasma concentrations of leptin. *J Clin Endocrinol Metab.* 1996; 81(9): 3424-7
- Rouillé Y, Martin S, Steiner DF. Differential processing of proglucagon by the subtilisin-like prohormone convertases PC2 and PC3 to generate either glucagon or glucagon-like peptide. *J Biol Chem.* 1995; 270: 26488-96
- Rouillé Y, Westermark G, Martin SK, Steiner DF. Proglucagon is processed to glucagon by prohormone convertase PC2 in alpha TC1-6 cells. *Proc Natl Acad Sci U S A.* 1994; 91: 3242-6

- Sakata I, Nakamura K, Yamazaki M, Matsubara M, Hayashi Y, Kangawa K, and Sakai T. Ghrelin-producing cells exist as two types of cells, closed- and opened-type cells, in the rat gastrointestinal tract. *Peptides*. 2002; 23: 531–536
- Sakata I, Park WM, Walker AK, Piper PK, Chuang JC, Osborne-Lawrence S, Zigman JM. Glucose-mediated control of ghrelin release from primary cultures of gastric mucosal cells. *Am J Physiol Endocrinol Metab*. 2012; 302: E1300-10
- Schmittgen TD, Livak KJ. Analyzing real-time PCR data by the comparative C(T) method. *Nat Protoc*. 2008; 3(6): 1101-8
- Schwartz GJ. The role of gastrointestinal vagal afferents in the control of food intake: current prospects. *Nutrition*. 2000; 16: 866-73
- Schwartz MW, Woods SC, Porte D Jr, Seeley RJ, Baskin DG. Central nervous system control of food intake *Nature*. 2000; 404(6778): 661-71
- Sedbazar Ul, Ayush EA, Maejima Y, Yada T. Neuropeptide Y and α -melanocyte-stimulating hormone reciprocally regulate nesfatin-1 neurons in the paraventricular nucleus of the hypothalamus. *Neuroreport*. 2014; 25(18): 1453-8
- Seminara SB, Messager S, Chatzidaki EE, Thresher RR, Acierno JS Jr, Shagoury JK, Bo-Abbas Y, Kuohung W, Schwinof KM, Hendrick AG, Zahn D, Dixon J, Kaiser UB, Slaugenhaupt SA, Gusella JF, O'Rahilly S, Carlton MB, Crowley WF Jr, Aparicio SA, Colledge WH. The GPR54 gene as a regulator of puberty. *N Engl J Med*. 2003; 349(17): 1614-27
- Shimizu H O-IS, Okada S, Mori M. Nesfatin-1: an overview and future clinical application. *Endocr J*. 2009; 56: 537-43
- Shimizu H, Oh-I S, Hashimoto K, Nakata M, Yamamoto S, Yoshida N, Eguchi H, Kato I, Inoue K, Satoh T, Okada S, Yamada M, Yada T, Mori M. Peripheral administration of nesfatin-1 reduced food intake in mice: the leptin-independent mechanism. *Endocrinology*. 2009; 150: 662-71
- Shimizu H, Ohsaki A, Oh-I S, Okada S, Mori M. A new anorexigenic protein, nesfatin-1. *Peptides*. 2009; 30: 995-8
- Shintani M, Ogawa Y, Ebihara K, Aizawa-Abe M, Miyanaga F, Takaya K, Hayashi T, Inoue G, Hosoda K, Kojima M, Kangawa K, and Nakao K. Ghrelin, an endogenous growth hormone secretagogue, is a novel orexigenic peptide that antagonizes leptin action through the activation of hypothalamic neuropeptide Y/Y1 receptor pathway. *Diabetes*. 2001; 50: 227–232
- Shlimun A, Unniappan S. Ghrelin o-acyl transferase: bridging ghrelin and energy homeostasis. *Int J Pept*. 2011; 2011: 217957
- Solcia E, Capella C, Vassallo G, and Buffa R. Endocrine cells of the gastric mucosa. *Int Rev Cytol*. 1975; 42: 223–286

Stanley S, Wynne, K, McGowan, B, Bloom, S. Hormonal regulation of food intake. *Physiol Rev.* 2005; 85: 1131–58

Steiner DF, James DE. Cellular and molecular biology of the beta cell. *Diabetologia.* 1992; 35 Suppl 2: S41-8

Stengel A, Goebel M, Wang L, Rivier J, Kobelt P, Monnikes H, Lambrecht NW, Tache Y, Sachs G, Lambrecht NW. Central nesfatin-1 reduces dark-phase food intake and gastric emptying in rats: differential role of corticotropin-releasing factor2 receptor. *Endocrinology* 2009a; 150: 4911-9

Stengel A, Goebel M, Wang L, Taché Y, Sachs G, Lambrecht NW. Differential distribution of ghrelin-Oacyltransferase (GOAT) immunoreactive cells in the mouse International Journal of Peptides 5 and rat gastric oxyntic mucosa. *Biochem Biophys Res Commun.* 2010; 392: 67–71

Stengel A, Goebel M, Yakubov I, Wang L, Witcher D, Coskun T, Taché Y, Sachs G, Lambrecht NW. Identification and characterization of nesfatin-1 immunoreactivity in endocrine cell types of the rat gastric oxyntic mucosa. *Endocrinology.* 2009b; 150(1):232-8

Stengel A, Goebel-Stengel M, Wang L, Kato I, Mori M, Taché Y. Nesfatin-1(30-59) but not the N- and C-terminal fragments, nesfatin-1(1-29) and nesfatin-1(60-82) injected intracerebroventricularly decreases dark phase food intake by increasing inter-meal intervals in mice. *Peptides.* 2012a; 35(2): 143-8

Stengel A, Hofmann T, Goebel-Stengel M, Lembke V, Ahnis A, Elbelt U, Lambrecht NW, Ordemann J, Klapp BF, Kobelt P. Ghrelin and NUCB2/nesfatin-1 are expressed in the same gastric cell and differentially correlated with body mass index in obese subjects. *Histochem Cell Biol.* 2013; 139(6): 909-18

Stengel A, Tache Y. Ghrelin - a pleiotropic hormone secreted from endocrine x/a-like cells of the stomach. *Front Neurosci.* 2012b; 16: 24

Stoka A. Phylogeny and Evolution of Chemical Communication: An Endocrine Approach. *Journal of Molecular Endocrinology.* 1999; 22: 207-25

Su Y, Zhang J, Tang Y, Bi F, Liu JN. The novel function of nesfatin-1: anti-hyperglycemia. *Biochem Biophys Res Commun.* 2010; 391: 1039-42

Takaya K, Ariyasu H, Kanamoto N, Iwakura H, Yoshimoto A, Harada M, Mori K, Komatsu Y, Usui T, Shimatsu A, Ogawa Y, Hosoda K, Akamizu T, Kojima M, Kangawa K, and Nakao K. Ghrelin strongly stimulates growth hormone release in humans. *J Clin Endocrinol Metab.* 2000; 85: 4908–4911

Tanaka T, Katsuma S, Adachi T, Koshimizu TA, Hirasawa A, Tsujimoto G. Free fatty acids induce cholecystokinin secretion through GPR120. *Naunyn Schmiedebergs Arch Pharmacol.* 2008; 377: 523-527

- Tanaka T, Yano T, Adachi T, Koshimizu TA, Hirasawa A, Tsujimoto G. Cloning and characterization of the rat free fatty acid receptor GPR120: in vivo effect of the natural ligand on GLP-1 secretion and proliferation of pancreatic beta cells. *Naunyn Schmiedebergs Arch Pharmacol*. 2008; 377: 515-522
- Tena-Sempere M, Barreiro ML, Gonzalez LC, Gaytan F, Zhang FP, Caminos JE, Pinilla L, Casanueva FF, Dieguez C, Aguilar E. Novel expression and functional role of ghrelin in rat testis. *Endocrinology*. 2002; 143: 717–725
- Tolson KP, Garcia C, Yen S, Simonds S, Stefanidis A, Lawrence A, Smith JT, Kauffman AS. Impaired kisspeptin signaling decreases metabolism and promotes glucose intolerance and obesity. *J Clin Invest*. 2014; 124(7): 3075-9
- Topaloglu AK, Tello JA, Kotan LD, Ozbek MN, Yilmaz MB, Erdogan S, Gurbuz F, Temiz F, Millar RP, Yuksel B. Inactivating KISS1 mutation and hypogonadotropic hypogonadism. *N Engl J Med*. 2012; 366(7): 629-35
- Toshinai K, Mondal MS, Nakazato M, Date Y, Murakami N, Kojima M, Kangawa K, and Matsukura S. Upregulation of ghrelin expression in the stomach upon fasting, insulin-induced hypoglycemia, and leptin administration. *Biochem Biophys Res Commun*. 2001; 281: 1220–1225
- Tschop M, Smiley DL, and Heiman ML. Ghrelin induces adiposity in rodents. *Nature*. 2000; 407: 908–913
- Tsuneki H., Murata S., Anzawa Y., Soeda Y., Tokai E., Wada T., Kimura I., Yanagisawa M., Sakurai T. and Sasaoka T. Age-related insulin resistance in hypothalamus and peripheral tissues of orexin knockout mice. *Diabetologia*. 2008; 51, 657–667
- Ueta Y, Ozaki Y, Saito J, Onaka T. Involvement of novel feeding-related peptides in neuroendocrine response to stress. *Exp Biol Med (Maywood)*. 2003; 228: 1168-74
- Unniappan S, Cerda-Reverter JM, Peter RE. In situ localization of preprogalanin mRNA in the goldfish brain and changes in its expression during feeding and starvation. *Gen Comp Endocrinol*. 2004; 136: 200–7
- Van Nas A, Guhathakurta D, Wang SS, Yehya N, Horvath S, Zhang B, Ingram-Drake L, Chaudhuri G, Schadt EE, Drake TA, Arnold AP, Lusis AJ. Elucidating the role of gonadal hormones in sexually dimorphic gene coexpression networks. *Endocrinology*. 2009; 150: 1235–49
- Varricchio E, Russolillo MG, Russo F, Lombardi V, Paolucci M, Maruccio L. Expression and immunohistochemical detection of Nesfatin-1 in the gastrointestinal tract of Casertana pig. *Acta Histochem*. 2013; S0065-1281: 00223-00227
- Vas S, Ádori C, Könczöl K, Kátai Z, Pap D, Papp RS, Bagdy G, Palkovits M, Tóth ZE. Nesfatin-1/NUCB2 as a potential new element of sleep regulation in rats. *PLoS One*. 2013; 8(4): e59809

- Vincent M, Guz Y, Rozenberg M, Webb G, Furuta M, Steiner D, Teitelman G. Abrogation of protein convertase 2 activity results in delayed islet cell differentiation and maturation, increased alpha-cell proliferation, and islet neogenesis. *Endocrinology*. 2003; 144: 4061-9
- Volante M, Allia E, Gugliotta P, Funaro A, Broglio F, Deghenghi R, Muccioli G, Ghigo E, Papotti M. Expression of ghrelin and of the GH secretagogue receptor by pancreatic islet cells and related endocrine tumors. *J Clin Endocrinol Metab*. 2002; 87: 1300–1308
- Walia P, Asadi A, Kieffer TJ, Johnson JD, Chanoine JP. Ontogeny of ghrelin, obestatin, preproghrelin, and prohormone convertases in rat pancreas and stomach. *Pediatric research*. 2009; 65: 39-44
- Walker AK, Gong Z, Park WM, Zigman JM, Sakata I. Expression of Serum Retinol Binding Protein and Transthyretin within Mouse Gastric Ghrelin Cells. *PLoS One*. 2013; 8: e64882
- Wang Q, Guo F, Sun X, Gao S, Li Z, Gong Y, Xu L. Effects of exogenous nesfatin-1 on gastric distention-sensitive neurons in the central nucleus of the amygdala and gastric motility in rats. *Neurosci Lett*. 2014; 582: 65-70
- Weinhaus A, Poronnik P, Cook D, Tuch B. Insulin secretagogues, but not glucose, stimulate an increase in $[Ca^{++}]_i$ in the fetal rat beta-cell. *Diabetes*. 1995; 44: 118-24
- Wendel M, Sommarin Y, Bergman T, Heinegard D. Isolation, characterization and primary structure of a calcium-binding 63-kDa bone protein. *J Biol Chem*. 1995; 270: 6125–33
- Wierup N, Yang S, McEvelly RJ, Mulder H, Sundler F. Ghrelin is expressed in a novel endocrine cell type in developing rat islets and inhibits insulin secretion from INS-1 (832/13) cells. *J Histochem Cytochem*. 2004; 52: 301–10
- Winslow JT, Hastings N, Carter CS, Harbaugh CR, Insel TR. A role for central vasopressin in pair bonding in monogamous prairie voles. *Nature*. 1993; 365(6446): 545-8
- Wu D YM, Chen Y, Jia Y, Ma ZA, Boden G, Li L, Yang G. Hypothalamic nesfatin-1/NUCB2 knockdown augments hepatic gluconeogenesis that is correlated with inhibition of mTOR-STAT3 signaling pathway in rats. *Diabetes*. 2014; 63: 1234-47
- Xia ZF, Fritze DM, Li JY, Chai B, Zhang C, Zhang W, Mulholland MW. Nesfatin-1 inhibits gastric acid secretion via a central vagal mechanism in rats. *Gastrointest Liver Physiol*. 2012; 303: G570-G577
- Xu G, Li Y, An W, Li S, Guan Y, Wang N, Tang C, Wang X, Zhu Y, Li X, Mulholland MW, Zhang W. Gastric mammalian target of rapamycin signaling regulates ghrelin production and food intake. *Endocrinology*. 2009; 150: 3637–3644
- Yang J, Brown MS, Liang G, Grishin NV, Goldstein JL. Identification of the acyltransferase that octanoylates ghrelin, an appetite-stimulating peptide hormone. *Cell*. 2008; 132: 387-396

- Yang Y, Zhao TJ, Goldstein JL, Brown MS. Inhibition of ghrelin O-acyltransferase (GOAT) by octanoylated pentapeptides. *Proc Natl Acad Sci U S A*. 2008; 105: 10750–10755
- Yoshida N, Maejima Y, Sedbazar U, Ando A, Kurita H, Damdindorj B, Takano E, Gantulga D, Iwasaki Y, Kurashina T, Onaka T, Dezaki K, Nakata M, Mori M, Yada T. Stressor-responsive central nesfatin-1 activates corticotropin-releasing hormone, noradrenaline and serotonin neurons and evokes hypothalamic-pituitary-adrenal axis. *Aging (Albany NY)*. 2010; 2: 775-84
- Yoshimura M, Matsuura T, Ohkubo J, Maruyama T, Ishikura T, Hashimoto H, Kakuma T, Mori M, Ueta Y. A role of nesfatin-1/NucB2 in dehydration-induced anorexia. *Am J Physiol Regul Integr Comp Physiol*. 2014; 307(2): R225-36
- Yosten GL, Redlinger L, Samson WK. Evidence for a Role of Endogenous Nesfatin-1 in the Control of Water Drinking. *Journal of Neuroendocrinology*. 2012; 24: 1078–84
- Yosten GL, Samson WK. The anorexigenic and hypertensive effects of nesfatin-1 are reversed by pretreatment with an oxytocin receptor antagonist. *American Journal of Physiology Regulatory, Integrative and Comparative Physiology*. 2010; 298: R1642–R7
- Zegers D, Beckers S, de Freitas F, Jennes K, Van Camp JK, Mertens IL, Van Hoorenbeeck K, Rooman RP, Desager KN, Massa G, Van Gaal LF, Van Hul W. Identification of mutations in the NUCB2/nesfatin gene in children with severe obesity. *Mol Genet Metab*. 2012; 107:729-34
- Zegers D, Beckers S, Mertens IL, Van Gaal LF, Van Hul W. Association between polymorphisms of the Nesfatin gene, NUCB2, and obesity in men. *Mol Genet Metab*. 2011; 103:282-6
- Zhang AQ, Li XL, Jiang CY, Lin L, Shi RH, Chen JD, Oomura Y. Expression of nesfatin-1/NUCB2 in rodent digestive system. *World J Gastroenterol*. 2010; 16: 1735-41
- Zhang C, Suckow A, Chessler SD. Altered pancreatic islet function and morphology in mice lacking the Beta-cell surface protein neuroligin-2. *PLoS One*. 2013; 8: e65711
- Zhao TJ, Liang G, Li RL, Xie X, Sleeman MW, Murphy AJ, Valenzuela DM, Yancopoulos GD, Goldstein JL, Brown MS. Ghrelin O-acyltransferase (GOAT) is essential for growth hormone-mediated survival of calorie-restricted mice. *Proc Natl Acad Sci U S A*. 2010; 107: 7467–7472
- Zhu X, Cao Y, Voogd K, Steiner DF. On the processing of proghrelin to ghrelin. *J Biol Chem*. 2006; 281: 38867–38870
- Zimin AV, Delcher AL, Florea L, Kelley DR, Schatz MC, Puiu D, Hanrahan F, Pertea G, Van Tassell CP, Sonstegard TS, Marçais G, Roberts M, Subramanian P, Yorke JA, Salzberg SL A whole-genome assembly of the domestic cow, *Bos taurus*. *Genome Biol*. 2009; 10: R42